Volume 7, Number 5
September–October 1999

ISSN: 0869-5938

STRATIGRAPHY AND GEOLOGICAL CORRELATION

Official English Translation of *Stratigrafiya, Geologicheskaya Korrelyatsiya*

Editor-in-Chief
Boris S. Sokolov

http://www.maik.rssi.ru

Journal of the Fundamental and Applied Aspects of Stratigraphy and the Correlation of Geologic Events and Processes in Time and Space

МАИК "НАУКА/INTERPERIODICA" PUBLISHING

Stratigraphy and Geological Correlation

(Stratigrafiya, Geologicheskaya Korrelyatsiya)

ISSN: 0869-5938

Editor-in-Chief
Boris S. Sokolov

Member of the Russian Academy of Sciences,
Counsellor of the Presidium of the Russian Academy of Sciences (RAS)

Address for correspondence: Staromonetnyi per. 22, Moscow, 109180 Russia
Phones: 7 (095) 951-2164; Fax: 7 (095) 233-5590.

Deputy Editor-in-Chief

Mikhail A. Semikhatov
Member of the Russian Academy of Sciences
Head of Laboratory, Geological Institute, RAS
E-mail: semikhatov@ginran.msk.su

Assistant Editor

Aleksei B. Herman
Senior Scientist,
Geological Institute, RAS
E-mail: herman@ginran.msk.su

EDITORIAL BOARD

Mikhail A. Akhmet'ev
Dr. Sci. (Geol.–Min.),
Head of Laboratory, Geological Institute, RAS
akhmetev@ginran.msk.su

Aleksandr S. Alekseev
Professor, Department of Paleontology,
Moscow State University
alekseev@ginran.msk.su

Mikhail N. Alekseev
Dr. Sci. (Geol.–Min.),
Chief Scientist, Geological Institute, RAS
aaleks@geol.msu.ru

Ivan A. Basov
Dr. Sci. (Geol.–Min.), Deputy Director,
Institute of the Lithosphere, RAS
basov@ilsan.msk.ru

Michael G. Basset
Professor, National Museum of Wales,
Cardiff, UK

William A. Berggren
Professor, Department of Geology and
Geophysics, Woods Hole Oceanographic
Institute, USA

Elena V. Bibikova
Dr. Sci. (Geol.–Min.), Chief Scientist,
Vernadskii Institute of Geochemistry and
Analytical Chemistry, RAS
sergei@bibikov.genebee.msu.su

Nikita A. Bogdanov
Corresponding Member of
the Russian Academy of Sciences,
Director, Institute of the Lithosphere, RAS
bogdanov@ilsan.msk.ru

Kiyotaka Chinzei
Professor, Institute of Geology,
University of Tokyo,
Tokyo, Japan

Nikolai M. Chumakov
Dr. Sci. (Geol.–Min.),
Chief Scientist, Geological Institute, RAS
chumakov@ginran.msk.su

Yurii B. Gladenkov
Dr. Sci. (Geol.–Min.),
Head of Laboratory, Geological Institute, RAS
gladenkov@ginran.msk.su

Dmitrii L. Kaljo
Professor, Institute of Geology, Tallinn, Estonia

Victor E. Khain
Member of the Russian Academy of Sciences,
Chief Scientist, Institute of the Lithosphere, RAS

Lidiya A. Nevesskaya
Dr. Sci. (Biol.), Laboratory Chief,
Institute of Paleontology, RAS
lenin33@paleo.ru

Aleksandr G. Ponomarenko
Dr. Sci. (Biol.), Chief Scientist,
Institute of Paleontology, RAS
vtopor@paleo.ru

Jurgen Remane
Professor, Institute de Géologie,
Université de Neuchâtel, Switzerland

Aleksei Yu. Rozanov
Dr. Sci. (Geol.–Min.),
Director, Institute of Paleontology, RAS
aroza@paleo.ru

Boris A. Sokolov
Dr. Sci. (Geol.–Min.), Professor, Dean, Faculty
of Geology, Moscow State University
mfedon@paleo.ru

Otto Walliser
Professor, Göttingen University, Göttingen,
Germany

Sun Weigo
Professor, Nanjing Institute of Geology
and Paleontology, Academia Sinica, China

Victor A. Zakharov
Dr. Sci. (Geol.–Min.), Head of Laboratory,
Institute of Geology, Geophysics, and
Mineralogy, Siberian Branch, RAS, Novosibirsk

Aleksandr I. Zhamoida
Corresponding Member of the Russian Academy of
Sciences, Russian Geological Institute, St. Petersburg

Staff Editor Tamara V. Trishkina

Editor of the English Translation Anatolii Ya. Sharas'kin, Dr. Sci. (Geol.–Min.)

SCOPE

Stratigraphy and Geological Correlation (Stratigrafiya, Geologicheskaya Korrelyatsiya) is the only journal in the world designed to provide comprehensive coverage of the fundamental and applied aspects of stratigraphy and the correlation of geological events and processes in time and space. Articles are based on the results of multidisciplinary research and are directed toward researchers, university professors, students, and geologists interested in understanding stratigraphy and the chronological features of the world's geological record.

Stratigraphy and Geological Correlation is abstracted and/or indexed in *Petroleum Abstracts*, *Research Alert*, *SciSearch*, *Current Contents* (*Physical*, *Chemical*, and *Earth Sciences*) and *World Translations Index*.

SUBSCRIPTION OFFICE
INTERPERIODICA
P.O. BOX 1831, BIRMINGHAM, AL 35201-1831 USA
PHONE: (800) 633-4931; (205) 995-1567 (outside US and Canada);
FAX: (205) 995-1588

PUBLISHER
МАИК "НАУКА/INTERPERIODICA"
PROFSOYUZNAYA UL. 90, MOSCOW, 117864 RUSSIA
PHONE: 7 (095) 336-1600; FAX: 7 (095) 336-0666
E-mail: compmg@maik.rssi.ru
Web Site: http://www.maik.rssi.ru

SUBSCRIPTION PRICES (1999, Volume 7, 6 issues)
US $906.00 (North America), $1041.00 (elsewhere). A 5% discount is given on 2-year orders. Subscriptions may be entered at any time. Orders may be placed at agencies or directly. There is a 5% discount to all subscription agencies. Cancellations not allowed except for duplicate payment. Prepayment required. Advance payment required in US$/US bank. MasterCard/Visa accepted. Make checks payable to *Stratigraphy and Geological Correlation* or Interperiodica.

Stratigraphy and Geological Correlation (ISSN: 0869-5938) is published bimonthly for US $906.00 (North America), outside North America for $1041.00 per year by MAIK "Nauka/Interperiodica", 5724 Hwy. 280 East, Birmingham, Alabama 35242-5724 USA. Periodical postage paid at Birmingham, Alabama, and additional mailing offices. POSTMASTER: Send address changes to *Stratigraphy and Geological Correlation*, P.O. Box 1831, Birmingham, Alabama 35201 USA.

The journal was founded in 1993.

Original Russian Edition Copyright © 1999 by the Russian Academy of Sciences
and Division of Geology, Geophysics, Geochemistry, and Mining Sciences.
English Translation Copyright © 1999 by МАИК "Наука/Interperiodica" (Russia).

Contents

Vol. 7, No. 5, 1999

Simultaneous English language translation of the journal is available from МАИК "Наука/Interperiodica" (Russia).
Stratigraphy and Geological Correlation ISSN 0869-5938.

Biotic Events and Positive δC_{carb} Anomaly at 2.3–2.06 Ga
M. A. Semikhatov, M. E. Raaben, V. N. Sergeev, A. F. Veis, and O. V. Artemova 413

Neoproterozoic Age of Oldest Rocks from the Tom' Inlier (Mountainous Shoriya): Implication of U–Pb, Sm–Nd, Rb–Sr, and Ar–Ar Dating
A. G. Vladimirov, A. P. Ponomareva, S. A. Kargopolov, G. A. Babin, A. V. Plotnikov, A. S. Gibsher, A. E. Izokh, S. P. Shokal'skii, E. V. Bibikova, D. Z. Zhuravlev, V. A. Ponomarchuk, V. A. Khalilov, and A. V. Travin 437

Acritarchs from Upper Beds of the Upper Cambrian–Lower Tremadocian of the Moscow Syneclise
N. A. Volkova 452

Permian–Triassic Conchostracan Faunas from the North of Central Siberia
E. F. Orlova 465

Jurassic Radiolarians from Northern Russia
V. S. Vishnevskaya and I. E. Pral'nikova 473

The Upper Cretaceous Radiolarians, Foraminifers, and Stratigraphy of the Southeastern Russian Plate, the Right-Bank Volga Region near Volgograd
L. G. Bragina, V. N. Ben'yamovskii, and A. S. Zastrozhnov 492

Stratigraphy and Structural Peculiarities of the Lower Paleozoic Carbonate–Siliceous–Tuffaceous Complex of the Chingiz Range (Eastern Kazakhstan)
K. E. Degtyarev, S. V. Dubinina, and A. P. Orlova 501

Triassic Siliceous Formation in the Khor River Basin (Central Sikhote Alin)
Yu. G. Volokhin, E. V. Mikhailik, and G. I. Burii 508

Personalia

A Tribute to the 90th Birthday of Boris Borisovich Chernyshev (1909–1941) 519

Stratigraphy and Geological Correlation, Vol. 7, No. 5, 1999, pp. 413–436. Translated from Stratigrafiya. Geologicheskaya Korrelyatsiya, Vol. 7, No. 5, 1999, pp. 3–27.
Original Russian Text Copyright © 1999 by Semikhatov, Raaben, Sergeev, Veis, Artemova.
English Translation Copyright © 1999 by МАИК "Наука/Interperiodica" (Russia).

Biotic Events and Positive δC_{carb} Anomaly at 2.3–2.06 Ga

M. A. Semikhatov, M. E. Raaben, V. N. Sergeev, A. F. Veis, and O. V. Artemova

Geological Institute, Russian Academy of Sciences, Pyzhevskii per. 7, Moscow, 109017 Russia

Received January 27, 1998

Abstract—A comprehensive analysis of taxonomic composition of pre-Riphean silicified and organic-walled microfossils described in publications is performed and dynamics of stromatolite abundance during the Archean and Paleoproterozoic is reconstructed based on a calculation of a number of stromatolite-bearing formations in seven time periods 300–400 m.y. long for the Archean and 200–300 m.y. long for the Paleoproterozoic. It is shown that the Jatulian positive $\delta^{13}C_{carb}$ anomaly, the largest one in the Earth's history that occurred 2.3–2.06 Ga ago was not related to evolutionary innovations in the ancient microbiota but was synchronous with the sharpest, in geological history, increase in the global stromatolite abundance. This event was controlled by a favorable combination of climatic, paleogeographic, and geodynamic factors and occurred under condition of the prevalence of the mantle flux into the World ocean over the continental runoff. Simultaneously, the transition to "normal marine" $\delta^{13}C_{carb}$ values that marked the termination of the Jatulian anomaly was accompanied by a slight increase in abundance of Paleoproterozoic stromatolites, which was reduced again only 1.8–1.6 Ga ago. It is concluded that the Jatulian anomaly was mainly related to the unique-scale expansion of cyanobacterial ecosystems that is recorded in stromatolite succession and occurred against the background of increasing oxygenation of atmosphere and surficial part of hydrosphere. Peculiarities of the C-isotope and paleontological records of the second half of the Paleoproterozoic are briefly discussed with consideration of probable factors responsible for the disappearance of the anomaly in question.

Key words. *Archean, Paleoproterozoic, microfossils, stromatolites, C-isotope anomaly, biosphere evolution.*

INTRODUCTION

Recently, it was established that the positive C_{carb} isotope anomaly ($\delta^{13}C$ to 12–15‰ PDB) that occurred in the first half of the Early Proterozoic (Paleoproterozoic) about 2.3–2.06 Ga ago (Schidlowski *et al.*, 1976; Yudovich *et al.*, 1990; Karhu, 1993; Tikhomirova and Makarikhin, 1993; Melezhik and Fallick, 1994, 1996; Pokrovskii and Melezhik, 1995; Melezhik *et al.*, 1997a, 1997b, 1997c; Karhu and Holland, 1996; Akhmedov *et al.*, 1996; and references therein) was the most significant one in the entire Earth's history. Its manifestations are recorded in North America, Africa, Australia, and Europe (Fennoscandia, Karelia, Scotland), which allows it to be considered as a global-scale phenomenon.

Various models differing in mechanism and scale are used to explain the latter (see review in Melezhik and Fallick, 1996). Some of them assume an influence of biotic or related factors on the C-isotope composition in paleobasins. Therefore, of interest is a critical analysis of available data on those events in the Precambrian biota evolution that preceded them is of interest, were synchronous, and directly followed the Early Paleoproterozoic (Jatulian) positive C-isotope anomaly. Our analysis involved available incomplete data on pre-Riphean organic-walled microfossils and carbonaceous submacroscopic fossils, more extensive data on silicified microbiotas, and sufficiently representative information on abundance dynamics of the stromatolites, which represent mostly organic–sedimentary structures whose formation is related to the metabolic activity of benthic prokaryotic microorganisms, mainly cyanobacteria.

When performing the analysis, we used the following units of the Archean chronometric scale of the International Subcommission on Precambrian Stratigraphy: Paleoarchean (3.6–3.2 Ga), Mesoarchean (3.2–2.8 Ga), and Neoarchean (2.8–2.5 Ga). The age constraints for Paleoproterozoic microbiotas was defined by isotopic dates of enclosing deposits, whereas dynamic of stromatolite abundance was analyzed using four informal chronometric units (2.5–2.3, 2.3–2.0, 2.0–1.8, and 1.8–1.6 Ga), which were applied earlier when considering dynamics of the stromatolite diversity (Semikhatov and Raaben, 1994, 1996). In their time-range, this units are close or correspond to periods established for the Paleoproterozoic by the above-mentioned subcommission (Plumb, 1991).

MICROFOSSILS

The Precambrian organic-walled and silicified microfossils represent remains of biologically close but slightly different facies of microrganisms. Data on both

types of remnants of their Riphean and Vendian representatives well supplement each other and generally allow an adequate understanding of evolution of pertinent communities and their paleoecological structure. However, an information on Paleoproterozoic and, particularly, Archean organic-walled remnants very sharply decreases against the background of general decrease in abundance and diversity of all recorded microbiotas. This is very easily explained: silicified microfossils are enveloped by a siliceous "sarcophagus" just after the postmortem burial of microorganisms in carbonate sediments (Maliva *et al.*, 1989) and therefore, they are more resistant to an impact of external factors than the mummified organic-walled remnants confined to siliciclastic sequences and not protected by outer barriers.

Silicified microfossils. In the 1960–1990s, after attempts to multiply finds of the most ancient life traces, a lot of silicified microfossils more than 2.5–3.0 Ga old were described, but later, after their comprehensive analysis, almost all of them appeared to be pseudofossils (mineral artefacts or structureless aggregates of organic matter—kerogen) or modern contaminants (see reviews in Schopf and Walter, 1983; Hofmann and Schopf, 1983; Schopf and Klein, 1992). Only thin non-septate filaments from the Paleoarchean Onverwacht and Fig Tree groups of South Africa and the Warrawoona Group of Western Australia (about 3.5–3.4 Ga old) as well as probably small coccoidal forms reported from the first of the listed groups represent those Paleoarchean structures, whose organic nature is recently well substantiated (Buick, 1991; Awramik, 1992b; Walsh, 1992; Knoll, 1996).

More abundant finds of microfossils are confined to the Mesoarchean and Neoarchean. In India, rod-like and spherical structures several microns across that are interpreted to represent fossil bacteria (Venkatachala *et al.*, 1986) are enclosed in the Bababudan Iron Formation (2.9–2.8 Ga, Chadwick *et al.*, 1997), whereas probable filamentous microorganisms are recorded from the Sandur Schist Belt (Naqvi *et al.*, 1987) 2.75–2.65 Ga old (Nutman *et al.*, 1966; Chadwick *et al.*, 1997). The Fortescue Group of Western Australia (2.76–2.69 Ga old; Arndt *et al.*, 1991; Pidgeon and Horwitz, 1991) yields trichome-like structures about 10 μm wide (Schopf and Walter, 1983) and vertically oriented siliceous filament molds (Buick, 1992). In size and morphology, the latter are comparable with hormogonian cyanobacteria, although it is not inconceivable that they represent remnants of other microorganisms (sulfur or sulfate-reducing bacteria). Most remarkable Neoarchean microfossils originate from the South African Gamohaan carbonate formation (Transvaal Supergroup) 2550–2520 Ma old (Barton *et al.*, 1994; Altermann, 1996). Rocks of this unit host sufficiently wide filamentous (diameter to 35 μm) and small coccoidal (1–5 μm) forms (Klein *et al.*, 1987; Schopf and Klein, 1992), which judging from their morphology and dimensions may be considered, with a high degree of confidence, as representing fossil cyanobacteria. This unit also encloses very small rod-like structures, which are interpreted to be remnants of heterotrophic bacteria (Lanier, 1986; Knoll, 1996) or, sometimes, as pseudofossils.

The early Paleoproterozoic silicified microfossils are represented only by very small and poorly preserved coccoidal forms from the Kolasioki Group of the Pechenga Supergroup in the Kola Peninsula (Ivanova *et al.*, 1988) and small problematic coccoidal and filamentous remnants from the Aravalli Supergroup of India (Chauhan, 1989). The Kolasioki Group is dated back to 2.1–2.06 Ga (Melezhik *et al.*, 1997c), whereas the Aravalli Supergroup ranges from 2.3 to 2.0 Ga in age (Semikhatov and Raaben, 1994 and references therein). In the higher Paleoproterozoic strata (2.0–1.6 Ga), the abundance and diversity of recorded silicified microbiotas increases stepwise and their preservation becomes substantially better. First undoubted cyanobacteria remnants are reported just from these deposits.

The aforesaid first concerns colonial coccoidal microfossils *Eoentophysalis belcherensis* Hofmann from peritidal McLeary and Kasegalik carbonate formations of the Belcher Supergroup of Canada (Hofmann, 1976; Hofmann and Schopf, 1983); the age of the supergroup is bracketed between 2000 and 1960 Ma (Hofmann, 1988, 1989; Chandler and Parrish, 1989). In the morphology and succession of development stages, these fossils are identical to modern entophysalidacean cyanobacteria *Entophysalis major* Ercegovič (Golubic and Hofmann, 1976). In addition, the above-mentioned formations yield small microfossils of ellipsoidal, spherical, and filamentous forms, which also may be referred to cyanobacteria. Silicified microbiotas similar in composition and known as the Belcher-type microbiotas are reported, in addition to the Belcher Supergroup, from the Epworth Group (1.92–1.90 Ga; Grotzinger, 1988) of northwestern Canada (Hofmann, 1976; Hofmann and Schopf, 1983; Hofmann and Grotzinger, 1985; Schopf, 1992) and also from slightly younger (1.69–1.60 Ga; Plumb, 1990; Page *et al.*, 1994; Page and Sweet, 1998) deposits of Australia: the McArthur Group, Bungl Bungl Dolomite and Paradise Creek Formation (Muir, 1976; Oehler, 1978; Hofmann and Schopf, 1983). All these microbiotas are dominated by remnants of morphologically simple shallow-water entophysalidacean and chroococcoidal cyanobacteria with subordinate hormogonian cyanobacteria remnants. Almost all genera and even species of these microbiotas are reported from the Riphean (Golubic and Hofmann, 1976; Knoll, 1985, 1996; Sergeev, 1992; Schopf and Klein, 1992), where they form a core of evolutionary conservative shallow-water communities of carbonate platforms.

Deeper-water deposits of the upper part of the Paleoproterozoic enclose taxonomically different microfossils known as the Gunflint-type microbiotas. Most char-

acteristic here are microbiotas described from the Gunflint and Biwabik iron formations of the Animikie Supergroup. The age of this supergroup is constrained by the following data: (1) its lower strata experienced silicification 1930 ± 25 Ma ago and contain gravel-sized grains of apatite with the Pb–Pb age of 1929 ± 17 Ma; (2) the entire supergroup was affected by the Penokean orogeny that culminated approximately at 1850 Ma; and (3) the U–Pb age of zircons from tuffs of the Gunflint Formation is 1878 ± 2 Ma (Morey and Van Schmus, 1988; Morey, 1996; Fralick *et al.*, 1998). The Animikie Supergroup encloses two groupings of microfossils (Hofmann and Schopf, 1983; Hofmann and Grotzinger, 1985; Schopf and Klein, 1992). The first of them includes morphologically simple filamentous and coccoidal microremnants (*Gunflintia, Animikia, Huroniospora*, and others), which represent hormogonian and chroococcoidal cyanobacteria (Cloud, 1976; Hofmann and Schopf, 1983; Lanier, 1989) and partly, in all likelihood, iron-oxidizing bacteria, The second grouping is composed of morphologically more complex forms (*Kakabekia, Xenothrix, Archaeorstis, Eoastrion, Eosphaera, Eomicrhystridium*, and others), which include probable bacteria remnants including iron bacteria (*Eoastrion*) and probably lower unicellular eukaryotic organisms (*Eosphaera, Eomicrhystridium*).

The Gunflint-type assemblages that differ only in the list of microfossils of complex morphology are described from other successions of the Upper Paleoproterozoic: the Odjick Formation of the Epworth Group (Hofmann and Grotzinger, 1985) and the Sokoman Formation of the Kaniapiskau Supergroup of Canada (Knoll and Simonson, 1981) as well as from the Frere Formation of the Earaheedy Group (Walter *et al.*, 1976; Hofmann and Schopf, 1983) and the Duck Creek Formation of Australia (Hofmann and Schopf, 1983; Knoll *et al.*, 1988). As was mentioned, the age of the Epworth Group is 1.92–1.90 Ga and that of the Sokoman Formation, 1.88 Ga (Hoffman, 1988a, 1988b), whereas the Duck Creek Formation is slightly older than 1.84 Ga but younger than 2.0 Ga (Plumb, 1990; Thorne and Seymour, 1991). As for the Earaheedy Group, radiometric measurements show only that its age ranges between 2.4 and 1.6–1.7 Ga, though paleontological data suggest that this group is 1.9–1.8 Ga old (Grey, 1994b; Semikhatov and Raaben, 1996). Similar microfossil assemblage was macerated from shales of the Chuanlinggou Formation of China (Zhang, 1984), whose age is actively debated in the Chinese literature, but usually estimated to be in the range of 2.0–1.8 Ga (see Zhu and Chen, 1992; Semikhatov and Raaben, 1994; and references therein).

Thus, pre-Riphean silicified microbiotas are spatially widespread but irregularly scattered through the sequence (Fig. 1). Their first representatives, scarce and poorly diverse, are reported from the Paleoarchean and Mesoarchean. In the Neoarchean, these microbiotas become more frequent and informative, though they are virtually absent in the lower part of the Paleoproterozoic. The upper strata of the latter unit yield sufficiently abundant and diverse microbiotas, which include representatives of all classes and main families of cyanobacteria as well as first remnants of probable lower eukaryotic fossils.

Due to an ambiguous nature of oldest microfossils, data obtained by molecular biology are undoubtedly important for interpreting the Early Precambrian paleontological record. In this connection, the following should be noted. Ellipsoidal remnants recorded in the Rocknest Formation of the Epworth Group and first classed with *Brevitrichoides* (Hofmann and Grotzinger, 1985) are morphologically almost identical to Riphean microfossils of the *Archaeoellipsoides* genus, which are confidently correlated with akinetes (spores) of nostocalean or *Anabaena*-like cyanobacteria (Sergeev *et al.*, 1995; Golubic *et al.*, 1995.[1] An analysis of succession of 16-S ribosomal RNA in representatives of modern cyanobacteria (Fig. 2) allow the akinete-forming nostocalean and stigonematalean cyanophytes to be considered as a terminal group at the cyanobacteria philogenetic tree (Giovannoni *et al.*, 1988; Wilmotte and Golubich, 1991). If this interpretation is correct, then akinete finds in the Rocknest Formation determine a minimum age limit for the origination of main morphological groups of cyanobacteria, whose radiation process, according to molecular biology, was very rapid.

Nonetheless, the potential of such approach to deciphering cyanobacteria philogeny should not be overestimated because there are examples of inconsistency between the 16-S RNA succession in modern cyanobacteria and secular succession of some microfossils. For instance, the modern cyanobacteria *Spirulina* fall out of a generally correct succession of their morphologically complex representatives (Wilmotte and Golubic, 1991), and the paleotype analogue of the genus—*Obruchevella*—appears only near the Middle–Upper Riphean boundary, much later than other relatively complex cyanobacteria (Golovenok and Belova, 1983, 1994; Sergeev, 1992, 1997).

Organic-walled microfossils. The purposeful study of pre-Riphean organic-walled microfossils has been carried out only in Russia and China. In the 1960–1980s, B.V. Timofeev and his collaborators reported on abundant remnants of variable morphology from Lower Proterozoic and, less commonly, also from Archean deposits of North Eurasia, which were referred to several dozens of species belonging to many genera (Timofeev, 1982; and references therein). The essential taxonomy of Precambrian organic-walled microfossils (Yankauskas *et al.*, 1989) and comprehensive revision of previously published data allow us to state that all these Archean and Paleoproterozoic fossils

[1] Sometimes, thickenings on *Gunflintia* trichomes from the Gunflint Formation were described as akinetes and heterocysts (Cloud 1976), but nowadays such structures are usually considered as representing posthumous transformation of homogenous filament (Gerasimenko and Krylov, 1983; Wilmotte and Golubic, 1991).

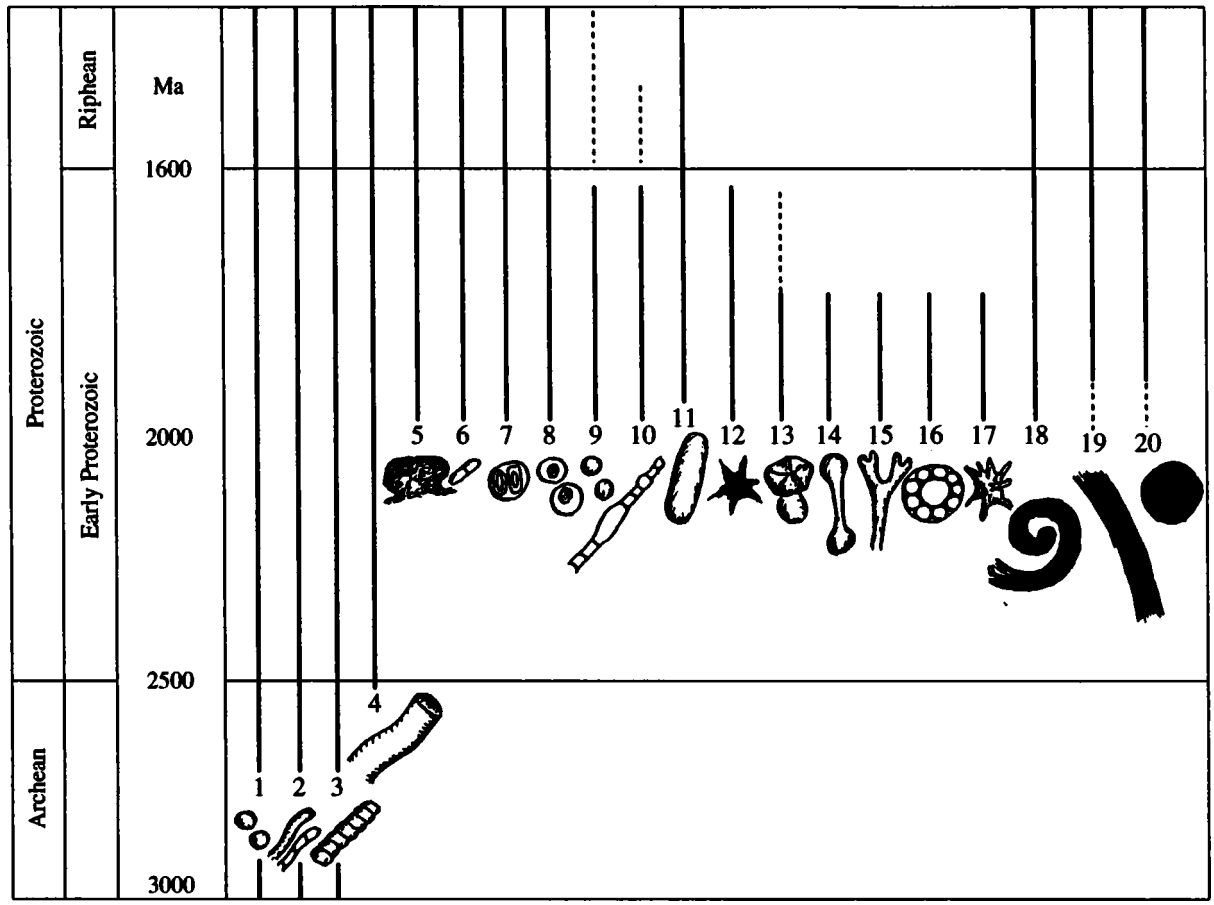

Fig. 1. Distribution of main types of microfossils in Archean and Paleoproterozoic: (1) small (<10μm) isolated spherical microfossils; (2) small (diameter <10 μm) filamentous microfossils; (3) trichomes and trichome-like structures more than 10 μm across; (4) large (diameter to 35 μm) nonseptated filaments—probable empty envelopes of oscillatorian cyanobacteria; (5) remnants of entophysalidacean cyanobacteria (genus *Eoentophysalis*); (6) unicellular ellipsoidal chroococcoidal cyanobacteria of the *Synechococcus* type (genus *Eosynechococcus*); (7) unicellular chroococcoidal cyanobacteria of the *Gloeocapsa* type (genus *Gloeodiniopsis*); (8) coccoidal microfossils with inclusions of compressed bodies; (9) coccoidal microfossils without inclusions (genus *Myxococcoides*); (10) trichomes with separate enlarged cells (genus *Gunflintia*); (11) large ellipsoidal envelopes—probable akinetes of cyanobacteria; (12–17) microfossils of complex morphology from associations of the *Gunflintia* type: (12) *Eoastrion*, (13) *Kakabekia*, (14) *Xenothrix*, (15) *Archaeorestis*, (16) *Eosphaera*, (17) problematic acanthomorph acritarchs *Eomicrhystridium*; (18) impressions of large spiral structures (genus *Grypania*); (19) impressions of large band-like structures; (20) impressions of large *Chauria*-like spherical forms.

correspond to three simplest morphotypes that are included into their modern classification. These are small acritarchs (from 5–6 to 60 and, sometimes, 100 μm across), colonial coccoidal forms with cells to 10–14 μm across, and thin (2–12 μm) filaments lacking the cellular structure. In the context of modern classification, first forms can be referred to *Leiominuscula* and *Leiosphaeridia*, whereas the second to *Myxococcoides* and the third one to *Eomycetopsis* and *Leiotrichoides* genera.

The oldest organic-walled microfossils originate from the Mesoarchean (3.0–2.8 Ga; Bibikova *et al.*, 1989) Gimola Group of central Karelia, where *Leiominuscula* and *Myxococcoides* representatives occur. The Paleoproterozoic deposits of the Baltic shield, namely the Jatulian succession (2.3–2.06 Ga; Melezhik *et al.*, 1997c), the Besovets Formation of the Ludikovian (2.06–1.9 Ga), and the Pechenga Group in the Kola superdeep hole (mainly the interval of 3759–1981 m) yields listed genera and also *Leiosphaeridia* species. The same very simple microfossils are present in the Krivoi Rog Group of Ukraine (2.5–2.0 Ga; Bibikova *et al.*, 1989) and in the Kodar Subgroup (2.5–2.18 Ga; Berezhnaya *et al.*, 1988) representing the lower part of the Udokan Group of central Siberia. In higher layers of this group (2.18–2.0 Ga), the above-mentioned microfossils are associated with structureless filaments of *Eomycetopsis* and *Leiotrichoides*.

The cited data confirm the prevalent opinion that Late Archean basins hosted relatively diverse prokaryotes, which in the Late Paleoproterozoic basins were accompanied by eukaryotic phytoplankton. Few reliable data on the composition of pre-Riphean organic-walled, partly mineralized microbiotas of North Amer-

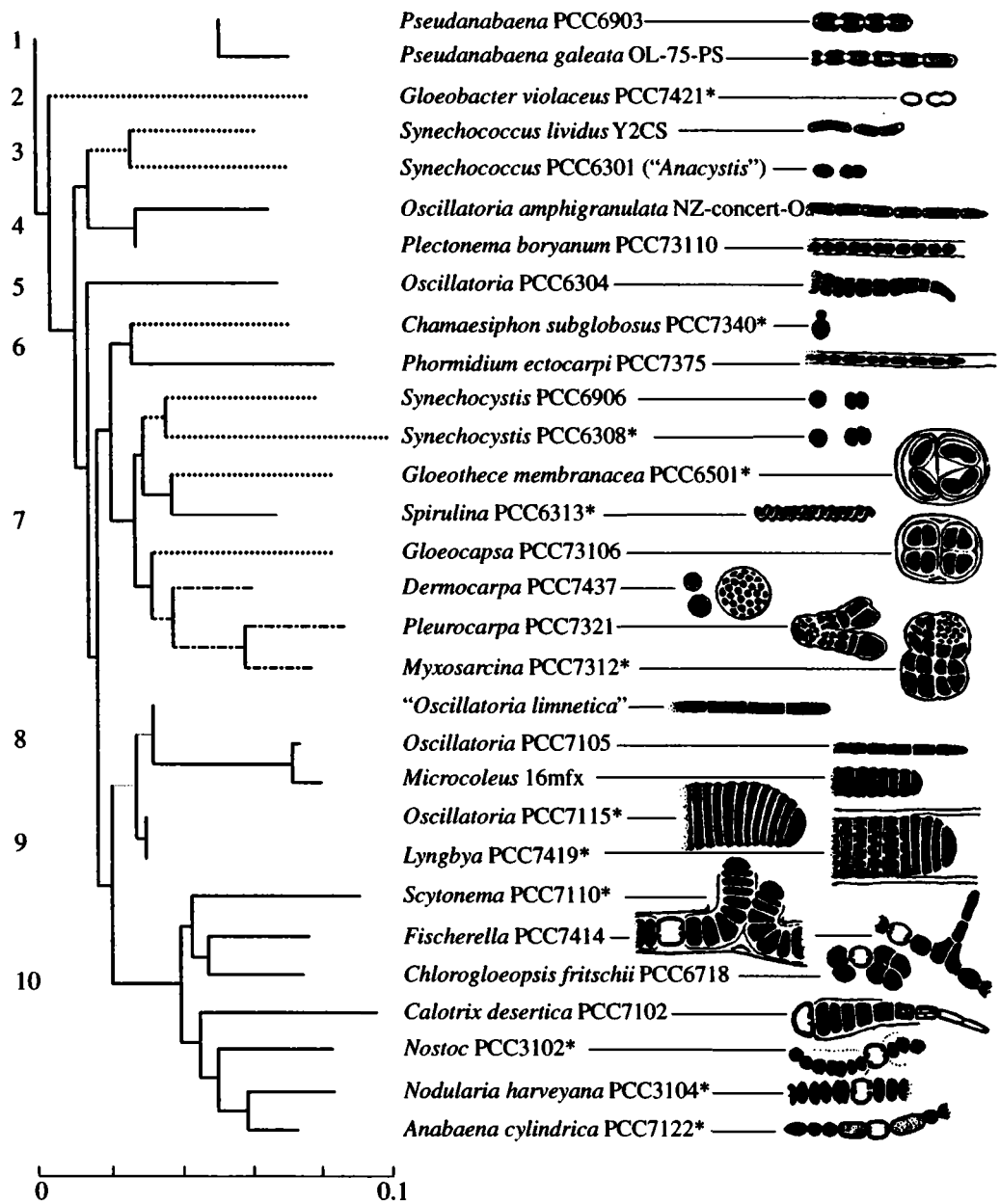

Fig. 2. Dendrogram showing philogenetic relationships between different morphologic groups of cyanobacteria based on the succession of 16-S ribosomal RNA (Wilmotte and Golubic, 1991).

Dotted lines designate simple filamentous forms, punctate lines—coccoidal forms, dotted–punctuate lines—baeocyth-forming organisms, and solid lines—heterocyst akinete-forming organisms. Indices to the right of taxa names designate laboratory numbers of different strains used in the original work (Giovannoni *et al.*, 1988) when studying molecular philogeny of cyanobacteria.

ica and Australia (Schopf and Walter, 1983; Hofmann and Schopf, 1983; Mendelson *et al.*, 1992) are consistent with this conclusion.

This picture is slightly violated by publications of Chinese geologists concerning the composition of microfossils from Upper Paleoproterozoic deposits (Zhang, 1995; Yan, 1995; references therein). The Changzhougou and Taunshanzi formations representing the lower part of the Changcheng "System," whose age ranges from 1850 to 1620 Ma (for references, see Semikhatov and Raaben, 1994), enclose abundant well-preserved acritarchs (including those to 250 μm across) and associated carbonaceous films variable in morphology. Amid the latter, *Chuaria*- and *Tawuia*-like varieties prevail being accompanied by subordinate morphologically more complex structures, which reveal, in the opinion of the researchers who described them, a similarity with green, red, and brown algae. The language barrier and low quality of images of paleontological

remains in Chinese publications prevent the correct estimate of these opinions. Therefore, they are omitted from further consideration.

The occurrence of *Chuaria* in the lower part of the Changcheng "System" is better substantiated (Hofmann and Chen, 1981; Hofmann, 1994), although some researchers (including one of us) cast doubt on the accuracy of their determinations. Recently, these fossils were considered as representing remnants of either the lower eukaryots (giant acritarchs) or large nostocalean colonial cyanobacteria (Sun, 1987; Sergeeev, 1992, 1994; Knoll, 1992, 1996; Hofmann, 1994; Steiner, 1986). Older impressions of large spherical carbonaceous microfossils are reported from North America as occurring in deposits 2.0–1.85 Ga old (the Nastapoka and Knob Lake groups). These fossils are interpreted to represent remnants of cyanobacteria colonies and are mainly referred to the Moraniacea and Beltinacea families (Hofmann, 1994).

Remnants of the oldest proven eukaryotic organisms, known by the moment, are recorded in the Negaunee Formation that terminates the Minnominee Group section in the Superior Lake area. They include small narrow (0.7–1.5 mm) carbonaceous bands of two size categories forming flat spire. Some of them are close to *Grypania spiralis* (Walcott) from the Lower Riphean of Montana (Walter *et al.*, 1990), whereas others probably represent a new genus. Morphology and dimensions of these fossils allow them to be classed with lower algae, which probably have no modern analogues (Han and Runnegar, 1992; Hofmann, 1994). The available isotopic–geochronologic data and regional relationships show that the age of the Negaunee Formation is close to 1900 Ma, rather than 2100 Ma, as had been estimated in recent publications. This estimate is based on the following data: (1) the Minnominee Group is predated by basic dikes with the Sm-Nd isochron age of 2110 ± 52 Ma and its lower and middle strata underlying the Negaunee Formation enclose volcanics with the U-Pb age of 1910 ± 10 Ma; (2) the group is unconformably overlain by the Baraga Group metamorphosed 1852 ± 6 Ma ago and correlated with the Animikie Supergroup whose accumulation commenced about 1900 Ma ago (Gerlach *et al.*, 1988; Morey, 1996; Fralick *et al.*, 1998).

The occurrence of *Grypania* remnants in the Negaunee Formation provides strong evidence that the eukaryots appeared on the Earth slightly earlier than it stems from the analysis of maximum dimensions of microfossils and biomarker studies (for a bibliography see Knoll, 1992, 1996; Hofmann, 1994). In this connection, it should be noted that data of molecular biology (Sogin *et al.*, 1989; Sepkoski, 1993) indicate that eukaryotes are close to archaeobacteria, not to eubacteria, as was considered previously, and consequently, they appeared evolutionary earlier.

Thus, the following time constraints are obtained for oldest fossils: (a) about 2.0 Ga for definite cyanobacteria remnants (Belcher Supergroup); (b) 2.52–2.55 and probably 2.69–2.76 Ga for their very probable remnants (Transvaal Supergroup and Fortescue Group, respectively); (c) slightly older than 1.9 Ga for remnants of the early eukaryotic organisms (Negaunee Formation); and (d) 2.69–2.76 Ga for remnants of heterotrophic bacteria (Fortescue Group) and probably 3.4–3.5 Ga for those from the Onverwacht, Fig Tree, and Warrawoona groups. It is clear that distribution of the listed finds in the geological record reflects not only evolutionary but also taphonomic factors. The role of the latter is particularly emphasized by an extreme impoverishment of fossil microbiotas in deposits accumulated 2.5–2.0 Ga ago. To some extent, this lacuna in the paleontological record is bridged by stromatolites.

STROMATOLITES

Stromatolites were the first group of paleontologic remains, whose evolutionary peculiarities established with a relatively high stratigraphic resolution were considered when explaining the Jatulian C-isotope anomaly (Semikhatov and Raaben, 1994, 1996; Melezhik *et al.*, 1997b, 1997c).[2] This consideration was based, first of all, on the chronological coincidence of the anomaly with the peak of the stromatolite diversity on the regional (Baltic shield) or global scales, and second, on a conclusion that precisely this time-interval was marked by a maximum in the stromatolite abundance. The latter conclusion, in turn, was based either on an assumption of a direct dependence between the stromatolite diversity and abundance (Semikhatov and Raaben, 1994, 1996) or on empirical evidence from the Baltic shield (Melezhik *et al.*, 1997c). As a result, it was assumed that expansion of shallow-water benthic cyanobacterial communities responsible for the peak diversity and abundance of stromatolites and coupled with explosion of phytoplankton followed by enhanced C_{org} burial in deep-water settings were combined driving forces for emergence of the Jatulian $\delta^{13}C$ anomaly. Transition from abnormally high to low $\delta^{13}C_{carb}$ values that occurred in the post-Jatulian time (about 2.0 Ga ago) was related to stromatolite reduction. In opinion of some researchers, the latter reflected a collapse of benthic microbiotas (Melezhik *et al.*, 1997c), whereas others believe that only slight reduction in distribution areas of the stromatolite ecosystems occurred in the considered period (Semikhatov and Raaben, 1996).

When estimating the validity of these assumptions, the following points should be kept in mind. Melezhik *et al.* (1997c) did not take into consideration that a sharp decline in the stromatolite abundance and diversity 2.0 Ga ago is recorded only in the Baltic shield and northern China platform regions, whereas in Australia

[2] Earlier reconstructions of the abundance and/or diversity dynamics of Proterozoic stromatolites (Awramik, 1971, 1992a; Walter and Heys, 1985) were performed with the low stratigraphic resolution, which hindered their application for the above-mentioned purpose.

and North America, this period was marked by an increase in the above-mentioned parameters. Semikhatov and Raaben (1994, 1996) who leaned upon global data, analyzed only those stromatolites whose generic and species affinity was without question and, thus, many microbialites were inevitably left out of consideration. Finally, both concepts did not consider the stromatolite nature although conclusions on the abiogenic origin of some of them is recently gaining in popularity (Hofmann, 1969; Grotzinger, 1989, 1990; Lowe, 1994; Knoll and Semikhatov, 1998). It should be added that the dynamics of the Archean stromatolite development were never considered. In other words, there are no available data to estimate changes in the global stromatolite abundance in the time interval enclosing the Jatulian anomaly of the organic carbon isotope composition.

Below, we have made an attempt to fill this gap in knowledge, analyzing only the abundance parameter in terms of the objective statistics, namely the number of stromatolite-bearing formations in every unit of the selected chronological scale. When estimating this parameter, we discarded corrections that were used by our forerunners to correct the raw statistical data on Proterozic stromatolites (Walter and Heys, 1985; Melezhik *et al.*, 1997c). Results of the calculation are shown in two histograms, one presenting data on the Archean and another on the Paleoproterozoic stromatolites. The usage of separate histograms is explained by the fact that most of Paleoproterozoic stromatolite sequences prevail in the thickness and extension over similar Archean sequences by one–two orders of magnitude and more. Therefore, these sequences should be considered as being of a different statistical significance when estimating the stromatolite abundance.

Archean

Archean stromatolites were repeatedly considered as resulting from the metabolic activity of oldest microbial communities, although nowadays some researchers call into question the contribution of biotic factors to the formation of some of these structures.

Paleoarchean. Stromatolites of a definitely Paleoarchean age are recorded in three sequences: at the base (the Towers Formation, 3556 ± 32 Ma) and in the upper third (the Strelly Pool Formation, (3471 ± 5)–(3458 ± 1.9) Ma; Thorpe *et al.*, 1992) of the Warrawoona Group of West Australia (Lowe, 1980, 1983; Walter *et al.*, 1980; Walter, 1983) and also in the Onverwacht Group of South Africa (3.5–3.3 Ga; Byerly *et al.*, 1986; Lowie, 1994).[3] These stromatolites are siliceous in composition and compose thin (20–80 cm) beds of small-scale extension (usually less than 1 km), which occur among siliceous beds alternating with siliciclastic and/or carbonate rocks and, in total, form a very small part of the mentioned volcanogenic rock groups in greenstone belts. Buildups are represented by stratiform, nodular, and strato-columnar forms; the latter were first erroneously classed with conophytons (Lowe, 1980). Stromatolites encountered in the Rhodesian craton in the Mushandike area (Zimbabwe) and correlated with the Sebakwian Group that is intruded by granitoids about 3.5 Ga old (Orpen and Wilson, 1981; Abel *et al.*, 1985b) are probably also the Paleoarchean in age. Nonetheless, their Mesoarchean age is not inconceivable.

Because of their morphology, Paleoarchean stromatolites were considered for a long time as representing organo-sedimentary structures (Schopf *et al.*, 1971; Walter, 1983; Byerly *et al.*, 1986); recently, however, an opinion appeared that some of them are abiogenic in origin (Buick and Dunlop, 1990; Lowe, 1994). Nevertheless, the microbialitic nature of stratiform structures from the Onverwacht and Warrawoona groups enclosing signs of microbial mats is doubtless (Walter, 1983; Awramik, 1991; Walsh, 1992; Knoll, 1996). The C-isotope data, though limited (see below), support this conclusion.

Mesoarchean. Stromatolites of this age are reported from South Africa, India, Canada, the Kola Peninsula, and Australia. Oldest of them are recorded in the Insuzi Group of the Kaapvaal craton of South Africa. The U-Pb and Rb-Sr age of volcanics from the middle part of the group is 3090 ± 90 and (3150 ± 150)–(3048 ± 50) Ma, respectively (Mason and Von Brunn, 1977; Walter, 1983; Cahen *et al.*, 1984). These stromatolites are confined to beds of silicified dolomites (thickness 1–30 m), which are developed in the small area amid shallow-water siliciclastic metasediments prevailing in the group and less common metavolcanics. Stromatolites are represented by small nodular, strato-columnar, and stratiform buildups. Some of them show the preserved relics of probable filamentous microorganisms (Walter, 1983). In India, Mesoarchean stromatolites are detected in the Singhboom Group, ranging from 3.2 to 2.95 Ga in age (Moitra and Raha, 1991). There, beds of silicified dolomites enclosing sufficiently large columnar structures occur among iron quartzites, jaspers, phillites, and volcanics.

Three stromatolite localities are recorded in the Mesoarchean of the Canadian shield. In the Uchi greenstone belt located in its central part, stromatolites occur in a 350-m-thick unit of silicified marbles, rare BIF, and schists, which locally occur in the upper third of a thick (6.5 km) metavolcanic sequence. The U-Pb age of this sequence is younger than 2940 and older than 2925 Ma. The sequence yields small biostromes of stratiform buildups and scattered nodular and, sometimes, strato-columnar stromatolites, at least part of which was formed in relatively deep water environments (Hofmann *et al.*, 1985). Stromatolites of the adjacent Uchi-Confederation greenstone belt represent stratiform, small nodular, and miniature columnar structures. They

[3] Initially, these stromatolites were referred to the overlying Fig Tree Group, which is also older than 3.3 Ga (Byerly *et al.*, 1986).

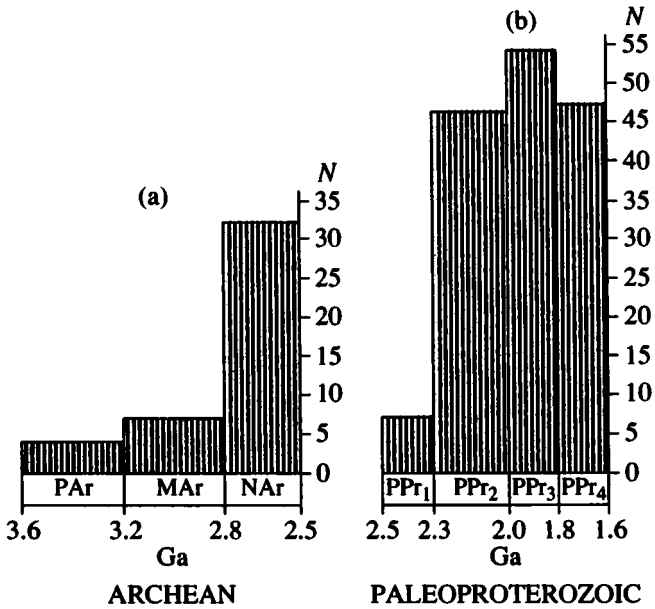

Fig. 3. Histogram demonstrating changes in abundance of stromatolite-bearing lithostratigraphic units (formations) in the Archean (a) and Paleoproterozoic (b); (*N*) number of formations with stromatolites; letter indices designate chronometric subdivisions: (PAr) Paleoarchean, (MAr) Mesoarchean, (Nar) Neoarchean; (PPr_1–PPr_4) four Paleoproterozoic subdivisions.

are confined to the thin horizon of siliceous–carbonate rocks occurring at the top of thick succession of submarine and subaerial volcanics. The U-Pb zircon age of this horizon ranges between 2830 ± 6 and 2793 ± 8 Ma (Hofmann *et al.*, 1985).

In the southern part of the Canadian shield, Mesoarchean stromatolites form large (to 500 m thick and more than 12 km across) fringing reef that is located within the shallow-water carbonate platform composed of rocks of the lower Steep Rock Group (Grotzinger, 1989). There, small columnar branching and nodular as well as large dome-like structures are recorded. These deposits are likely correlative to a 2990 ± 1-Ma-old unit; the age of underlying gneisses is estimated to be 3.0 Ga and that of postdating intrusions, 2.66 Ga (Nisbet and Wilks, 1988). Finally, the Mesoarchean in age are nodular stromatolites of the granulite belt in the Kola Peninsula (Ivliev, 1971) and stratiform structures from the Gundokerta Formation of West Australia (2.8–2.9 Ga) determined as *Thyssagetes* sp. (Grey, 1981; Grey, oral communication). Sometimes, stromatolites from the Sandur schist belt of India are also referred to the Mesoarchean (Murthy and Reddy, 1984), but recent data show their Neoarchean age (see below).

Thus, Mesoarchean stromatolites differ from those in the Paleoarchean sequences in the following features: they are wider spread, occur also beyond greenstone belts, compose oldest sufficiently thick bodies, some of the reefal type, and are more variable in morphology.

Neoarchean. In the Neoarchean, the amount of stromatolite-bearing deposits sharply increased (Fig. 3a), although most of them were confined, as before, to the greenstone belts. Stromatolite carbonate and siliceous rocks developed within these belts represent only insignificant shares in predominantly volcanogenic successions, and their bodies are usually no more than several meters thick and several kilometers across; in one case (Hofmann and Masson, 1994), they occur as allochthonous blocks in metaturbidites.

Namely greenstone belts host Neoarchean stromatolites in the Canadian shield, where they are recorded in the Joutel Volcanic Complex of the Abitibi Belt (2730–2720 Ma; Hofmann and Masson, 1994) and also in the Michipicoten (Helen Formation; 2749–2702 Ma; Hofmann *et al.*, 1991), Yellowknife (2650–2600 Ma; Henderson, 1975; Walter, 1983), and Kaminak (about 2700 Ma; Patterson, 1986) groups; they are also mentioned from three other localities in other belts (Hofmann *et al.*, 1991). Similar structures enclose stromatolites of the Gindalbie Formation in western Australia (2.8–2.7 Ga; Grey, 1981) and those of the Belingwe (Manjeri and Cheshire formations; Bickle *et al.*, 1975; Martin *et al.*, 1980; Abel *et al.*, 1985a) and Bulawayan groups in South Africa, where they range in age between 2.7 and 2.8 Ga (Macgregor, 1941; Cloud and Semikhatov, 1969; Schopf *et al.*, 1971; Walter, 1983). All these stromatolites were formed in a wide range of settings, from relatively deep water to coastal shallow-water, and are represented by nodular, stratiform (including *Thyssagetes*-form buildups) and less common strato-columnar and columnar branching structures. Dark thin (to 5 μm) filaments similar to cyanobacteria remnants *Phormidium* were described from the *Thyssagetes*-like buildups of the Gindalbie Formation (Grey, 1981). Columnar buildups from the Bulawayan Group contain kerogen filaments 2–7 μm thick and oriented perpendicularly or at an angle to bedding; they may represent either relicts of filamentous microbes or a result of kerogen redistribution along the spiny carbonate crystals (Walter, 1983).

Neoarchean stromatolites of South India are mainly developed in the so-called young schist belts in the western part of the Dharwar craton, which were formed over the Mesoarchean (older than 2.9 Ga) crystalline basement (Pencat *et al.*, 1995; Chadwick *et al.*, 1997). Beds of stromatolithic, usually silicified dolomites are up to 70 m thick and united sometimes into thicker members, but generally they are subordinate members in the volcanogenic–sedimentary and IBF sequences of the Chitradurga Group. Volcanics from the lower part of the latter are dated back to 2848 ± 70 and 2747 ± 15 Ma (Sm-Nd isochrone) and those from its middle portion, to 2614 ± 8 Ma (U-Pb, zircon), whereas the U-Pb age of granitoids, which intrude the entire group, is 2605 ± 18 Ma (Nutman *et al.*, 1996; Chadwick *et al.*,

1997). Stromatolites of the Chitradurga Group recorded in the correlative Degiri, Vanivilas, and Joldal formations within three schist belts are represented by columnar, strato-columnar, stratiform, and nodular forms. In morphology, they are more variable in relatively deep water deposits and show the diversity decrease in shallow-water sediments (Baral, 1986; Venkatachala *et al.*, 1989; Vasudev *et al.*, 1989; Shrinavasan *et al.*, 1990). In addition, Neoarchean stromatolites of India include those developed within schists of the Sandur Belt in the eastern part of the Dharwar craton (Murthy and Reddy, 1984); their age ranges from 2750 to 2650 Ma (Nutman *et al.*, 1996; Chadwick *et al.*, 1997).

The Neoarchean intermontane basins are characterized by stromatolites from the Ventersdorp Supergroup of South Africa (2643 ± 80–2709 ± 4 Ma; Armstrong *et al.*, 1991) and Fortescue Group of West Australia (2756 ± 8–2684 ± 6 Ma; Arndt *et al.*, 1991), both representing thick terrigenous–volcanogenic successions accumulated in freshwater or coastal-marine settings with differentiated topography. The Ventersdorp Supergroup (Klippan and Bothaville formations) enclose stratiform, strato-columnar, nodular, and rare small columnar buildups, whereas the Fortescue Group (Mount Jope volcanics and Tumbiana Formation) contains microstromatites, nodular and stratiform buildups (Cloud and Semikhatov, 1969; Walter, 1972, 1983). These stromatolites form isolated bioherms or biostromes to 2–3 m thick and to 300–400 m across. Relics of microbial filaments are reported from the stratiform buildups of the Tumbiana Formation (Walter, 1972).

Stromatolites from the Whalen Group of Michigan and Transvaal Supergroup of South Africa are of particular type among others considered here. The Whalen Group that experienced a regional metamorphism 2.6 Ga ago comprises two carbonate formations 900–1500 and 60–900 m thick and a thick terrigenous–volcanogenic sequence separating these two units. The carbonate formations accumulated in shallow-shelf environments yield abundant stromatolite domes composed of stratiform and strato-columnar structures (Hofmann and Snyder, 1985). Stromatolites of the Transvaal Supergroup are confined to thick (500–1700 m) carbonate sequences, which are distinguished in different parts of the Caapvaal craton as the Campbellrand and Malmani subgroups. These subgroups, containing only rare interbeds of siliciclastic and tuffaceous rocks, were deposited within a vast (more than 900 × 350 km in the modern structure) carbonate platform, which evolved, according to U-Pb zircon age determinations, 2550–2520 Ma ago, although the oldest carbonate rocks were formed there approximately 2590 Ma ago (Sumner and Bowring, 1996; Altermann, 1996). Stromatolite dolomites take part or prevail in eleven of twelve formations that are distinguished within the above-mentioned subgroups. In their eastern shallow-water sequences, most common are stratiform buildups, whereas microstromatites, columnar and, particularly, nodular varieties occur less frequently. In western sections accumulated in deeper settings, the share of columnar forms increases (Truswell and Eriksson, 1972, 1973, 1975; Betrand-Sarfati and Eriksson, 1977). In abundance, the Transvaal stromatolitic dolomites are highly competitive with the most prominent examples of stromatolite-bearing Paleoproterozoic sequences and, in distribution range, they are amid unique Lower Precambrian objects.

Thus, there are 32 stromatolite-bearing formations with all main stromatolite morphotypes, except conophytons, recorded to date in the Neoarchean. Some of buildups developed there preserve structures similar to remnants of filamentous microorganisms, including cyanobacteria. In addition, it should be noted that in light of actualist data, it is reasonable to consider an accretion of the *Thyssagetes*-like buildups that appeared at the end of the Mesoarchean as resulting from the metabolic activity of phototrophic and phototaxic filamentous organisms (Grey, 1981; Hofmann and Masson, 1994). In other words, Neoarchean stromatolites show the further development of the tendency that appeared in the Mesoarchean time: the lateral expansion to new biotopes, grows of taxonomic diversity of buildups, and increasing number of their localities (Fig. 3a). These trends can hardly be related to the taphonomic factor. Judging from all available data, they reflect general regularities in evolution of early ecosystems on the Earth.

Paleoproterozoic

Data on spatial–chronological distribution of formal genera (groups) and species (forms) of Paleoproterozoic stromatolites from Eurasia, Africa, Australia, and North America, as well as on the isotope age of enclosing lithostratigraphic units, were recently summarized by Semikhatov and Raaben (1994, 1996). The results of this analysis are directly used in this work, but because of limited space, data on age of these units as well as references to many original articles listed in the abovementioned publications are not repeated here. At the same time, information on the distribution and age of the formations and groups, which contain stromatolites of unknown taxonomy, is considered below. In the context of this paper, they are as important as lithostratigraphic units with well-defined stromatolite taxa.

The first subdivision of the Paleoproterozoic (2.5–2.3 Ga) is very poor in stromatolites (Fig. 3b). They are recorded only in seven formations, which represent subordinate members of thick volcanogenic–siliciclastic successions: the Hamersley and Turee Creek groups (2.49–2.34 Ga; Arndt *et al.*, 1991; Pidgeon and Horwitz, 1991) of western Australia; The Lower Huronian (2.45–2.3 Ga; Morey, 1996) of southern Canada; the lower subgroup (2.5–2.36 Ga; Zhu and Chen, 1992) of the Huto Group of North China (for review and bibliography see Semikhatov and Raaben, 1994, 1996); and also the Lapponian and Sumian of the Baltic shield (2.50–2.42 Ga; Melezhik *et al.*, 1997c). All these formations accumulated in rift structures are characterized

by a limited lateral distribution, consist predominantly of stromatolite-free rocks, and usually have an insignificant thickness amounting to dozens of meters. Stromatolites from these formations are represented by all morphotypes recorded in the Proterozoic, including the oldest conophytons.

In *the second subdivision* of the Paleoproterozoic (2.3–2.0 Ga), a number of stromatolite-bearing formations and groups sharply increases mainly in the Baltic shield, North China platform, and North America. In first of these region, there are 17 units of this kind, 14 of which are referred to the Jatulian, and three to the basal Ludikovian strata closely connected with the Upper Jatulian deposits (Melezhik *et al.*, 1997c). At present, the age of the Jatulian is estimated as ranging from 2.33 to 2.06 Ga, and that of the Ludikovian, from 2.06 to 1.9 Ga (op. cit.). In the available publications on the coeval deposits of the North China platform, 13 stromatolite-bearing formations are described (Zhu *et al.*, 1987; Zhu and Chen, 1992; Semikhatov and Raaben, 1994; and references therein). Seven of them are reported to compose the entire middle subgroup (2.3–2.05 Ga) of the Huto Group in the Shangxi Province and others belong to correlative Zhongtiao and Gantaohe groups (each hosting two formations) in the adjacent regions, as well as to the Langhe Group of the Lulang Mts and Liaohe Group of Eastern Liaoning Province.[4] In addition, the stromatolite-bearing deposits of Eurasia include the Butun Formation of the Udokan Group in East Siberia (the age slightly older than 2180 ± 50 Ma; Berezhnaya *et al.*, 1988) and the phosphate-bearing limestone of the Aravalli Supergroup of Hindustan (age is bracketed between 2.3 and 2.0 Ga; Semikhatov and Raaben, 1994).

In North America, stromatolites as old as 2.3–2.0 Ga are most widespread in the Labrador trough and southern provinces of the Canadian shield. They compose extended beds and members in the Portage and Alder formations of the Knob Lake Group in the western zone of the Labrador trough and form reefal bodies in the overlying Denault and Abner formations of the same group; they are also mentioned in the Dunphy Formation developed in the eastern part of the trough and correlative with the Portage Formation. First, two formations are sandwiched between volcanogenic sequences with the U-Pb zircon age of 2169 ± 7 and 2142 ± 4 Ma, whereas other two conformably rest upon the highest of these sequences and are unconformably overlain by deposits with the U-Pb age of 1880 ± 6 Ma (Hofmann, 1981; Wardle and Bailey, 1981; Hofmann and Grotzinger, 1988; Hofmann, 1989; Melezhik *et al.*, 1997a). In the Southern Province, the deposits in question compose mutually correlative Trout Lake, Randvill, Kona, and Bad River formations of the Mille Lake and Chocolay groups, whose age ranges from 2200 to 2110 ± 52 Ma (Hofmann, 1969, 1981; Sims *et al.*, 1981; Morey, 1996).

In addition, stromatolites 2.3 to 2.0 Ga old compose in North America a series of beds and members in the Nastapoka Group and in the Lower and Upper Albanel formations in the southeastern Canadian shield. Beyond this structure, they form significant bodies in the Nash Fork Formation of the central part of the Rocky Mts (for references see Semikhatov and Raaben, 1996; Melezhik *et al.*, 1997a). The Nash Fork Formation is younger than analogues of the Upper Huronian tillites (2.3–2.19 Ga; Morey, 1996) and older than granitoids dated by the Rb-Sr method back to 2.0–2.1 Ga. Rocks of the Nastapoka Group contain diagenetic apatite with the U-Pb age of 2025 ± 25 Ma and volcanics dated by the Pb-Pb method back to 1960 ± 80 Ma (Chandler and Parrish, 1989). Available radiometric data constrain the age of the Lower and Upper Albanel formations within a wide range (from 2.5 to 1.7 Ga), but the transition from relatively high positive $\delta^{13}C$ values to "normal marine" ones observed in the section of these deposits is similar to that documented in other sequences, including well-dated carbonate-bearing successions of the eastern Canadian shield and can be used for their chemostratigraphic correlation (for details see Melezhik *et al.*, 1997a). Beyond Eurasia and North America, stromatolite successions with the definite age of 2.3–2.0 Ga are known only in Equatorial Africa, where they are represented by the Francevillian Formation of Gabon, whose age is close to 2.06 Ga (Sarfati, 1992). Stromatolites of the second subdivision of the Paleoproterozoic are most commonly composed of columnar branching forms and sometimes of microstromatites, whereas stratiform and nodular forms and particularly conophytons are sufficiently rare.

Thus, a number of stromatolite-bearing lithostratigraphic units recorded in the second subdivision of the Paleoproterozoic increases in comparison with its first subdivision (at least 46 versus 7, respectively); simultaneously distribution areas and thicknesses of these units also strongly increase. For instance, the average thickness of carbonate rocks is 6 m in the Sumian of the Baltic shield and 69 to 142 m in the Lower and Upper Jatulian, respectively (Melezhik *et al.*, 1997c), whereas that of stromatolite-bearing formations of the middle Huto Group is estimated to be hundreds of meters (Zhu *et al.*, 1987). All these changes reflect an extensive development of intracontinental rifts occupied by shallow-water basins, the first wide marine transgression onto the epi-Archean stable massifs, the development of carbonate platforms, transition from the glacial to warm climate, and evaporite accumulation (Semikhatov and Raaben, 1994, 1996; Akhmedov *et al.*, 1996; Melezhik *et al.*, 1997c; and references therein).

The third subdivision of the Paleoproterozoic (2.0–1.8 Ga) was characterized, similarly to the second one, by a wide stromatolite development, but their distribu-

[4] It is interesting to note that dolomites in the middle of the Huto Group show no enrichment in the ^{13}C isotope ($\delta^{13}C$ ranges from –3.7 to +2.0‰; Hua and Yongsheng, 1997) as opposed to their analogues in the Baltic and Canadian shields.

tion areas moved from Eurasia to North America and Australia.

In North America, they are widespread in the Canadian shield, mainly in its northwestern part. There, stromatolite dolomites and less frequent limestones compose, entirely or partly, 15 formations, which are enclosed in the Epworth, Goulburn, Snare, Recluse, and Great Slave (super)groups (Hofmann, 1973, 1974, 1988a; Cecile and Campbell, 1978; Campbell and Cecile, 1981; Semikhatov, 1978; Grotzinger, 1986, 1988, 1989; Grotzinger *et al.*, 1987; Jakson, 1988; Hoffman, 1988b; Sami and James, 1994; Semikhatov and Raaben, 1996). The age of these (super)groups estimated using the U-Pb zircon dating of enclosed volcanics and intrusions ranges between 2.0 and 1.85 Ga (Hoffman, 1988b, 1989; Grotzinger, 1988). In addition, a thin member of stromatolitic dolomites occurs in the LaBine Group in the northwestern part of the shield, whose age ranges from 1.92 to 1.87 Ga (Hofmann, 1981; Hildebrand, 1981). The thickness and distribution areas of the aforementioned formations vary over a wide range, although some of them, being several hundreds of meters thick, are developed over vast carbonate platforms and locally enclose stromatolite reefs of variable size range.

In the central part of the Canadian shield, stromatolites of the considered age form considerable bodies, some of the reefal type, in four formation of the Belcher Supergroup, whose age ranges between 1960 ± 80 and 1810 ± 30 Ma (Hoffman, 1988b, 1989). They also occur as thin members and packets in the Sutton Lake and Hurwitz groups that correlate with the Belcher Supergroup (Douglas, 1972; Hofmann, 1981; Ricketts and Donaldson, 1981, 1988). Coeval stromatolite-bearing deposits occurring along the southern margin of the shield in the Southern Province are represented by three thin so-called "algal" members within the Gunflint and Biwabik formations of the Animikie Group and lower part of the Baraga Group correlative to each other (Hofmann, 1969; Morey, 1996). Recent isotopic dates for these deposits are given above in this paper. Judging from scarce Rb-Sr dates and lithostratigraphic correlation, the third subdivision of the Paleoproterozoic also includes mainly detrital and volcanogenic–detrital deposits of the Otish and Ramah groups in the southeastern part of the shield, where they enclose isolated beds of stromatolite dolomites (Hofmann, 1981; Khight and Morgan, 1981; Wardle and Bailey, 1981).

Thus, in the Canadian shield, deposits 2.0–1.8 Ga old contain at least 27 stromatolite-bearing formations of variable thickness and distribution range. Morphology of these buildups is also variable (Hofmann, 1969, 1978; Donaldson, 1976, Semikhatov, 1978). Columnar branching "walled" forms occurring in them served, in due time, as a basis for an erroneous inferences about the presence of characteristic Late Riphean taxa in pre-Riphean deposits.

The Australian (more exactly, North and West Australian) sequences add to the list 19 stromatolite-bearing formations of the Wyloo, Earaheedy, South Alligator, Glengarry, Batchelor, Kimberley, and Crowhurst groups (Walter, 1972; Preiss, 1976; Plumb and Derrick, 1976; Grey, 1984, 1994a, 1994b; Bunting, 1986; Plumb, 1990; Thorne and Seymour, 1991; Gee and Grey, 1993). In most of these formations, stromatolithic carbonate and, less commonly, siliceous rocks play a subordinate role, and only the Duck Creek Dolomite of the Wyloo Group represent a thick substantially stromatolithic succession. The inference that the first three of the listed formations belong to the considered subdivision of the Paleoproterozoic is leaned upon the isotopic–geochronologic data mainly obtained on volcanogenic zircons (Plumb, 1990; Gee and Grey, 1993; review in Semikhatov and Raaben, 1996); for the Earaheedy Group the latter were supplemented by the Pb-Pb dating of carbonate rocks (2010 ± 70 and 1950 ± 70 Ma; Russel *et al.*, 1994). A similar conclusion regarding the age of the Glengarry Group is mainly inferred from the taxonomic analysis of enclosed silicified microfossils and stromatolites and also from regional correlation (Grey, 1994a, 1994b; Semikhatov and Raaben, 1996). The Batchelor Group overlies unconformably the Archean deposits and is conformably overlain by the South Alligator Group with volcanics in the lower part, whose U-Pb zircon age is 1877 ± 11 to 1883 ± 3 Ma. The Kimberley Group is separated by unconformity from underlying volcanics showing the U-Pb age of 1850 ± 5 Ma and together with conformably overlying Crowhurst Group is intruded by dolerites yielding the Rb-Sr age of 1760 ± 25 Ma (Plumb and Derrick, 1976; Page, 1988; Needham *et al.*, 1988; Plumb, 1990). A leading part of stromatolites from the listed groups of Australia belongs to columnar buildups, whereas thyssagetides, conophytons, and microstromatites are subordinate.

Beyond North America and Australia, stromatolite-bearing deposits of the third subdivision of the Paleoproterozoic are sporadically developed in North Eurasia, India, China, and South Africa. In the Baltic shield, they are enclosed in upper parts of two relatively thick carbonate sequences (Pitkyaranta and Rantamaa formations) corresponding to the entire Ludikovian (2.06–1.9 Ga) and also occur, as subordinate members, in the Kondopoga Formation of the Kalevian, whose age ranges between 1.90 and 1.80 Ga (Melezhik *et al.*, 1997c). In Siberia, the considered deposits compose lenses within the continental terrigenous–volcanogenic Akitkan Group (Dol'nik, 1978) with the U-Pb zircon age of (1865 ± 6)–(1823 ± 38) Ma (Semikhatov *et al.*, 1991), whereas in India, they form thin horizons in mostly siliciclastic Dehli Group arbitrary ranging in age between 2.0 and 1.8 Ga (Semikhatov and Raaben, 1994; and references therein). In China, rocks in question occur as rare members in the lower part of the Changcheng "System" in the Yangshang Mts. Most of Chinese researchers estimate the isotopic age the

Changzhougou Formation hosting these deposits as ranging from 2.0 to 1.8 Ga (for review and bibliography see Zhu and Chen, 1992; Semikhatov and Raaben, 1994). Stromatolites from the Kaindy Group of Tien Shan, whose age is apparently close to 1.9–1.85 Ga (Semikhatov *et al.*, 1991), and those from the South African Umkondo Group, which is older than 1780 ± 50 Ma (Cahen *et al.*, 1984), probably belong to the same time interval.

Thus, the third subdivision of the Paleoproterozoic includes at least 54 stromatolite-bearing formations, and this abundance rate is slightly higher that of similar formations in the second subdivision (Fig. 3b). Most of them (85%) occur in North America and Australia, and namely in America, stromatolites of the considered age are known within a vast carbonate platform, where they locally compose reefs of variable extension and thickness and characterize a wide range of environments from intratidal and, probably, supratidal to relatively deep water settings (Hoffman, 1974) marked by distal turbidite accumulation. Consequently, there are no grounds to speak about general decline of stromatolite ecosystems about 2.0 Ga ago (Melezhik *et al.*, 1997c), although in China and the Baltic shield their distribution area was indeed reduced dramatically at that time. The fact that the third subdivision appears to be significantly poorer worldwide in reliably determined stromatolite genera and species as compared with the second one is noteworthy (Semikhatov and Raaben, 1994, 1996). However, the aforementioned data make us consider this impoverishment as representing an artifact resulting from stromatolite decline in those regions, where they are relatively well studied with respect to taxonomy, and from the limited knowledge of their generic and species composition in those areas, were they were widespread 2.0–1.8 Ga ago. Suffice it to say that the second subdivision of the Paleoproterozoic in North Eurasia and China encloses 31 stromatolite-bearing formations and 134 reliably determined species, whereas in North America and Australia, only 53 species were determined in 45 formations of the third subdivision.

The opposite trends of stromatolite abundance in the second half of the Paleoproterozoic within North Eurasia and China, on the one hand, and in North America and Australia, on the other, are explained first of all by tectonic and paleogeographic factors. In the Baltic shield, a system of shallow-water basins was replaced about 2.06 Ga ago by the vast Svecofennian ocean that resulted in a sharp reduction of carbonate accumulation. To the contrary, a significant part of Siberia was drained 1.95–1.9 Ga ago and some areas accumulated terrestrial terrigenous–volcanogenic deposits, whereas in China, molasses of the Lulang orogeny were widespread at that time. In Australia, the period of 2.0–1.8 Ga was marked by the development of a system of epicratonic shallow-water basins, whereas in North America, it was characterized by intensified rifting and formation of carbonate platforms at a certain stage of evolution of riftogenic and conjugated structures (Grotzinger, 1989; Hoffman, 1989; Rozen *et al.*, 1994; Semikhatov and Raaben, 1994, 1996; Melezhik *et al.*, 1997c). Changes in position of plates and terranes relative to paleolatitudes could also contribute to reorganization of areas with the mass development of stromatolites.

The fourth, terminal subdivision of the Paleoproterozoic was marked by a slight reduction of the global stromatolite abundance. The decline was dramatic for the formerly abundant microbialites of North America, whereas in Australia and China, they widened their distribution areas.

In Australia, stromatolithic rocks of youngest Paleoproterozoic strata are concentrated in the north of this continent, in the McArthur basin and Mount Isa Province, where they are enclosed in two successions, which are chronologically close but separated by an unconformity and granitoid intrusions (Plumb and Derrick, 1976; Plumb *et al.*, 1980; Page, 1988; Walter *et al.*, 1988; Plumb, 1990). Volcanics located in the lower and middle horizons of the oldest succession have U-Pb zircon ages of 1790 ± 9 and 1750 ± 7 Ma; granitoid intrusions are dated back to 1735 ± 5 Ma (Plumb *et al.*, 1980; Page and Sun, 1998). Stromatolite-bearing rocks are enclosed here in the approximately coeval Tawallah (Sly Creek Sandstone), Ketherin River (Cottee Formation), Malbon (Mitakoodi Quartzite), Merry Kathleen (Billara Quartzite, Corella Formation), Haslingden (Lochness Formation) groups, and in the Quilalar Formation usually as thin beds and members within preponderant siliciclastic sequences. Exceptions are the Corella, Lochness, and, partly, Quilalar formations, where stromatolithic dolomite beds play a significant role.

In the upper succession, stromatolitic rocks are most widespread in the spacious McArthur platform basin. There, they form a significant share in the McArthur Group (Amelia, Emmerugga, Teena, and Reward dolomites, Mallapunyah, Tooganinie, Barney Creek, Linott, and Yalko formations) and less commonly occur in the Mount Rigg (Dook Creek Formation) and Habgood (Gunpowder Creek, Gwakura, Ulunourwi, and Yarowoy formations) groups corresponding to the lower and middle parts of the McArthur succession. In correlative deposits of the Mount Isa Province, stromatolites are quite common in the McNamara Group (Paradise Creek, Lady Loretta, and Esperanza formations) and sometimes occur in the Surprise Creek Beds (Plumb and Derrick, 1976; Plumb *et al.*, 1980; Walter *et al.*, 1988; Page and Sweet, 1998). The U-Pb age of volcanogenic zircons from the basal and upper parts of this succession in the Mount Isa Province is (1709 ± 3)–(1678 ± 2), and 1595 ± 6 Ma, whereas that for its lower and terminal parts in the McArthur basin ranges from 1690 ± 27 to 1625 ± 2 Ma, respectively (Page and Sweet, 1998; Page and Sun, 1998). Approximately coeval stromatolites are recorded in the Scorpion Group and Capricorn Formation in Western Australia (Grey, 1982; Thorne

and Seymour, 1991). The Capricorn Formation rests uncomfortably upon the Wyloo Group, the middle part of which contains volcanics with the U-Pb age of 1843 ± 2 Ma, and is intruded by granodiorites dated by the Rb-Sr method back to 1680 ± 30 Ma (Thorne and Seymour, 1991). The Scorpion Group is separated by unconformities from both the older Earaheedy Group (slightly older than 1.8 Ga; see above) and the younger Bangemall Group, whose basal layers began to accumulate at about 1.6 Ga ago (Williams, 1990).

Thus, the terminal subdivision of the Australian Paleoproterozoic encloses at least 27 stromatolite-bearing lithostratigraphic units (formations, beds), some of which are developed within extensive carbonate platforms. Judging from available fragmentary descriptions, they are represented by columnar branching, subordinate stratiform (including Thyssagaetacean) buildups, and also rare conophytons and microstromatites.

In North America, stromatolite-bearing deposits 1.8–1.6 Ga old occur in the northwest of the Canadian shield. There, they are enclosed, similarly to Australia, in two regional lithostratigraphic complexes bounded by unconformities (Douglas, 1972; Hofmann, 1981; Kerans *et al.*, 1981; Ramaekers, 1981; Hoffman, 1989). The lower of them is composed of terrestrial volcanogenic–detrital deposits with subordinate thin (0.5–2.0 m) stromatolite bioherms and biostromes of the Et-Then Group and Martin Formation. This rock complex is separated by an unconformity from intrusive and supracrustal rocks 1.9–1.86 Ga old, being intruded by granitoids with the U-Pb age of 1753 ± 4 Ma (Lowerindge *et al.*, 1988; Hoffman, 1989; Ritts and Grotzinger, 1994). According to isotopic–geochronologic data, the upper complex comprises a succession of sandy–clayey and sandy–carbonate rocks of the Hornby Bay Group of the Canadian Arctic coast and, according to lithostratigraphic correlation and regional relationships, the similar successions from adjacent southerly areas of the Canadian shield. In the upper carbonate members of these successions (terminal members of the Hornby Bay and Dubawnt groups and also Perry Bay and Carswell formations), stromatolites form beds to 7–10 m thick. The considered deposits rest unconformably upon the aforementioned granites 1753 ± 4 Ma old and older rocks; volcanics from the top part of the Hornby Bay Group yield the U-Pb age of 1663 ± 8 Ma (Lowerindge *et al.*, 1988; Ritts and Grotzinger, 1994).

In China, the terminal subdivision of the Paleoproterozoic comprises upper members of the Changcheng "System," which include the stromatolite-rich Tuanshanzi and Dahongyu formations in the stratotype of the group, Jixian County. Carbonates from the first of these formations yield the Pb-Pb isochron age of 1.77 Ga, and the topmost part of the second formation encloses volcanics with the U-Pb zircon age of 1621 ± 6 Ma (Lu and Li, 1991), whereas overlying deposits show the Pb-Pb age of 1600–1520 Ma (for review and bibliography see Semikhatov and Raaben, 1994). Stromatolites of two aforementioned formations compose two successive associations, which in the opinion of Chinese researchers are of a great correlative significance and replace each other in the upper layers of the Dahongyu Formation. Beyond Jixian County, representatives of the first association are recorded in several distant areas both in northern and southern China (Gao, 1983, 1992; Liang *et al.*, 1985; Xing *et al.*, 1985; Zhu and Chen, 1992). In the north of the country, they are reported from Xinjiang (five formations subordinate to the Tekesi, Bolohouloshau, Kuximuqike, Beishan, and Baihu groups), Inner Mongolia (the Norgong Formation and the lower part of the Obo Group), and in Shanxi Province (analogues of the Tuanshanzi and Dahongyu formations). In the southern areas, they are indicated in the Hubei (two lower formations of the Shennougjia Group) and Yunnang (the Louxe Formation of the Kungyan Group) provinces. The second association has a wider distribution, though it cannot be used for identification of strata correlative with highest layers of the Changcheng "System," because similar stromatolites occur also in younger deposits. Therefore, deposits enclosing this association are not considered here, although some of them can belong to the terminal subdivision of the Paleoproterozoic.

Thus, the subdivision in question encloses at least 47 stromatolite-bearing formations in total on different continents, which appear to be slightly less abundant than in the previous subdivision (Fig. 3b). Most of these formations accumulated in spacious platform basins, which emerged almost simultaneously in Australia and the Canadian North and slightly earlier appeared in the northern China craton. It is precisely Chinese and Australian sections, which become enriched in stromatolites about 1.8 Ga ago, and this event contributes significantly to the general patterns of subglobal distribution of stromatolites at the end of the Paleoproterozoic. To the contrary, a number of stromatolite-bearing formations in America simultaneously declined in response to reduction of the distribution area of relevant deposits and changes in their composition (transition to the preponderant detrital and volcanogenic–detrital deposits). As for North Eurasia and Africa, stromatolites of the fourth subdivision of the Paleoproterozoic did not show any significant development there because of dominant subaerial settings on continental blocks in the first of the aforementioned superregions and because of the absence of carbonate rocks among coeval deposits of a limited distribution in the second one.

In other words, distribution of the stromatolite ecosystems at the end of the Paleoproterozoic was controlled, similarly to earlier periods, by long-lasting tectonic and paleogeographic factors (Semikhatov and Raaben, 1994, 1996). The cited authors related to their influence also a decline in the taxonomic diversity of Late Paleoproterozoic stromatolites. However, the above-mentioned data suggest that such decline should be substantially or entirely considered as apparent and related to a poor knowledge of taxonomy of stromato-

lites enclosed in many stromatolite-rich deposits. For instance, 27 stromatolite-bearing lithostratigraphic units of the considered age (about 57% of their total amount) recorded in Australia yield only 10 reliably determined stromatolite species, whereas for China, corresponding values are 14 and 36.

Thus, the histogram showing the occurrence rate of Paleoproterozoic stromatolite-bearing formations that is considered, at a first glance, as reflecting the stromatolite abundance, is monomodal and asymmetric. It shows the very sharp increase of this parameter in passing from the first subdivision to the second one, another slight increase in the third subdivision, and insignificant decline in the fourth one (Fig. 3b).

DISCUSSION AND CONCLUSION

The performed analysis of pre-Riphean microbiotas shows that the representative paleontologic record appeared only about 2.0 Ga ago (Fig. 1). Nonetheless, fragmentary paleontologic data allows an assumption that cyanobacteria existed already in the Neoarchean (2.52–2.55 Ga and, probably, 2.7 Ga ago) and, in opinion of some researchers, they occurred in the Paleoarchean, about 3.5 Ga ago as well (i.e., Awramik, 1991, 1992b; Schopf and Klein, 1992; Schidlowski, 1983). This opinion is based on interpretation of the nature of oldest microfossils, on extrapolation of all features of Proterozoic stromatolite-forming microbiotas, to the most ancient stromatolites and/or on evaluation of C-isotope record. However, the validity of such extrapolation seems not undeniable, and biological interpretation of Paleoarchean microfossils may be ambiguous. Therefore, it would be more safe to say that the presence of cyanobacteria amid first stromatolite-forming organisms is probable but not proved (Knoll, 1979; 1996; Schidlowski *et al.*, 1983; Walter, 1983; Knoll and Canfield, 1998). Nonetheless, the available C-isotope data suggest that autotrophic organisms in the Paleoarchean were capable of fixing CO_2 and point to the intense development in the Neoarchean of both oxygenic photosynthetic and also methanogenic and methylotrophic bacteria, which increased a degree of the carbon isotope fractionation in the course of transformation of organic compounds (Buick, 1992; Strauss *et al.*, 1992; Schidlowski, 1993; Hayes, 1994; Des Marais *et al.*, 1997a, 1997b; Knoll and Canfield, 1998). Consequently, one can confidently state that cyanobacteria and, the more so, heterotrophic organisms existed well before the Jatulian anomaly, although their indisputable remnants are recorded only in the post-Jatulian deposits. As for the first eukaryotic organisms, which are thought to be of prime significance for reconstruction of Paleoproterozoic evolution of the atmosphere, they appeared in the geological record about 1900 Ma rather than 2100 Ma ago as is usually accepted (see above), i.e., 150 m.y. after the anomaly ceased to exist. The anomaly disappearance was followed by origination of first diverse microbial communities, the oldest of which are dated back to 2.0–1.9 Ga ago (Fig. 1).

Thus, the available data evidence that the Jatulian anomaly was not related to evolutionary innovations of biota. At the same time, the reconstructed dynamics of pre-Riphean stromatolite distribution allows a definite conclusion that *quantitative* changes in biota represented one of the main factors responsible for the anomaly emergence.

As noted above, the Archean and, particularly, Neoarchean were marked by the steadily growing abundance of stromatolite-bearing sequences, which increased in thickness within a series of paleotectonic and facies settings. However, the stromatolite abundance even in the Neoarchean deposits is generally lower than in the Proterozoic sequences and, thus, corresponding histograms displaying changes in the abundance of stromatolite-bearing formations (Figs. 3a, 3b) reflect the different-scale events.

Nonetheless, a sharp decline in the abundance of such formations at the beginning of the Paleoproterozoic, as compared with the Neoarchean, reflects a real and strong reduction of stromatolite settings 2.5–2.3 Ga ago. It is emphasized by the fact that some Neoarchean stromatolite formations are characterized by a significant extension and thickness, whereas 2.5–2.3-Ga-old deposits comprise only rare and small stromatolite bodies. True enough, the sharp abundance contrast, well seen in histograms, will be less if one appreciates that the Neoarchean lasted one and half times longer than the first subdivision. However, the sharp decline in the global stromatolite abundance across the Neoarchean–Paleoproterozoic transition and the lowest, for the entire Proterozoic, value of this parameter 2.5–2.3 Ga ago remain undeniable.

Abiotic factors, which governed such a drastic stromatolite reduction at the very beginning of the Paleoproterozoic, are obvious. The leading role among them belonged to the severe climate of the Huronian Glacioera (Chumakov, 1984; Ojakangas, 1988, Akhmedov *et al.*, 1996), general low sea-level stand, and preponderance of volcanogenic–terrigenous sediments in those not numerous and small, partly freshwater basins of the rift type, which existed at that time (Semikhatov and Raaben, 1994, 1996; Rosen *et al.*, 1994; Melezhik and Fallick, 1996; Melezhik *et al.*, 1997c). Carbonates that accumulated in a small proportion in these basins usually show "normal" $\delta^{13}C$ values ranging between –4 and 0‰ (Karhu and Holland, 1996; Melezhik *et al.*, 1997a, 1997c) being only sometimes slightly enriched in ^{13}C (Bekker *et al.*, 1998).

The sharp, almost seven-fold increase in the abundance of stromatolite-bearing units that occurred during the second subdivision of the Paleoproterozoic was accompanied by a significant growth in their thickness, lateral extension, and proportion in the total sediment accumulation. As a result, a unique increase in the stromatolite abundance 2.3–2.0 Ga ago has no analogues in

the preceding or subsequent geological history. Precisely since that time, stromatolites became dominant members of Proterozoic carbonate deposits, and cyanobacterial communities responsible for their formation acquired a role of an important regulator of the carbon cycle in the biosphere.

Such succession of events was caused by a fortunate combination of several abiotic factors (Semikhatov and Raaben, 1994, 1996; Akhmedov *et al.*, 1996; Melezhik *et al.*, 1997c; and references therein) with the following ones being most important: significant sea-level rise and related sea transgression onto the epi-Archean stable massifs; intensification of rifting in some areas that favored the growth of basin dimensions; termination of the Huronian Glacioera and transition from the cold to warm biosphere, with relevant oceanographic changes (Chumakov, 1995); and intense evaporite accumulation. It should be noted that the role of sea-level rise was likely not limited by an expansion of shallow-water basins, the favorable biotopes of cyanobacterial communities. Recolonization of these biotopes in the course of transgressions was usually accompanied by transformations in the structure of communities themselves and by significant changes in the stromatolite record (Gebelein, 1974).

An important regulating role in dynamics of this record is often ascribed to secular changes in the sea water composition, and first to the degree of water saturation with Ca and Mg carbonates (Grotzinger, 1990; Semikhatov and Raaben, 1996; Knoll and Semikhatov, 1998; and references therein). In our case, however, this factor probably did not play a significant role. An example of the Transvaal Supergroup convinces that favorable physicochemical (and biological) prerequisites of intense stromatolite formation appeared as early as in the terminal Archean, but they were completely realized only after additional influence of other larger-scale factors (see above) favorable for the extensive development of shallow-water carbonate deposits with corresponding stromatolite formations 2.3–2.0 Ga ago. It is logical to assume that this expansion of benthic cyanobacterial stromatolite ecosystems was also accompanied by an increase in biomass of planktonic photosynthetic organisms responsible for changes in the C-isotope balance.

The conclusion on the cyanobacterial expansion and its age is highly consistent with the enhanced oxygenation rate of the atmosphere and upper parts of the ocean of the early Earth, i.e., with the dramatic increase of free O_2 content in the atmosphere 2.22–2.06 Ga ago from approximately 1 to ≥15% of its modern value (Holland, 1994; Karhu and Holland, 1996).[5] After the classic works by P. Cloud, the above oxygenation event is thought to be related to two opposite processes: (a) the enhanced O_2 flux resulting from the productivity increase of cyanobacterial communities and/or the enhanced rate of the organic matter burial; and (b) the reduced flux of volcanic gases, Fe^{2+}, and other redox-sensitive compounds into outer shells of the Earth and the exhaustion of their reserves in the atmosphere and hydrosphere as a result of oxidation; this is very well exemplified by the avalanche accumulation of banded iron formations (BIF) at the beginning of the Paleoproterozoic (Cloud, 1972, 1974; Knoll, 1979; Schidlowski, 1984; Des Marais *et al.*, 1992b; Kasting, 1993; Melezhik and Fallick, 1996; Des Marais *et al.*, 1997a, 1997b; Knoll and Canfield, 1998; and others). The above data emphasize the role of the increased abundance of cyanobacterial communities in this process.

The chronological coincidence of the global cyanobacterial expansion with the beginning of the Jatulian $\delta^{13}C$ anomaly allows the causal–consequential relation between these events to be formulated with a high degree of confidence. Earlier, such a conclusion was based on either the regional data or the assumption that there is an indispensable direct correlation between the stromatolite diversity and abundance (Semikhatov and Raaben, 1994, 1996; Melezhik and Fallick, 1996; Melezhik *et al.*, 1997b, 1997c). However, under the modern state of knowledge of microbialites, such a correlation is not characteristic of all Paleoproterozoic subdivisions (see above). As for the stromatolite diversity proper, it could influence the biogeochemical cycle of carbon only if stromatolite taxa are correlated with the photosynthetic activity of microbial communities controlling their formation. However, as is known, the available system of the Precambrian stromatolites allows us to define only form taxa based on a certain combination of features, the functional role of which is unclear, whereas some are known to be abiogenic in origin. Therefore, we should admit that changes in the C-isotope composition cannot be related to dynamics of stromatolite taxonomic diversity.[6] The changes in their global abundance, which reflect variations in distribution of cyanobacterial benthic communities and, correspondingly, their total productivity, is a different matter.

In this connection, it should be recalled that the change in balance of buried organic and carbonate carbon in favor of the first one because of the growth of its absolute or relative content is considered to be the main or one of the main factors responsible for the positive $\delta^{13}C$ anomalies, whereas the enhanced rate of C_{org} burial is thought to be related to tectonic factors, such as orogeny, active rifting, and formation of supercontinents, which controlled the high denudation and sedimentation rates (Derry *et al.*, 1992; Karhu, 1993; Des Marais, 1994, 1997a, 1997b; Karhu and Holland, 1996; Melezhik *et al.*, 1997a, 1997b, 1997c; Knoll and Canfield, 1998; and references therein). When applying this

[5] A different point of view on the change in the O_2 content in the early Earth's atmosphere is presented in (Ohmoto, 1996) and its criticism, in (Holland and Rye, 1997).

[6] M.E. Raaben holds to another viewpoint that it is impossible to estimate to what extent the degree of carbon isotopic discrimination could be related to the stromatolite diversity).

model to the Jatulian anomaly, the following should be kept in mind.

(1) Isotopic mass balance considerations indicate that the main role in disturbance of the C_{org}/C_{carb} ratio 2.3–2.06 Ga ago should be related to the increased absolute amount of the isotopically light organic carbon. The point is that this period was marked not only by a significant increase in the $\delta^{13}C_{carb}$ values in sedimentary carbonate rocks but also by a sharp increase in the amount of such rocks (Fig. 3b).

(2) The decreased carbon isotope fractionation between its carbonate and organic reservoirs in the Jatulian time, as compared with that at the beginning of the Paleoproterozoic and particularly in the Neoarchean, does not contradict to the aforementioned conclusion, because it is easily explained by changes in the carbon exogenic cycle related to the appearance of free O_2 in the biosphere and to the relevant reduction of biotopes of anaerobic heterotrophic organisms (Des Marais, 1997a, 1997b; Knoll and Canfield, 1998). Nonetheless, under conditions of high CO_2 content in the atmosphere and hydrosphere (Kasting, 1993; Holland, 1994), photosynthetic organisms could produce the C-isotope fractionation with the maximum intensity precisely at that time. A suppression of this activity under CO_2 deficiency is exemplified by modern cyanobacterial mats formed in hypersaline and hydrothermal environments (Schidlowski *et al.*, 1984; Des Marais *et al.*, 1992a).

(3) Sr-isotope data on the Upper Jatulian (2.1–2.06 Ga) carbonates of Karelia show that the $^{87}Sr/^{86}Sr$ ratio in open sea basins of that time was very low and ranged from 0.70343 to 0.70419 (Gorokhov *et al.*, 1998). Consequently, the mantle influx into the World ocean sharply prevailed over the continental runoff, and this conclusion essentially precludes the high siliciclastic sedimentation rate. In the light of the data on Jatulian rocks, the initial $^{87}Sr/^{86}Sr$ ratios (0.70600) in approximately coeval dolomites of Canada (Miorta and Veizer, 1994) can be related to the semiclosed state of the basin. The influence of this factor on the Sr-isotope composition is clearly shown using the Jatulian as an example (Gorokhov *et al.*, 1998).

(4) The Lower Paleoproterozoic ^{13}C-enriched carbonate rocks are characterized by the low organic matter content, whereas approximately coeval clayey deposits enriched in the latter occur only sporadically, and no clear secular trends in changes of the C_{org} content is established in the Proterozoic sedimentary rocks (Strauss *et al.*, 1992; Karhu, 1993; Des Marais, 1997a; Melezhik *et al.*, 1997a). Two points are very important when interpreting these facts.

First, the estimated degree of postdepositional thermal degradation of Paleoproterozoic kerogen on the basis of evaluation of C/H and $^{12}C/^{13}C$ ratios and the corresponding correction of measured $\delta^{13}C_{org}$ values allowed (reasoning from the isotopic mass balance) a conclusion that a share of buried C_{org} 2.1–1.8 Ga ago was twice as much as in the earliest and terminal Paleoproterozoic (Des Marais *et al.*, 1992b). It is significant that this time interval (2.1–1.8 Ga) broadly comprises both the Jatulian anomaly and the abundance peak of Paleoproterozoic stromatolites.

Second, in the anoxic zone of cyanobacterial mats located below the photosynthesis zone, organic matter produced in the latter is reworked by heterotrophic (sulfate-reducing and methane-producing) bacteria, and this process is accompanied by oversaturation of porous waters with calcium bicarbonate and $CaCO_3$ precipitation simultaneously with organic matter degradation (Canfield and Rainswell, 1991; Knoll and Semikhatov, 1998; and references therein). Naturally, the further C-isotope fractionation and ^{12}C-enriched CH_4 and CO_2 fluxes into the atmosphere occur in the course of this process. Besides, the general patterns of ^{12}C and ^{13}C distribution in mats are complicated because of opposite HCO_3^- fluxes with different $\delta^{13}C$ values during the day (from water into mats) and night time (from mats into water, approximately 80% of the volume accepted by mats in the day time; Des Marais *et al.*, 1992a). The aforementioned processes may significantly influence the ^{13}C isotope content in the anaerobic part of mats. It is important for us that the most probable ^{13}C acceptor is represented by the very early (in fact, almost synsedimentary) carbonate precipitating within mats in parallel with decomposition of the mats' organic substance, and that this carbonate is present in Precambrian stromatolites playing a significant role in lithification of at least some of them (Walter, 1983; Burne and Moore, 1987; Knoll and Semikhatov, 1998). On this note, it is interesting to note that the Jatulian stromatolite facies of Karelia are marked by higher $\delta^{13}C$ values (to +14.2‰) as compared with those in stromatolite-free deposits (Akhmedov *et al.*, 1996).

(5) The question about abiogenic or biogenic origin of Proterozoic microstromatites (*Asperia*-like or microdigitate buildups; Grotzinger, 1990; Raaben, 1998), which is recently debated, directly has nothing to do with the considered problem. These buildups represent common, but subordinate members of many Paleoproterozoic stromatolite deposits (Semikhatov and Raaben, 1996), and only locally become comparable in abundance, with other morphotypes never completely replacing the latter.

All the aforesaid allows us to avoid some difficulties in an interpretation of the Jatulian anomaly (e.g., Yudovich *et al.*, 1990; Tikhomirova and Makarikhin, 1993; Melezhik and Fallick, 1996) and to exclude the enhanced sedimentation rate as a probable cause of the anomaly. At the same time, the data discussed allow this anomaly to be related, with sufficient confidence, to the expansion of cyanobacterial ecosystems that was unique in the Earth's history and to the enhanced C_{org} absolute mass under growing oxygenation of the atmosphere.

In the light of this conclusion, one could expect that the transition from the Jatulian anomaly to the "normal

marine" $\delta^{13}C_{carb}$ values occurred against the background of a sharp decline of the above-mentioned ecosystems and related stromatolites (Melezhik *et al.*, 1997b, 1997c). In fact, this transition proceeded, however, against the background of some increase in the stromatolite abundance (Fig. 3b) and still elevated share of buried organic carbon (Des Marais *et al.*, 1992b; Des Marais, 1997a, 1997b). Both these parameters decreased only in the latest Paleoproterozoic, about 1.8 Ga ago. This occurred after the global-scale orogenic processes 1.92–1.85 Ga ago (Page 1988; Hoffman, 1989; Rozen *et al.*, 1994), which resulted in draining of vast territories, increased continental erosion, and intensified siliciclastic sedimentation, as it is evident from direct geological data and from the $^{87}Sr/^{86}Sr$ ratio increase in seawater at the end of the Paleoproterozoic (Veizer *et al.*, 1992).

A slight reduction of the stromatolite abundance that occurred at that time accords well with the succession of aforementioned abiotic events, but the simultaneous decrease in the buried C_{org} content is inconsistent with these events. As was mentioned, an increase (not decrease) in the C_{org} burial rate is usually related to orogeny and enhanced sedimentation rate (e.g., Derry *et al.*, 1992; Des Marais, 1997a, 1997b; Knoll and Canfield, 1998; and others). Moreover, the listed abiotic events of the second half of the Paleoproterozoic as well as the mass appearance of diverse microbial communities 2.0–1.9 Ga ago and first eukaryots about 1.9 Ga ago—all these biospheric phenomena should be seemingly reflected in the C-isotope record, but they have not been recorded. After the Jatulian anomaly, the isotope composition of carbonate carbon fluctuated for a long time within a very narrow interval around zero, whereas $\delta^{13}C_{org}$ values notably increased, but dispersion of this parameter decreased; they clustered between –25 to –35‰ at the end of the Paleoproterozoic versus –20 to –65‰ in rocks older than 2.1 Ga (Des Marais, 1997a, 1997b). Such behavior of the C-isotope system allowed its stasis at the end of the Paleoproterozoic–beginning of the Riphean to be postulated (Brasier and Lindsay, 1998; Knoll and Canfield, 1998).

The aforesaid suggests that the origination and disappearance of the Jatulian anomaly were controlled by the interaction of different factors, a full range of which is to be yet defined. The following factors can be listed amid obvious causes responsible for the anomaly disappearance: (1) a decreased degree of the carbon isotope fractionation in the course of photosynthesis and further significant reduction of anoxic heterotrophic organisms in response to the decreased CO_2 and increased O_2 content in the atmosphere and surficial part of the hydrosphere that occurred at that time (Kasting, 1993; Holland, 1994); and (2) the appearance of oxic respiration as globally dominant way for utilization and decomposition of organic matter and, probably, the nutritions deficiency (nitrates and phosphates) that commenced in cyanobacterial ecosystems (Des Marais, 1997a, 1997b; Brasier and Lindsay, 1998; Knoll and Canfield, 1998). This deficiency could be related to significant geodynamic events (activated rifting, ocean opening, and shallow sea reduction) and relevant oceanographic reorganizations at the beginning of the second half of the Paleoproterozoic.

The more comprehensive analysis of the post-Jatulian C-isotope and paleontological records along with relevant contradictions revealed in the course of such analysis will be considered in further papers. Here, we should like to emphasize the main conclusion of this work: the unique expansion of cyanobacterial ecosystems reflected in the stromatolite record was the main factor responsible for the Jatulian C_{carb} positive anomaly, the largest one in the Earth's history.

ACKNOWLEDGMENTS

We are sincerely grateful to M.A. Fedonkin for constructive discussion of problems considered in this paper.

The work was supported by the INTAS–RFBR (project 95-05-0928) and Russian Foundation for Basic Research (projects 96-05-64329 and 98-05-64259).

Reviewers M.A. Fedonkin and B.S. Sokolov

REFERENCES

Abel, P.J., McClory, J., Martin, A., and Nisbet, E.G., Archean Stromatolites from the Ngesi Group, Belingwe Greenstone Belt, Zimbabwe; Preservation and Stable Isotopes—Preliminary Results, *Precambrian Res.*, 1985a, vol. 27, no. 4, pp. 357–383.

Abel, P.J., McClory, J., Martin, A., Nisbet, E.G., and Kyzer, T.K., Petrography and Stable Isotope Rations from Archean Stromatolites, Mushandive Formation, Zimbabwe, *Precambrian Res.*, 1985b, vol. 27, no. 4, pp. 385–398.

Akhmedov, A.M., Travin, L.V., and Tikhomirova, M., Glacial and Evaporitization Epochs in the Early Proterozoic and Interregional Correlation, *Regional Geology and Metallogeny*, 1996, no. 5, pp. 84–97.

Altermann, W., Discussion on "Zircon Pb-Evaporation Age Determination of the Oax Tree Formation, Chuniesport Group, Transvaal Sequence: Implication the Transvaal-Griqualand West Basin Correlations," *S. Afr. J. Geol.*, 1996, vol. 99, no. 3, pp. 337–338.

Armstrong, R.A., Compston, W., Retief, E.A., *et al.*, Zircon ion Microprobe Studies Beating on the Age and Evolution of the Witwatersrand Triad, *Precambrian Res.*, 1991, vol. 53, no. 1, pp. 243–266.

Arndt, N.T., Nelson, D.R., Compston, W., and Thorne, A.M., The Age of the Fortescue Group, Hamersly Basin, Western Australia, from Ion Microprobe Zircon-U-Pb Results, *Aust. J. Earth Sci.*, 1991, vol. 38, no. 2, pp. 261–281.

Awramik, S.M., Archean and Proterozoic Stromatolites, in *Calcareous Algae and Stromatolites*, Berlin: Springer, 1991, pp. 289–304.

Awramik, S.M., Precambrian Columnar Stromatolite Diversity: Reflection of Metazoan Appearance, *Science*, 1971, vol. 174, pp. 825–827.

Awramik, S.M., The History and Significance of Stromatolites, in *Early Organic Evolution: Implications for Mineral and Energy Resources*, Berlin: Springer, 1992a, pp. 435–449.

Awramik, S.M., The Oldest Records of Photosynthesis, *Photosynthesis Res.*, 1992b, vol. 33, no. 1, pp. 75–89.

Baral, M.C., Archean Stromatolites from Dodguni Belt of Karnataka Craton, India, *J. Geol. Soc. India*, 1986, vol. 28, no. 10, pp. 328–333.

Barton, E.S., Altermann, W., Williams, J.S., and Sims, C.B., U-Pb Zircon Age for a Tuff in the Campbell Group, Griqualand West Sequence, South Africa: Implication for Early Proterozoic Rock Accumulation Rate, *Geology*, 1994, vol. 23, no. 3, pp. 343–346.

Bekker, A., Karhu, J.A., Beukes, N.J., *et al.*, Early Paleoproterozoic Climate Changes in Relation to Biogechemical Cycling of Carbon, in *Paleoklimaty i evolyutsiya paleogeograficheskikh obstanovok v istorii Zemli. Tez. dokladov* (Paleoclimates and Evolution of Paleogeographic Settings in the Earth's History. Abstracts), Petrozavodsk: Karel'skii Nauchn. Tsentr RAS, 1998, pp. 14–16.

Berezhnaya, N.G., Bibikova, E.V., Sochava, A.V., *et al.*, Isotopic Age of the Chinei Subgroup of the Udokan Group in the Korodo–Ydokan Depression, *Dokl. Akad. Nauk SSSR*, 1998, vol. 302, no. 5, pp. 1209–1212.

Bertrand-Sarfati, J. and Eriksson, K.A., Columnar Stromatolites from the Early Proterozoic Schmidtsdrift Formation, Northern Cape Province, South Africa, Part 1: Systematic and Diagnostic Features, *Paleontol. Afric.*, 1977, vol. 20, no. 1, pp. 1–26.

Bibikova, E.V., Lobach-Zhuchenko, S.B., Semikhatov, M.A., *et al.*, Precambrian Geochronological Scale of the East European Platform and Framing Structures, *Izv. Akad. Nauk SSSR, Ser. Geol.*, 1989, no. 4, pp. 8–22.

Bickle, M.J., Martin, A., and Nisbet, E.G., Basaltic and Peridotitic Komatiites and Stromatolites above a Basal Unconformity in the Belingwe Greenstone Belt, Rhodesia, *Earth Planet. Sci. Lett.*, 1975, vol. 27, no. 2, pp. 155–162.

Brasier, M.D. and Lindsay, J.F., A Billion Years of Environmental Stability and Emergence of Eucaryotes: New Data from Northern Australia, *Geology*, 1998, vol. 26, no. 6, pp. 555–558.

Buick, R., Microfossil Recognition in Archean Rocks: an Apprisal of Spheroides and Filaments from a 3500 M.Y. Old Chert-Barite Unit at North Pole, Western Austr., *Palaios*, 1991, vol. 5, no. 4, pp. 441–459.

Buick, R., The Antiquity of Oxigenic Photosynthesis: Evidence from Stromatolites in Sulfate-Deficient Archean Lakes, *Science*, 1992, vol. 225, no. 5033, pp. 74–77.

Buick, R., and Dunlop, J.S.R., Evaporitic Sediments of Early Archean Age from the Warrawoona Group, North Pole, Western Australia, *Sedimentology*, 1990, vol. 37, no. 2, pp. 247–277.

Bunting, J.A., Geology of the Eastern Part of the Nabberu Basin, Western Australia, *Geol. Surv. West. Austral.*, 1986, bull. 131, pp. 1–130.

Burne, R.V. and Moore, L.S., Microbialites: Organosedimentary Deposits of Benthic Microbial Communities, *Palaios*, 1987, vol. 2, no. 2, pp. 241–254.

Byerly, G.R., Lowie, D.R., and Walsh, M.M., Stromatolites from the 3.300-3.500 Myr Swaziland Supergroup, Barberton Mountain Land, South Africa, *Nature*, 1986, vol. 319, pp. 499–491.

Cahen, L., Snelling, N.J., Delhal, J., *et al.*, *The Geochronology and Evolution of Africa*, Oxford: Clarendon Press, 1984.

Campbell, F.H.A. and Cecile, M.P., Evolution of the Early Proterozoic Kilohigok Basin, Bathurst Inlet-Victoria Island, Northwest Territories, *Pap. Geol. Surv. Can.*, 1981, no. 81-10, pp. 103–132.

Canfield, D.E. and Raiswell, R., Carbonate Precipitation and Dissolution: Its Relevance to Fossil Preservation, in *Taphonomy: Releasing and Data Locked in the Fossil Record*, London: Plenum Press, 1991, pp. 411–453.

Cecile, M.P. and Campbell, F.H.A., Regressive Stromatolite Reefs and Associated Facies, Iddle Goulbern Group (Lower Proterozoic), *Bull. Can. Pet. Geol.*, 1978, vol. 26, no. 2, pp. 237–267.

Chadwick, B., Vasudev, V.N., and Hegde, G.V., The Dharwar Craton, Southern India, and Its Late Archean Plate Tectonic Setting: Current Interpretation and Controversies, *Proc. Indian Acad. Sci. (Earth Planet. Sci.)*, 1997, vol. 106, no. 4, p. 249–258.

Chandler, F.W. and Parrish, R.R., Age of the Richmond Gulf Group and Implications for Rifting in the Trans-Hudsonian Orogen, Canada, *Precambrian Res.*, 1989, vol. 44, no. 2, pp. 277–288.

Chauhan, D.C., Microbial Activities and Genesis of Aravalli Phosphorite, Udaipur, Rajasthan, *Himalayan Geology*, 1989, vol. 13, no. 1, pp. 39–51.

Chumakov, N.M., Main Past Glacial Events and Their Geological Significance, *Izv. Akad. Nauk SSSR. Ser. Geol.*, 1984, no. 7, pp. 35–53.

Chumakov, N.M., The Problem of the Warm Biosphere, *Stratigr. Geol. Korrelyatsiya*, 1995, vol. 3, no. 3, pp. 3–14.

Cloud, P.E., A Working Model of the Primitive Earth, *Am. J. Sci.*, 1972, vol. 272, no. 6, pp. 537–548.

Cloud, P.E., Beginnings of Biospheric Evolution and Their Biogeochemical Consequences, *Paleobiology*, 1976, vol. 2, no. 3, pp. 351–387.

Cloud, P.E., Evolution of Ecosystems, *Am. Sci.*, 1974, vol. 62, no. 1, p. 54–66.

Cloud, P.E. and Semikhatov, M.A., Proterozoic Stromatolite Zonation, *Am. J. Sci.*, 1969, vol. 267, no. 11, pp. 1017–1060.

Derry, L.A., Kaufman, A.J., and Jacobsen, S.B., Sedimentary Cycling and Environmental Change in the Late Proterozoic: Evidence from Stable and Radiogenic Isotopes, *Geochim. Cosmochim. Acta*, 1992, vol. 56, no. 12, pp. 1317–1329.

Des Marais, D.J., Tectonic Control of the Crustal Organic Carbon Reservoir during the Precambrian, *Chem. Geol.*, 1994, vol. 114, no. 3, pp. 303–314.

Des Marais, D.J., Long-term Evolution of the Biogeochemical Carbon Cycle, *Rev. in Mineralogy, vol. 35, Geomicrobiology: Interactions between Microbes and Minerals*, Washington: Min. Soc. Amer., 1997a, pp. 428–448.

Des Marais, D.J., Isotopic Evolution on the Biogeochemical Carbon Cycle during the Proterozoic Eon, *Org. Geochem.*, 1997b, vol. 27, nos. 5–6, pp.185–193.

Des Marais, D.J., Bauld, J., Palmisano, A.C., *et al.*, The Biochemistry of Carbon in Modern Microbial Mats, in *The Proterozoic Biosphere*, New York: Cambridge Univ., 1992a, pp. 287–293.

Des Marais, D.J., Strauss, H., Summons, R.E., and Hayes, J.M., Carbon Isotope Evidence for the Stepwize Oxidation of the Proterozoic Environments, *Nature*, 1992b, vol. 359, pp. 605–609.

Dol'nik, T.A., Stromatolites of the Akitkan Group of the Northwestern Baikal Region, in *Nizhnyaya granitsa rifeya i stromatolity afebiya* (The Lower Riphean Boundary and Aphebian Stromatolites), Moscow: Nauka, 1978, pp. 106–110.

Donaldson, J.A., Aphebian Stromatolites in Canada: Implication for Stromatolite Zonation, in *Stromatolites. Development in Sedimentology*, Amsterdam: Elsevier, 1976, vol. 20, pp. 371–380.

Douglas, R.J.W. (Ed.), *Geology and Economic Minerals of Canada*, Ottawa: Geol. Surv. Can., 1972.

Fralick, P.W., Kissin, S.A., and Davis, D.W., Age and Provenance of the Gunflint Lapilli Tuff, in *Prog. and Abstr., 44th Annual Meeting, Inst. Lake Superior Geol. Minneapolis*, Minnesota, May 6–10, 1998, pp. 66–67.

Gao, Zh., Report of Activity, *Stromatolite Newsletters*, 1983, no. 10, pp. 76–79.

Gao, Zh., Stromatolites and Their Stratigraphic Significance of Middle and Late Proterozoic at the Tian Shan Mts and Contiguous Regions, Xinjiang, in *Intern. Symposium on Stromatolites and Plenary Meeting of IGCP 261 Project, Tianjin*, 1992.

Gebelein, C.D., Biotic Control on Stromatolite Microstructure: Implication for Precambrian Time Stratigraphy, *Am. J. Sci.*, 1974, vol. 274, no. 6, pp. 575–598.

Gee, R.D. and Grey, K., Proterozoic Rocks on the Glengarry 1 : 250000 Sheet: Stratigraphy, Structure, and Stromatolite Biostratigraphy, *West. Aust. Geol. Surv. Rep., 41*, 1993.

Gerasimenko, L.M. and Krylov, I.N., Posthumous Cyanobacteria Alterations in the Algal–Bacterial Films from Thermal Springs of Kamachatka, *Dokl. Akad. Nauk SSSR*, 1983, vol. 272, no. 1, pp. 201–203.

Gerlach, D.C., Shirey, R.W., and Carlson, A.H., *Eos*, 1988, vol. 69, no. 1515.

Giovannoni, S.J., Turner, S., Olsen, G.J., *et al.*, Evolutionary Relationships among Cyanobacteria and Green Chloroplasts, *J. Bacteriology*, 1988, vol. 170, pp. 3584–3592.

Golovenok, V.K. and Belova, M.Yu., Finds of *Obruchevella* in the Riphean of the Patoma Highland and in the Vendian of Southern Kazakhstan, *Dokl. Akad. Nauk SSSR*, 1983, vol. 262, no. 3, pp. 675–678.

Golovenok, V.K. and Belova, M.Yu., Gigantism in Precambrian Microfossils and Its Biostratigraphical Significance, *Stratigr. Geol. Korrelyatsiya*, 1994, vol. 2, no. 6, pp. 33–39.

Golubich, S. and Hofmann, H.J., Comparision of Holocene and Mid-Precambrian Entophysaliceae (Cyanophyta) in Stromatolitic Algal Mats: Cell Division and Degradation, *J. Paleontol.*, 1976, vol. 50, no. 9, pp. 1074–1082.

Golubic, S., Sergeev, V.N., and Knoll, A.H., Mesoproterozoic *Archaeolellipsoides*: Akinetes of Heterocystous Cyanobacteria, *Lethaia*, 1995, vol. 28, no. 2, pp. 285–298.

Gorokhov, I.M., Kuznetsov, A.B., Melezhik, V.A., *et al.*, Sr Isotope Composition in Upper Jatulian Dolomites of the Tulomozero Formation, Southeastern Karelia, *Dokl. Ross. Akad. Nauk*, 1998, vol. 360, no. 4, pp. 609–678.

Grey, K., Small Conical Stromatolites from the Archean near Kanowna, Western Australia, *Geol. Surv. West. Austral. Ann. Rep. 1980*, 1981, pp. 90–94.

Grey, K., Aspects of Proterozoic Stromatolite Biostratigraphy in Western Australia, *Precambrian Res.*, 1982, vol. 18, no. 3, pp. 347–365.

Grey, K., Biostratigraphic Studies of Stromatolites from the Proterozoic Earaheedy Group, Nabberu Basin, Western Australia, *Geol. Surv. West. Aust. Bull.*, 1984, no. 130.

Grey, K., Stromatolites from the Proterozoic Earaheedy Group, Earaheedy Basin, Western Australia, *Alcheringa*, 1994a, vol. 18, no. 1, pp. 187–218

Grey, K., Stromatolites from the Paleoproterozoic (Orosirian) Glengarry Group, Glengarry Basin, Western Australia, *Alcheringa*, 1994b, vol. 18, no. 2, pp. 275–300.

Grotzinger, J.P., Cyclicity and Paleoenvironmental Dynamics, Rocknest Platform, Northwest Canada, *Bull. Geol. Soc. Am.*, 1986, vol. 97, no. 11, pp. 1208–1231.

Grotzinger, J.P., Introduction to Precambrian Reefs, *Mem. Can. Soc. Petrol. Geol.*, 1988, no. 13, pp. 9–12.

Grotzinger, J.P., Facies and Evolution of Precambrian Carbonate Depositional Systems: Emergence of the Modern Platform Archetype, in *Controls on carbonate platform and basinal development*, Soc. Econ. Paleontol. Mineral. Spec. Publ., 44, 1989, pp. 79–106.

Grotzinger, J.P., Geochemical Model for Proterozoic Stromatolite Decline, *Am. J. Sci.*, 1990, vol. 290-A, pp. 80–103.

Grotzinger, J.P., McCormic, D.S., and Pelechaty, S.M., Progress Report on the Stratigraphy, Sedimentology, and Significance of the Kimerot and Bear Creek Groups, Kilohigon Basin, District of Mackenzie, *Pap. Geol. Surv. Can.*, 1987, no. 87-1A, pp. 219–238.

Han, T.-M. and Runnegar, B., Megascopic Eucaryotic Algae from the 2.1-Billion-Year-Old Negaunee Iron Formation, Michigan, *Science*, 1992, vol. 257, pp. 232–235.

Hayes, J.M., Global Methanotropy at the Archean-Proterozoic Transition, in *Early Life on Earth. Nobel Symp. 84*, New York: Columbia Univ., 1994, pp. 220–236.

Henderson, J.B., Archean Stromatolites in the Northern Slave Province, Northwest Territories, Canada, *Can. J. Earth Sci.*, 1975, vol. 12, no. 9, pp. 1619–1630.

Hildebrand, R.S., Early Proterozoic LaBine Group of Wopmay Orogen: Remnant of a Continental Volcanic Arc Developed during Oblique Convergence, *Pap. Geol. Surv. Can.*, 1981, no. 81-10, pp. 133–156.

Hoffman, P.F., Evolution of an Early Proterozoic Continental Margin: the Coronation Geosyncline and Associated Aulacogens of the Nortwestern Canadian Shield, *Philos. Trans. Roy. Soc. London, Ser. A*, 1973, vol. 273, pp. 547–581.

Hoffman, P.F., Shallow and Deepwater Stromatolites in Lower Proterozoic Platform-to-Basin Facies Change, Great Slave Lake, Canada, *Bull. Am. Assoc. Petrol. Geol.*, 1974, vol. 58, no. 5, pp. 856–867.

Hoffmann, P.E., Pethei Reef Complex (1.9 Ga), Great Slave Lake. N.W.T., *Mem. Can. Soc. Pet. Geol.*, 1988a, no. 13, pp. 38–48.

Hoffman, P.E., United Plates of America, the Birth of a Craton: Early Proterozoic Assembley and Growth of Laurentia, *Ann. Rev. Earth Planet. Sci. Lett.*, 1988b, vol. 16, no. 5, pp. 543–603.

Hoffman, P.F., Precambrian Geology and Tectonic History of North America, in *The Geology of North America—an Overview*, 1989, vol. A, pp. 447–512.

Hofmann, H.J., Stromatolites from the Proterozoic Animikie and Sibley Groups, Ontario, *Pap. Geol. Surv. Can.*, 1969, nos. 68–69, pp.1–77.

Hofmann, H.J., Precambrian Microflora, Belcher Island, Canada: Significance and Systematics, *J. Paleontol.*, 1976, vol. 50, no. 10, pp. 1040–1073.

Hofmann, H.J., New Stromatolites from the Aphebian Mistassini Group, Ontario, *Can. J. Earth Sci.*, 1978, vol. 1, no. 4, pp. 571–585.

Hofmann, H.J., Precambrian Fossils in Canada—the 1970s in Retrospect, *Pap. Geol. Surv. Can.*, 1981, no. 81-10, pp. 419–443.

Hofmann, H.J., Proterozoic Carbonaceous Compression ("Metaphytes" and "Worms"), in *Early Life on Earth, Nobel Symp. 84*, New York: Columbia Univ., 1994, pp. 342–357.

Hofmann, H.J. and Chen, J., Carbonaceous Megafossils from the Precambrian (1800 Ma) near Jixian, Northern China, *Can. J. Earth Sci.*, 1981, vol 18, no. 4, pp. 443–447.

Hofmann, H.J. and Grotzinger, J.P., Shelf-facies Microbiota from the Odjick and Rocknest Formations (Epworth Group, 1.89 Ga), NW Canada, *Can. J. Earth Sci.*, 1985, vol. 22, no. 12, pp. 1781–1792.

Hofmann, H.J., and Grotzinger, J.P., Abner/Denault Reef Complex (2.1 Ga), Labrador Trough, N.E. Quebec, *Mem. Can. Soc. Petrol. Geol.*, 1988, no. 13, pp. 49–54.

Hofmann, H.J. and Masson, M., Archean Stromatolites from Abitili Greenstone Belt, Quebec, Canada, *Bull. Geol. Soc. Am.*, 1994, vol. 106, no. 4, pp. 424–429.

Hofmann, H.J. and Schopf, J.W., Early Proterozoic Microfossils, in *Earth's Earliest Biosphaere: Its Origin and Evolution*, Schopf, J.W., Ed., Princeton: Princeton Univ., 1983, pp. 321–360.

Hofmann, H.J. and Snyder, G.L., Archean Stromatolites from the Hartville Uplift, Eastern Wyoming, *Bull. Geol. Soc. Am.*, 1985, vol. 96, no. 8, pp. 842–849.

Hofmann, H.J., Sage, R.P., and Berdusco, E.N., Archean Stromatolites in Michipicoten Group Siderite Ore at Wawa, Ontario, *Econ. Geol.*, 1991, vol. 86, no. 5, pp. 1023–1030.

Hofmann, H.J., Thurston, P.C., and Wallace, H., Archean Stromatolites from Uchi Greenstone Belt, Northwestern Ontario, in *Evolution of Archean Supracrustal Strucrures, Pap. Geol. Assoc. Can.*, 1985, no. 28, pp. 125–132.

Holland, H.D., Early Proterozoic Atmospheric Change, in *Early Life on Earth, Nobel Symp. 84*, New-York: Columbia Univ., 1994, pp. 237–244.

Holland, H.D. and Rye, R., Evidence in Pre-2.2 Ga Paleosoils for the Early Evolution of Atmospheric Oxygen and Terrestrial Biota. Comment, *Geology*, 1997, vol. 25, no. 9, pp. 857–858.

Hua, Zh., and Yongsheng, Ma., Carbon Isotope Stratigraphy of Dolomites in the Early Proterozoic Succession, North China, *Geol. Mag.*, 1997, vol. 134, no. 6, pp. 763–770.

Jackson, M.J., Lower Proterozoic Cowles Lake Foredeep Reef, N.W.T., Canada, *Mem. Can. Soc. Petrol. Geol.*, 1988, no. 13, pp. 64–71.

Ivanova, L.V., Chapina, O.S., and Melezhik, V.A., First Finds of Coccoidal Microphytofossils in Lower Proterozoic Metamorphosed Cherts of the USSR, *Dokl. Akad. Nauk SSSR*, 1988, vol. 303, no. 1, pp. 210–212.

Ivliev, A.I., Stromatolite Finds in the Granulite Complex of the Kola Peninsula, *Dokl. Akad. Nauk SSSR*, 1971, vol. 198, no. 3, pp. 661–664.

Karhu, J.A., Paleoproterozoic Evolution of the Carbon Isotope Ratios of Sedimentary Carbonates in the Fennoscandian Shield, *Bull. Geol. Surv. Finland*, 1993, no. 371.

Karhu, J.A. and Holland, H.D., Carbon Isotopes and Rise of Atmospheric Carbon, *Geology*, 1996, vol. 24, no. 10, pp. 867–870.

Kasting, J.F., Earth's Early Atmosphere, *Science*, 1993, vol. 259, no. 5097, pp. 920–926.

Kerans, C., Ross, G.M., Donaldson, J.A., and Geldsetzer, H.J., Tectonism and Depositional History of the Helikan Hornby Bay and Dismal Lake Groups, District of Mackenzie, *Pap. Geol. Surv. Can.*, 1981, no. 81-10, pp. 157–182.

Klein, C., Beukes, N.J., and Schopf, J.W., Filamentous Microfossils in the Early Proterozoic Transvaal Supergroup: Their Morphology, Significance, and Paleoenvironmental Setting, *Precambrian Res.*, 1987, vol. 36, no. 1, pp. 81–94.

Knight, J. and Morgan, W.C., The Aphebian Ramah Group, Northern Labrador, *Pap. Geol. Surv. Can.*, 1981, no. 81-10, pp. 313–356.

Knoll, A.H., Archean Photoantotrophy: Some Alternatives and Limits, in *Origins of Life*, Dordrecht: Reider Publ. Co., 1979, vol. 9, pp. 313–327.

Knoll, A.H., A Paleobiological Perspective on Sabkhas, *Ecological Studies*, 1985, vol. 53, no. 4, pp. 407–425.

Knoll, A.H., The Early Evolution of Eukaryotes: A Global Perspective, *Science*, 1992, vol. 256, pp. 622–627.

Knoll, A.H., Archean and Proterozoic Paleontology, in *Palynology: Principles and Applications*, Jansonius, J. and McGregor, D.C., Eds., Am. Assoc. Stratigr. Palynol. Foundation, 1996, vol. 1, pp. 51–80.

Knoll, A.H. and Canfield, D.E., Isotopic Inference on Early Ecosystems, *Pap. Paleontol. Soc.*, 1998, vol. 4, pp. 212–243.

Knoll, A.H. and Semikhatov, M.A., The Genesis and Time-Distribution of Two Distinctive Proterozoic Stromatolite Microstructures, *Palaios*, 1998, vol. 13, no. 4, pp. 408–422.

Knoll, A.H. and Simonson, D., Early Proterozoic Microfossils and Penecontemporeneous Quartz-Cementation in the Sokoman Iron Formation, Canada, *Science*, 1981, vol. 211, pp. 478–480.

Knoll, A.H., Strother, P.K., and Rossi, S., Distribution and Diagenesis of Microfossils from the Lower Proterozoic Duck Creek Dolomite, Western Australia, *Precambrian Res.*, 1988, vol. 38, pp. 257–279.

Lanier, W.P., Approximate Growth Rates of Early Proterozoic Microstromatolites as Deduced by Biomass Productivity, *Palaios*, 1986, vol. 1, no. 5, pp. 525–542.

Lanier, W.P., Interstitial and Peloid Microfossils from the 2.9 Ga Gunflint Formation: Implication for the Paleoecology of the Gunflint Stromatolites, *Precambrian Res.*, 1989, vol. 45, pp. 291–318.

Liang, Yu., Zhang, J., *et al.*, Stromatolite Assemblages of Late Precambrian in China, *Precambrian Res.*, 1985, vol. 29, nos. 1–3, pp. 15–32.

Lowerindge, W.D., Eade, K.E., and Sullivan, R.W., Geochronological Studies of Precambrian Rocks from the Southern District of Keewatin, *Pap. Geol. Surv. Can.*, 1988, no. 88-18.

Lowe, D.R., Stromatolites 3400 Myr Old from the Archean of W. Australia, *Nature*, 1980, vol. 284, pp. 441–443.

Lowe, D.R., Restricted Shallow-Water Sedimentation on Early Atchean Stromatolitic and Evaporitic Strata of the Strelley Pool Chert, Pilbara Block, W. Australia, *Precambrian Res.*, 1983, vol. 19, no 2, pp. 239–283.

Lowe, D.R., Abiological Origin of Described Stromatolites Older Than 3.2 Ga, *Geology*, 1994, vol. 22, no. 4, pp. 387–390.

Lu, S. and Li, H., A Precise U-Pb Single Zircon Age Determination for the Volcanics of the Dahongyu Formation, Changcheng System in Jixian, *Bull. Chin Acad. Geol. Sci.*, 1991, vol. 22, pp. 137–145.

Macgregor, A.M., A Pre-Cambrian Algal Limestones in South Rodesia, *Trans. Geol. Soc. S. Afr.*, 1941, vol. 43, no. 1, pp. 9–16.

Maliva, R.G., Knoll, A.H., and Siever, R., Secular Change in Chert Distribution: a Reflection of Evolving Biological Participation in the Silica Cycle, *Palaios*, 1989, vol. 4, no. 5, pp. 519–532.

Martin, A., Nisbet, E.G., and Bickle, M.Y., Archean Stromatolites of the Belingwe Greenstone Belt, Zimbabwe (Rodesia), *Precambrian Res.*, 1980, vol. 13, no. 3, pp. 337–362.

Mason, T.R. and Von Brunn, V., 3-Gyr-old Stromatolites from South Africa, *Nature*, 1977, vol. 266, pp. 47–49.

Melezhik, V.A. and Fallick, A.E., A World-Wide 2.0-2.0 Ga-old Positive $\delta^{13}C_{carb}$ Anomaly as a Phenomenon in Relation to the Earth's Major Paleoenvironmental Changes, *Mineral. Mag.*, 1994, vol. 58A, no. 6, pp. 593–594.

Melezhik, V.A. and Fallick, A.E., A Widespread Positive $\delta^{13}C_{carb}$ Anomaly at Around 2.33–2.06 Ga on the Fennoscandian Shield: a Paradox?, *Terra Nova*, 1996, vol. 8, no. 2, pp.141–157.

Melezhik, V.A., Fallick, A.E., and Clark, T., Two Billion Year Old Isotopically Heavy Carbon: Evidence from the Labrador Trough, Canada, *Can. J. Earth Sci.*, 1997a, vol. 34, no. 3, pp. 217–285.

Melezhik, V.A., Semikhatov, M.A., and Fallick, A.E., The Positive Carbon Anomaly and Stromatolite Explosion at Around 2.3–2.0 Ga Ago: Are They Linked?, *EUG-9 Abstr.*, Strasbourg, 1997b, p. 252.

Melezhik, V.A., Fallick, A.E., Makarikhin, V.V., and Lyubtsov, V.V., Links between Paleoproterozoic Palaeogeography and Rise and Decline of Stromatolites: Fennoscandian Schield, *Precambrian Res.*, 1997c, vol. 82. no. 3, pp. 311–348.

Mendelson, C.V., Bauld, J., Horodyski, R.J., *et al.*, Proterozoic and Selected Early Cambrian Microfossils: Prokaryotes and Protists, in *The Proterozoic Biosphere: A Multidisciplinary Study*, New York: Cambridge Univ., 1992, pp. 175–245.

Miorta, M.D. and Veizer, J., Geochemistry of Precambrian Carbonates: VI. Aphebian Albanel Formation, Quebec, Canada, *Geochim. Cosmochim. Acta*, 1994, vol. 58, no. 7, pp. 1735–1745.

Moitra, A.K. and Raha, P.K., Research on Precambrian Life and Biostratigraphy: Search for Biota in Archean Sediments of Singhbhum Iron Ore Group in Parts of Orissa and Bihar, *Rec. Geol. Surv. India*, 1991, vol. 124, no. 2, pp. 5–6.

Morey, G.B., Continental Margin Assemblages, *U.S.Geol. Surv. Prof. Pap.*, 1996, no. 1556, pp. 34–44.

Morey, G.B. and Van Schmus,W.R., Correlation of Precambrian Rocks of the Lake Superior Region, United States, *U.S. Geol. Surv. Prof. Pap.*, 1988, no. 1241-F.

Muir, M.D., Proterozoic Microfossils from the Amelia Dolomite, McArthur Basin, Northern Territory, *Alcheringa*, 1976, vol. 1, no. 1, pp. 143–158.

Murthy, P.S.N. and Reddy, K.K., 2900 M.Y. Old Stromatolites from Sandur Greenstone Belt of Karnataka Craton, India, *J. Geol. Soc. India*, 1984, vol. 25, no. 5, pp. 263–266.

Naqvi, S.M., Venkatachala, B.S., and Shukla, M., *et al.*, Silicified Cyanobacteria from the Cherts of the Archaean Sandur Schist Belt–Karnataka, India, *J. Geol. Soc. India*, 1987, vol. 29, pp. 535–539.

Needman, R.S., Stuart-Smith, P.G., and Page, R.W., The Stratigraphy, Metamorphism and Tectonics of the Early Proterozoic Litchfield Province and Western Pine Creek Geosyncline, Northern Territories, *Precambrian Res.*, 1988, vos. 40/41, pp. 543–564.

Nisbet, E.G. and Wilks, M.E., Archean Stromatolite Reefs at Steep Rock Lake, Atikotan, Northwestern Canada, *Mem. Can. Soc. Petrol. Geol.*, 1988, no. 13, pp. 89–92.

Nutman, A.P., Chadwick, B., Krishna, R.B., and Vasudev, V.N., SRIMP U/Pb Zircon Ages of Acid Volcanic Rocks in the Chitradurga and Sandur Groups, and Granites Adjacent to the Sandur Schist Belt, Karnataka, South India, *J. Geol. Soc. India*, 1996, vol. 39, no 3, pp. 367–374.

Oehler, D.Z., Microflora of the Middle Proterozoic Balbirini Dolomite (McArthur Group) of Australia, *Alcheringa*, 1978, vol. 2, pp. 269–309.

Ohmoto, H., Evidence in Pre-2.2 Ga Paleosoils for the Early Evolution of Atmospheric Oxygen and Terrestrial Biota, *Geology*, 1996, vol. 24, no. 12, pp. 1135–1138.

Ojakangas, R.W., Glaciation: an Uncommon "Mega-event" as a Key to Intracontinental and Intercontinental Correlation of Early Proterozoic Basin Fill, North America and Baltic Shield, in *New Perspective in Basin Analysis*, Berlin: Springer, 1988, pp. 431–444.

Orpen, J.L. and Wilson, J.F., Stromatolites at 3500 Myr and a Greenstone-granite Unconformity in the Zimbabwean Archean, *Nature*, 1981, vol. 291, pp. 218–220.

Page, R.W., Geochronology of Early to Middle Proterozoic Fold Belts in Northern Australia, *Precambrian Res.*, 1988, vos. 40/41, pp. 1–20.

Page, R.W. and Sun, S.S., Aspects of Geochonology and Crustal Evolution in the Eastern Fold Belt, Mt Isa Inlier, *Aust. J. Earth Sci.*, 1998, vol. 45, no. 3, pp. 343–361.

Page, R.W. and Sweet, J.P., Geochronology of Basin Phases in Western Mount Isa Inlier, and Correlation with the McArthur Basin, *Aust. J. Earth Sci.*, 1998, vol. 45, no. 2, pp. 219–232.

Page, R.W., Sun, S.-S., and Carr, G.R., U-Pb Zircon and Pb Isotopes Studies in Relation to Proterozoic Sediment-Hosted Lead-Zink-Silver Deposits in Northern Australia, in *Abstr. 8-th Intern. Conf. on Geochron., Cosmochronol. and Isotope Geol., Berkeley, California., U.S. Geol. Surv. Circular 1107*, 1994, p. 240.

Patterson, J.G., The Amer Belt: Remnants of an Aphebian Foreland Fold and Thrust Belt, *Can. J. Earth Sci.*, 1986, vol. 23, no. 12, pp. 2012–2023.

Pencat, J.J., Honhallier, H., Fanning, G.M., and Jayananda, M., Age of the Holenarsipur Greenstone Belt and Relationship

with the Surrounding Gneisses (Karnataka, S. India), *J. Geol.*, 1995, vol. 103, no. 6, pp. 701–711.

Pidgeon, R.T. and Horwitz, R.G., The Origin of Olistoliths in Proterozoic Rocks of the Ashburton Trough, Western Australia, Using Zircon U-Pb Isotopic Characteristics, *Aust. J. Earth Sci.*, 1991, vol. 38, no. 1, pp. 55–63.

Plumb, K.A., Subdivision and Correlation of the Australian Precambrian, in *Geology of the Mineral Deposits of Australia and Papua New Guinea. Mongraph 14*, Parkvill: Austral. Inst. of Mining and Metallurgy, 1990, pp. 27–32.

Plumb, K.A., New Precambrian Time Scale, *Episodes*, 1991, vol. 14, no. 2, pp. 139–140.

Plumb, K.A. and Derrick, G.M., Geology of the Proterozoic Rocks of the Kimberley to Mount Isa Region, in *Econom. Geol. of Australia and Papua New Guinea*, Parkvill: Austral. Inst. Mining Metallurgy, 1976, pp. 217–252.

Plumb, K.A., Derrick, G.M., and Wilson, J.H., Precambrian Geology of the McArthur River–Mount Isa Region, Northwestern Australia, in *The Geology and Geophysics of Northeastern Australia*, Brisbane: Geol. Soc. Austral., Queensland Division, 1980, pp. 71–88.

Pokrovskii, B.G. and Melezhik, V.A., Carbon and Oxygen Isotopic Variations in the Lower Proterozoic Carbonates of the Kola Peninsula, *Stratigr. Geol. Korrelyatsiya*, 1995, vol. 3, no. 3, pp. 42–53.

Preiss, W.V., Proterozoic Stromatolites from the Naberru and Officer Basin, Western Australia, and Their Biostratigraphic Significance, *South Aust. Geol. Surv. Rep.*, 1976, no. 47, pp. 1–33.

Raaben, M.E., Microstromatites and Their Nature, *Litol. Polezn. Iskop.*, 1998, no. 2, 153–161.

Ramaekers, P., Hudsonian and Helikian Basins of the Athabosca Region, Northern Saskatchewan, *Pap. Geol. Surv. Can.*, 1981, no. 81-10, pp. 219–234.

Ricketts, B.D. and Donaldson, J.A., Sedimentary History of the Belcher Group of Hudson Bay, *Pap. Geol. Surv. Can.*, 1981, no. 81-10, pp. 235–254.

Ricketts, B.D. and Donaldson, J.A., Stromatolite Reef Development on a Mud-Dominated Platform in the Middle Precambrian Belcher Group of Hudson Bay, *Mem. Can. Soc. Petrol. Geol.*, 1988, no. 13, pp. 113–119.

Ritts, B.D. and Grotzinger, J.P., Depositional Facies and Detrital Composition of the Proterozoic Et-Then Group, N.W.T., Canada: Sedimentary Response to Intercratonic Indentation, *Can. J. Earth Sci.*, 1994, vol. 31, no. 12, pp. 1736–1778.

Rosen, O.M., Condie, K.C., Natapov, L.M., and Nozhkin, A.D., Archean and Early Proterozoic Evolution of the Siberian Craton: a Preliminary Assessment, in *Archean Crustal Evolution*, Amsterdam: Elsevier, 1994, pp. 411–459.

Russell, J., Grey, K., Whitehous, M., and Moorbath, S., Direct Pb/Pb Age Determination of Proterozoic Stromatolites from the Ashburton and Nabberu Basins, Western Australia, in *Abstr. 8th Internat. Conf. on Geochronol., Cosmochronol., and Isotope Geol., U.S. Geol. Surv. Circular 1107*, 1994, p. 275.

Sami, T.T. and James, W.P., Peritidal Carbonate Platform Growth and Cyclicity in an Early Proterozoic Foreland Basin, Upper Pithei Group, Northwest Canada, *J. Sediment. Res.*, 1994, vol. B64, no. 2, pp. 11–131.

Sarfati, J., Cherty Stromatolites in the 2000 Ma Fransevillian Cherts, Gabon, in *Intern. Symposium on Stromatolites and Plenary Meeting of IGCP 261 Project*, Tianjin, 1992, p. 23.

Schidlowski, M., Early Atmospheric Oxygen Level: Constraints from Archean Photoautotrophy, *J. Geol. Soc. London*, 1984, vol. 141, part 2, pp. 243–250.

Schidlowski, M., The Initiation of Biological Processes in Early Biogeochemical Evolution on Earth, in *Organic Geochemistry*, Eugel, M.N. and Macko, S.A., Eds., New-York: Plenum, 1993, pp. 639–655.

Schidlowski, M., Eichmann, R., and Junge, C.E., Carbon Isotope Geochemistry of the Precambrian Lomagundi Carbonate Province, Rhodesia, *Geochim. Cosmochim. Acta*, 1976, vol. 40, no. 4, pp. 449–455.

Schidlowski, M., Hayes, J.M., and Kaplan, J.P., Isotopic Inferences of Ancient Biochemistries: Carbon, Sulfur, Hydrogen, and Nitrogen, in *Earth's Earliest Biosphere, Its Origin and Evolution*, Princeton: Princeton Univ., 1983, pp. 147–186.

Schidlowski, M., Matzigkeit, U., and Krumbein W.E., Superheavy Organic Carbon from Hypersaline Microbial Mats: Assimilatory Pathways and Geochemical Implications, *Naturwissenschaften*, 1984, vol. 71, no. 3, pp. 303–308.

Schopf, J.W., Paleobiology of the Archean, in *The Proterozoic Biosphaere: A Multidisciplinary Study*, Schopf, J.W. and Klein, C., Eds., Cambridge: Cambridge Univ. Press, 1992, pp. 24–39.

Schopf, J.W. and Walter, M.R., Archean Microfossils, New Evidence of Ancient Microbes, in *Earth's Earliest Biosphaere: Its Origin and Evolution*, Schopf, J.W., Ed., Princeton: Princeton Univ. Press, 1983, pp. 241–239.

Schopf, J.W. and Klein C., Eds., *The Proterozoic Biosphaere: A Multidisciplinary Study*, Cambridge: Cambridge Univ., 1992.

Schopf, W., Oehler, D.Z., Horodyski, J., and Kvenvolden, K.A., Biogenecy and Significance of the Oldest Known Stromatolites, *J. Paleontol.*, 1971, vol. 45, no. 3, pp. 477–485.

Semikhatov, M.A., Some Carbonate Stromatolites of the Aphebian in the Canadian Shield, in *Nizhnyaya granitsa rifeya i stromatolity afebiya* (The Lower Riphean Boundary and Aphebian Stromatolites), Moscow: Nauka, 1978, pp. 111–147.

Semikhatov, M.A. and Raaben, M.E., Dynamics of the Global Diversity of Preterozoic Stromatolites. Article 1: Northern Eurasia, China, and India, *Stratigr. Geol. Korrelyatsiya*, 1994, vol. 2, no. 6, pp. 10–32.

Semikhatov, M.A. and Raaben, M.E., Dynamics of the Global Diversity of Preterozoic Stromatolites. Article 2: Africa, Australia, North America, and General Synthesis, *Stratigr. Geol. Korrelyatsiya*, 1996, vol. 4, no. 1, pp. 26–54.

Semikhatov, M.A., Shurkin, K.A., Aksenov, E.M., *et al.*, New Precambrian Stratigraphic Scheme of the USSR, *Izv. Akad. Nauk SSSR., Ser. Geol.*, 1991, no. 4, pp. 3–16.

Sepkoski, J.J., Jr., Chapter One Foundational Life in the Oceans, in *The Book of Life*, Gould, S.J., Ed., New York: Norton and Co., 1993, pp. 34–63.

Sergeev V.N., *Okremnennye mikrofossilii dokembriya i kembriya Urala i Srednei Azii* (Precambrian and Cambrian Silicified Microfossils of the Urals and Central Asia), Moscow: Nauka, 1992.

Sergeev, V.N., Microfossils in Cherts from the Middle Riphean (Mesoproterozoic) Avzyan Formation, Southern Ural Mountains, Russian Federation, *Precambrian Res.*, 1994, vol. 1, no. 2, pp. 231–254.

Sergeev, V.N., Mesoproterozoic Microbiotas of the Northern Hemisphere and the Meso-Neoproterozoic Transition, *Proc. 30th Intern. Geol. Congress, Beijin*, 1997, vol. 1, pp. 177–185.

Sergeev, V.N., Knoll, A.H., and Grotzinger, G.P., Paleobiology of the Mezoproterozoic Billyach Group, Anabar Uplift Northern Siberia, *Mem. Paleontol. Soc.*, 1995, no. 39, pp. 1–37.

Shrinavasan, R., Nagvi, S.M., and Kumar, B.V., Archean Shelf-Facies and Stromatolites Proliferation in Dharwar Supergroup, North Karnataka, District Karnataka, *J. Geol. Soc. India*, 1990, vol. 35, no. 2, pp. 203–212.

Sims, P.K., Card, K.D., and Lumbers, S.B., Evolution of Early Proterozoic Basins of the Great Lakes Region, *Pap. Geol. Surv. Can.*, 1981, no. 81-10, pp. 379–398.

Sogin, M.L., Gunderson, J.H., Elwood, H.J., *et al.*, Philogenetic Meaning of the Kingdom Concept: an Unusual Ribosomal RNA from Giardia Lamblia, *Science*, 1989, vol. 243, no. 4887, pp. 75–77.

Steiner, M., *Chuaria circularis* Mascot 1899—Megaspheromorphic Acritarchs or Prokaryotic Colony?, *Acta Univ. Carolinae. Geol.*, 1996, vol. 40, nos. 3–4, pp. 645–665.

Strauss, H., Des Marais, D.J., Hayes, J.M., and Summons, R.E., The Carbon-Isotopic Record, in *The Proterozoic Biosphere: A Multidisciplinary Study*, Schopf, W.B. and Klein, C., Eds., Cambridge: Cambridge Univ., 1992, pp. 117–127.

Sumner, D.Y. and Bowring, S.A., U-Pb Geochronologic Constrains on Deposition of the Camberland Subgroup, Trasvaal Supergroup, South Africa, *Precambrian Res.*, 1996, vol. 79, no. 1, pp. 25–35.

Sun, W.G., Palaeontology and Biostratigraphy of Late Precambrian Macroscopic Colonial Algae: *Chuaria* Walcott and *Tawuia* Hofmann, *Palaeontographica B*, 1987, vol. 203, no. 1, pp. 109–134.

Thorne, A.M. and Seymour, D.B., Geology of the Aushburton Basin, Western Australia, *Bull. Geol. Surv. West. Aust.*, 1991, no. 139.

Thorpe, R.I., Hickman, A.H., Davis, D.W., *et al.*, U-Pb Zircon Geochronology of Archean Felsic Units in the Marble Bar Region, Pilbara Craton, Western Australia, *Precambrian Res.*, 1992, vol. 56, no. 1, pp. 169–189.

Tikhomirova, M. and Makarikhin, V.V., Possible Reasons for the ^{13}C Anomaly of Lower Proterozoic Sedimentary Carbonate, *Terra Nova*, 1993, vol. 5, no. 2, pp. 244–248.

Timofeev, B.V., *Mikrofossilii rannego dokembriya* (Early Precambrian Microfossils), Leningrad: Nauka, 1982.

Truswell, J.F. and Eriksson, K.A., The Morphology of Stromatolites from the Transvaal Dolomite Northwest of Johannesburg, South Africa, *Trans. Geol. Soc. S. Africa*, 1972, vol. 75, part 2, pp. 99–110.

Truswell, J.F. and Eriksson, K.A., Stromatolitic Associations and Their Palaeoenvironmental Significance: a Re-Apprisal of a Lower Proterozoic Locality from the Northern Cape Province, South Africa, *Sediment. Geol.*, 1973, vol. 10, no. 10, pp. 1–23.

Truswell, J.F. and Eriksson, K.A., A Palaeoenvironmental Interpretation of the Early Proterozoic Malmani Dolomite from Zwartkopf, South Africa, *Precambrian Res.*, 1975, vol. 2, no. 2, pp. 227–303.

Vasudev, V.N., Naqvi, S.M., Shukla, M., and Raj, B.U., Stromatolites from the Chert-Dolomites of Archean Shimoga Schist Belt, Dharwar Craton, India, *J. Geol. Soc. India*, 1989, vol. 33, no. 3, pp. 201–205.

Veizer, J., Plumb, K.A., Clayton, R.N., *et al.*, Geochemistry of Precambrian Carbonates: V. Late Paleoproterozoic Seawater, *Geochem. Cosmochem. Acta*, 1992, vol. 56, no. 12, pp. 2487–1501.

Venkatachala, B.S., Sharma, M., Srinivasan, R., *et al.*, Bacteria from the Archaean Banded Iron Formation of Kudremukh Region, Dharwar Craton, South India, *The Palaeobotanist*, 1986, vol. 35, pp. 200–203.

Venkatachala, B.S., Naqvi, S.M., Chada, M.S., *et al.*, Paleobiology and Geochemistry of the Precambrian Stromatolites and Associated Sedimentary Rocks from the Dharwar Craton: Constraints on Archean Biogenic Processes, *Himalayan Geol.*, 1989, vol. 13, no. 1, pp. 1–20.

Xing, Yu., Duan, Ch., Liang, Yu., *et al.*, *Late Precambrian Paleontology of China*, Beijing: Geol. Publ. House, 1992, pp. 28–106.

Walsh, M.M., Microfossils and Possible Microfossils from the Early Archean Onverwacht Group, Barberton Mountain Land, South Africa, *Precambrian Res.*, 1992, vol. 54, no. 2, pp. 271–293.

Walter, M.R., Stromatolites and the Biostratigraphy of the Australian Precambrian and Cambrian, *Paleontol. Assoc. Spec. Pap.*, 1972, no. 11, pp. 1–190.

Walter, M.R., Archean Stromatolites: Evidence of the Earth's Earliest Benthos, in *Earth's Earliest Biosphere: Its Origin and Evolution*, Princeton: Princeton Univ., 1983, pp. 187–213.

Walter, M.R. and Heys, G.R., Links between the Rise of the Metazoa and the Decline of Stromatolites, *Precambrian Res.*, 1985, vol. 29, no. 1, pp. 149–174.

Walter, M.R., Bauld, J., and Brock, T.D., Microbiology and Morphogenesis of Columnar Stromatolites (*Conophyton, Vacerrilla*) from Hot Springs in Yellowstone National Park, in *Stromatolites. Development in Sedimentology*, Amsterdam: Elsevier, 1976, vol. 20, pp. 273–311.

Walter, M.R., Buick, R., and Dunlop, J.S.R., Stromatolites 3.400–3.500 My Old from the North Pole Area, Western Australia, *Nature*, 1980, vol. 284, pp. 443–445.

Walter, M.R., Krylov, J.N., and Muir, M.D., Stromatolites from Middle and Late Proterozoic Sequences in the McArthur and Georgina Basins and the Mount Isa Province, Australia, *Alcheringa*, 1988, vol. 12, no. 1, pp. 79–106.

Walter, M.R., Du, R., and Horodyski, R.J., Coiled Carbonaceous Megafossils from the Middle Proterozoic of Jixian (Tianjin) and Montana, *Am. J. Sci.*, 1990, vol. 200-A, pp. 133–148.

Wardle, R.J. and Bailey, D.G., Early Proterozoic Sequences in Labrador, *Pap. Geol. Surv. Can.*, 1981, no. 81-10, pp. 331–360.

Williams, J.R., Bangemall Basin, *Mem. Geol. Surv. West. Aust.*, 1990, no. 3, pp. 308–329.

Wilmotte, A. and Golubic, S., Morphological and Genetic Criteria in the Taxonomy of Cyanophyta, *Cyanobacteria. Algological Studies*, 1991, vol. 64, no. 1, pp. 1–24.

Yan, Yu-Zh., Microflora from Shaly Facies of Lower Chancheng System, Kuangchan District, Hubei, and Its Comparision with That of Adjacent Areas, *Acta Micropaleontol. Sinica*, 1995, vol. 12, no. 4, pp. 453–456.

Yakauskas, T.V., Mikhailova, N.S., German, T.N., *et al.*, *Mikrofossilii dokembriya SSSR* (Precambrian Microfossils of the USSR), Moscow: Nauka, 1989.

Yudovich, Ya.E., Makarikhin, V.V., Medvedev, P.V., and Sukhanov, N.V., Carbon Isotopic Anomalies in Carbonates of the Karelian Complex, *Geokhimiya*, 1990, no. 7, pp. 972–978.

Zhang, Zh., Discovery of Microfossils from the 1848-Ma-old Changzhoigou Formation, Jixian Section, North China, *J. Nanjing Univ. Nat. Sci. Sect.*, 1995, vol. 31, no. 2, pp. 198–199.

Zhang, Y., A Gunflint Type of Microfossil Assemblage from Early Proterozoic Stromatolite Cherts in China, *Nature*, 1984, vol. 309, no. 5968, pp. 547–579.

Zhu, Sh. and Chen H., Characteristics of Paleoproterozoic Stromatolites in China, *Precambrian Res.*, 1992, vol. 57, no. 1, pp. 135–163.

Zhu, Sh., Xu, Ch., and Gao, R., Early Proterozoic Stromatolites from Wutai Mt. and Its Adjacent Regions, *Bull. Tianjin Inst. Geol., Mineral. Resources*, 1987, no. 7, pp. 1–180.

Stratigraphy and Geological Correlation, Vol. 7, No. 5, 1999, pp. 437–451. Translated from Stratigrafiya. Geologicheskaya Korrelyatsiya, Vol. 7, No. 5, 1999, pp. 28–42.
Original Russian Text Copyright © 1999 by Vladimirov, Ponomareva, Kargopolov, Babin, Plotnikov, Gibsher, Izokh, Shokal'skii, Bibikova, Zhuravlev, Ponomarchuk, Khalilov, Travin. English Translation Copyright © 1999 by МАИК "Наука/Interperiodica" (Russia).

Neoproterozoic Age of Oldest Rocks from the Tom' Inlier (Mountainous Shoriya): Implication of U–Pb, Sm–Nd, Rb–Sr, and Ar–Ar Dating

A. G. Vladimirov*, A. P. Ponomareva*, S. A. Kargopolov*, G. A. Babin, A. V. Plotnikov*, A. S. Gibsher*, A. E. Izokh*, S. P. Shokal'skii**, E. V. Bibikova***, D. Z. Zhuravlev****, V. A. Ponomarchuk*, V. A. Khalilov*****, and A. V. Travin***

** Joint Institute of Geology, Geophysics, and Mineralogy, Siberian Division, Russian Academy of Sciences, Universitetskii pr. 3, Novosibirsk, 630090 Russia*

*** State Enterprise "Zapsibgeols"emka," Elan' Settlement, Novokuznetsk District, Kemerovskaya oblast, 654919 Russia*

**** Vernadsky Institute of Geochemistry and Analytical Chemistry, Russian Academy of Sciences, ul. Kosygina 19, Moscow, 117975 Russia*

***** Institute of Geology of Ore Deposits, Petrography, Mineralogy, and Geochemistry, Russian Academy of Sciences, Staromonetnyi per. 35, Moscow, 109017 Russia*

****** Institute of Geology, Kazakhstan Academy of Sciences, ul. Kalinina 69a, Almaty, 480100 Kazakhstan*

Received January 21, 1997; in final form, January 28, 1998

Abstract—Age of metamorphic and magmatic rocks from the Mountainous Shoriya is measured using U–Pb, Sm–Nd, Rb–Sr, and Ar–Ar dating. As established, the oldest rocks of the region are metabasites of the Konzhin Complex (Sm–Nd isochron data $T = 694 \pm 43$ (2σ) Ma, $\varepsilon_{Nd}(T) = 7.1 \pm 0.1$ (2σ), MSWD = 2.0), whose isotopic composition corresponds to that of abyssal and ocean island basalts. Geochronological dates obtained show that the crystalline schists, and gneissoid to normal granites of the Tom' inlier, which have been attributed earlier to the deep Precambrian, range in age from the Carboniferous to Late Triassic. None of the geochronological methods revealed dates older than the Late Riphean. The same age constraint for oldest rocks from the Mountainous Shoriya is inferred from the Sm–Nd model ages $T_{Nd}(DM\text{-}2st) = 590$–$920$ Ma calculated for protoliths of granitoids. Maximum values $\varepsilon_{Nd}(T) = +6.0$ are shown to be characteristic of the Early Cambrian plagiogranites of the ophiolite association, whereas low parameters $\varepsilon_{Nd}(T) = +2.5$ mark the Late Triassic potassium granitoids. The geochronological dates obtained and correlation of geological complexes in the Mountainous Shoriya and adjacent regions suggest a conclusion that the Early Precambrian crystalline crust is missing in the study area.

Key words: *isotopic dating, Sm–Nd model age, crystalline basement, Precambrian*

INTRODUCTION

The Mountainous Shoriya is the key area of the Altai–Sayan folded system, where the Altai, Salair, and West Sayan structures are conjoined. Geological and stratigraphic problems have been the focal point of researchers studying this area for nearly a century, yet these still provide matter for keen discussion. Most intriguing among the problems is one concerning the age of metamorphic complexes composed of amphibolites, crystalline and green schists, gneisses, marbles, and gneissoid granites, which are exposed within the Tom' inlier. There are two viewpoints on the age and origin of these rocks. According to one of them, they are constituents of the Early Precambrian sialic basement (Churakov, 1927; Monich, 1938; Dodin, 1948; Kuznetsov, 1954; Lepezin *et al.*, 1975; *Geologicheskaya...*, 1977; *Rabochaya...*, 1996). However, another group of researchers (Khomentovskii, 1960; Dolgushin, 1969; and some others) considers these rocks as related in origin to the local metamorphism and granitization, which affected the Early Paleozoic sequences around the deep-rooted Kuznetsk Alatau fault. Plentiful K–Ar geochronological dates obtained some time ago (Klyarovskii, 1972) revealed a wide age spectrum for the rocks with determination maximums at 170, 220, 270, 360, and 450 Ma. In this work, we put forth effort to solve the problem using simultaneously several modern methods of geochronological dating of metamorphic and magmatic rocks. Understanding that newly obtained geochronological dates and their interpretation bear the far-reaching consequences and may provoke new debates, some of us reserve an opportunity to explain later the personal viewpoint on the geological structure of the Mountainous Shoriya that is not described in this short paper.

FORMATION STAGES OF GEOLOGICAL COMPLEXES IN THE TOM' INLIER AND NEARBY

The Tom' inlier and surrounding structures demonstrate an intricate ensemble of metamorphic and mag-

matic rock complexes located in the Kuznetsk Alatau fracture zone (Fig. 1). Rocks most widespread within the inlier are gneissoid gabbros and diorites, gneissoid and normal granites associated with metamorphic sequences composed of predominant amphibolites and less abundant metasediments. These rocks are exposed inside a belt 10–25 km wide and about 90 km long. Striking eastward of the Kuznetsk depression, the belt is separated from this structure by a narrow wedge of the Lower–Middle Paleozoic sedimentary and volcanogenic sequences crosscut by the Middle Paleozoic granitoids. In the east, it is rimmed by greenschist metasediments and metavolcanics enclosing the intrusive bodies of gabbro, diorite, and Na-granitoids, which range in age, according to various stratigraphic schemes, from the Early Proterozoic to Early Cambrian.

Our geological and geochronological investigations showed that the oldest rocks of the Tom' inlier and surrounding structures are of the Late Riphean age. The

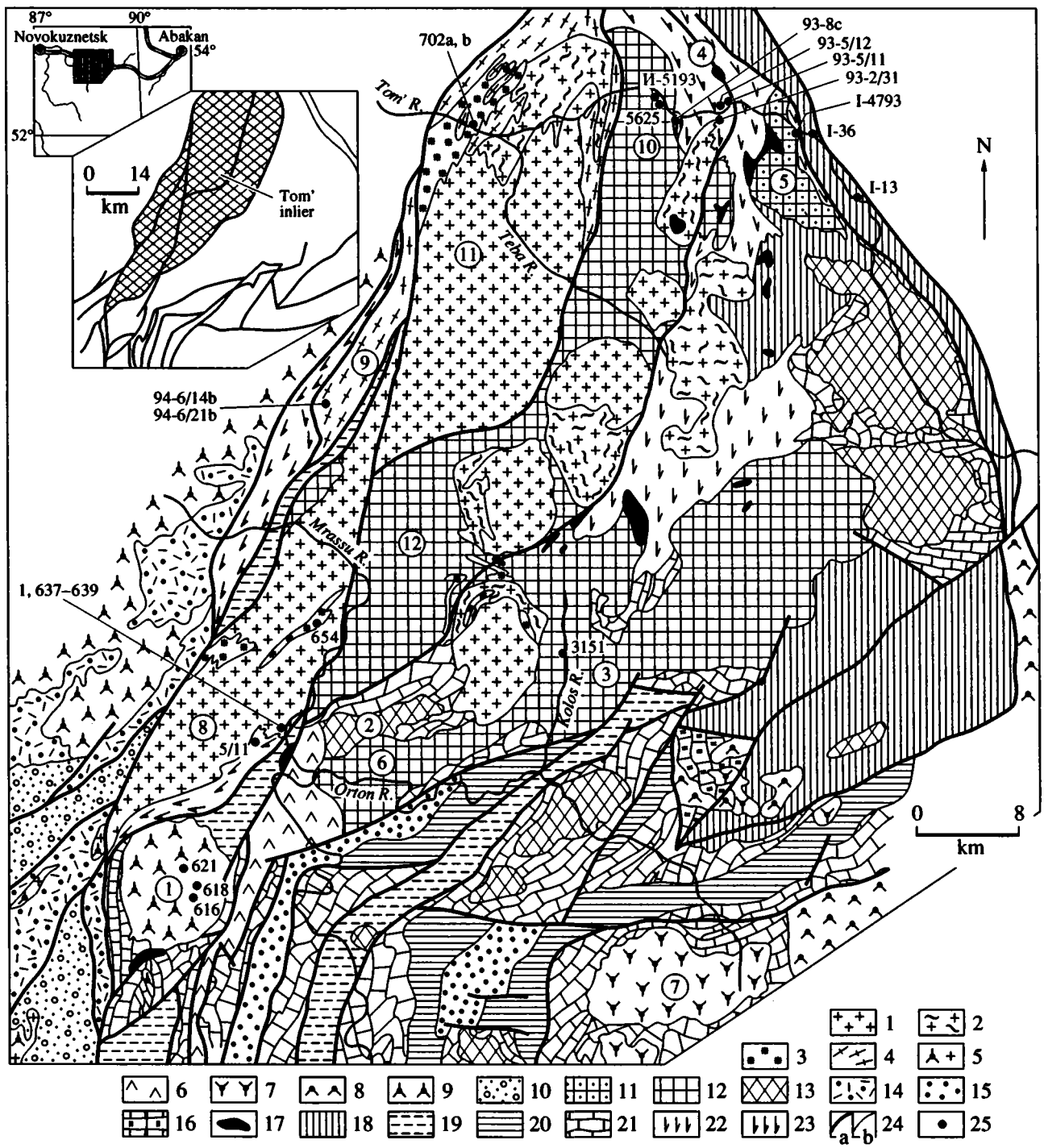

tectono-thermal history of rock transformations lasted long, up to the Early Mesozoic, inclusive, and locally involved the amphibolite-grade metamorphism and anatexis. Geological characteristics, lithology, and formation stages of the studied rock complexes, as they are understood in this work, are presented in Table 1, where we have also indicated their stratigraphic ranges suggested in previous works.

OBJECTS AND INVESTIGATION METHODS

The U–Pb zircon dating was applied to a series of metamorphic and magmatic rock complexes briefly characterized below.

Migmatized gneisses, gneissoid and normal granites of the Tom' Complex have been traditionally considered as the oldest rocks of the region. Recently (Ponomareva *et al.*, 1995), it was established that the complex, in its former scope, is heterochronous and divisible into three autonomous rock associations: the Barsuk Complex of small bodies of gneissoid syenite-diorites and quartz-syenites; the Tom' Complex proper, incorporating predominant gneissoid granites with injection veins of granites; and the Porog Complex of the granodiorite–granite–leucogranite composition. Zircon fractions from all these rock associations were used to measure their U–Pb ages (Table 1).

With respect to the analyzed migmatitic gneisses (metapelites) of the Tashelga Complex, it should be mentioned that these rocks have been formerly attributed to the Konzhin Formation assumed to be of the Early Proterozoic age. We consider them as representing an independent metamorphic complex because of the peculiar substratum lithology and disthene-sillimanite grade of metamorphism (Kargopolov and Plotnikov, 1995).

The next group of rocks used for the U–Pb dating is that of gabbro, gabbro-diorite, diorite, and Na-granitoid massifs exposed in the northern part of the Tom' inlier and to the east from this structure (Fig. 1). Due to the various extent of cataclasis and schistosity, these rocks have been earlier considered as different in age, being attributed to Early Proterozoic intrusions within the Tom' inlier and to later intrusive formations outside of the latter (see Table 1). Data on the composition and structure of the analyzed massifs (Izokh *et al.*, 1995) suggest that they represent two autonomous rock series: the gabbro–diorite–Na-granite association of the calc-alkaline type (Teba, Khomutovka, Orton, and Kolos massifs) and the subalkaline gabbro–diorite association (Luzhba massif) much less widespread than the former.

In order to elucidate the age of ophiolites known in the Mountainous Shoriya, we studied plagiorhyolites and subvolcanic plagiogranites associated with tholeiitic basalts of the volcanic Koltas Complex.

The results of isotopic measurements are presented in Table 2 characterizing as well the peculiarity of laboratory measurements, used equipment, and also reproducibility of the results and method of processing them.

The Sm–Nd isotopic analysis is used to study metabasites (amphibolites) of the Konzhin Complex attributed previously to the Early Proterozoic (Table 1). In order to reveal principal stages of crust formation in the region, we analyzed the Sm–Nd isotope systems in heterochronous granitoids. Table 3 shows the results obtained and data on analytical procedure, equipment type, and method of calculating the Sm–Nd parameters.

Fig. 1. Geological scheme of the Tom' inlier and surrounding structures with indicated sampling localities (compiled using data of G.F. Gorelov, I.O. Ivonin, V.P. Isaev, G.A. Kokov, P.F. Lavrenov, V.N. Pen'kin, Yu.A. Speit, A.B. Shepel', and original observation results). *Late Paleozoic–Early Mesozoic*: (1) Porog Complex of subalkaline monzodiorites, granodiorites, granites, and leucogranites, T_3; (2) Tom' Complex of gneissoid to normal granites, P_2–T_1; (3) Barsuk Complex of syenodiorites and quartz-syenites, P_2; (4) Tashelga Complex of crystalline schists and gneisses, Pz_3–Mz_1. *Middle Paleozoic*: (5) Kistal Complex of granosyenites, granites, and leucogranites, D_2; (6) calc-alkaline and shoshonite volcanic series undivided, D_{1-2}; (7) Patyn Complex of gabbro and syenites, D_1; (8) alkali basalt–phonolite volcanic series, D_1; (9) norite–diorite (Bol'shaya Rechka) and monzodiorite–granodiorite–granite (Tel'bes) complexes undivided, D_1. *Late Riphean–Early Paleozoic*: (10) molassic and flyschoid deposits, $\in_3$–O_3; (11) Luzhba Complex of subalkaline leucogabbroids, $\in_3 : O_1$; (12) Teba Complex of Na-gabbro, diorites, and granites, $\in_3 : O_1$; (13) Sadra Complex of Na-gabbro, diorites, and granodiorites, $\in_2$; (14) shoshonite volcanic series (Tashtagol and Mundybash formations), $\in_2$; (15) carbonate–terrigenous deposits intercalated with molasse beds and calc-alkaline volcanics (Mrassu Formation), $\in_1^2$; (16) carbonate deposits (Mazas Formation), $\in_1$; (17) dunite–harzburgite Salan (Tersa) and wehrlite–clinopyroxenite-gabbro Usa complexes of the ophiolite sequence, $\in_1$; (18) Koltas Formation of MORB- and OIB-type volcanics of the ophiolite sequence, $\in_1$?; (19–20) Ust Anzas Formation of OIT (19) and OIA (20) basalts, V-$\in_1$; (21) limestone–dolomite and clay–chert–carbonate sequences (Spas Group, Kabyrza and West Siberian formations, undivided), V-$\in_1$; (22) Tersa Complex of MORB- and OIB-type metabasites, R_3; (23) Konzhin Complex of MORB-type metabasites, R_3; (24) principal faults (a) and other geological boundaries (b); (25) sampling localities and sample nos. as in Tables 2–4.

Encircled numbers denote massifs and tectonic blocks: (1) Azas; (2) Zaslon; (3) Kolos; (4) Konzhin and Tersa; (5) Luzhba; (6) Orton; (7) Patyn; (8) Porog; (9) Tashelga; (10) Teba; (11) Tom'; (12) Khomut.

Table 1. Formation sequence of rock complexes in the Tom' inlier and surrounding structures

Geochronology	Metamorphic or magmatic complex; groups and formations	Investigated type massifs, areas, and sections	Rock types	Metamorphic facies	Age			
					Geologiya ..., 1967	*Regional'nye...*, 1978 *Resheniya...*, 1983	*Rabochaya...*, 1996	Radiological dates, Ma (method)
T_3	Porog Complex	Porog massif	Monzodiorites, granodiorites, granites, leucogranites (massive to cataclastic and gneissoid at the periphery)		AR	PR_1	PR_1	211 ± 4 (U–Pb)
$P_2 : T_1$	Tom' Complex	Tom' massif (section at the Tom' River)	Granite gneisses, migmatites, gneissoid granites, granite veins	Epidote–amphibolite and amphibolite	AR	PR_1	PR_1	251–236 (U–Pb)
	Barsuk Complex	Tom' massif (Barsuk group of intrusions at the Tom' River)	Syenodiorites and quartz- syenites (gneissoid)	?	AR	PR_1	PR_1	251 ± 4 (U–Pb)
$C_2 : P_1$	Tashelga Complex	Tashelga area	Migmatitic gneisses, crystalline schists, amphibolite, marbles	Epidote-amphibolite and amphibolite	PR	PR_1–Pz_1	PR_1–R_2	~300 (U–Pb)
D_{1-2}	Kistal Complex of granosyenites, granites, and leucogranites; Patyn Complex of syenites and gabbros; Goryachegorsk Complex of alkaline gabbroids; calc-alkaline volcanics and shoshonites intercalated with red beds (Tel'bes Group and Palatninsk, Belaya Osipovka, and Abramovsk formations); alkali basalt–phonolite volcanic series (Sokolinaya Gora and Karatag formations)				D_{1-2}	D_{1-2}	D_{1-2}	n. a.
D_1	Tel'bes and Bol'shaya Rechka complexes	Azas massif	Gabbros, diorites, granodiorites, granites		D_{1-2}	O_3	S_2–D_1	385 ± 15 (U–Pb)
ϵ_3–O_3	Molassic and flyschoid deposits of the Gornaya Shoria, Alga, and Amzas formations; calc-alkaline and shoshonite volcanic series (Kitat, Taimen', and Alzas formations) in the lower part of the sequence				ϵ_3–O	ϵ_3–O	ϵ_3–O_3	n. a.
$\epsilon_3 : O_1$	Luzhba Complex	Luzhba massif	Subalkaline leucogabbros and diorites		Pz_1	V–ϵ_1		490 ± 19 (U–Pb)
	Teba Complex	Teba and Kolos massifs	Gneissoid diorites and gabbro-diorites		PR_1 Pz_1	PR_1 V–ϵ_1	PR_1	499 ± 14 485 ±5 (U–Pb)
ϵ_2	Sadra Complex of gabbros, diorites, and granodiorites associated with flyschoid and molassic deposits of Ust-Tel'bes and Bol'shoi Sii formations					Pz_1	ϵ_1?	n. a.
	Shalym Complex of monzogabbro and syenites; shoshonite and calc-alkaline volcanic series (Tashtagol and Mundybash formations); Ulutag Formation of flyschoid rocks			Greenstone to greenschist	ϵ_{1-2}	ϵ_{2-3}	ϵ_2	n. a.

Table 1. (Contd.)

Geochronology	Metamorphic or magmatic complex; groups and formations	Investigated type massifs, areas, and sections	Rock types	Metamorphic facies	Age			
					Geologiya..., 1967	*Regional'nye....*, 1978 *Resheniya...*, 1983	*Rabochaya...*, 1996	Radiological dates, Ma (method)
$V + \epsilon_1$	Complex of siliceous, terrigenous, and carbonate sediments intercalated with calc-alkaline volcanics and molassic deposits (Adiak, Mazas, Mrassu and other formations)				ϵ_1	ϵ_1		n.a.
	Ophiolite sequence of			Greenstone				
	(1) Koltas Complex (Formation) of MORB and OIT volcanics,				R_3–V	R_1	R_2	544 ± 8 (U–Pb)
	(2) Usa Complex of wehrlites, clinopyroxenites, and gabbros, and				ϵ_2	ϵ_{1-3}	R_1	n.a.
	(3) Salan (Tersa) Complex of dunites and harzburgites				ϵ_2	ϵ_{1-2}	R_1	n.a.
	Ust-Anzas Complex (Formation) of OIA and OIT volcanics			Greenstone to greenschist			V–ϵ_1	n.a.
	Siliceous–carbonate deposits (Belka and Karchit formations)					V, ϵ_1		n.a.
	Limestone–dolomite (Kabyrza and West Siberian formations) and chert–limestone (Spas Group) complexes				R_3–V	R_3–V		
R_3	Tersa Complex of carbonate–siliceous deposits intercalated with MORB and OIB metabasites			Greenschist	PR_1	PR_1	PR_1	n.a.
	Konzhin Complex	Konzhin section at the Tom' River	MORB-type metabasites	Epidote–amphibolite	PR_1	PR_1	PR_1	694 ± 43 (Sm–Nd)

n.a.—Not analyzed.

Table 2. Results of U–Pb zircon dating of magmatic and metamorphic rocks from the Tom' inlier and surrounding structures (Mountainous Shoria)

Sample no. (fraction, μm)	Rock type	U (ppm)	Pb (ppm)	$^{206}Pb/^{204}Pb$	$^{206}Pb/^{207}Pb$	$^{206}Pb/^{208}Pb$	$^{206}Pb/^{238}Pb$	$^{207}Pb/^{235}Pb$	Remarks
Ophiolite sequence, Koltas Complex, Tom' River section									
I-13	plagiorhyolite	250.7	17.7	317.5	9.88	4.09	0.05943	0.4541	$T = 544 \pm 8$ Ma, MSWD = 0.21; discordia is plotted using $T =$ 260 Ma for the lower intersect with concordia; samples donated by A.E. Izokh
I-36	plagiogranite	762.5	50.8	579.7	1.38	4.86	0.06166	0.4742	
Teba Complex, synonymous massif									
I-5193 (+100)	diorite	152	11.9	5059	16.70	9.75	0.078	0.6131	$T = 499 \pm 14$ Ma, MSWD = 6.1; discordia is plotted using $T =$ 260 Ma for the lower intersect with concordia; samples donated by A.E. Izokh
I-5193 (+100, r. f.)		121	9.7	6621	16.81	9.80	0.07975	0.63	
I-5193 (–100)		190	14.5	7216	17.01	10.43	0.07663	0.6	
I-5193 (–100, r. f.)		174	13.5	3172	16.26	9.47	0.07681	0.6029	
Teba Complex, Konchik–Koltas massif									
I-4793 (+100)	leucogabbro	319	25.5	7634	17.01	7.58	0.07785	0.6106	$T = 490 \pm 19$ Ma, MSWD = 12; discordia is plotted using $T =$ 260 Ma for the lower intersect with concordia; samples donated by A.E. Izok
I-4793 (+100, r. f.)		369	30.7	1397	17.15	7.44	0.08095	0.6392	
I-4793 (–100)		378	30.6	8369	17.04	7.35	0.07859	0.6172	
I-4793 (–100, r. f.)		330	27.6	11987	17.14	7.50	0.08057	0.6346	
I-4793 (–100 + 75)		330.8	24.6				0.07813	0.6102	
Teba Complex, Kolos massif									
3151 (–80 + 50)	gabbro	437.9	32.95				0.06966	0.5429	$T = 485 \pm 5$ Ma; lower intersect with concordia corresponds to 111 ± 53 Ma; samples donated by V.N. Pen'kin
3151 (+ 125)		209.4	17.04				0.07678	0.6011	
Tel'bes Complex, Azas massif									
615	granodiorite	770	39.1	3111	16.91	11.33	0.05113	0.3837	$T = 385 \pm 15$ Ma, MSWD = 16; discordia is plotted using $T =$ 0 Ma for the lower intersect with concordia; samples donated by A.P. Ponomareva
615 (r. f.)		674	36.8	6243	17.60	11.49	0.05532	0.4154	
617	melagranite	819	41.5	5423	17.59	10.48	0.05094	0.3803	
617 (r.f.)		765	39.9	7911	17.80	10.79	0.05264	0.3944	
Tashelga Complex, synonymous area									
94-6/14b (90)	metapelite (migmatitic Gr–Bi-gneiss)	342	26.3	1940	14.55	5.28	0.0708	0.5991	Preliminary data, see text for explanation; samples donated by S.A. Kargopolov and A.V. Plotnikov
94-6/14b (+100)		360	29.2	2050	14.68	6.81	0.0774	0.6518	
94-6/21b (60)		755	46.3	5208	16.40	31.92	0.0657	0.5274	
94-6/21b (90 + 75)		740	46.5	7042	16.80	10.14	0.0632	0.5013	
94-6/21b (90 + 60)		923	57.6	8000	16.57	14.38	0.0644	0.5206	
Tom' Complex, Tom' River section									
93-8c (+100)	Gr–Bi-granite gneiss	1387	53.5	1230	15.55	9.95	0.0373	0.2698	$^{206}Pb/^{238}U$ age $T = 236 \pm$ 10 Ma is calculated for the subconcordant point; sample donated by S.A. Kargopolov and A.V. Plotnikov
93-8c (+75)		668.3	27.3	3160	16.76	7.78	0.0403	0.3067	
93-8c (100–75)		866.9	35.3	3900	16.76	7.67	0.04015	0.3099	
Tom' Complex, granite vein in Teba massif									
5625 (–125 + 100)	granite	959	37.2				0.03929	0.2776	Concordant age $T = 251 \pm$ 4 Ma; sample donated by V.N. Pen'kin
Barsuk Complex, synonymous group of intrusions at the Tom' River									
702a (+100)	quartz-syenite	647	22.8				0.0342	0.243	Concordant age $T = 251 \pm$ 3.6 Ma; sample donated by A.P. Ponomareva
702a (–100 + 75)		730	29.7				0.0397	0.2838	
702a (–60)		1264	43.6				0.0336	0.238	

Table 2. (Contd.)

Sample no. (fraction, μm)	Rock type	U, (ppm)	Pb, (ppm)	$\frac{^{206}Pb}{^{204}Pb}$	$\frac{^{206}Pb}{^{207}Pb}$	$\frac{^{206}Pb}{^{208}Pb}$	$\frac{^{206}Pb}{^{238}Pb}$	$\frac{^{207}Pb}{^{235}Pb}$	Remarks
Porog Complex, synonymous massif									
637	granite	1347	51	14486	18.33	10.43	0.03821	0.2821	$T = 211 \pm 4$ Ma; the upper intersect with concordia corresponds to $T = 950 \pm 169$ Ma, MSWD = 8.7; samples donated by A.P. Ponomareva
637 (r. f.)		1433	49.5	14419	19.02	9.69	0.0347	0.2475	
638		1708	56.1	21621	19.76	9.47	0.03299	0.2272	
1		1791	60.2	10861	19.14	10.15	0.03389	0.2379	
639		1770	58	14414	19.59	9.53	0.03291	0.227	

Note: Zircons were separated using the standard heavy-liquid technique. The dissolution procedure was that described by Krogh (1973). Isotopic analysis at the Institute of Geochemistry and Analytical Chemistry in Moscow [sample nos. I-13, I-36, I-5193 (+100), I-5193 (–100), I-4793 (+100), I-4793 (–100), I-4793 (–100 to +75), 94-6/14b, 94-6/21b, 93-8c, 702a] was performed using the thermoionic emission method and CAMECA mass spectrometer TSN 206A with aluminosilicate gel as the ion emitter; precision of isotope dilution technique used to measure U and Pb concentrations is ±0.5%, and Pb contamination in the blank run not greater than 0.5 ng. The multicollector mass spectrometer Finnigan MAT-261 was used to analyze samples nos. 3151 and 5625 at the Institute of Precambrian Geology and Geochronology, St. Petersburg; in this case, the analytical precision for U and Pb concentrations is ±0.5%, and the blank run Pb contamination is below 0.2 ng. Other samples were analyzed at the Institute of Geology, Kazakhstan Academy of Sciences, Almaty, using the MI-1320 mass spectrometer equipped with a PRM-2 unit for the mass spectra registration; Pb contamination in the blank run is not greater than 0.5 ng. Measurements at different laboratories for the control zircon fractions showed the satisfactory convergence of results. Experimental data were processed using the ISOPOLT program by Ludwig (1990). The uranium decay constants used to calculate rock ages are those reported by Steiger and Jager (1976), and correction for common leads is done in accordance with model by Stacey and Kramers (1975). Size of zircon fractions is indicated in brackets, e.g., as (+100), meaning that grains are greater than 100 μm; undivided samples are without this indication; abbreviations (r.f.) mark residual fractions of crystal cores after 30–50% dissolution in hydrofluoric acid.

The Rb–Sr isotopic study is performed for granitoids of the Azas massif attributed either to Early, or to Middle Paleozoic in different cartographic legends for magmatic rocks of the region. In this case, our main purpose was to evaluate the state of disturbance in the Rb–Sr isotopic systems using the comparative analysis of data obtained for the whole rock samples and monomineral biotite fractions. In order to reveal the initial Sr-isotope ratios in granitoids, we studied their whole rock samples from those massifs, where we measured the U–Pb zircon ages. The used method of Rb–Sr isotope analysis was standard (Faure, 1990). The analytical equipment and procedure of data processing are indicated in Table 4 also showing the experimental results.

The Ar–Ar age measurements are used to study the monomineral amphibole and plagioclase fractions from amphibolites of the Konzhin Complex. Before the Ar–Ar isotope analysis, weighted mineral fractions (grain-size of 0.15–0.5 mm) enveloped together with tracer (biotite OCO MCA-11) in Al-foil were sealed in evacuated quartz vials and irradiated in the cadmium-platted channel of research reactor at the Tomsk Polytechnic University. The neutron flux variations were not grater than 2% in each run. The argon isotope composition was measured using the standard equipment for the K–Ar age method. Analyzing pure K_2SO_4 and CaF_2, we determined correction factors: $(^{36}Ar/^{37}Ar)_nCa = 0.798 \times 10^{-4}$; $(^{39}Ar/^{37}Ar)_nCa = 8.37 \times 10^{-4}$; $(^{40}Ar/^{39}Ar)_nK = 0.0573$. Criteria suggested by Fleck *et al.* (1977) were used by interpretation of Ar–Ar isotope measurements (incremental age spectra).

U–Pb, Sm–Nd, Rb–Sr, AND Ar–Ar DATES OF ROCK COMPLEXES AND Sm–Nd SYSTEMATICS OF GRANITOIDS

Considering the results of U–Pb, Sm–Nd, Rb–Sr, and Ar–Ar age measurements, we can draw the principal conclusion that none of metamorphic or magmatic rocks of the Tom' inlier is older than the second half of the Late Riphean.

The U–Pb zircon ages, obtained for gneissoid quartz-syenites of the Barsuk Complex, gneissoid granites of the Tom' Complex, and granitoids of the Porog Complex, correspond to concordant and subconcordant dates ranging within the interval of 251–211 Ma, i.e., within the Permian–Triassic interval (Fig. 2). As it is calculated from experimental data on zircon fractions bearing admixture of ancient radiogenic lead (including the crystal-core fraction after the 50% leaching), the granitoid protolith of the Porog Complex is 950 ± 170 Ma old, thus being within the range of the Late Riphean. This model date most likely represents the lower age limit of crust formation in the region.

The U–Pb zircon dating of gabbro and diorite samples from the Teba, Luzhba, and Kolos massifs point to

Table 3. Sm–Nd isotopic data for magmatic and metamorphic rocks from the Tom' inlier and surrounding structures (Mountainous Shoriya)

Sample no.	Rock or mineral	Age, Ma	Sm, μg/g	Nd, μg/g	$^{147}Sm/^{144}Nd$	$^{143}Nd/^{144}Nd$ ($\pm 2\sigma_{cp.}$)	$\varepsilon_{Nd}(0)$	$\varepsilon_{Nd}(T)$	T_{Nd} (DM)	T_{Nd} (DM-2st)
Metamorphic Konzhin Complex, Tom' River section										
93-2/31	MORB-type metabasalt	694	4.262	11.64	0.22131	0.513108 ± 7	+9.17	+6.10	–	–
93-5/12	ditto	"	4.887	13.46	0.21949	0.513109 ± 7	+9.19	+7.18	–	–
93-5/11wr	ditto	"	2.080	5.488	0.22913	0.513156 ± 7	+10.10	+7.24	–	–
93-5/11pl	plagioclase	"	4.962	19.14	0.15669	0.512832 ± 9	–	–	–	–
93-5/11am	amphibole	"	2.720	10.28	0.16000	0.512826 ± 6	–	–	–	–
93-7/10	tholeiitic microgabbr	"	2.763	8.793	0.18995	0.513022 ± 8	+7.49	+8.10	830	–
93-6/1	ditto	"	1.758	6.973	0.15243	0.512577 ± 9	–1.19	+2.74	1427	–
Ophiolite sequence, Koltas Complex of volcanic rocks ($\in_1$), Tom' River section										
I-37-94	subvolcanic plagiogranite	544	3.760	20.14	0.11286	0.512647 ± 9	+0.18	+6.01	762	782
Tel'bes Complex, synonymous massif ($\in_1$–O_1)										
I-54-93	diorite	499	3.375	18.51	0.11025	0.512584 ± 8	–1.05	+4.46	836	866
Tel'bes Complex, synonymous massif (D_1)										
T-65	quartz-diorite	385	3.487	15.96	0.13210	0.512749 ± 8	+2.17	+5.35	752	712
T-66	granodiorite	"	6.492	33.35	0.11766	0.512678 ± 7	+0.78	+4.67	751	761
T-67	granite	"	2.125	11.42	0.11254	0.512680 ± 8	+0.82	+4.96	710	730
Tel'bes Complex, Azas massif (D_1)										
616	granodiorite	385	4.214	21.47	0.11863	0.512582 ± 8	–1.09	+2.75	913	923
Barsuk Complex, synonymous group of intrusions (P_2–T_1)										
702B	syenodiorite	251	18.96	98.08	0.11685	0.512741 ± 6	+2.01	+4.57	646	656
Porog Complex, synonymous massif (T_3)										
654	quartz-diorite	211	6.773	41.61	0.09841	0.512632 ± 8	–0.12	+2.5	687	797
638	granite	"	3.111	20.72	0.09078	0.512675 ± 8	+0.72	+3.5	591	711

Note: Samples are analyzed by D.Z. Zhuravlev at the Institute of Ore Deposits, Petrography, Mineralogy, and Geochemistry, Russian Academy of Sciences. The standard procedure described by Richard *et al.* (1976) was used to extract Sm and Nd from rock or mineral samples. Mass spectrometers MI-1320 and Finnigan MAT-262 were used to analyze Sm and Nd isotope compositions, respectively. Analytical precision for Sm/Nd ratios is ±0.2%. The Nd isotopic ratios are normalized to $^{146}Nd/^{144}Nd = 0.7219$. Control analyses of the La Jolla Nd standard yielded the average value $^{143}Nd/^{144}Nd = 0.511842 \pm 14$ (N = 17). The indicated error magnitude was used to calculate the isochron confidence parameters. Values of $\varepsilon_{Nd}(T)$ are calculated on the basis of $^{143}Nd/^{144}Nd = 0.512638$ and $^{147}Sm/^{144}Nd = 0.1967$ characterizing CHUR, the homogeneous chondrite reservoir (Jacobsen and Wasserburg, 1984). Model ages $T_{Nd}(DM)$ are calculated in accordance with model by Goldstein and Jacobsen (1988) assuming $(^{143}Nd/^{144}Nd)_0 = 0.513151$ and $^{147}Sm/^{144}Nd = 0.21365$ in the depleted mantle reservoir. Calculating the protolith ages on the basis of two stage model (Liew and Hofman, 1988), we accepted the average crustal ratio $^{147}Sm/^{144}Nd = 0.12$ (Taylor and McLennan, 1985).

the Late Cambrian–Early Ordovician age of these rocks. Fallen into this age interval are not only "diorite-gneisses," but also massive gabbros and diorites (Fig. 3), although different rock groups have been formerly considered as heterochronous, and some of them have been attributed to the Early Proterozoic.

Analyzing amphibolites (N-MORB-type metabasalts) of the Konzhin Complex, we established the Sm–Nd isochron age of metamorphism: $T = 694 \pm 43$ (2σ) Ma, MSWD = 2.0, $\varepsilon_{Nd}(T) = 7.1 \pm 0.1$ (Fig. 4). The model Nd ages, which are calculated using various approaches, show that these rocks originally corresponded to basalts, which have been derived from the Late Riphean (or Middle–Late Riphean, not older) mantle reservoir depleted to a much greater extent than that of recent MORB. However, the Ar–Ar age spectra of the analyzed mineral fractions (Fig. 5) are much younger and correspond to the Early Devonian (amphibole, $T = 398 \pm 12$ Ma) and Permian–Triassic interval (amphibole, $T = 260 \pm 3$ Ma; plagioclase, $T = 238 \pm 4$ Ma). These dates reveal the multistage thermal history characterizing the Konzhin Complex of amphibolites, because the sealing temperature of K–Ar isotopic system is 600 ± 50°C for amphibole and 200 ± 50°C for plagioclase (Berger and York, 1981).

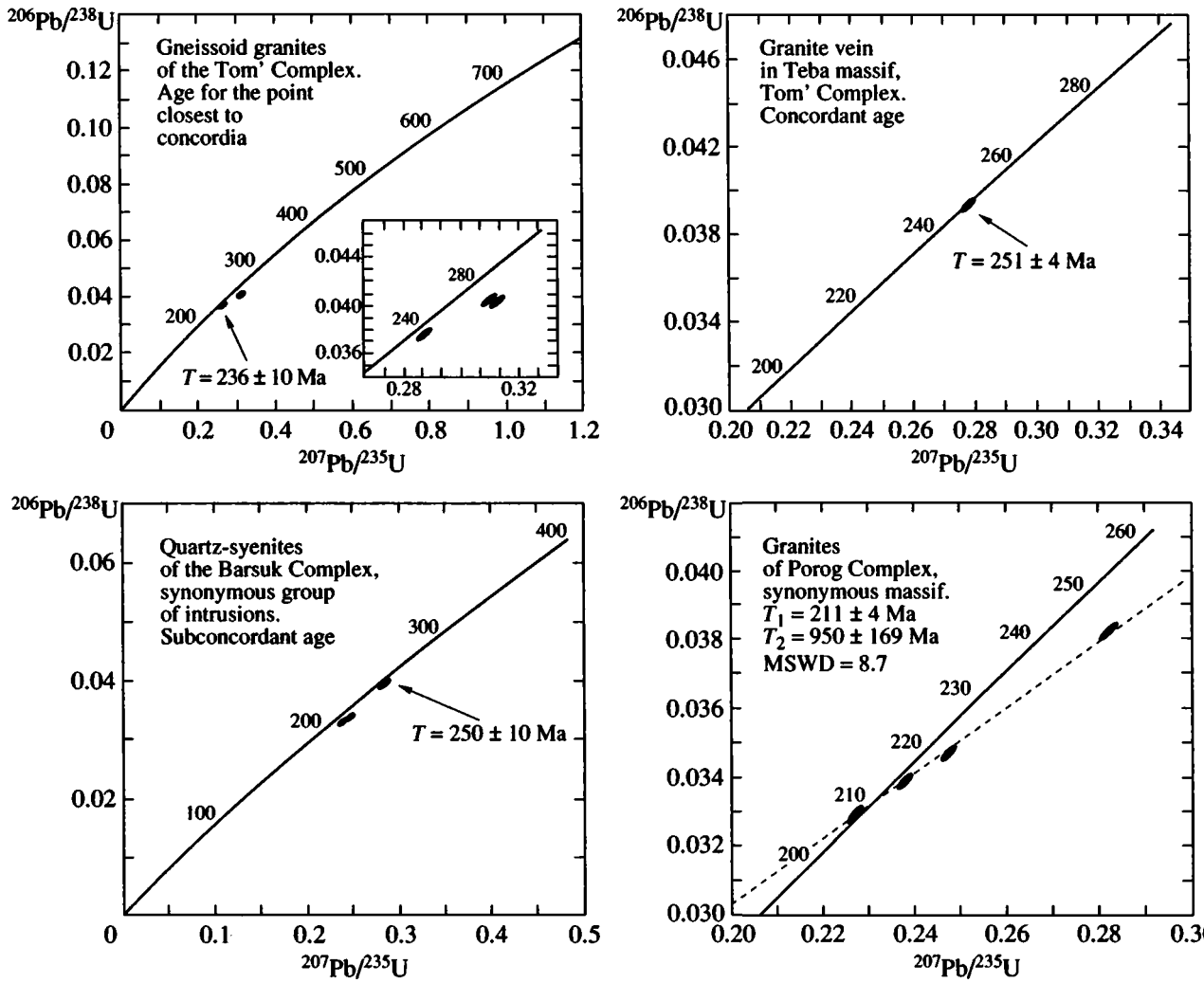
$^{206}Pb/^{238}U$
Gneissoid granites of the Tom' Complex. Age for the point closest to concordia
$T = 236 \pm 10$ Ma
$^{207}Pb/^{235}U$
Granite vein in Teba massif, Tom' Complex. Concordant age
$T = 251 \pm 4$ Ma
Quartz-syenites of the Barsuk Complex, synonymous group of intrusions. Subconcordant age
$T = 250 \pm 10$ Ma
Granites of Porog Complex, synonymous massif.
$T_1 = 211 \pm 4$ Ma
$T_2 = 950 \pm 169$ Ma
MSWD = 8.7

Fig. 2. U-Pb Concordia plots for zircons from the Barsuk, Tom', and Porog complexes of Mountainous Shoriya.

The tectono-thermal events, which are recorded in K–Ar isotopic systems of minerals from the Konzhin Complex, influenced as well other rock complexes of the Tom' inlier and surrounding structures. For instance, three whole rock samples of granitoids from the Azas massif (Tel'bes Complex) plot along an Rb–Sr isochron corresponding to the age of 407 ± 25 Ma, whereas the model Rb–Sr age calculated for the biotite fraction is 237 ± 2 Ma, i.e., much younger (Fig. 6). The older Rb–Sr age of whole rock samples is comparable, within limits of the analytical errors, with the U–Pb zircon age measured for the same granitoids (Ponomareva *et al.*, 1995; Vladimirov *et al.*, 1996). These preliminary results allow us to believe that the Early Devonian date marks the crystallization stage of granitoids, while the Triassic one corresponds to subsequent heating and cooling of rocks, because the sealing temperature of Rb–Sr isotopic system in biotite (300 ± 50°C) is much lower than that of U–Pb isotopic system in zircon (Harrison and McDougall, 1980; Farver and Giletti, 1989; Faure, 1990).

The above data demonstrate that U–Pb, Rb–Sr, and K–Ar isotopic systems are disturbed in all metamorphic and magmatic rocks of the Mountainous Shoriya. This factor appears to be responsible for discordant U–Pb isotopic ratios in zircons, for rejuvenated Rb–Sr ages of biotite from granitoid intrusions, and for resetting of K–Ar isotopic systems in amphiboles and plagioclases. Most of the intense tectono-thermal events, which upset the isotopic systems, apparently took place at the Late Paleozoic–Early Mesozoic boundary, for it was a time of intrusion of relatively large granitoid massifs (Barsuk, Tom', and Porog complexes).

The established disbalance of isotopic systems presents a special problem for dating plagiogranites of the volcanic Koltas Complex (those of the ophiolite rock association) and migmatitic gneisses of the Tashelga Complex.

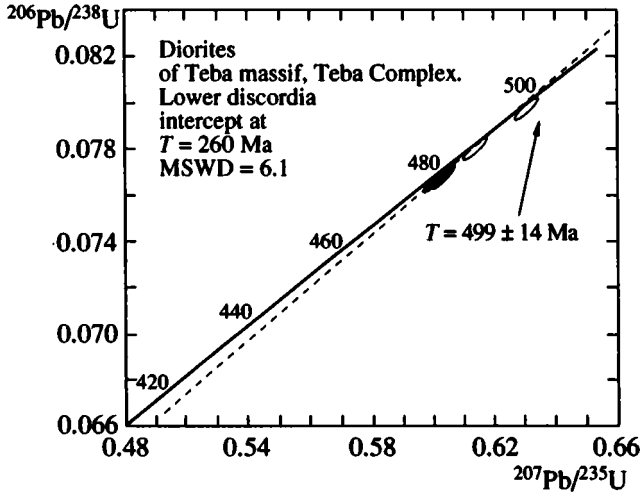

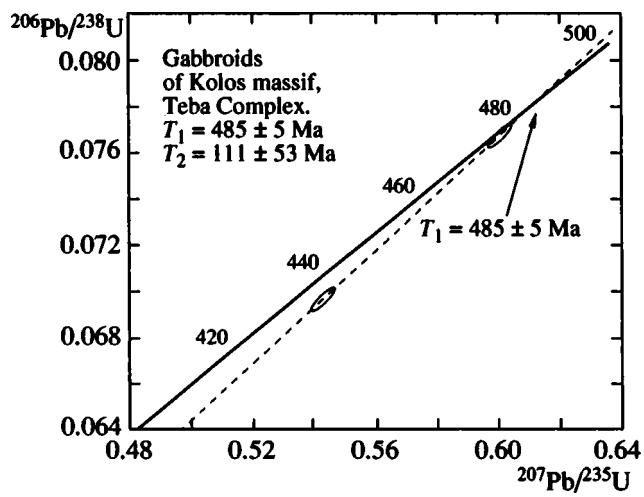

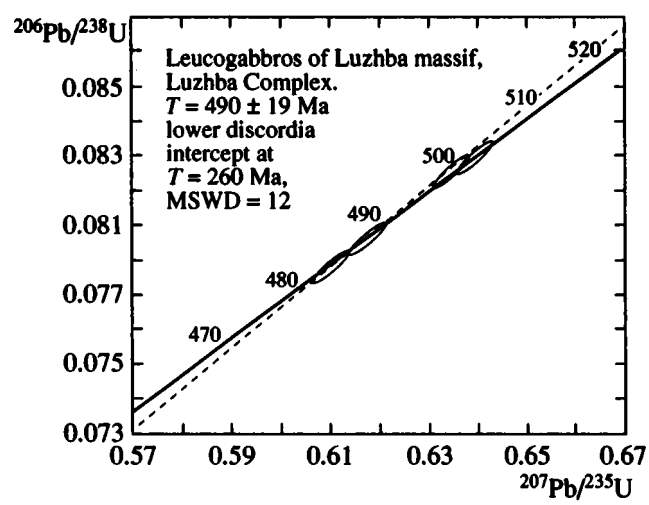

Fig. 3. U-Pb Concordia plots for zircons from the Teba and Luzhba complexes of Mountainous Shoriya.

Zircons from plagiorhyolites and subvolcanic plagiogranites of the Koltas Complex yielded two highly discordant U–Pb isotopic ratios. If T = 260 Ma can be taken for the time mark of most intense tectono-thermal events in the region, then, recalculating the experimental data, we obtain an admissible isochron relation corresponding to T = 544 ± 8 Ma (Fig. 7). This tentative result points to the Early Precambrian age of ophiolites. The one-stage model age of plagiogranites is therewith T_{Nd}(DM) 760 Ma and $\varepsilon_{Nd}(T)$ = +5.86 (Table 3).

Zircons from migmatitic gneisses of the Tashelga Complex, whose critical sillimanite–K-feldspar mineral assemblage corresponds to the amphibolite grade of metamorphism, yielded five discordant U–Pb isotopic ratios displaced toward the lower discordia intersect (see Table 1). Calculations on the basis of York's method suggest that the rocks recorded two isotopic events happened in Late Paleozoic–Early Mesozoic and Late Riphean times ($T_1 \approx 300$ Ma and $T_2 \approx 900$ Ma), however the disbalance of U–Pb isotopic systems and low separation degree of experimental data points are responsible for the insufficient confidence level of the calculated discordia. Superposing the lower intersection point at T = 260 Ma (see above explanation for this date), we obtain the protolith age of 790 ± 120 Ma (Fig. 7). This age value is concordant, within limits of the analytical errors, with the U–Pb age of protolith for granitoids of the Porog Complex (950 ± 170 Ma).

The Late Riphean age of crust-forming processes in the region is also evident from Sm–Nd isotopic data on other granitoids. As established (Table 3, Fig. 8), all granitoids of the region show $\varepsilon_{Nd}(T)$ values greater than zero. The maximum value $\varepsilon_{Nd}(T)$ = +6.0 is characteristic of plagiogranites from the ophiolite rock association

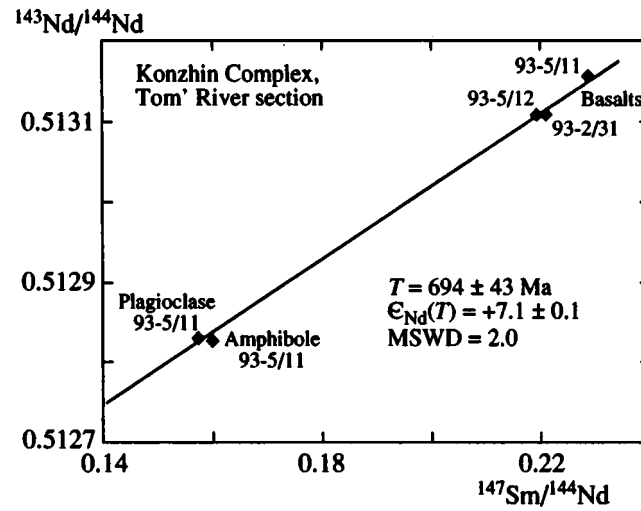

Fig. 4. Sm–Nd isochron plot for metabasites (amphibolites) of the Konzhin Complex of Mountainous Shoriya.

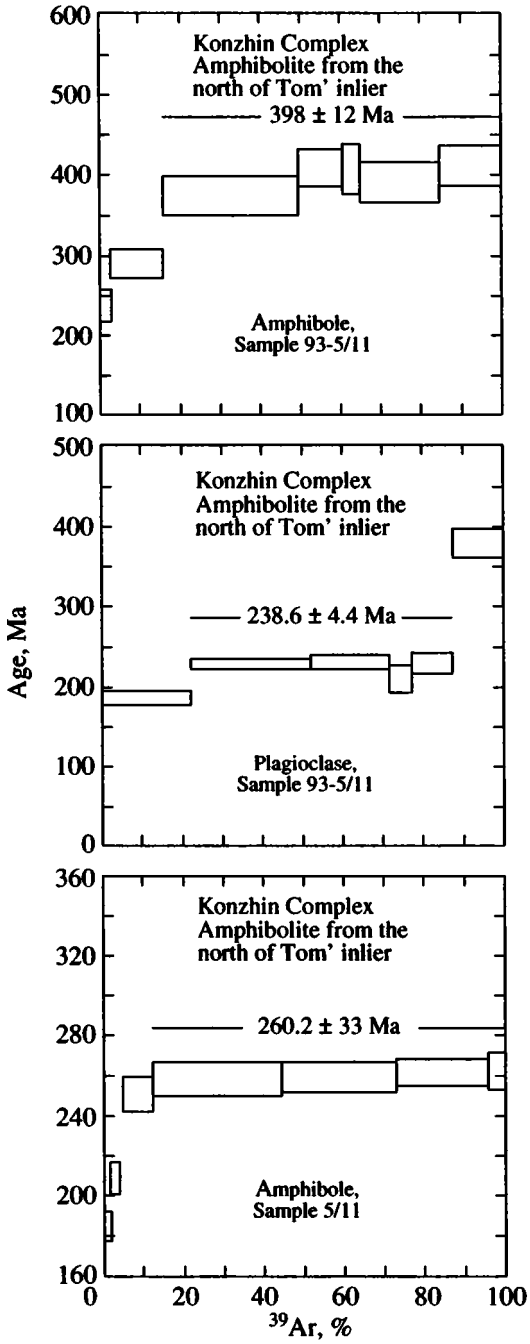

Fig. 5. Ar–Ar age spectra for mineral fractions of amphibolites of the Konzhin Complex of Mountainous Shoriya (results obtained by A.V. Travin and V.A. Ponomarchuk at the Analytical Center of Joint Institute of Geology, Geophysics, and Mineralogy, Novosibirsk; samples donated by S.A. Kargopolov and A.V. Plotnikov).

(ϵ_1^1), whereas $\varepsilon_{Nd}(T) = +2.5$ is typical of granitoids of the Porog Complex (T_3). The calculated one- and two-stage Sm–Nd model ages range between 590 and 920 Ma, thus being within the Late Riphean–Vendian stratigraphic interval. It is remarkable as well that data

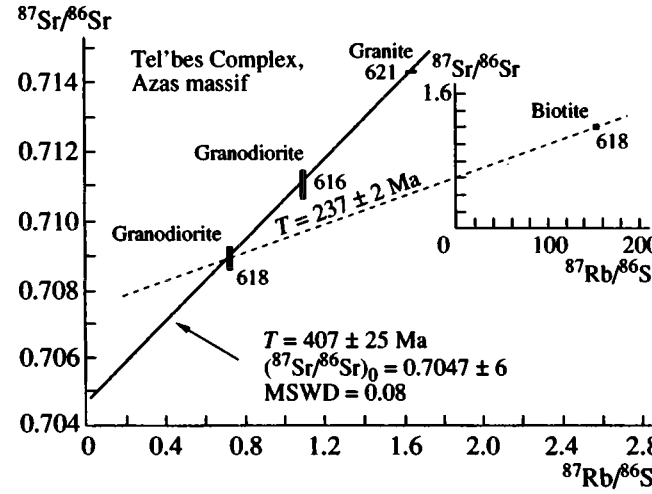

Fig. 6. Estimated Rb–Sr isochron relationships for whole rock samples and biotite fraction from the Azas massif, Tel'bes Complex of Mountainous Shoriya.

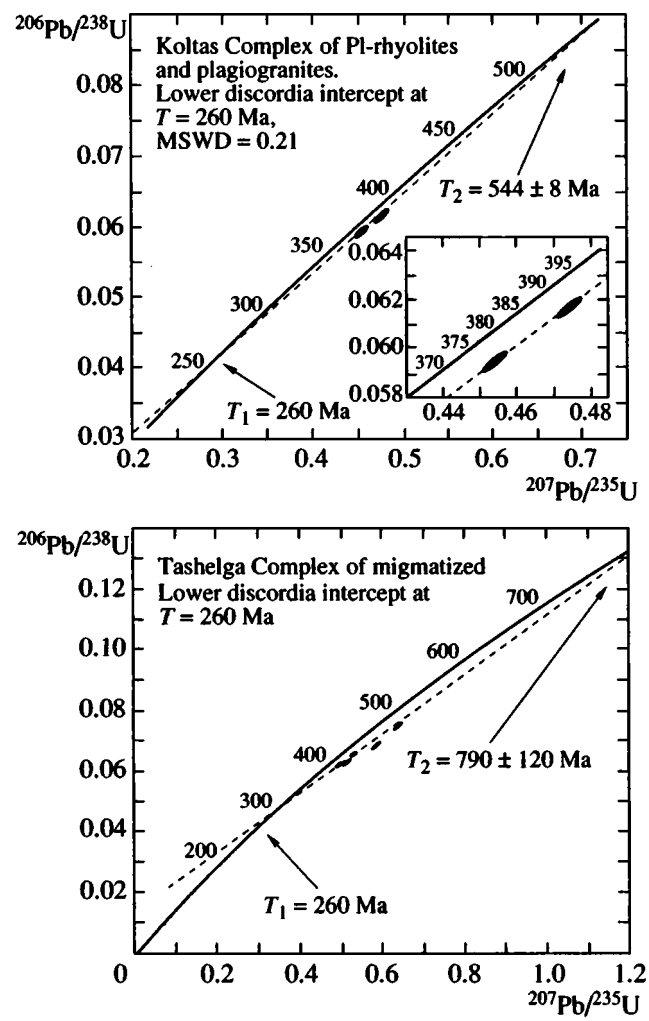

Fig. 7. U-Pb Concordia plots for zircons from Pl-rhyolites and subvolcanic plagiogranites of the Koltas Complex (ophiolite sequence) and from migmatitic gneisses of the Tashelga Complex.

Table 4. Rb–Sr isotopic data for magmatic and metamorphic rocks from the Tom' inlier and surrounding structures (Mountainous Shoriya)

Sample no.	Rock or mineral	Rb (ppm)	Sr (ppm)	$^{87}Rb/^{86}Sr$	$^{87}Sr/^{86}Sr$	$(^{87}Sr/^{86}Sr)_0$	$\varepsilon_{Sr}(T)$
Tel'bes Complex, Azas massif (D_1)							
616	granodiorite	97.4	255.9	1.1	0.71100 ± 45	0.7047 ± 9	+13.03
618	granodiorite	89.0	361.1	0.707	0.70880 ± 3.7	0.7048 ± 9	+12.38
621	granite	159.26	216.8	1.637	0.71417 ± 1	0.7048 ± 51	+16.24
618	biotite	440.3	8.7	153.3	1.22299 ± 23	–	–
Barsuk Complex, synonymous group of intrusions (P_2)							
702‡	quartz-syenite	134.2	1183.1	0.328	0.70523 ± 8	0.70402 ± 6	–2.08
702,	syenodiorite	116.3	691.2	0.486	0.70916 ± 23	0.7073 ± 4	+45.8
Tom' Complex (P_2–T_1)							
93-9/12	leucogranite	103.0	289.0	1.026	0.70822 ± 10	0.7046 ± 8	+7.8
Porog Complex, synonymous massif (T_3)							
670	granodiorite	68.0	370.2	0.528	0.70554 ± 11	0.70393 ± 6	–4.25
662	granite	110.8	261.9	1.220	0.70523 ± 8	0.7015 ± 6	–38.14

Note: Rb–Sr isotopic systems are studied by V.A. Ponomarchuk at the Analytical Center of the Joint Institute of Geology, Geophysics, and Mineralogy, Siberian Division, Russian Academy of Sciences. Measurements in two-tape regime have been carried out using mass spectrometer MI-1201"T". Blank values for Rb and Sr are 2 and 4 ng, respectively. The analytical error for Rb/Sr ration is below 1.5%. According to a series of control measurements, the average $^{87}Sr/^{86}Sr$ ratio for the VNIIM standard is 0.70802 ± 11 (95%). Experimental data are processed using the ISOPLOT program (Ludwig, 1990) and conventional decay constant of rubidium (Faure, 1990). Parameters $(^{87}Sr/^{86}Sr)_0$ and $\varepsilon_{Sr}(T)$ are calculated with due account for the U–Pb ages corresponding to 385 Ma for the Azas massif, 250 Ma for the Barsuk Complex, 236 Ma for the Tom' Complex, and 211 Ma for the Porog massif.

points of Nd isotope composition in heterochronous granitoids of the Mountainous Shoriya plot in the diagram of $\varepsilon_{Nd}(T)$ versus age (Fig. 8) along an evolutionary trend considerably deviating from that characterizing the Early Precambrian continental crust of Siberian platform.

The high $\varepsilon_{Nd}(T)$ values suggest that granitoids of the Mountainous Shoriya originated in a substrate whose rocks have been derived from a depleted mantle source. The low and abnormally low values of initial Sr isotope ratios typical of Devonian and Permian–Triassic granitoids (Table 4) also indicate that the region is lacking an ancient sialic basement.

DISCUSSION AND CONCLUSIONS

The obtained geochronological data on metamorphic and magmatic rocks of the Tom' inlier and surrounding structures allow us to discuss, with due account for available results of stratigraphic studies, the development of crystalline basement in the Mountainous Shoriya.

As noted above (see also Table 1), we failed to reveal rock complexes of the region (or their protoliths), which can be considered as predating the Late Riphean. Metabasites of the Konzhin Complex can be classed with basalts of the past open ocean (Kargopolov *et al.*, 1995; Plotnikov *et al.*, 1996; Plotnikov *et al.*, in press) and correspond in age to the latest Riphean. A rock sequence widespread to the east of the Tom' inlier (Fig. 1) consists predominantly of carbonates and is attributed to the Vendian–Lower Cambrian (?). Judging from the composition and inner structure, this sequence is an analogue of the Kabyrza and West Siberian formations and of the Spassk Group widespread in the Mrassu Uplift. Accordingly, it is conceivable that metabasites represent as well the basement rocks of this uplift corresponding to a past intraoceanic rise crowned with the carbonate platform. Another intraoceanic rise with the carbonate platform has been recently distinguished nearby (the Batenevskii Range) by Kheraskova and Gavrilova (1996). This range is separated from the Mrassu Uplift by the distribution area of Vendian–Lower Cambrian basaltic sequence. The sequence is composed of OIA- and OIT-basalts of the Ust-Anzas Formation associated with tholeiites of the Koltas Formation. Rocks of the last type are attributed to ophiolites of the Mountainous Shoriya.

As is established in this study, rock complexes of the Late Paleozoic–Early Mesozoic age are quite widespread in the Mountainous Shoriya that is an unexpected result. Exactly these complexes of predominant granitoids, attributed formerly to the deep Precambrian, were traditionally interpreted as indicators of

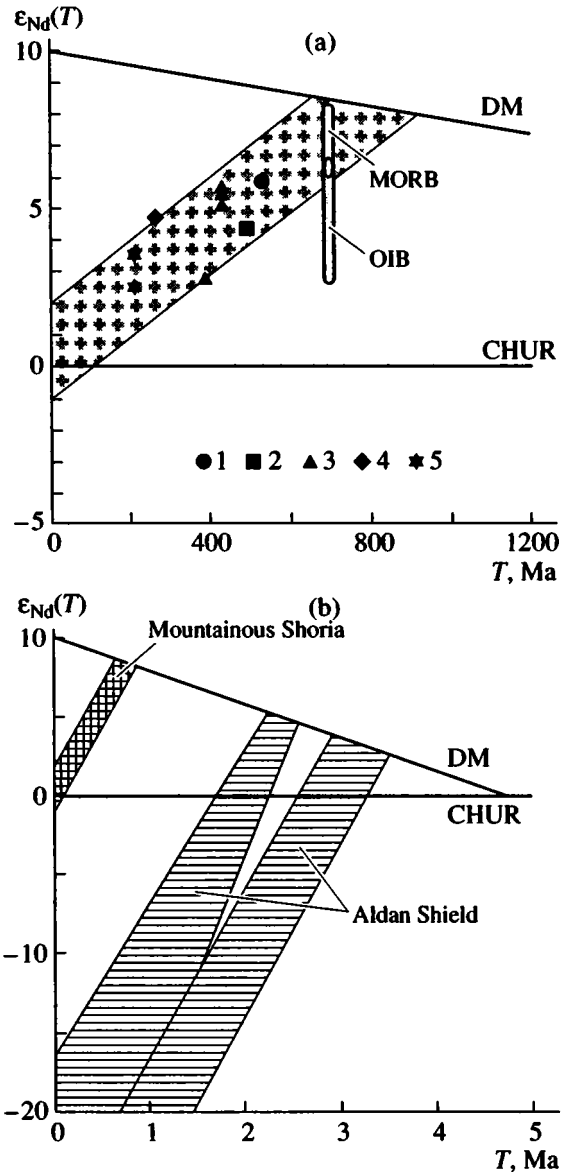

Fig. 8. A model of Nd isotope evolution for magmatic rocks of the Mountainous Shoria. (a) Age-dependent variations of $\varepsilon_{Nd}(T)$ for various rock types of the region: (1) plagiogranites of ophiolite sequence, ϵ_1; (2) diorites ϵ_3–O_1; (3) quartz-diorites, granodiorites, and granites, D_1; (4) syenodiorites, P_2–T_1; (5) quartz-diorites and granites, T_3. (b) Variations of Nd isotope composition at the Late Riphean stage of crust formation in the Mountainous Shoriya as compared to principal stages of continental crust formation in the Aldan shield (Sal'nikova *et al.*, 1993; Kotov *et al.*, 1995; Kovach *et al.*, 1996).

ancient sialic basement underlying other rocks of the region. Our results demonstrate, however, that they are related in origin to the development of the Kuznetsk Alatau shear zone characterized by intense stress-dislocations, blastic deformation, and mylonitization of rocks. In some tectonic slices thrown up from different depth levels, we distinguished rheomorphic transformations of the amphibolite grade, which were responsible for migmatization and anatexis of the rocks (the polymetamorphic Tashelga Complex and the second sillimanite–K-feldspar stage of metamorphism dated back to 320–260 Ma). Magmatic rocks of this stage are gneissoid granites of the Tom' and syenites of the Barsuk complexes (P_2–T), and also granitoids of the Porog Complex (T_3). Equally remarkable are the isotopic specifics of the Late Triassic K-granitoids of the Porog Complex, which are most widespread inside the Tom' inlier. These rocks show low $\varepsilon_{Sr}(T)$ values ranging from –38.2 to –4.3 and high magnitudes of $\varepsilon_{Nd}(T)$ from +2.5 to +3.5 (Table 4). Isotopic parameters of this kind are characteristic of mantle rocks, but their significance should be discussed elsewhere, as the respective problems are beyond the scope of our current study. The only thing we would like to mention here is that they do not contradict our main conclusion concerning the absence of Precambrian crystalline basement beneath the study region.

ACKNOWLEDGMENTS

This work is supported by the Russian Foundation for Basic Research (RFBR), project nos. 96-05-66227, 96-05-65961, 96-05-65970, 97-05-65303, and 98-05-65294, and also by the Yuzhsibgeolkom project no. 13-93-96/1 and INTAS–RFBR project no. 95-0934.

Reviewers M.A. Semikhatov and V.V. Khomentovskii

REFERENCES

Berger, G.W. and York, D., Geothermometry from $^{40}Ar/^{39}Ar$ Dating Experiments, *Geochim. Cosmichim. Acta*, 1981, vol. 45, pp. 795–811.

Churakov, A.N., History of Our Concepts Concerning the Northwestern Margin of "Ancient Crown of Asia," *Izv. Geol. Kom.*, 1927, vol. 46, no. 1, pp. 45–69.

Dodin, A.L., *Geologiya i poleznye iskopaemye Kuznetskogo Ala-Tau* (Geology and Mineral Resources of the Kuznetsk Alatau), Moscow: Ugletekhizdat, 1948.

Dolgushin, S.S., The Kuznetsk Alatau Deeply Rooted Fault and Related Metamorphism and Granite Magmatism, *Izv. Akad. Nauk SSSR, Ser. Geol.*, 1969, no. 2, pp. 98–104.

Farver, J.R. and Giletti, B.J., Oxygen and Strontium Diffusion Kinetics in Apatite and Potential Applications to Thermal Theory Determinations, *Geochim. Cosmochim. Acta*, 1989, vol. 53, pp. 1621–1631.

Faure, G., *Principles of Isotope Geology*, New York: Wiley and Sons, 1986. Translated under the title *Osnovy isotopnoi geologii*, Moscow: Mir, 1989.

Fleck, R.J., Sutter, J.F., and Elliot, D.H., Interpretation of Discordant $^{40}Ar/^{39}Ar$ Age-Spectra of Mesozoic Tholeiites from Antarctica, *Geochim. Cosmochim. Acta*, 1977, vol. 41, pp. 15–32.

Geologicheskaya karta zapadnoi chasti Altae-Sayanskoi skladchatoi oblasti, masshtab 1 : 500 000 (Geological Map of the Western Altai–Sayan Foldbelt, Scale 1 : 500 000), Gintsinger, A.B., Ed., Moscow: VANPO "Aerogeologiya," 1977.

Geologiya SSSR, tom XIV, Zapadnaya Sibir'. Ch. 1: Geologicheskoe opisanie (Geology of the USSR, vol. XIV, part 1: Geological Description), Moscow: Nedra, 1967.

Goldstein, S.J. and Jacobsen, S.B., Nd and Sr Isotopic Systematics of Rivers Water Suspended Material: Implications for Crustal Evolution, *Earth Planet. Sci. Lett.*, 1988, vol. 87, pp. 249–265.

Harrison, T.M. and McDougall, I., Investigations of an Intrusive Contact, Northwest Nelson, New Zealand: Thermal, Chronological and Isotopic Constraints, *Geochim. Cosmochim. Acta*, 1980, vol. 44, pp. 1985–2003.

Izokh, A.E., Gibsher, A.S., Vladimirov, A.G., and Tokarev, V.N., Ordovician Gabbro Associations in the Mountainous Shoria and Salair: Geodynamic Interpretaion, in *Novye dannye o geologii i poleznykh iskopaemykh Altae-Sayanskoi skladchatoi oblasti* (New Data on Geology and Mineral Resources of the Altai–Sayan Folded Zone), Novokuznetsk: YUZHSIBGEOLKOM, 1995, pp. 200–202.

Jacobsen, S.B. and Wasserburg, G.J., Sm–Nd Evolution of Chondrites and Achondrites, *Earth Planet. Sci. Lett.*, 1984, vol. 67, pp. 137–150.

Kargopolov, S.A. and Plotnikov, A.V., Metamorphism in the Tom' Inlier and Surrounding Structures, in *Novye dannye o geologii i poleznykh iskopaemykh Altae-Sayanskoi skladchatoi oblasti* (New Data on Geology and Mineral Resources of the Altai–Sayan Folded Zone), Novokuznetsk: YUZHSIBGEOLKOM, 1995, pp. 221–223.

Kargopolov, S.A., Esin, S.V., Plotnikov, A.V., and Kireev, A.D., Metavolcanics of the Tom' Inlier and Surrounding Structures, in *Novye dannye o geologii i poleznykh iskopaemykh Altae-Sayanskoi skladchatoi oblasti* (New Data on Geology and Mineral Resources of the Altai–Sayan Folded Zone), Novokuznetsk: YUZHSIBGEOLKOM, 1995, pp. 223–225.

Kheraskova, T.N. and Gavrilova, E.V., Tectonics and Sedimentology of Upper Riphean–Cambrian Carbonate Deposits in the Batenevskii Range (Kuznetsk Alatau), *Geotektonika*, 1996, no. 3, pp. 54–66.

Khomentovskii, V.V., Rock Formations of Structural-Lithologic Zones in the Southwest of Siberia and Related Mineral Deposits, in *Zakonomernosti razmeshcheniya poleznykh iskopaemykh* (Distribution Trends of Mineral Deposits), Moscow: Akad. Nauk SSST, 1960, vol. 3, pp. 7–87.

Klyarovskii, V.M., *Geokhronologiya gornykh oblastei yugozapadnoi chasti obramleniya sibirskoi platformy* (Geochronology of Orogenic Structures to the Southwest of Siberian Platform), Novosibirsk: Nauka, 1972, p. 257.

Kotov, A.B., Kovach, V.P., Sal'nikova, E.B., *et al.*, Stages of Continental Crust Formation in the Central Part of the Aldan Granulite–Gneiss Area: U–Pb and Sm–Nd Isotopic Data on Granitoids, *Petrologiya*, 1995, vol. 3, no. 1, pp. 99–110.

Kovach, V.P., Kotov, A.B., Sal'nikova, E.B., *et al.*, Sm–Nd Isotopic Systematics of the Kurumkan Subgroup, the Iengra Group of Aldan Shield, *Stratigr. Geol. Korrelyatsiya*, 1996, vol. 4, no. 3, pp. 3–10.

Krogh, T.E., A Low-Contamination Method for Hydrothermal Decomposition of Zircon and Extraction of U and Pb for Isotopic Age Determination, *Geochim. Cosmochim. Acta*, 1973, vol. 37, pp. 485–494.

Kuznetsov, V.A., Geotectonic Zoning of the Altai–Sayan Folded Area, in *Voprosy geologii Azii* (Problems of Geology in Asia), Moscow: Akad. Nauk SSSR, 1954, vol. 1, pp. 202–227.

Lepezin, G.G., Letuvninkas, A.I., Shepel', A.B., and Ivonin, I.P., Pecuiliarities of Regional Metamorphism in the Kuznetsk Alatau and Mountainous Shoria, *Geol. Geofiz.*, 1975, no. 8, pp. 45–53.

Liew, T.C. and Hofmann, A.W., Precambrian Crustal Components, Plutonic Associations, Plate Environment of the Hercynian Fold Belt of Central Europe: Implications from a Nd and Sr Isotopic Study, *Contrib. Mineral. Petrol.*, 1988, vol. 98, pp. 129–138.

Ludwig, K.R., ISOPLOT for MS-DOS, Version 2.0, *U.S. Geol. Survey Open-File Rept.*, 1990, no. 88-577, pp. 1–38.

Monich, V.K., *Geologiya i petrologiya raiona Mrasskikh porogov v Gornoi Shorii* (Geology and Petrology of the Mrassu Rapids, Mountainous Shoria), Moscow: Geolkom, 1938.

Plotnikov, A.V., Kargopolov, S.A., Vladimirov, A.G., and Zhuravlev, D.Z., MORB and OIB Rock Types in Metamorphic Sequences of the Tom' Inlier and Surrounding Structures (Mountainous Shoria), in *Materialy nauchnoi konferentsii RFFI "Geodinamika i evolyutsiya Zemli"* (Proc. Sci. RFBR Conference on the Earth's Geodynamics and Evolution), Novosibirsk, 1996, p. 101.

Plotnikov, A.V., Stupakov, S.I., Babin, G.A., *et al.*, Ophiolites of the Kuznetsk Alatau: Age and Geodynamic Setting, *Dokl. Ross. Akad. Nauk*, (in press).

Ponomareva, A.P., Vladimirov, A.G., Khalilov, V.A., and Ponomarchuk, V.A., Heterogeneous Granitoids of the Tom' Inlier and Surrounding Structures (Mountainous Shoria), in *Novye dannye o geologii i poleznykh iskopaemykh Altae-Sayanskoi skladchatoi oblasti* (New Data on Geology and Mineral Resources of the Altai–Sayan Folded Zone), Novokuznetsk: YUZHSIBGEOLKOM, 1995, pp. 189–191.

Rabochaya korrelyatsionnaya skhema magmaticheskikh i metamorficheskikh kompleksov Kuznetskogo Alatau (Practical Correlation Scheme for Magmatic and Metamorphic Rock Complexes of the Kuznetsk Alatau), Khomichev, V.L., Ed., Novosibirsk: SNIIGGIMS, 1996.

Regional'nye skhemy magmatizma Altae-Sayanskoi skladchatoi oblasti (Regional Stages of Magmatism in the Altai–Sayan Foldbelt), Leningrad: VSEGEI, 1978.

Resheniya Vsesoyuznogo stratigraficheskogo soveshchaniya po dokembriyu, paleozoyu i chetvertichnoi sisteme Srednei Sibiri, ch. 1, (Resolutions of the All-Union Stratigraphic Conference on Precambrian, Paleozoic, and Quaternary in Central Siberia, Pt. 1), Leningrad: VSEGEI, 1983.

Richard, P., Shimizu, N., and Allegre, C.J., $^{143}Nd/^{144}Nd$ as Natural Tracer: An Application to Oceanic Basalts, *Earth Planet. Sci. Lett.*, 1976, vol. 31, pp. 269–278.

Sal'nikova, E.B., Kovach, V.P., Kotov, A.B., and Nemchina, A.A., Stages of Formation and Evolution of the Aldan Shield Crust: Sm-Nd Data on Granitoids, Abstracts of Papers, *XIII Simposium po geokhimii izotopov* (13th Symposium on Isotope Geochemistry), Moscow: GEOKHI, 1992, pp. 172–173.

Stacey, J.S. and Kramers, I.D., Approximation of Terrestrial Lead Isotope Evolution by a Two-Stage Model, *Earth Planet. Sci. Lett.*, 1975, vol. 26, pp. 207–221.

Steiger, R.H. and Jager, E., Subcomission of Geochronology: Convention of the Use of Decay Constants in Geo- and Cosmochronology, *Earth Planet. Sci. Lett.*, 1976, vol. 36, pp. 359–362.

Taylor, S.R. and McLennan, S.M., *The Continental Crust: Its Evolution and Composition*, London: Blackwell, 1985.

Vladimirov, A.G., Shokal'skii, S.P., Khalilov, V.A., *et al.*, Stages and Intensity of Granite Formation in the Altai, Salair, and Kuznetsk Alatau, in *Materialy nauchnoi konferentsii RFFI "Geodinamika i evolyutsiya Zemli* (Proc. Sci. RFBR Conference on the Earth's Geodynamics and Evolution), Novosibirsk, 1996, pp. 87–89.

Stratigraphy and Geological Correlation, Vol. 7, No. 5, 1999, pp. 452–464. Translated from Stratigrafiya. Geologicheskaya Korrelyatsiya, Vol. 7, No. 5, 1999, pp. 43–55.
Original Russian Text Copyright © 1999 by Volkova.
English Translation Copyright © 1999 by МАИК "Наука/Interperiodica" (Russia).

Acritarchs from Upper Beds of the Upper Cambrian–Lower Tremadocian of the Moscow Syneclise

N. A. Volkova

Geological Institute, Russian Academy of Sciences, Pyzhevskii per. 7, Moscow, 109017 Russia

Received November 15, 1997; in final form, January 20, 1998

Abstract—The Cambrian–Ordovician boundary beds of the Moscow syneclise contain three acritarch assemblages; one of them is from the uppermost part of the Upper Cambrian (UC4B-1) and the other two from the lower Tremadocian (OT1 and OT2). In taxonomy, the studied assemblages are similar to those of the lower Tremadocian in the Peri-Gondwana cold-water province owing to the climatic cooling of that time.

Key words: *acritarchs, Upper Cambrian, lower Tremadocian, Moscow syneclise, Baltic province*

The Tremadocian acritarchs of the Moscow syneclise have bun little studied, though some information about them can be obtained from publications by Aristova (1980a, 1980b). The acritarch assemblages of the Kuvshinovo and Obolidae Beds of the Moscow syneclise, i.e., assemblages VIII–XII (Umnova and Fanderflit, 1971) and assemblages I–III (Umnova, 1975), lack the typical Tremadocian taxa and apparently belong, as was shown earlier (Volkova, 1990), to the Middle–Late Cambrian.

The age of the acritarch assemblage from the upper part of the Bugino Formation is reassessed (borehole Rybinsk-1; 1785.4–1793.4-m interval). At first, this assemblage was considered as an equivalent of the Cambrian–Tremadocian assemblage US5 (Volkova, 1990). Later, it was referred to the lower Tremadocian assemblage OT1 (Volkova, 1995). In the present paper, it is identified as a separate assemblage UC4B-1 and is dated back to the latest Cambrian, if the base of the conodont *Cordylodus proavus* zone is assumed to be marking the Cambrian–Ordovician boundary (Apollonov *et al.*, 1985).

Three acritarch assemblages were recovered for the first time from the Ukhrino (2131–2154-m interval) and Sementsovo (2119–2131-m interval) formations of the Mar'ino-1 borehole drilled in the Danilov area in the central part of the Moscow syneclise (see figure). Their age was determined on the basis of fauna from the neighboring reference sections drilled in the Danilov area. The Ukhra Formation of this region is dated back to the late Tremadocian on the basis graptolites: *Dyctyonema* aff. *uralense* Obut, *D. murrayi* (Mons.), *Bryograptus ramosus* (Brögg), *Clonograptus flexilis* (Hall.), and others. The Sementsovo Formation, the age of which corresponds to that of the lower part of the Arenigian Stage, contains *Tetragraptus phyllograptoides* (Linn.), *T. approximatus* Nich., *Didymograptus geometricus* Töernq, and others; there are also articulate brachiopods and conodonts (Dmitrovskaya,1991). Recently, *Dictyonema* cf. *flabelliforme* (Eichw.) was found within the Sementsovo Formation in the Mar'ino-1 borehole at the depth of 2119.2 m (oral communication by A.R. Orlova).

Acritarchs were also found in the four samples from the Mar'ino-1 borehole. Two of them are from the depth interval of 2141.7–2147.1 m, which is referred to the Ukhra Formation, and the other two from the interval of 2118.4–2127.8 m corresponding to the Sementsovo Formation. The studied intervals are composed of alternating light-gray quartz sandstones, gray siltstones, mudstones, and argillaceous clays.

All samples yielded a considerable amount of well-preserved acritarchs. Apart from the undamaged specimens, there was a large number of destroyed and semidestroyed forms (up to 50% and more) almost undeterminable. Three acritarch assemblages are distinguished; the assemblage UC4B-1 is recovered from the interval of 2141.7–2147.1 m of the Ukhra Formation, and assemblages OT1 and OT2 characterize the interval of 2118.4–2127.8 m of the Sementsovo Formation. The species of these assemblages and quantitative distribution parameters of separate taxa are listed in Table 1. The diacrodian acritarchs dominate in all assemblages; there are also many representatives of the Herkomorphitae subgroup and the *Polygonium* genus (Plates I–IV).

The acritarch studied indicate that the Ukhra and Sementsovo formations of the Mar'ino-1 borehole in the interval of 2118.4–2147.1 m are of the Late Cam-

brian–early Tremadocian age. These data, however, cannot be applied to the Ukhra and Sementsovo formations penetrated in other reference sections of the Danilov area, if we assume the diachronous age of these formations in the region.

The assemblage UC4B-1 consisting of *Arbusculidium ornatum, A. ramusculosum, Nellia acifera,* and *N. sukatschevii* was obtained from two samples of the Ukhra Formation (interval of 2141.7–2147.1 m). It is established for the first time and is as yet found only in the Moscow syneclise. The typical species of the assemblage are *A. ornatum* (Combaz) Fensome *et al.*, *A. ramusculosum* (Combaz) Fensome *et al.*, *Multiplicisphaeidium* sp. I, and *Vulcanisphaera* cf. *V. capillata* Jardine *et al.*, which appear at the lower boundary of the interval. Also typical are *N. acifera* (N. Umn.) Volk., *N. sukatschevii* (Tim.) Volk., *Polygonium sexradiatum* (Tim.) Volk., *Schizodiacrodium digermulense* (Welsch), and *S. fibrosum* Golub et Volk., all these species passed from the Upper Cambrian assemblage UC4B (Volkova, 1990) and disappear at the level of the upper boundary of the assemblage range. Moreover, there are species of a wider Cambrian–Tremadocian distribution. These are *Arbusculidium destombesii* Deunff, *Baltisphaeridium capillatum* (Naum.) N. Umn., *Cymatiogalea cuvillieri* (Deunff) Deunff, *C. velifera* (Downie) Martin, *Dasydiacrodium palmatilobum* Tim. ex Downie et Sarjeant, *Izhoria angulata* Golub et Volk., *Raphesphaera turbata* (Martin) Volk., *Saharidia fragilis* (Downie) Combaz, and others (Tables 1, 2).

The age of the assemblage UC4B-1 is not unambiquous. It is younger than the Late Cambrian assemblage UC4B, because it lacks many typical Late Cambrian species, such as *Calyxiella izhoriensis* Golub et Volk., *Lusatia* sp., *Ooidium rossicum* Tim., *Vogtlandia cervinacornua* (Welsch), *V. petropolitana* (German) Volk., *Timofeevia* forms, and others (Table 2). The representatives of the *Timofeevia* genus, which are widespread in the Middle and Upper Cambrian deposits of the East European platform, including the Moscow syneclise, probably disappear at the lower boundary of the assemblage interval. Accordingly, they are absent in the lower Tremadocian of the Moscow syneclise. Single specimens of this genus were found only in the lower Tremadocian of the glint belt of Estonia at the Toila (Volkova, 1989a) and Vihula (Volkova, 1990) localities.

The assemblage UC4B-1, however, is older than the early Tremadocian assemblage OT1, which is known in the East European platform (Volkova, 1995), where it overlies the Sementsovo Formation of the studied section. The assemblage UC4B1 lacks species typical of the lower Tremadocian, i.e., *Acanthodiacrodium angustum* (Downie) Combaz and *A. comptulum* Rasul. As shown earlier, these species appeared later than *A. ornatum* and *A. ramusculosum,* which mark the lower boundary of beds bearing the assemblage UC4B-1, though it was assumed earlier (Volkova, 1995) that all four species appear concurrently.

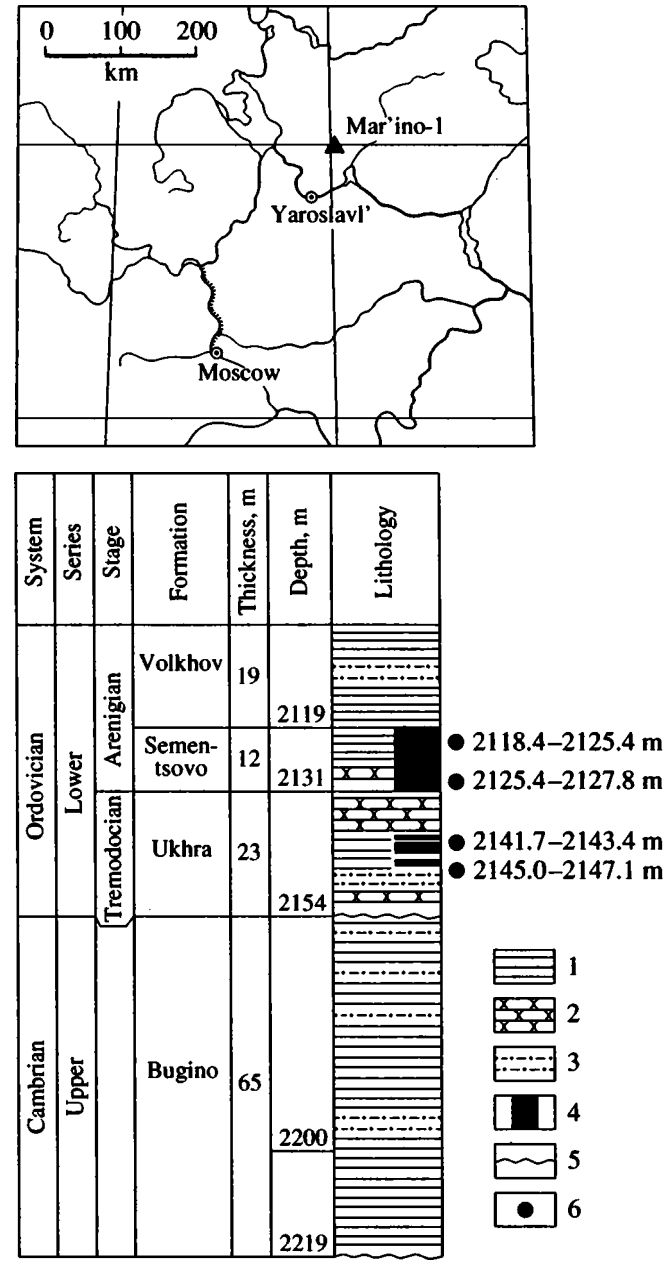

Locality, lithology, and inferred ages of formations in the Mar'ino-1 borehole section: (1) claystone; (2) sandstone; (3) siltstone; (4) argillaceous clay; (5) hiatus; (6) sampling points.

Since the assemblage UC4B-1 is younger than the Late Cambrian assemblage UC4B, the upper boundary of which lies inside the *Acerocare* Zone (Volkova, 1995), and older than the early Tremadocian assemblage OT1, which approximately corresponds to the *Cordylodus proavus* Zone, it can be deduced that the assemblage range corresponds to the middle part of the

Table 1. Distribution of acritarchs (%) in the Borehole Mar'ino-1, the interval of 2118.4–2147.1 m

Species	Assemblage UC4B-1		OT1	OT2
	interval 2145.0–2147.1 m	2141.7–2143.4 m	2125.4–2127.8 m	2118.4–2125.4 m
Acanthodiacrodium invictum		0.5		
Acanthodiacrodium sp.	11.0	10.0	9.5	1.0
Actinotodissus aff. *A. achrasii*	1.5	2.0	3.5	11.0
Arbusculidium destombesii	2.5	1.0		
Arbusculidium aff. *A. destombesii*	12.5	5.0	0.5	0.5
A. ornatum		0.5	2.0	0.5
A. ramusculosum	2.0	0.5	0.5	
Baltisphaeridium capillatum	0.5	6.0	4.0	1.0
B. setaceum	1.0			
Buedingisphaeridium tremadocum	1.5	1.0		
Caldariola glabra		0.5	0.5	
Cymatiogalea cuvillieri	0.5	0.5	2.0	0.5
C. velifera	1.0	1.0	3.5	4.0
Cymatiogalea sp. 1		0.5	1.0	0.5
Cymatiogalea sp.	2.5	4.0	11.0	11.0
Dactylofusa sp.		0.5	0.5	0.5
Dasydiacrodium palmatilobum	4.0	0.5	0.5	
Dasydiacrodium sp.	1.5	0.5		
Izhoria angulata	0.5	0.5	0.5	0.5
Ladogella sp.	7.5	12.0	1.0	
Leiosphaeridia spp.	7.0	8.0	3.0	3.0
Lophodiacrodium sp.	3.0			0.5
Micrhystridium sp.		2.0	2.0	2.0
Multiplicisphaeridium sp. 1	0.5			
Multiplicisphaeridium sp.	3.5			
Nellia acifera	7.0	1.0		
N. sukatschevii	7.0	10.0		
Plygonium akrochordum		2.0		1.0
P. minimum	1.0	1.0	3.0	7.0
P. pellicidum		1.0	4.0	0.5
P. pungens		3.5	6.0	11.0
P. sexradiatum	11.0	4.5		
P. tuberatum		1.0	1.0	
Polygonium sp.			6.0	1.0
Pterospermella sp.		0.5		
Raphesphaera turbata	0.5	0.5	1.0	1.0
Saharidia fragilis		0.5	0.5	0.5
Schizodiacrodium digermulense	6.0	6.0		
Schizodiacrodium fibrosum	1.0			
Stellechinatum uncinatum	2.0	1.0	5.0	14.0
Stelliferidium cortinulum	7.0	6.0	2.0	1.5
Stelliferidium sp.			1.0	1.0
Trachydiacrodium coarctatum		2.0		

Table 1. (Contd.)

Species	Assemblage UC4B-1		OT1	OT2
	interval 2145.0–2147.1 m	2141.7–2143.4 m	2125.4–2127.8 m	2118.4–2125.4 m
Trichosphaeridium hirtum		2.0	1.0	2.0
Veryhachium sp.	0.5			0.5
Vulcanisphaera cf. *V. capillata*		0.5		
Acanthodiacrodium angustum			5.0	4.0
Acanthoduacrodium aff. *A. angustum*			11.0	6.0
A. comptulum			1.0	0.5
Actinotodissus sp.			3.0	4.0
Arbusculidium striatulum			0.5	0.5
Baltispaeridium aciculare			0.5	
Cymatiogalea bellicosa			0.5	
C. cristata			0.5	
C. aff. *C. multarea*			0.5	
Cymatiogalea sp. 2			0.5	
Filisphaeridium sp.			0.5	
Vesiculosphaera sp.			0.5	0.5
Actinotodissus ubuii				2.0
Dactilofusa squama				0.5
Dictyotidium sp.				0.5
Vulcanisphaera britannica f.1				1.5
V. imparilis f. 3				0.5
Gen. et sp. nov. no. 1				0.5
Gen. et sp. nov. no. 2				1.5
Number of counted up specimens	500	1000	1100	1000

Acerocare Zone. Taking into consideration its proximity to the assemblage OT1, the assemblage is conditionally placed at the level of the upper part of the *Cordylodus andresi* zone (Table 2).

Apart from the studied deposits, the assemblage UC4B-1 was also distinguished in samples from the upper part of the Bugino Formation, the interval of 1785.4–1793.4 m in the Rybinsk borehole, the Moscow

Plates I–IV. Acritarchs of the uppermost Cambrian and lower Tremadocian of the Moscow syneclise. Scale bar for all figures is 10 μm long.

Plate I. (1–3) *Actinotodissus* aff. *achrasii* (Martin) Yin: (1) slide GIN 3939/3713-1; (2) slide GIN 3939/3713-2, interval of 2125.4–2127.8 m, Sementsovo Formation; (3) slide GIN 3939/3711-1, interval of 2145.0–2147.1 m, Ukhra Formation. (4), (8)*Acanthodiacrodium angustum* (Downie) Combaz; 4—slide GIN 3939/3713-1, interval of 2125.4–2127.8 m; (8) Slide GIN 3939/3714-1, interval of 2118.4–2125.4 m (0.5 m below the top), Sementsovo Formation. (5), (9) *Acanthodiacrodium comptulum* Rasul: (5) slide GIN 3939/3713-1; (9) slide GIN 3939/3713-2, interval of 2125.4–2127.8 m, Sementsovo Formation. (6)*Schizodiacrodium digermulense* (Welsch), slide GIN 3939/3711-1, interval of 2145.0–2147.1 m, Ukhra Formation. (7)*Actinotodissus* sp., slide GIN 3939/3713-1, interval of 2125.4–2127.8 m, Sementsovo Formation. (10)*Actinotodissus ubuii* (Martin) Fensome *et al.*, slide GIN 3939/3714-2, interval of 2118.4–2125.4 m, Sementsovo Formation. (11) *Acanthodiacrodium* aff. *A. angustum* (Downie) Combaz, slide GIN 3939/3713-2, interval of 2125.4–2127.8 m, Sementsovo Formation. (12)*Actinotodissus* sp., slide GIN 3939/3714-1, interval of 2118.4–2125.4 m (0.5 m below the top), Sementsovo Formation. (13)*Acanthodiacrodium* sp., slide GIN 3939/3713-2, interval of 2125.4–2127.8 m, Sementsovo Formation. (14) *Actinotodissus* sp., slide GIN 3939/3713-2, interval of and formation as above. (15)*Actinotodissus* sp., slide GIN 3939/3713-2, interval of and formation as above. (16) *Raphesphaera turbata* (Martin) Volkova, slide GIN 3939/3713-3, interval of and formation as above. (17) *Izhoria angulata* Golub et Volk., slide GIN 3939/3713-1, interval of and formation as above. All specimens are from the Yaroslavl district, Mar'ino-1 borehole.

Plate I

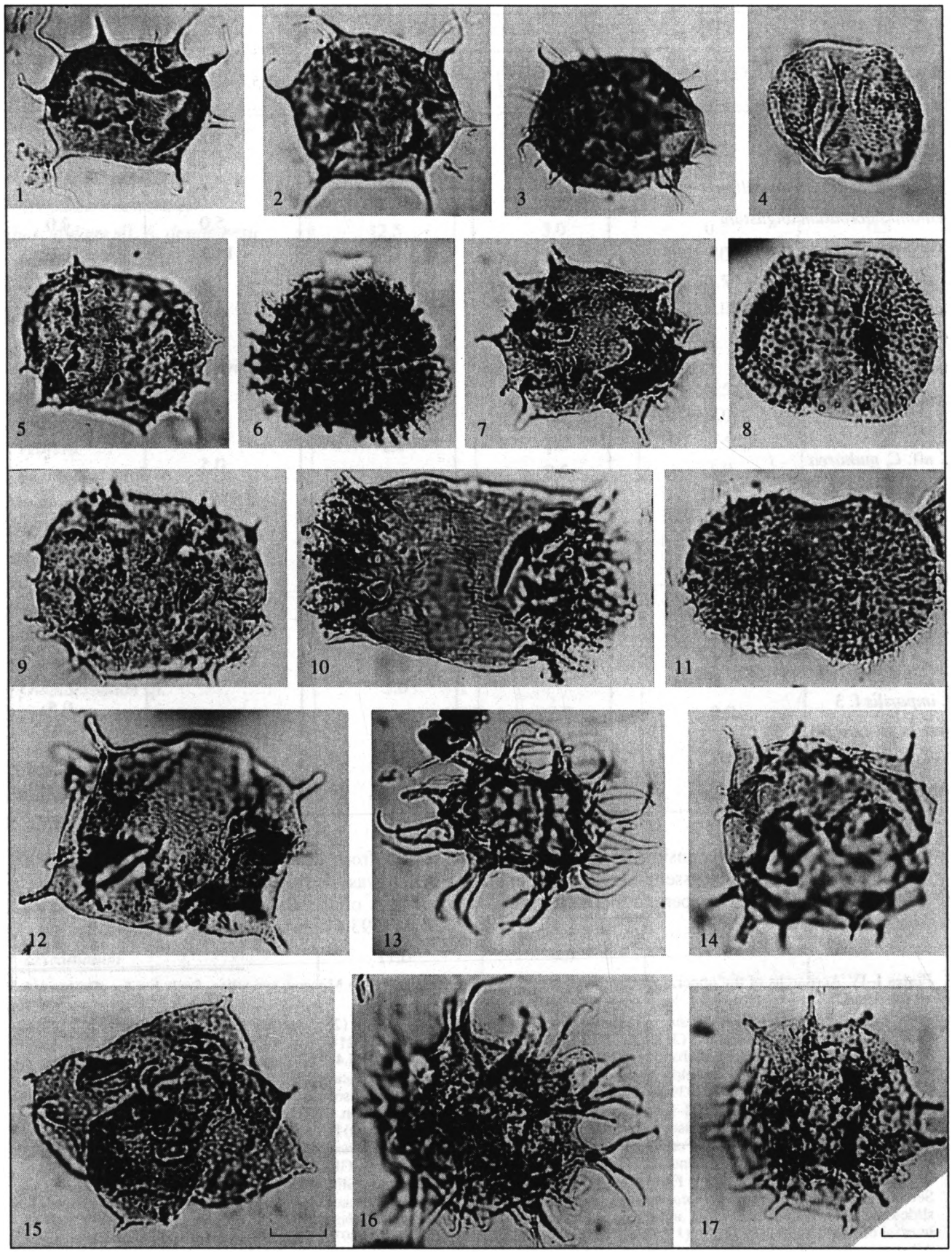

Plate II

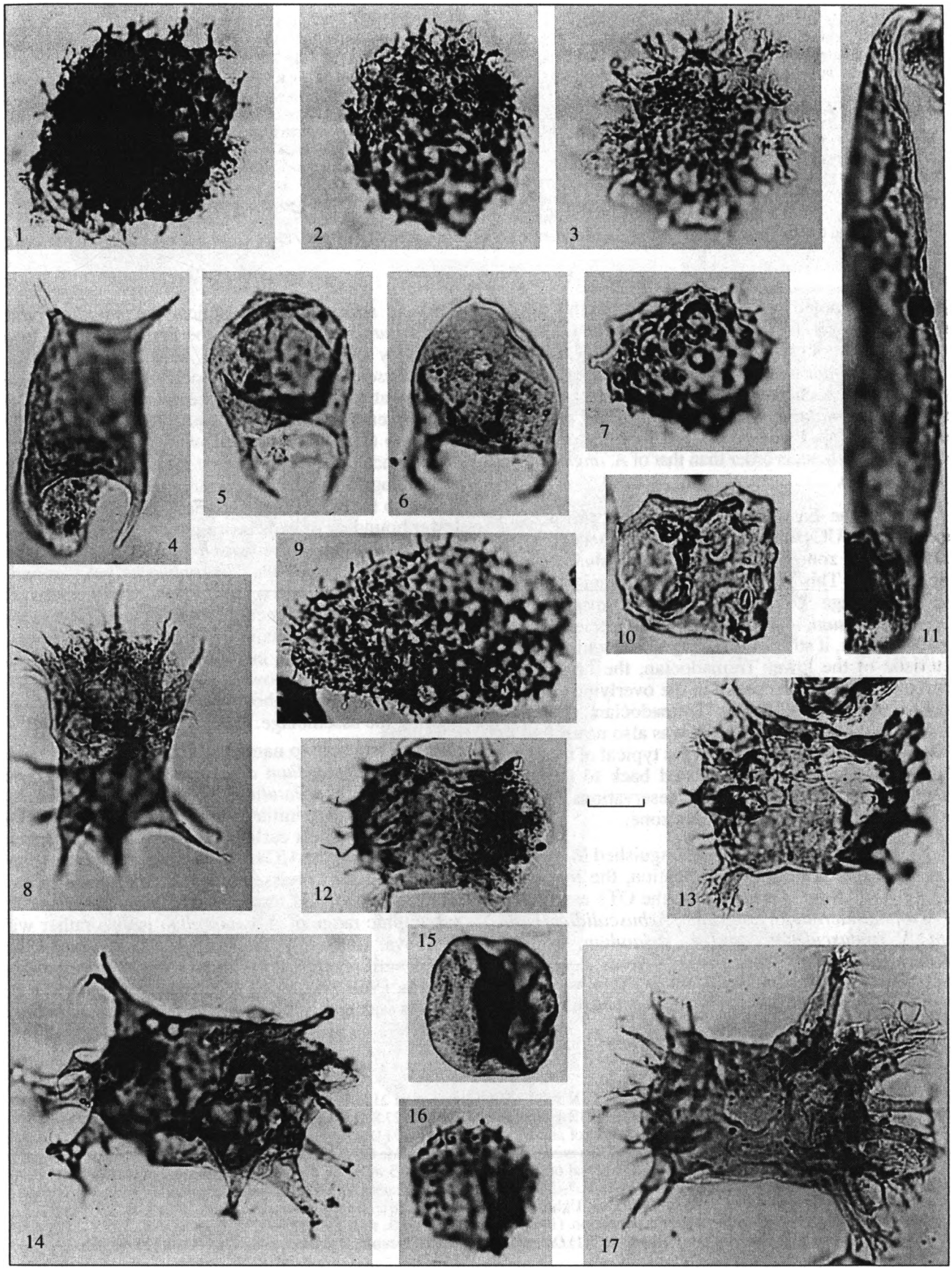

Plate II. (1–3) *Vulcanisphaera britannica* f.1 Rasul: (1, 3) slide GIN 3939/3714-1, (2) slide GIN 3939/3714-2, interval of 2118.4–2125.4 m, Sementsovo Formation. (4, 5) *Nellia sukatschevii* (Tim.) Volk., slide GIN 3939/3711-1, interval of 2145.0–2147.1 m, Ukhra Formation; (6) *Nellia acifera* (N. Umn.) Volk., slide GIN 3939/3712-3, interval of 2141.7–2143.4 m, Ukhra Formation. (7) *Vulcanisphaera imparilis* f.3 Rasul, slide GIN 3939/3714-1, interval of 2118.4–2125.4 m (0.5 m below the top), Sementsovo Formation. (8) *Dasydiacrodium palmatilobum* Tim. ex Downie et Sarjeant, slide GIN 3939/3711-1, interval of 2145.0–2147.1 m, Ukhra Formation. (9) *Filisphaeridium* sp., slide GIN 3939/3713-1, interval of 2125.4–2127.8 m, Sementsovo Formation. (10) *Vesiculosphaera* sp., slide GIN 3939/3714-1, interval of 2118.4–2125.4 m (0.5 m below the top), Sementsovo Formation. (11) *Dactylofusa* sp., slide GIN 3939/3713-3, interval of 2125.4–2127.8 m, Sementsovo Formation. (12) *Arbusculidium* aff. *A. destombesii* Deunff, slide GIN 3939/3711-1, interval of 2145.0–2147.1 m, Ukhra Formation. (13) *Arbusculidium ornatum* (Combaz) Fensome *et al.*, slide GIN 3939/3713-1, interval of 2125.4–2127.8 m, Sementsovo Formation. (14) *Arbusculidium ramusculosum* (Combaz) Fensome *et al.*, slide GIN 3939/3711-1, interval of 2145.0–2147.1 m, Ukhra Formation. (15) *Trachydiacrodium coarctatum* Tim., slide GIN 3939/3712-3, interval of 2141.7–2143.4 m, Ukhra Formation. (16) *Buedingisphaeridium tremadocum* Rasul, slide GIN 3939/3712-3; interval of and formation above. (17) *Arbusculidium destombesii* Deunff, slide GIN 3939/3712-3, interval of and formation as above.

syneclise. As noted earlier, acritarchs from this sample are in the Lower Tremadocian assemblage OT1 (Volkova, 1995), though some species typical of the latter, e.g., *A. angustum and A. comptulum* missing here. Of typical species characterizing the assemblage OT1, only *Arbusculidium ramusculosum* and *Multiplicisphaeridium* sp. 1 were found, and their first occurrence level as shown here, is order than that of *A. angustum* and *A. comptulum.*

Outside the East European platform, the possible analogue of UC4B-1 assemblage is detected in the palynological zone BO of the Algerian Sahara (Jardine *et al.*, 1974). This zone yields the nominal species of the assemblage UC4B-1, namely *A. ornatum* and *A. romusculosum*, and also the typical species *V. capillata.* However, it still lacks *A. angustum*, which is characteristic of the lower Tremadocian; the first appearance of the latter is recorded in the overlying zone B1, which contains the lower Tremadocian graptolites *Rhabdinopora flabelliformis.* It was also noted that the BO zone lacks ooidal morphotypes typical of the Upper Cambrian. The BO zone is dated back to the lower Tremadocian with considerable reservations, because graptolites were not found in this zone.

The second assemblage is distinguished in one samples from the Sementsovo Formation, the interval of 2125.4–2127.8 m. It is similar to the OT1 assemblage of *Acanthodiacrodium angustum, Arbusculidium ornatum, A. ramusculosum, and A. striatulum*, which is characteristic of the *Cordylodus proavus* Zone in the glint belt of Estonia (Volkova, 1995). This assemblage contains all nominal OT1 species, among which *A. angustum, A. striatulum* and typical *Acanthodiacrodium comptulum* are detected for the first time at the lower boundary of the assemblage beds. *A. ornatum* and *A. ramusculosum*, which appeared earlier, are still present at this level. Only one species typical of the OT1 assemblage in Estonia, namely *Dasydiacrodium tumidum* (Deunff) Tongiorgi, was not found. The first appearance of *Vesiculosphaera* genus in the second assemblage is remarkable, though it has not been established so far in the lower Tremadocian of Estonia. The lower boundary of beds bearing the second assemblage lacks *Nellia acifera, N. sukatschevii, Polygonium sexradiatum, Schizodiacrodium digermulense* (=*S. armatum* Volk.), and *S. fibrosum.* In the Estonian sections, the last two species still occur at the OT1 level. The second assemblage also contains a series of Late Cambrian species (Table 2), among which *Dasydiacrodium palmatilobum* Tim. ex Downie et Sarjeant and *Ladogella* forms do not appear above the upper boundary of beds bearing the assemblage.

I suggest here to name the OT1 assemblage as that of *Acanthodiacrodium angustum, A. comptulum,* and *Arbusculidium striatulum*, because *A. ornatum* and *A. ramusculosum*, initially used in nomenclature (Volkova, 1995), appear earlier and are the nominal species of the assemblage UC4B-1. Among the nominal species of the second assemblage, *A. angustum* is most widespread beyond the East European platform. The geographic range of *A. comptulum* is also rather wide (Volkova, 1995). The third species *A. striatulum*, was found until recently only in the lower Tremadocian of Estonia (Volkova, 1995; Paalits, 1995), but later this species was recovered from the lower Tremadocian of

Plate III. (1) *Multiplicisphaeridium* sp. 1, slide GIN 3939/3711-1, interval of 2145.0–2147.1, Ukhra Formation. (2) *Stellechinatum uncinatum* (Downie) Molyneux, slide GIN 3939/3713-1, interval of 2125.4–2127.8 m, Sementsovo Formation, (3) *Polygonium pungens* (Tim.) Rauscher, slide GIN 3939/3713-1, interval of and formation as above. (4) *Polygonium* (Tim.) Volk., slide GIN 3939/3713-2, interval of and formation as above. (5) *Polygonium minimum* (Tim.) Volk., slide GIN 3939/3713-1, interval and formation as above. (6) *Polygonium* sp., slide GIN 3939/3714-1, interval of 2118.4–2125.4 m (0.5 m below the top), Sementsovo Formation. (7) *Ladogella* sp., slide GIN 3939/3712-3, interval of 2141.7–2143.4 m, Ukhra Formation. (8) *Polygonium sexradiatum* (Tim.) Volk., slide GIN 3939/3711-1, interval of 2145.0–2147.1 m, Ukhra Formation. (9) *Arbusculidium striatulum* Volk., slide GIN 3939/3713-2, interval of 2125.4–2127.8 m, Sementsovo Formation. (10) Gen. et sp. nov. no. 1, slide GIN 3939/3714-1, interval of 2118.4–2125.4 m (0.5 m below the top), Sementsovo Formation. (11) *Dactylofusa squama* (Deunff) Rauscher, slide GIN 3939/3714-1, interval and formation as above.

Plate III

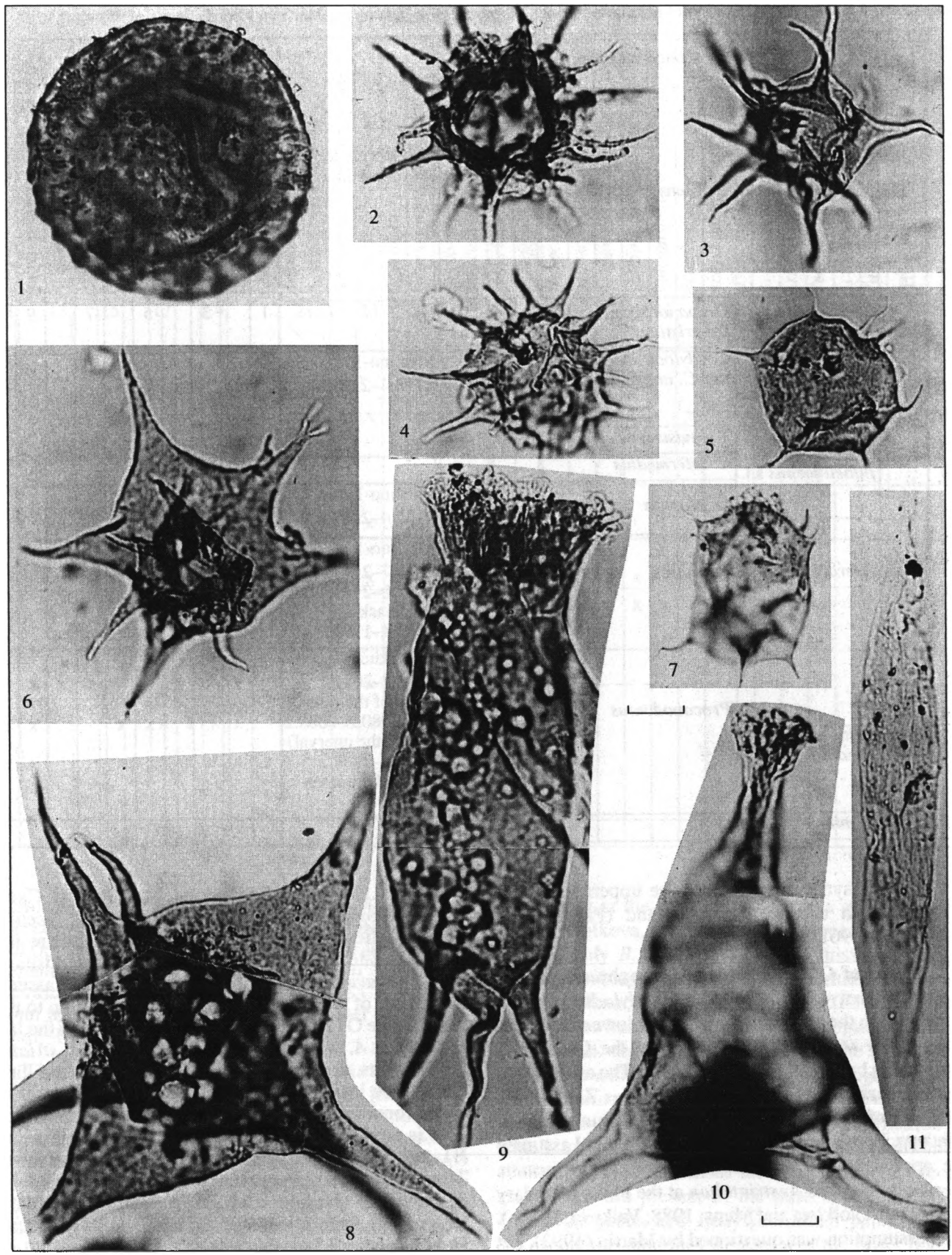

Table 2. Distribution of typical acritarch taxa in the Cambrian–Ordovician boundary deposits of the Moscow syneclise (data on the Tolbukhino-1 and Rybinsk-1 boreholes are quoted from Volkova, 1990); data on the Mar'ino-1 borehole are of this work)

Age	Horizon	Trilobite and graptolite zones (Kaljo *et al.*, 1986; Mens *et al.*, 1993)	Conodont zones (Kaljo *et al.*, 1986; Mens *et al.*, 1993)	Acritarch assemblage	Borehole, depth in m	*Bychinia variabilis*	*Calyxiella izhoriensis*	*Cristallinium pilosum*	*Lusatia* sp.	*Nellia longiuscula*	*N. magna*	*Ooidium rossicum*	*O. timofeevii*	*Schizodiacrodium breviciritum*	*Timofeevia janischewskyi*
						1		3		5		7		9	
O_1t	Itinu	*Clonograptus–Didymograptus*	*Drepanoistodus dellifer pristinus*												
			Cordylodus rotundatus–C. angulatus	OT2	Mar'ino-1, 2118.4–2125.4										
		Rhabdinopora flabelliformis s.l.	*C. lindstroemi*												
			C. intermedius	?											
			C. proavus	OT1	Mar'ino-1, 2125.4–2127.8										
ϵ_3	?	*Acerocare*	*C. andresi*	UC4B-1	Mar'ino-1, 2141.7–2143.4 2145.0–2147.1 PRybinsk-1, 1785.4–1793.4										
	Ladoga		*Proconodontus*	UC4B	Tolbukhino-1, 2063.7–2071.7 (base of the interval) 2080.2–2088.2 (top of the interval) 2080.2–2088.2 (base of the interval)	x	x x x	x	x x x	 x x	x x x	x	x	x x x	 x x
		Peltura scarabaeoides													
		P. minor													

the Moscow syneclise and from the uppermost Cambrian beds in eastern Newfoundland (Parsons and Anderson, 1996).

The age of OT1 assemblage approximately corresponds to that of the conodont *Cordylodus proavus* Zone, i.e., to the lowermost part of the lower Tremadocian, if the zone base is assumed at the Cambrian–Ordovician boundary (Volkova, 1995). The assemblage was originally detected in the *C. proavus* Zone of the glint belt of Estonia (the Vihula and Suhkrumaegi denudations, borehole M-9; Volkova, 1995), and I assumed the appearance of its nominal species *A. angustum*, *A. comptulum*, and *A. striatulum* at the lower boundary of the zone (Volkova and Mens, 1988; Volkova, 1989a). This assumption was questioned by Martin (1993), but the latest results confirm it.

Paalits (1995) studied acritarchs from the Cambrian–Ordovician boundary deposits in the Toenismaegi section, Tallinn district of Estonia, where the rocks are dated on the basis of conodonts. In deposits of the *C. proavus* Zone, Paalits distinguished the assemblage A-2, of which is very close in composition to the assemblage OT1 and includes all typical taxa of the latter, such as *A. angustum*, *A. comptulum*, and *A. striatulum*. Paalits arrived at the conclusion that the first occurrence level of *A. angustum* is coeval with that of zonal conodont species, or even older. The assemblage OT1 is presumably correlative with the acritarch zones B1 and B2 of the Algerian Sahara, where the lower Tremadocian graptolites were found in association with *A. angustum* (Jardine *et al.*, 1974), and also with the assemblage from upper beds of the Bordj–Nili Sandstones penetrated by the borehole NL2 (Vecoli *et al.*, 1995). The latter assemblage includes typical lower

11	13	15	17	19	21	23	25	27	29	31	33	35	37	39	41	43
Veryhachium dumontii	*Vogtlandia cervinacornua*	*V. petropolitana*	*Nellia acifera*	*N. sukatschevii*	*Polygonium sexradiatum*	*Schizodiacrodium digermulense*	*S. fibrosum*	*Dasydiacrodium palmatilobum*	*Ladogella rotundiformis*, *Ladogella* sp.	*Arbusculidium destombesii*, *A.* aff. *A. destombesii*	*Baltisphaeridium capillatum*	*Cymatiogalea cuvillieri*	*C. velifera*	*Izhoria angulata*	*Polygonium pellicidum*, *P. pungens*	*Saharidia fragilis*	*Stelliferidium cortinulum*	*Stellechinatum uncinatum*	*Arbusculidium ornatum*	*A. ramusculosum*	*Multiplicisphaeridium* sp. 1	*Vulcanisphaera* cf. *V. capillata*	*Acanthodiacrodium angustum*	*Acanthodiacrodium* aff. *A. angustum*	*A. complutum*	*Arbusculidium striatulum*	*Vesiculosphaera* sp.	*Actinotodissus ubuii*	*Vulcanisphaera britannica* f.1.	*V. imparilis* f. 3	Gen. et sp. nov. no. 1	Gen. et sp. nov. no. 2
					x	x	x	x	x	x	x	x	x	x	x	x	x	x				x	x	x	x	x	x	x	x	x
				x	x	x		x	x	x	x	x	x	x	x	x	x	x	x	x			x	x	x	x	x				
			x	x	x	x		x	x	x	x	x	x	x	x	x	x	x	x	x		x									
			x	x	x	x	x	x	x	x	x	x	x	x			x	x		x	x										
			x	x	x	x	x	x	x	x	x	x	x	x	x	x	x	x		x	x	x									
	x	x	x	x	x	x		x	x	x	x	x	x	x			x	x													
x					x	x	x	x	x	x	x	x	x	x	x	x	x	x													
					x	x	x	x	x	x	x	x	x	x	x																

Tremadocian taxa *Acanthodiacrodium* aff. *A. angustum* and *Dasydiacrodium tumidum*. However, it lacks the typical Upper Cambrian *Veryhachium dumontii* and *Multiplicisphaeridium cervinacornuum* Welsch (= *Vogtlandia cervinacornua*), which are present in the Upper Cambrian acritarch assemblage from the lower part of the Bordj–Nili Sandstones.

The third assemblage is distinguished in one sample from the Sementsovo Formation, the interval of 2118.4–2125.4 m (0.5 m below the top of the core from the depth of 2119 m). The characteristic species of the assemblage are *Vulcanisphaera britannica* Rasul, *V. imparilis* Rasul, and *Actinotodissus ubuii* (Martin) Fensome *et al.*, which appear at the lower boundary of the interval. The assemblage is identical to the OT2 assemblage of *Vulcanisphaera britannica*, *V. imparilis*, and *Baltisphaeridium setaceum*, which is established in the glint belt of Estonia and Leningrad district (Volkova, 1995). Out of the three nominal OT2 species, only *B. setaceum* (Tim.) is missing from the third assemblage and should be excluded from the group of characteristic species of the OT2 assemblage. This species has a very simple morphological structure, and its peak abundance is confined to the black shaly claystones with considerable amount of organic matter (*Dictyonema* shales), which are known in the clint belt of Estonia and Leningrad District, and formation of which took place in a specific facies environment (Volkova, 1989b). Almost all species of the second assemblage are present in the third assemblage. The *Ladogella* genus and *Dasydiacrodium palmatilobum* are exceptions, and they disappear at the lower boundary of beds bearing the second assemblage.

The age of the third assemblage, which is similar to the OT2 assemblage of the Baltic sections, is determined as corresponding to the interval of the *Cordylodus lindstroemi–C. angulatus/C. rotundatus* Zone. The assemblages A4 and A5 distinguished by Paalits (1995) also correspond to the OT2 assemblage in the Toenismaegi section, where the first one ranges from the *C. lindstroemi* Zone and the next one from the *C. angulatus–C. rotundatus* Zone. The taxonomic composition of both assemblages is poor, probably owing to certain facies conditions. Typical OT2 species *V. britannica, V. imperialis,* and *A. ubuii* are present either in the studied section proper, or, in association with *C. lindstroemi*, in other reference sections of the glint belt. Thus, the age similarity of the OT2 interval and *C. lindstroemi–C. angulatus/C. rotundatus* Zone is confirmed once again. The later appearance of *V. britannica* and *V. imparilis*, as compared to that of *C. angustum* and *A. comptulum*, is likewise observed in North Africa. The Tremadocian Fezouata Formation of Morocco is dated on the basis of graptolites, and *A. ubuii* and *V. britannica?* appear here only in the uppermost lower Tremadocian acritarch zone 4, whereas the *A. comptulum* range begins from zone 2 (Elaouad-Debbaj, 1988). In the section of the NL2 borehole in Algerian Sahara, *V. britannica* is also detected much higher in the section than *Acanthodiacrodium* aff. *A. angustum* (Vecoli *et al.*, 1995).

Even the youngest OT2 assemblage from the upper part of the Sementsovo Formation cannot be attributed to the upper Tremadocian. The late Tremadocian acritarchs of the Moscow syneclise are known from Orekhovo-1 borehole in the Kostroma district (Aristova, 1980a). In addition to the late Tremadocian graptolites *Bryograptus ramosus* and *Dictyonema murrayi*, Aristova discovered in this borehole an assemblage of acritarchs, many of which have large polar openings (*Stelliferidium* and *Cymatiogalea* genera). The typical species of the assemblage are represented by rather large forms of diacrodian *Acanthodiacrodium rotundatum* Gorka and *A. formosum* Gorka, both described from the upper Tremadocian of Poland. A new diacrodian species *A. magnum* Arist. which is distinguished by its large size and conic appendices, was also detected here. The large diacrodian acritarchs of this type are characteristic of the upper Tremadocian of Poland (Gorka, 1969), Estonia (Volkova, 1993; Paalits, 1994), and Sweden (Bagnoli *et al.*, 1988). Moreover, the upper Tremadocian assemblages in these regions, as in the Moscow syneclise, are dominated by representatives of the *Stelliferidium* genus. In the OT2 assemblage, the diacrodian forms likewise prevail, but their large forms are missing. The appearance of large diacrodian acritarchs is recorded, according to Paalits (1994), in the lower part of the Varangu Formation of northern Estonia, where it is the age analogue of Ceratopyge shales.

The lower Tremadocian acritarch assemblages of the Moscow syneclise, as in other regions of the Baltic province (Volkova, 1995), are abundant and show diversity of the diacrodian forms (more than 30%) and Herkomorphitae (about 20%). The diacrodian acritarchs are represented by genera *Acanthodiacrodium, Actinotodissus, Dasydiacrodium, Lophodiacrodium, Schizodiacrodium, Trachydiacrodium, Arbusculidium,* and *Nellia.* Among Herkomorphitae, there are numerous and diverse *Cymatiogalea* species associated with *Stelliferidium, Caldariola,* and *Dictyotidium* genera. The *Baltisphaeridium* representatives are not large, and finds of *Vulcanisphaera* and *Saharidia* genera are occasional.

The lower Tremadocian assemblages of the Moscow syneclise somewhat differ in taxonomic composition from those of the Baltic reference sections. The main distinctive feature is a considerable abundance of *Polygonium* forms (up to 30%) in the Moscow syneclise whereas they are scarce in assemblages of the Baltic sections. Moreover, the Moscow syneclise has not yielded as yet the peculiar species *Brochos eisenackii* Vand. et Mikh., which are mainly confined to the *Dictyonema* shales of the Baltic region. These distinctive features of regional assemblages can perhaps be attributed to the differences in the facies environment.

The lower Tremadocian acritarch assemblages of the Moscow syneclise and Baltic sections are characterized by presence of taxa typical of the lower Tremadocian of the cold-water Peri-Gondwana province. These assemblages lack the lower Tremadocian taxa of warm-water provinces, which are known from northeastern China (Yin, 1986) and Canada (Martin, 1992). This fact presumes that the early Tremadocian climate was cold on the territory of the Moscow syneclise. The late Tremadocian acritarch assemblages of the Baltic province contain the warm-water forms implying a probable warming and migration of these forms into temperate latitudes.

Plate IV. (1) *Cymatiogalea cristata* (Downie) Rauscher, slide GIN 3939/3713-1, interval 2125.4–2127.8 m, Sementsovo Formation. (2) *Caldariola glabra* (Martin) Molyneux, slide GIN 3939/3712-3, interval 2141.7–2143.4 m, Ukhra Formation. (3) *Stelliferidium cortinulum* (Deunff) emend. Deunff *et al.*, slide GIN 3939/3713-1, interval 2125.4–2127.8 m, Sementsovo Formation. (4) *Cymatiogalea cuvillieri* (Deunff) Deunff, slide GIN 3939/3713-2, interval and formation as above. (5) *Cymatiogalea* sp. 2, slide GIN 3939/3713-1, interval and formation as above. (6) *Cymatiogalea velifera* (Downie) Martin, slide GIN 3939/3713-2, interval and formation as above. (7) *Cymatiogalea* sp. 1, slide GIN 3939/3713-2, interval and formation as above. (8) Gen. et sp. nov. no. 2, slide GIN 3939/3714-1, interval 2118.4–2125.4 m (0.5 m below the top), Sementsovo Formation. (9) *Veryhachium* sp., slide GIN 3939/3714-1, interval and formation as above. (10) *Cymatiogalea* aff. *multarea* (Deunff) Eisenack *et al.*, slide GIN 3939/3713-2, interval 2125.4–2127.8 m, Sementsovo Formation. (11) *Saharidia fragilis* (Downie) Combaz, slide GIN 3939/3713-3, interval and formation as above. (12) *Baltisphaeridium capillatum* (Naum.) N. Umn., slide GIN 3939/3713-1, interval and formation as above.

Plate IV

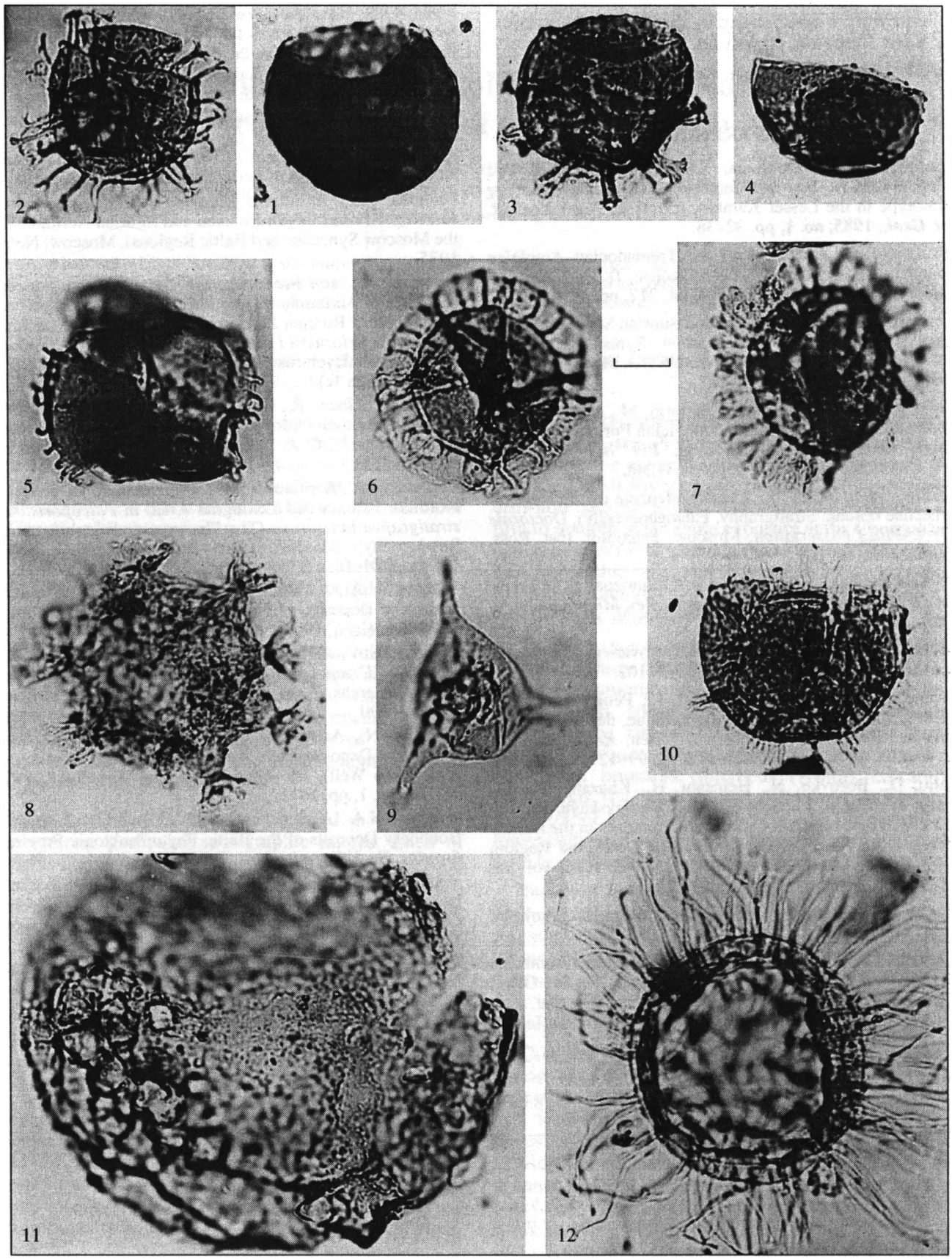

ACKNOWLEDGMENTS

This work was supported by the Russian Foundation for Basic Research, project no. 96-05-65559.

Reviewers T.N. Koren' and A.Yu. Rozanov

REFERENCES

Apollonov, M.K., Dubinina, S.V., Ergaliev, G.Kh., and Chugaeva, M.N., Possible Cambrian–Ordovician Boundary Stratotype in the Lesser Karatau, *Izv. Akad. Nauk KazSSR, Ser. Geol.*, 1985, no. 1, pp. 32–38.

Aristova, K.E., Acritarchs of the Tremadocian–Arenigian Boundary Beds of the Moscow Syneclise, *Tr. Vses. Nauch.–Issled. Geol. Razved. Inst.*, 1980a, no. 217, pp. 10–18.

Aristova, K.E., The Ordovician and Silurian Standard Microfossil Assemblages of the Moscow Syneclise, in *Palinologiya v SSSR* (Palynology in the USSR), Moscow: Nauka, 1980b, pp. 47–49.

Bagnoli, G., Stouge, S., and Tongiorgi, M., Acritarchs and Conodonts from the Cambro–Ordovician Furuhäll (Köpingsklint) Section (Öland, Sweden), *Riv. Ital. Paleontol. Stratigr.*, 1988, vol. 94, no. 2, pp. 163–248.

Dmitrovskaya, Yu.E., The Lower Paleozoic of the Moscow Syneclise (Fauna, Stratigraphy, Paleogeography), *Doctorate (Geol.–Min.) Dissertation*, Moscow: Paleontol. Inst. Ross. Akad. Nauk, 1991.

Elaouad-Debbaj, Z., Acritarches et Chitinozoaires du Tremadoc de L'Anti-Atlas Central (Maroc), *Rev. Micropaleontol.*, 1988, vol. 31, no. 2, pp. 85–128.

Gorka, H., Microorganismes de L'Ordovicien de Pologne, *Palaeontol. Polon.*, 1969, no. 22, pp. 1–102.

Jardine, S., Combaz, A., Magloire, L., Peniguel, G., and Vachey, G., Distribution Stratigraphique des Acritarches dans le Paleozoique du Sahara Algérien, *Rev. Palaeobot. Palynolog.*, 1974, vol. 18, nos. 1–2, pp. 99–129.

Kaljo, D., Borovko, N., Heinsalu, H., Khazanovich, K., Mens, K., Popov, L., Sergeeva, S., Sobolevskaya, R., and Viira, V., The Cambrian–Ordovician Boundary in the Baltic–Ladoga Clint Area (North Estonia and Leningrad Region, USSR), *Proc. Acad. Sci. ESSR. Ser. Geol.*, 1986, vol. 35, no. 3, pp. 97–108.

Martin, F., Acritarchs: A Review, *Biol. Rev.*, 1993, vol. 68, pp. 475–538.

Mens, K., Viira, V., Paalits, I., and Puura, I., Upper Cambrian Biostratigraphy of Estonia, *Proc. Est. Acad. Sci., Ser. Geol.*, 1993, vol. 42, no. 4, pp. 148–159.

Paalits, I., Late Tremadocian Acritarchs from Ceratopyge Shale at Ottenby, Öland, Sweden, *Proc. Est. Acad. Sci., Ser. Geol.*, 1994, vol. 43, no. 4, pp. 203–205.

Paalits, I., Acritarchs from the Cambrian–Ordovician Boundary Beds at Tõnismägi, Tallinn, North Estonia, *Proc. Est. Acad. Sci., Ser. Geol.*, 1995, vol. 44, no. 2, pp. 87–96.

Parsons, M.G. and Anderson, M.M., Late Cambrian Acritarch Assemblages from the *Peltura scarabaeoides* and *Acerocare* Trilobite Zones of Random Island, Southeastern Newfoundland, *Cimp. Newslett.*, 1996, no. 50, pp. 1–17.

Umnova, N.I., *Akritarkhi ordovika i silura Moskovskoi sineklizy i Pribaltiki* (Ordovician and Silurian Acritarchs of the Moscow Syneclise and Baltic Regions), Moscow: Nedra, 1975.

Umnova, N.I. and Fanderflit, E.K., Cambrian and Lower Ordovician Acritarch Assemblages of the Western and Northwestern Russian Platform, in *Palinologicheskie issledovaniya v Belorussii i drugikh raionakh SSSR* (Palynological Studies in Byelorussia and Other Regions of the USSR), Minsk: Nauka Tekh., 1971, pp. 45–73.

Vecoli, M., Albani, R., Ghomari, A., *et al.*, Précisions sur la Limite Cambrien–Ordovicien au Sahara Algérien (Secteur de Hassi-Rmel), *C. R. Acad. Sci.*, 1995, vol. 320; Sér. IIa, pp. 515–522.

Volkova, N.A., Acritarchs of the Upper Pakerort Horizon of Northern Estonia and Leningrad Area, in *Paleofloristika i stratigrafiya fanerozoya* (The Phanerozoic Paleobotany and Stratigraphy), Moscow: Geol. Inst. Akad. Nauk SSSR, 1989a, pp. 4–16.

Volkova, N.A., Acritarchs from the Cambrian–Ordovician Boundary Deposits of Northern Estonia, *Izv. Akad. Nauk SSSR, Ser. Geol.*, 1989b, no. 7, pp. 59–67.

Volkova, N.A., *Akritarkhi srednego i verkhnego kembriya Vostochno-Evropeiskoi platformy* (Middle and Late Cambrian Acritarchs of the East European Platform), Moscow: Nauka, 1990.

Volkova, N., Acritarchs from the Cambrian–Ordovician Boundary Deposits near the Klint Area of Estonia (the Maardu-56 Well), *Izv. Akad. Nauk Est., Ser. Geol.*, 1993, vol. 42, no. 1, pp. 15–22.

Volkova, N.A., Acritarchs from the Cambrian–Ordovician Boundary Deposits of the Baltic Phytoplanktonic Province, *Stratigr. Geol. Korrelyatsiya*, 1995, vol. 3, no. 4, pp. 31–43.

Volkova, N. and Mens, K., Acritarch Distribution in the Cambrian–Ordovician Boundary Beds of the Sukhkrumyagi Section (Northern Estonia), *Izv. Akad. Nauk ESSR, Ser. Geol.*, 1988, vol. 37, no. 3, pp. 97–101.

Yin, Leid-Ming. Acritarchs, in *Aspects of Cambrian–Ordovician Boundary in Dayangcha, China*, Chen Jun-Juan, Ed., Beijing: China Prospect., 1986, pp. 314–373.

Stratigraphy and Geological Correlation, Vol. 7, No. 5, 1999, pp. 465–472. Translated from Stratigrafiya. Geologicheskaya Korrelyatsiya, Vol. 7, No. 5, 1999, pp. 56–63.
Original Russian Text Copyright © 1999 by Orlova.
English Translation Copyright © 1999 by MAIK "Nauka/Interperiodica" (Russia).

Permian–Triassic Conchostracan Faunas from the North of Central Siberia

E. F. Orlova

Cosmoaerogelogical Expedition no. 3, ul. Krzhizhanovskogo 3, Moscow, 117292 Russia

Received November 10, 1997

Abstract—Eight conchostracan faunas described in the paper successively replace one another in the Upper Permian–Middle Triassic sedimentary sequence of the Siberian platform, Taimyr, and Verkhoyansk Range. Data on microsculpture of conchostracan shells are obtained using the scanning electron microscopy (SEM).

Key words: *conchostracan, microsculpture, Permian, Triassic, Siberian platform*

Phyllopoda is an important group of organisms whose remains are widespread in Permian and Triassic deposits of central Siberia. Conchostracans occur in beds bearing marine fauna in some localities and plant remains in others that is an advantage for correlation of different sedimentary facies.

In this work, I describe conchostracans from more than 50 localities of northern central Siberia. The abundant paleontological material was studied using the replica method (Orlova, 1978), and this yielded more comprehensive data on compositional variations in different-age conchostracan populations and allowed me to discriminate principal elements of faunas from those, which are not qualificative. The results substantiated the ecostratigraphical analysis of materials, which reveals more details and is more confident than the guide-fossil method.

Conchostracan faunas distinguished in this study characterize particular stratigraphic ranges. Each of them is dominated by representatives of one or several families (sometimes by a single species). In continuous sections, there are some mixed faunas incorporating younger and older forms. The faunas are distinguished in localities studied by myself and also on the basis of revised collections investigated formerly by Novojilov (1958, 1965). When original samples were inaccessible for revision, some genera and species identified by Novojilov were not included in composition of faunas described below.

In a series of localities bearing conchostracans, they occur together with other fossils studied by a group of researchers, for instance, with plant remains (G.N. Sadovnikov), bivalves (I.M. Malovetskaya), ammonites (A.S. Dagys), ostracodes (E.M. Mishina), fossil insects (A.G. Sharov), fishes (A.A. Selezneva), amphibians (I.A. Efimov), and reptiles (B.P. V'yushkov).

Distribution ranges of eight distinguished conchostracan faunas are shown in Fig. 1. Some faunas are detected in the same localities (e.g., the first and third near the Anakit River mouth, the third and fourth in the drill-hole section at the Yambukan River mouth, the fifth to seventh in the same exposure at the Chernokhrebetnaya River) thus characterizing the well-detectable biostratigraphic units and their time successions. Four lowermost faunas are recognized in terrigenous and volcanogenic deposits of the Tunguska syneclise.

The *first conchostracan fauna* of Bairdestheriidae [*Rohdendorfium* (*Bipemphigus*) *gennisi* (Nov.)] is the oldest one among others and characteristic of most localities (36, some designated further in brackets) studied in the Tunguska syneclise and North Anabar region. This fauna is detected in shaly aleurolites (Korbunchana), limestone interbeds (Avam), calcareous concretions (Delimekit), and tuffaceous sedimentary rocks (other localities) of the Gagarii Formation and lower beds of the Pirda Formation (Gagarii and Lebedeva horizons; Orlova, 1990).

The first conchostracan fauna is investigated, by applying the advanced method, on the basis of very representative collection (over 2000 of specimens) from 39 burials of 22 localities and six burials of two drill-hole sections (Orlova, 1978, 1990, 1991). Several dozens, usually from 100 to 600 specimens from each burial have been studied.

Conchostracan assemblages from burials consist almost entirely of species *Rohdendorfium* (*Bipemphigus*) *gennisi* (Nov.) displaying the striate-costate sculpture well-distinguishable in practice (Fig. 2). These forms coexist sometimes with single specimens of Leaiidae, Limnadiidae, and some other families. For instance, in the lower beds of the sequence (Korbunchana, Khoiro, Balagannakh), forms other than *R.* (*B.*) *gennisi* (Nov.) are usually missing. Higher in the section, there are representatives (up to 15%) of Limna-

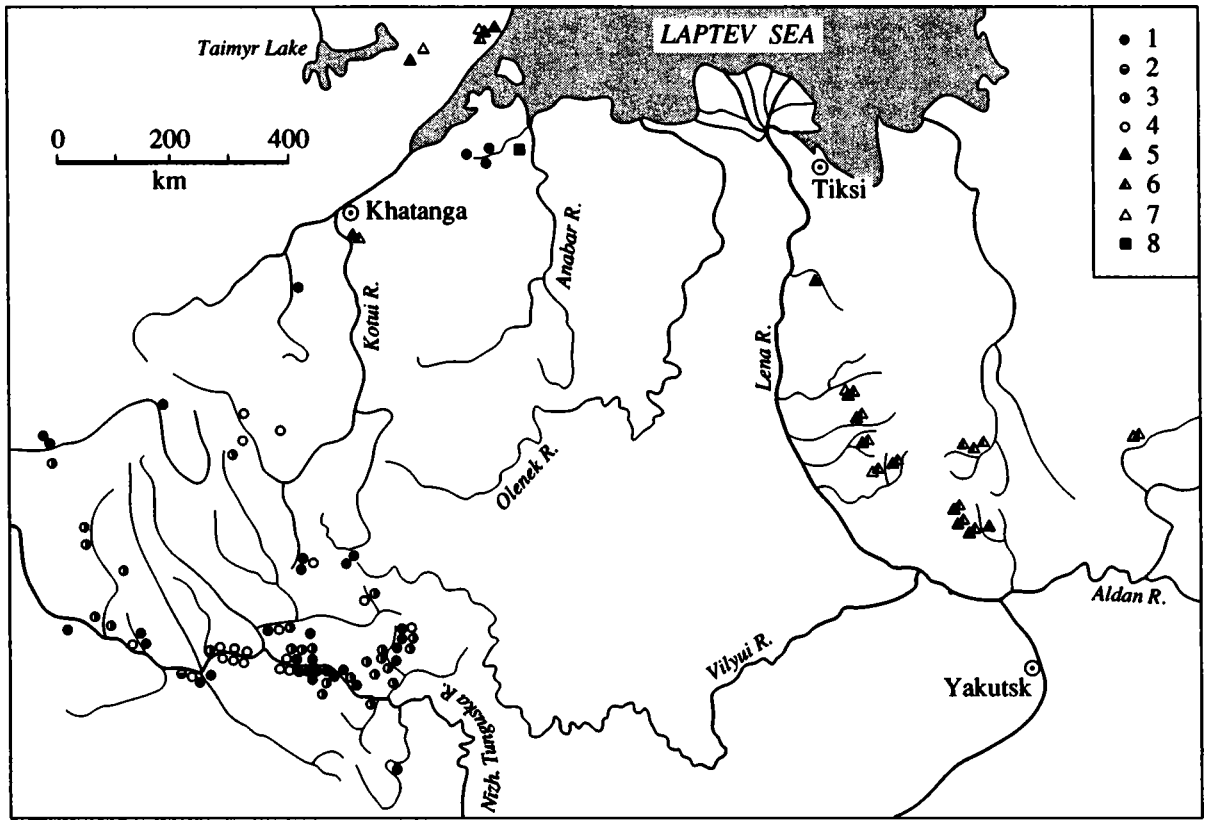

Fig. 1. Distribution areas of Permian and Triassic conchostracans in the north of Central Siberia (symbols and their number denote the distinguished conchostracan faunas).

diidae, Glyptoasmussiidae (Mol'daul', Yastrebok, Turka, Avam), and Leaiidae forms (Shadrinka) widespread in younger assemblages. At the boundary with deposits bearing the third fauna, the mixed assemblage includes *R. (B.) gennisi, Limnadia vana* Nov. (Delimekit), *Mimoleaia mitchelli* (Ether.) (Shadrinka), and some other species.

Remains of other organisms have been encountered in association with conchostracans or within neighboring interbeds almost everywhere. In the Gagarii Horizon (Korbunchana), the *R. (B.) gennisi* Beds bear ostracodes *Darwinula elegantella* Belous., *D. inornata* var. *macra* Lun., *D. parallela* (Spizh.), *Suchonella emphasis* Misch., *S. facilis* Misch., *S. stelmachovi* Spizh., and *Darwinuloides tatarica* Posn., whereas the overlying tuffaceous siltstones enclose leaf impressions of Cordaitanthales and remains of Dicynodontidae. In the Lebedeva Horizon (Anakit), conchostracans coexist with several groups of fossils: phytoleims of *Pecopteris crenata* (Pryn.), *Cladophlebis (Aurifolia) lobifera* Pryn., *Tungussopteris* cf. *sphenopteroides* Vlad., *Lepidopteris* cf. *arctica* Mog., and *Taeniopteris* (?) *prynadae* Mog.; fish bones of *Evenkia eunotoptera* Berg, *Arctosomus sibiricus* Berg, *Tungusichtys acentrophoroides* Berg, and *Perleidus borealis* Yakovl.; ostracodes *Darwinula inornata* (Spizh.), *D. interactata* Mand., *D. kassini* Belous., *D. sibirica* Mand., *Darwinuloides oviformis* Mand., *Suchonella stelmachovi* Spizh., and *Tatariella permiensis* Misch.; fossil insects of Schizocoleidae family; and amphibian species *Tungussogyrinus bergi* Efr. Plant remains of *Madygenia* aff. *borealis* Radcz. are known from the Balagannakh locality. Bivalves *Palaeanodonta* ex gr. *compressa* (Ludwig), *Microdontella (Abiella) maltseviensis* (Rag.), and *Antraconauta* (?) ex gr. *pseudophillipsi* Fed. are encountered at the Lopokol locality. Plant remains from the Khungtukun Horizon are represented by *Neokoretrophyllites annularioides* Radcz., *N. linearis* (Pryn.), and *Todites* aff. *borealis* Pryn. in the Mamilyakan locality, and by *Quadrocladus pachyphyllus* (Pryn.), and *Q.* cf. *sibiricus* (Neub.) in the Turka and Dvurogii localities. *Mertensides* cf. *lingulatus* (Mog.) and *Cladophlebis (Aurifolia)* cf. *lobifera* Pryn. occur in the nearby Avam locality. Bivalves *Abiella* cf. *subovata* (Jones) and *Microdontella plotnikovskiensis* (Fed.) are known from the Mamilyakan locality. Ostracodes *Darwinula postparallela* (Misch.), *D. regia* Misch., *Suchonella lucida* Mand., and *Gerdalia variabilis* (Misch.) are detected at the Turka locality.

As noted above, species *Rohdendorfium (Bipemphigus) gennisi* occur, beginning from the Gagarii Horizon, together with abundant remains of Cordaitantha-

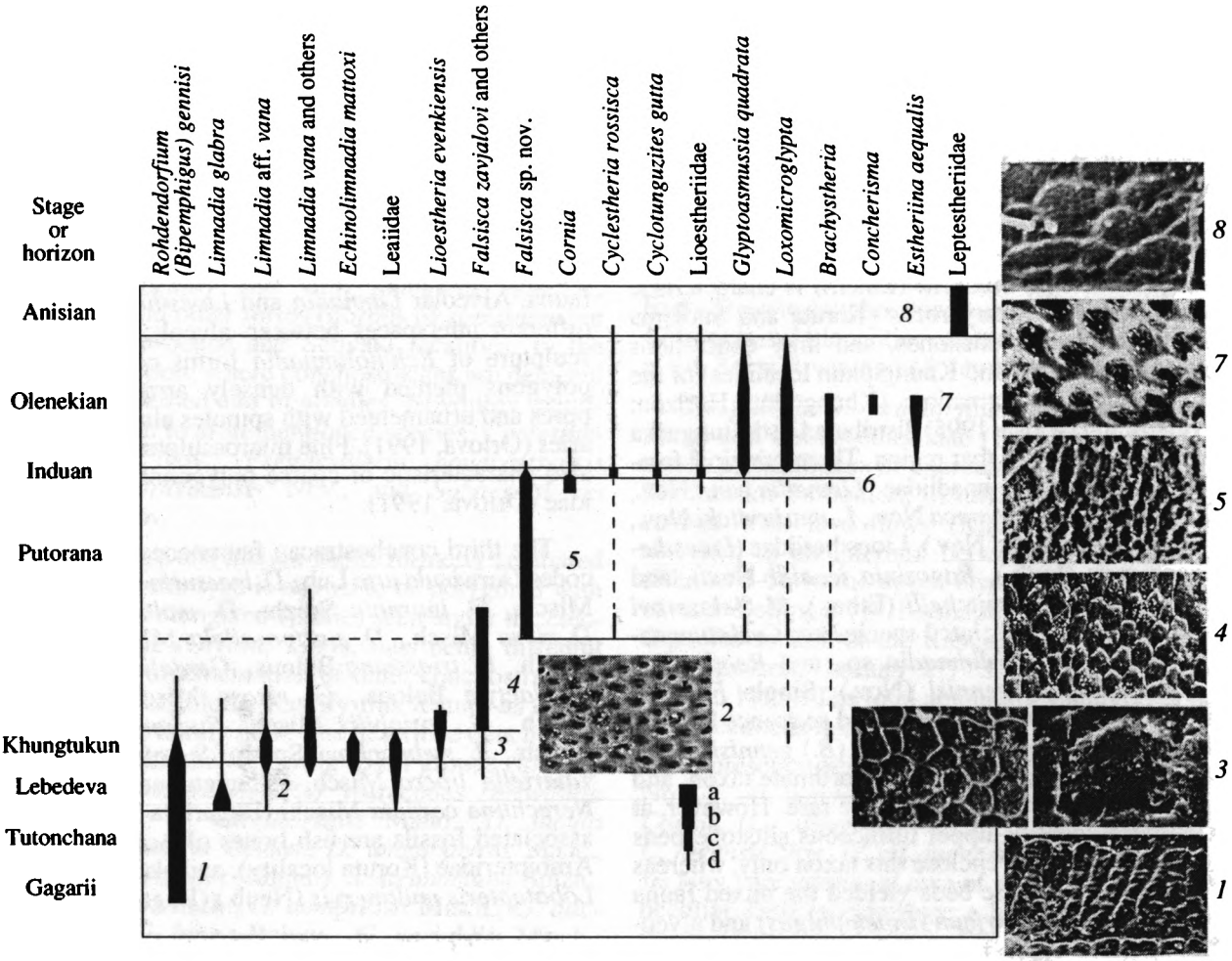

Fig. 2. Stratigraphic ranges and morphostructural types of conchostracan shells from the north of Central Siberia. Width of lines indicate the abundance rate of taxa in assemblages: (a) highly dominant; (b) dominant to subdominant; (c) subordinate; (d) accessory.

les. In some localities, they coexist with *Mimoleaia mitchelli* (Ether.) characteristic of uppermost Permian Belmont Beds in New South Wales, Australia (Novojilov, 1958). At the same time, I failed to identify the Triassic forms *Lioestheria aequalis* (Lutk.), *L. gutta* (Lutk.), and *Estherites evenkiensis* (Lutk.), E. tungussensis (Lutk.), in the new representative collection from the Balagannakh locality, although they have been reported earlier from this site. Accordingly, all data suggest the Late Permian age of the first conchostracan fauna.

Shell sculpture in all other conchostracan families representing the second to seventh of distinguished faunas was traditionally considered as alveolar. However, the scanning electron microscopy showed its variability, and now we can distinguish several morphological types of alveolar sculpture proper and also the polygonal ornamentation.

The *second conchostracan fauna* of Limnadiidae is tentatively considered here as being older than the third one, though it is not inconceivable that they are coeval. This fauna is detected only at the Gagarii locality (Sadovnikov and Orlova, 1995) in calcareous concretions from tuffites of the Dyuk Formation (Lebedeva Horizon). The fauna includes genera *Limnadia* (*L. glabra* Mitch., *L.* aff. *vana* Nov.) and *Eulimnadia* (*E. shorokhovi* Nov.). Only three of the more than 150 specimens mainly representing the *Limnadia* forms (about 80%) are identified as *Lioestheria evenkiensis* (Lutk.). Morphological distinctions between two the aforementioned *Limnadia* species are insignificant maybe because of their preservation state, and I suppose that they could be considered as representing one taxon (*L.* aff. *vana* Nov.) after the additional study. In this case, it would be reasonable to unite the second and third faunas. All species of the second fauna show alveolar, though slightly variable sculpture of shells (Orlova, 1991).

At the site where the second fauna is established, conchostracans coexist with bivalves *Abiella* cf. *elliptica* (Khalf.) and *Anthraconaia* aff. *vivi* Mal., and also with phytoleims of *Arthropitys prynadae* Sadovn.,

A. tunguskanus Sadovn., *Todites borealis* Pryn., *Acrostichides tunguskanus* Pryn., *Kirjamkenia lobata* Pryn., *Stiphorus crassus* Mog., and *Parajacutiella* (?) *angusta* Mog. The Late Permian age of the fauna is indicated by presence of *Limnadia glabra* Mitch. known from Permian Belmont Beds of New South Wales, Australia.

The *third conchostracan fauna* of Limnadiidae (*Limnadia vana* Nov., *Echinolimnadia mattoxi* Nov.), Lioestheriidae (*Lioestheria evenkiensis* (Lutk.)), and Leaiidae (*Mimoleaia mitchelli* (Ether.)) is characteristic of tuffaceous sedimentary rocks (Koruta and Suolema localities), calcareous siltstones, and limy concretions (Nizhnyaya Bugarikta and Khungtukun localities) of the Pirda and Bugarikta formations (Khungtukun Horizon; Sadovnikov and Orlova, 1995) distributed in the tunguska syneclise and North Anabar region. Three principal families of the fauna are Limnadiidae (*Limnadia vana* Nov., *L.* aff. *vana* Nov., *L. pygmaea* Nov., *L. markevitchi* Nov., *Echinolimnadia mattoxi* Nov.), Lioestheriidae (*Lioestheria evenkiensis* (Lutk.), *Ragozinia leonidi* Nov.), and Leaiidae (*Mimoleaia mitchelli* (Ether.), *M. belozerovi* Nov., and others). Associated species are *Cyclotunguzites gazimuri* Nov., *Eulimnadia* sp., and *Rohdendorfium* (*Bipemphigus*) *gennisi* (Nov.). Single *Falsisca* forms appear in the upper part of bed sequence bearing the third fauna. In the lower part, *R.* (*B.*) *gennisi* (Nov.) prevailing in the first fauna is a subordinate taxon, and higher in the section these forms are rare. However, at the Delimekit locality, upper tuffaceous siltstone beds of the Pirda Formation enclose this taxon only, whereas limy nodules from these beds yielded the mixed fauna of old striate *Rohdendorfium* (*Bipemphigus*) and alveolar Limnadiidae typical of younger deposits. Faunas from the limy nodules are variable in composition: in some of them, *R.* (*B.*) *gennisi* represents half of all specimens and about one third in others, being sporadic in particular nodules, where the remaining specimens belong to Limnadiidae. Very characteristic taxa of the third fauna are *Echinolimnadia mattoxi* with radial rows of spines and Leaiidae forms with radial carinae, which are missing in younger faunas and occasional in older ones. The mixed assemblages from boundary deposits include taxa characterizing either the first, second and third (Delimekit-2 and Shadrinka-1 localities), or the third and fourth faunas (Untuun-2 locality).

The third conchostracan fauna is known in 30 localities, eight of which I have studied personally (two yielded mixed assemblages; total amount of investigated specimens is over a thousand). Assemblages from individual burials differ from each other in proportions of main and subordinate taxa. In nodules and sedimentary beds of the Khungtukun locality, the principal taxon is *Limnadia vana* Nov. (hundreds of specimens) *Limnadia* aff. *vana* displaying some morphological distinctions as compared to holotype. Almost all nodules also bear *Echinolimnadia mattoxi* (single specimens to 50% of all taxa) (dozens of specimens). *Lioestheria evenkiensis, Ragozinia leonidi*, and *Cyclotunguzites gazimuri*, which are much less abundant than *Limnadia* forms, occur in nodules almost everywhere. The conchostracan assemblage from nodules of the Nizhnyaya Bugaricta locality consists predominantly of *Echinolimnadia mattoxi* (hundreds of specimens) associated with occasional specimens of *Limnadia vana, L. pygmaea, Mimoleaia mitchelli* (single specimens), and *Rohdendorfium* (*Bipemphigus*) *gennisi.*

The SEM analysis revealed the following morphological features of conchostracans shells from the third fauna. Alveolar *Limnadia* and *Lioestheria* forms have different interspaces between alveoli. The polygonal sculpture of *Echinolimnadia* forms consists of large polygons pierced with densely arranged prismatic pores and ornamented with spinules along their boundaries (Orlova, 1991). Fine microsculptural elements are also characteristic of coarse polygonal shells of Leaiidae (Orlova, 1991).

The third conchostracan fauna coexists with ostracodes *Darwinula arta* Lub., *D. inassueta* Misch., *D. innae* Misch., *D. inornata* Spizh., *D. malachovi* (Spizh.), *D. mera* Misch., *D. postparallela* Misch., *D. prisca* Misch., *D. triassiana* Belous., *Gerdalia clara* Misch., *G. dactyla* Belous., *G. rixosa* Misch., *G. sibirica* Misch., *G. variabilis* Misch., *Suchonella constricta* Neustr., *S. stelmachovi* Spizh., *S. tajmurica* Misch., *Tatariella libera* Misch. (Khungtukun locality), and *Nerechtina cordata* Misch. (Bugarikta locality). Other associated fossils are fish bones of Acrolepididae and Ambipteridae (Koruta locality), and also phytoleims of *Lobatopteris multinervis* (Neub.) (Bugarikta locality).

The third fauna from the Khungtukun locality consists mostly of local species. *Limnadia vana, Lioestheria evenkiensis, Ragozinia leonidi*, and *Cyclotunguzites gazimuri* were recorded in the Khungtukun locality. Novojilov (1958) and I failed to distinguish among them Triassic species *"Estheria" gutta* and *"E." aequale*, which have been reported by Lyutkevich (1938) from this site. Presence of *Mimoleaia mitchelli* characteristic of the Belmont Beds in Australia may indicate the Permian age of this fauna.

The *fourth conchostracan fauna* of Limnadiidae (*Falsisca zavjalovi* Nov., *F. turaica* Nov., *Limnadia vana* Nov.) and Lioestheriidae [*Lioestheria evenkiensis* (Lutk.)] characterizes tuffaceous sedimentary rocks and limy nodules from the Irgakta, Nidym, and Kochechumo formations (Putorana Horizon) of the Tunguska syneclise (Sadovnikov and Orlova, 1995). This fauna, consisting mainly of Limnadiidae and Lioestheriidae representatives, is distinct because of widespread *Falsisca* species (20–100%) displaying a characteristic bend of growth lines in the posterior dorsal area of shells. These species are extremely rare in underlying beds. Other Limnadiidae species are *Limnadia vana, L.* aff. *vana, L. markevithci, Eulimnadia* sp., and some others. Lioestheriidae forms are represented by *Lioestheria evenkiensis*, less abundant *Ragozinia leonidi* Nov., and occasional *Pseudestheria* species. Rare rep-

resentatives of Bairdestheriidae, Glyptoasmussiidae, and Cyclestheriidae occur locally.

The fourth fauna is known from 20 localities, six of which I have studied personally (600 specimens). At the Dakat, Turukan, and Khoktomo localities, almost all conchostracans belong to the genus *Falsisca* (dozens to hundreds of specimens). The widespread representatives of the genus associate with quite abundant (dozens of specimens) *Lioestheria evenkiensis* at the Irgakta Yar locality and with *Limnadia vana, L. markevitchi*, and other forms (dozens of specimens) at the Khekchekit-Seene and Sebyaki localities. In the Irgakta Yar section, where conchostracans are detected within nine interbed and in nodules, Novojilov identified, in addition to aforementioned species, *Cyclestheria krivickii* Nov., *Pseudestheria novacastrensis* Mitch., *P. nordvikensis* Nov., and *Sphaerestheria belorussica* Nov.

The sculpture of *Falsisca* shells formerly attributed to the fine alveolar type is shown to be polygonal with large rhomboid elongated cavities seen under the electron microscope (Orlova, 1991), thus being different from the shell ornamentation of other conchostracans. It appears reasonable to classify this feature as corresponding to the family rank. The described conchostracans coexist with the following fossil groups (locality names are given in brackets): ostracodes *Darwinula aceris* Misch., *D. curvidorsalis* Mand., *D. lucida* Mand., *D. triassiana* Belous., *D. tunguskiensis* Mand., *Suchonella interactata* (Mand.), *S. stelmachovi* Spizh., *Gerdalia clara* Misch., *G. compressa* Misch., *G. dactyla* Belous., *G. longa* Belous., *G. variabilis* Misch., *Wetluginella solers* Misch., *Tatariella constricta* Neustr. (Irgakta Yar), *Darwinula fragilis* Schneid., *D. longissima* Belous., *D. pseudoobliqua* Belous., *D. pseudooblonga* Belous., *D.* (?) *triassiana* Belous., *Gerdalia dactyla* Belous., *G. longa* Belous (?) and *Suchonella stelmachovi* Spizh. (Dakat); bivalves *Palaeomutela* (?) ex gr. *rectodonta* Amal., *Anaplophora* sp., and *Myoconcha* sp. (Dakat); Palaeoniscoidea fish remains (Dakat); phytoleims of *Acrostichides kirjamkensis* (Pryn.), *Cladophlebis* (*Aurifolia*) *lobifera* (Pryn.), *Parajacutiella* (?) *angusta* Mog. (Khoktomo), and *Cladophlebis* cf. *haiburnensis* (L. et H.) (Khekchekit-Seene). At the Turukan locality, *Pecopteris* cf. *crenata* (Pryn.) and *Parajacutiella* (?) cf. *angusta* are detected inside a bed bearing conchostracans, and *Quadrocladus* (?) sp. below this level.

Almost all conchostracans of the fourth fauna are endemics unsuitable for age determination. On the basis of single specimens of *Pseudestheria nordvikensis* known from the Permian Misailap Formation of the Khatanga Bay and *Pseudestheria novacastrensis* occurring in the Permian Belmont Beds of New South Wales, the age problem cannot be solved unambiguously.

Early and Middle Triassic conchostracans (fifth to seventh and eighth faunas, respectively) are distinguished for the first time in lagoonal and coastal-marine sediments of Taimyr and in continental volcanogenic deposits of the Kotui River lower courses. All three Early Triassic faunas are detected in one section exposed at the Chernokhrebetnaya River upstream from the Ostantsovaya River mouth. In addition, the fifth and sixth faunas characterize the Kotui River section, the fifth and seventh faunas occur in closely spaced exposures of the Kholid'e locality (Mt. Pervaya), and the seventh and eighth faunas are known from Well B-3 located in the North Anabar region. The Early Triassic conchostracans studied here characterize 17 burials in 11 localities of eastern Taimyr, four burials at the Kotui River, and 18 depth levels in Well B-3.

The *fifth conchostracan fauna* of Limnadiidae (*Falsisca*) and Gabonestheriidae (*Cornia*) is detected in a series of localities: in charcoal gray siltstones of the Marininskii Formation; in tuffaceous sediments intercalated with lava flows (Kholid'e localities 5, 14, and 15), in an interbed between two lava sequence (Kholid'e-6), in the upper lava sequence (Kholid'e-7) of the Betlinga (?) Formation; and finally, in the Ostuolba section of the Kapchan Formation, Marininskii Horizon, Induan (?) Stage (Sadovnikov and Orlova, 1995). The total amount of studied conchostracan specimens is over 600.

Representatives of genera *Falsisca* (*F.* aff. *turaica* Nov., *F.* aff. *verchojanica* Mol., *Falsisca* sp. Nov.) and *Cornia* (*C. sileenica* Mol., *C.* aff. *sileenica* Mol., *C. jugensis* Nov., *C.* aff. *jugensis* Nov., *C.* ex gr. *jugensis* Nov.) are dominant taxa of the fauna, all displaying peculiar shell morphology: a bend of growth lines in the posterior-dorsal area in *Falsisca* shells and a tubercle on the larval valve of *Cornia* shells. Species of Lioestheriidae, Cyclestheriidae, and Glyptoasmussiidae are accessory components of the fauna. Three localities (Kholod'e-15, Marininskii, and Ostuolba) yielded only *Falsisca* species and two (Kholid'e-7 and 14) only *Cornia* forms; a combination of both taxonomic groups is typical of other localities, where either the former (Kholid'e 5 and 7, Ostuolba), or the latter taxa (Kholid'e) are predominant. All *Falsisca* and almost all *Cornia* forms show some features distinguishing them from known representatives of these genera. Sculpture of *Falsisca* shell is similar to that described above, whereas *Cornia* shells are alveolar.

Plant remains associated with the fifth conchostracan fauna are *Pleuromeia taimyrica* Sadovn., *Tomiostrobus belozerovii* Sadovn., *T. fusiformis* Sadovn., *Lepidopteris arctica* Mog. and others (Marininskii locality), *Tomiostrobus belozerovii* Sadovn., *T. migayi* (Schved.), *Lepidopteris* sp., *Peltaspermum* sp. (Ostantsovaya locality), *Tomiostrobus* cf. *belozerovii* Sadovn. (Kholid'e localities), *Lepidopteris* sp. and *Quadrocladus sibiricus* (Neub.) (Ostuolba locality).

The *sixth conchostracan fauna* of Limnadiidae (*Falsisca*), Lioestheriidae (*Lioestheria ignatjevi* Nov., *Pseudestheria sibirica* Nov.), and Cyclestheriidae (*Cyclestheria rossica* (Chern.), *Cyclotunguzites gutta*

(Lutk.)) is recovered from the variegated terrigenous deposits of the Fad'yukuda Formation, Ust' Kel'ter Horizon, Induan Stage (Sadovnikov and Orlova, 1995). The amount of studied specimens is about 240. Conchostracans of this fauna are more diverse than in the previous community, and their composition is transitional between the fifth and seventh faunas. *Falsisca* species identical to those described above coexist here with abundant Lioestheriidae forms (one third in the Ostuolba assemblage and more than a half in the Ostantsovaya assemblage) such as *Lioestheria ignatjevi* Nov., *L. propinqua* Nov., *Pseudestheria sibirica* Nov., and *P. kashirtsevi* Nov. Other families from this level are Cyclestheriidae (*Cyclestheria rossica* Nov., *Cyclotunguzites gutta* (Lutk.)) and Glyptoasmussiidae (*Glyptoasmussia quadrata* Nov., *Brachystheria kotchetkovi* Nov.), the latter widespread in the next younger fauna. The listed taxa, except those of *Falsisca* genus, have alveolar shells ornamented like in identical forms from other faunas.

The fifth conchostracan fauna occurs together with phytoleims of *Tomiostrobus latus* Sadovn. Higher in the sequence, there are detected *Pleuromeia taimyrica* Sadovn. (Ostantsovaya locality), *Tomiostrobus belozerovii* Sadovn., *T. bulbosus* Sadovn., *T. deltoideus* Sadovn., *T. latus* Sadovn., *Lepidopteris* sp., and *Quadrocladus sibiricus* (Neub.) (Ostuolba locality).

The *seventh conchostravan fauna* of Glyptoasmussiidae is typical of variegated upper beds of the Fad'yukuda Formation (Ostantsovaya locality), lower beds of the Kiryakatas Formation (Pavlova River, Mt. Pervaya), and gray siltstone beds of the Ystanakh and Pastakh formations (Well B-3, Suolema locality). These beds span the upper Induan Substage and Olenekian Stage (Sadovnikov and Orlova, 1995). About 530 conchostracan specimens from these beds have been studied so far.

Representatives of Glyptoasmussiidae prevailing in the seventh fauna (30–90%) have the developed anterior part of dorsal margin and are distinct from older Early Triassic forms. These are *Loxomicroglypta sibiricularis* (Chern.), *L. nodosa* Nov., *Glyptoasmussia quadrata* Nov., *Brachystheria kotchetkovi* Nov., *B. taimyrensis* Nov., *Concherisma tomensis* Nov., and *C. sundyrensis* Nov. The listed species frequently associate with Estheriinidae forms: *Estheriina aequalis* (Lutk.) and *Notocrypta begitchevi* Nov. Other taxa of the seventh fauna are *Cyclotunguzites gutta* (Lutk.), *Pseudestheria sibirica* Nov., *P. putjatensis* Nov., *P. kashirtzevi* Nov., *Lioestheria ignatjevi* Nov., *L. propinqua* Nov., and *Sphaerestheria ovata* Nov. and others.

Being similar in general, conchostracan assemblages from the Ostantsovaya, Pavlova River, and Mt. Pervaya localities show slightly variable proportions of species from different families. A newcomer, the genus *Concherisma* of Glyptoasmussiidae appears in the fauna higher in the sequence (localities Pavlova River and Mt. Pervaya). Representatives of Estheriinidae, the *Notocrypta* genus included, become abundant at the same level (up to 30% at the locality Mt. Pervaya). At the same time, the conchostracan assemblage from Well B-3 (Suolema locality) is impoverished and includes a few specimens of *Glyptoasmussia quadrata* Nov., *Cyclotunguzites gutta* (Lutk.), and *Pseudestheria* aff. *rybinskensis* Nov.

According to SEM data, the alveolar sculpture of Glyptoasmussiidae shells consists of rounded, locally oval (drop-like) cavities (Orlova, 1991).

The seventh conchostracan fauna coexists with bivalves *Pseudocorbula* sp. (Suolema locality), ammonites *Arctoceras* cf. *oebergi* (Mojs.) (Pavlova River), and phytoleims of *Pleuromeia taimyrica* Sadovn. Plant remains of *Tomiostrobus migayi* (Schved.) and *Mesenteriophyllum* (?) sp. are encountered higher in the sequence at the Ostantsovaya locality.

In the West Verkhoyansk region, three Early Triassic conchostracan faunas were detected in 42 burials located along the right-hand tributaries of the Lena River, within the Dulgalakh River tributaries and Delin'ya River (Tompo River tributary) basins, and on both, western and eastern slopes of the Verkhoyansk Range. The faunas are similar to conchostracan assemblages from Induan and Olenekian deposits of Taimyr and North Anabar region. However, conchostracan shells from the West Verkhoyansk localities are poorly preserved and unsuitable for SEM investigation.

The complete succession of three Early Triassic faunas is established in the Syncha River section. In addition, the fifth and sixth faunas are detected in sections of the Sobopol, Seimcheen, and Kel'ter rivers, in the last case, together with upper mixed assemblages incorporating some species of the seventh fauna. The succession of sixth and seventh faunas is recognized in exposures of the Delin'ya and Yulegiir rivers.

The fifth conchostracan fauna is characteristic of seven burials in continental deposits of western slope of the Verkhoyansk Range (the Mol, Kel'ter, Seimcheen, Sobopol, Syncha, and Unguokhtaakh rivers). Mixed assemblages with subordinate species of the sixth fauna are established at three localities (Kel'ter, D'olobuun, Seimcheen) of this area. The amount of studied specimens from all these localities is over 1500. In the eastern slope of the range, I did not detect the fifth fauna, which, according to Molin (1965), is present in exposures near the Magan-Khaya River mouth on generally the left side of the Dulgalakh River. The fauna in question is similar to the fifth fauna of Taimyr, despite some minor differences in species composition.

In some of the Verkhoyansk Range localities (Seimcheen, D'olobuun), conchostracans closely associate with fossil plant remains *Tomiostrobus belozerovii* Sadovn. and *T.* cf. *radiatus* (Neub.). At the Sobopol locality, *T. bulbosus* Sadovn., *T. deltoideus* Sadovn. (Mol), and *T. latus* Sadovn. (Sobopol) occur immediately below and above interbeds bearing conchostracans.

The sixth conchostracan fauna is most widespread in the West Verkhoyansk region, where it is known from 26 burials in both continental (Kel'ter, Yulegiir, Sobopol, and Syncha localities) and marine deposits (Delin'ya, Echii, and Mataga sites), being represented by more than 200 specimens in my collection. Almost all species from this level are of a wide stratigraphic range and occur throughout the Lower Triassic sequence. Species of this kind are less abundant in the fifth and seventh faunas.

The sixth fauna from the West Verkhoyansk region is similar to but more diverse than that from Taimyr and North Anabar region. Another distinctive feature of this regional fauna is presence of rather abundant species *Wetlugites pronus* Nov. In some localities of the region (Kel'ter and Sobopol), conchostracans under consideration coexist with phytoleims of *Tomiostrobus latus* Sadovn. and *T. migayi* (Schved.), in others, with bivalves *Atomodesma errabunda* Popov (Delin'ya, Echii, and Mataga) or with ammonites *Wordieoceras* (Delin'ya). In deposits bearing the sixth fauna mixed with younger conchostracans, there are detected *Vavilovites* forms (Delin'ya).

The sevens conchostracan fauna is characteristic of six localities in the western (continental deposits in the Syncha and Yulegiir river basins) and eastern slopes (marine deposits at the Delin'ya locality) of the Verkhoyansk Range. The few localities with this fauna is likely a consequence of coarse-grained structure of the upper Induan deposits widespread within the range. The amount of studied specimens is over 700.

Despite some distinctions at the species level, the seventh fauna of the region is similar to that from Taimyr and North Anabar region. It coexists here with phytoleims of *Tomiostrobus latus* Sadovn. (Syncha River) and with ammonites *Vavilovites* sp. (Delin'ya River).

Considering the age of the fifth to seventh conchostracan faunas, I should mention first that Molin (1965) attributed the *Cornia–Falsisca* assemblage (the fifth fauna in my terminology) to the lower Induan Substage. This is an admissible, but not well-constrained interpretation. The early Induan *Otoceras* forms are known only from the eastern slope of the Verkhoyansk Range, whereas the fifth fauna is localized in the western slope. Molin reported on only one eastern burial of conchostracans, where ammonites are unknown. Consequently, it is not inconceivable that the fifth fauna is actually older than the *Otoceras* Zone.

The sixth fauna includes *Lioestheria ignatjevi* Nov., *Pseudestheria sibirica* Nov., *Cyclotunguzites gutta* (Lutk.), *Cyclestheria rossica* Nov., and others, all characteristic of the Vetluga Group in the Volga–Ural region and coexisting with the *Wordieoceras* genus of ammonites typical of upper beds of the lower Induan. The *Vavilovites* genus of late Induan ammonites is found to be coeval with conchostracan assemblages incorporating mixed taxa of the sixth and seventh faunas. The last one includes, in addition to species typical of the Vetluga Group and Induan–Olenekian deposits, the endemic forms of Glyptoasmussiidae, which have been described by Novojilov (1946) as occurring in living chambers of characteristic Olenekian ammonites *Keyserlingites subrobustus* (Mojs.) and *Arctomeeoceras sibiricum* (Mojs.), albeit the late Induan *Vavilovites* sp. are also known in association with this conchostracan fauna. Furthermore, the seventh fauna coexists with *Arctoceras* cf. *oebergi* (Mojs.) in upper variegated beds of the Kiryakatas Formation of Taimyr. All these data suggest that the sixth and seventh conchostracan faunas characterize the Induan–Olenekian boundary deposits.

The *eighth conchostracan fauna* of Leptestheriidae (*Tigjanum borchgrevinki* Nov., *Diaplexa tigjanensis* Nov.) is established in drill-hole sections of the Nordvik Peninsula. I have studied about 200 conchostracan specimens of this fauna from terrigenous deposits of the Gurimis Formation recovered by the drill hole at the Suolema locality within the depth interval of 1105–1118.6 m.

Besides forms encountered in the sixth and seventh faunas, such as *Loxomicroglypta subcircularis* Chern., *Glyptoasmussia quadrata* Nov., *Cyclotunguzites gutta* (Lutk.), *Pseudestheria rybinskiensis* Nov., and others, the conchostracan assemblage, which is youngest among others studied here, includes taxa displaying complex polygonal sculpture of shells and lacking below in older Triassic assemblages (Orlova, 1991). These are representatives of Leptestheriidae: *Tigjanum borchgrevinki* Nov. and *Diaplexa tigjanensis* Nov.

It is difficult to estimate real proportions between taxa on the basis of limited material from one drill hole. In the lower beds of studied depth interval, Leptestheriidae forms always coexist with other taxa. Higher in the section, they are either isolated from or combined with other families.

The eighth conchostracan fauna is associated with bivalves *Pseudocorbula* ex. gr. *gregaroides* Phill. According to Novojilov, both representatives of Leptestheriidae are characteristic only of Anisian deposits at the Laptev Sea coast (drill hole at the Tigyan River), where they are coeval with Anisian bivalves *Bakevellia arctica* Kipar., *Trigonodus praelongus* Kipar, and ammonites *Danubites* sp. and *Arctohungarites* sp. Thus, the described assemblage of conchostracans appears to be of the Anisian age as well.

To end the discussion, I should note that conchostracans occur in both marine and continental sediments and represent fossils of the euryfacies type. The oldest pre-Triassic taxon *Rohdendorfium* (*Bipemphigus*) *gennisi* Nov. is widespread over the Tunguska syneclise, being abundant in continental tuffaceous and bituminous-terrigenous sediments. In limy nodules, the same conchostracans coexist with *Limnadia* species characteristic of tuffaceous sedimentary rocks as well. In the Dvurogii Formation, *Rohdendorfium* (*Bipemphigus*)

gennisi Nov. is found within limestone interlayers in association with occasional Glyptoasmussiidae forms coexisting with lingulids and ammonites in coastal-marine deposits of Taimyr.

Falsisca species, widespread in tuffaceous sediments and calcareous nodules of the Tunguska basin and North Anabar region and also in variegated continental sediments in the east of the Verkhoyansk Range, are simultaneously the key fossils of gray terrigenous deposits in the east of Taimyr (Marininskii Creek). The mixed conchostracan assemblage from tuffaceous sediments of the North Anabar region includes some species characteristic of black siltstones of the Marininskii Formation and variegated sandstone and siltstone beds of the Fad'yukuda Formation.

At the same time, different conchostracan assemblages may characterize identical sedimentary facies in different parts of a sequence. For instance, the first and third to distinguished faunas are established in tuffaceous sediments, whereas the first and fifth–eighth faunas are typical of terrigenous deposits, and the first–fourth faunas are buried in carbonate nodules.

Reviewer A.S. Alekseev

REFERENCES

Lyutkevich, E.M., Triassic Estheriae from Upper Beds of the Tunguska Group, *Tr. Arkt. Inst.*, 1938, vol. 101, pp. 155–164.

Molin, V.A., Early Triassic Bivalve Phyllopoda from North Yakutia, in *Dvustvorchatye listonogie permi i triasa severa SSSR* (Permian and Triassic Bivalve Phyllopoda from the Northern USSR), Molin, V.A. and Novojilov, N.I., Eds., Moscow: Nauka, 1965, pp. 57–76.

Novojilov, N.I., New Phyllopoda from Permian and Triassic Deposits of the Nordvik–Khatanga Region, *Nedra Arktiki*, 1946, no. 1, pp. 172–202.

Novojilov, N.I., New Phyllopod Bivalves from the Korvunchan Group of the Lower Tunguska River Basin, in *Dvustvorchatye listonogie permi i triasa severa SSSR* (Permian and Triassic Phyllopod Bivalves of the Northern USSR Regions), Molin, V.A. and Novojilov, N.I., Eds., Moscow: Nauka, 1965, pp. 45–56.

Novojilov, N.I., Conchostraca du Permien et du Triass du littoral de la mer des Laptev et de la Toungouzka inferieure, *Ann. Serv. Inform. geol. BRGGM*, Paris, 1958, no. 26, pp. 15–80.

Orlova, E.F., Application of Replica Method for Investigation of Fossil Conchostracans, *Paleontol. Zh.*, 1978, no. 3, pp. 124–127.

Orlova, E.F., New Data on Conchostracans Rohdendorfium and Bipemphigus from Volcanogenic Permian–Triassic Deposits of the Tunguska Syneclise, *Paleontol. Zh.*, 1990, no. 1, pp. 66–75.

Orlova, E.F., Microsculpture of Conchostracan Shells from North Siberian Platform: First Data of Scanning Electron Microscopy, *Dokl. Akad. Nauk SSSR*, 1991, vol. 316, no. 6, pp. 1476–1478.

Sadovnikov, G.N. and Orlova, E.F., New Data on Stratigraphy of Permian–Triassic Volcanogenic Deposits in the Central Par of the Tunguska Syneclise, *Stratigr. Geol. Correlyatsiaya*, 1995, vol. 3, no. 1, pp. 34–42.

Stratigraphy and Geological Correlation, Vol. 7, No. 5, 1999, pp. 473–491. Translated from Stratigrafiya. Geologicheskaya Korrelyatsiya, Vol. 7, No. 5, 1999, pp. 64–83.
Original Russian Text Copyright © 1999 by Vishnevskaya, Pral'nikova.
English Translation Copyright © 1999 by МАИК "Наука/Interperiodica" (Russia).

Jurassic Radiolarians from Northern Russia

V. S. Vishnevskaya* and I. E. Pral'nikova**

** Institute of the Lithosphere of Marginal Seas, Russian Academy of Science, Staromonetnyi per. 22, Moscow, 109180 Russia*
*** Geological Institute, Russian Academy of Sciences, Pyzhevskii per. 7, Moscow, 109017 Russia*

Received November 26, 1997; in final form, May 21, 1998

Abstract—The latitudinal models of radiolarian paleogeographic provinces are considered, and Late Jurassic boreal radiolarian assemblages of Russia are characterized. Several Jurassic radiolarian assemblages from the Koryak Upland are correlated with the Boreal-Atlantic, Arcto-Boreal, and Tethyan assemblages of these organisms. The presented paleontological description is devoted to characteristic radiolarian species from the Pechora basin and Koryak Upland. Species occurring in both regions are *Parvicingula blowi, P. blackhornensis, P. burnsensis, P. elegans*, and *P. enormis*. The former conclusion that the Bathonian–Callovian and Kimmeridgian–Tithonian radiolarians from some tectonic sheets of the Koryak Upland (the Talovka River, Rarytkin Ridge, and the left-hand side of the Utesiki River) are of the North Tethyan type is found to be correct. The established proportions between parvicingulids, pantanelliids, and other radiolarian groups suggest that most of Late Jurassic radiolarian assemblages from the Kuyul terrane originated near the boundary between the southern and northern Tethyan provinces, whereas coeval radiolarian communities from the Rarytkin Ridge can be considered as subboreal, dwelled close to the frontal zone of southern Boreal provinces.

Key words: *radiolarians, Late Jurassic, paleoclimatic affinity*

INTRODUCTION

Ideas of terrane tectonics considerably changed our understanding of geological structure of northern and northeastern Russia. As is known, fossil faunas play the key part in interpretation of terranes' ages and paleogeographic settings of their formation either in the study region, or in other areas far remote from the latter. Siliceous deposits are dominant among the Middle Mesozoic sedimentary sequences around the Pacific, and, accordingly, they bear only the radiolarian fauna. Exactly radiolarians were used to establish ages of sediments in many terranes accreted to the Eurasian continent in northeastern Russia. The investigation of radiolarians from individual tectonic sheets of the Koryak Upland terranes (Bogdanov and Vishnevskaya, 1990; Sokolov, 1992; Vishnevskaya, 1992; Vishnevskaya and Filatova, 1994, 1996) showed, however, that it is difficult to establish here an unambiguous stratigraphic scheme on the basis of this fossil group, because radiolarian assemblages from Boreal and Tethyan provinces are now conjoined in tectono-stratigraphic sections of the region (Vishnevskaya and Filatova, 1994; Pral'nikova and Vishnevskaya, 1996).

Solving stratigraphic problems when accretionary terranes of the Koryak–Kamchatka foldbelt are under study, we should understand as well the climatic (latitudinal) affinity of particular radiolarian assemblages (class them with the Boreal, Subboreal, North Tethyan, or Tethyan types). The fact is that the paleomagnetic data on some terranes reveal the primary rock magnetization not everywhere because of remagnetization at the accretionary and subsequent evolutionary stages of the Earth's crust. Thus the latitudinal characteristics of radiolarians are of prime significance for palinspastic reconstructions requiring data on relative original disposition of terranes. Since interpretation of the geodynamic regime, geological and tectonic structure of the region is dependent on information about past latitudes of radiolarian habitats, the inference on paleoclimatic affinity of radiolarians must be based on comprehensive and detailed analysis of their distribution ranges. This was the main reason why we investigated once again the radiolarian assemblages from well-known sections of European Russia (Pechora and Sysola river basins) and northern Siberia (Paksa Peninsula), which consist of Boreal-Atlantic and Arcto-Boreal taxa (Khudyaev, 1931; Khabakov, 1937; Kozlova, 1971, 1994; Vishnevskaya and Malinovskii, 1995).

Available models of latitudinal zoning of Jurassic radiolarians are based on the concept by Pessagno *et al.* (1984, 1987) who developed their ideas using materials obtained from Tithonian–Kimmeridgian siliceous deposits of the Californian terranes. In this concept, however, the latitudinal position of boundaries between radiolarian assemblages of different climatic affinities is detected using not the paleomagnetic parameters of the studied sedimentary sequences, but the presumable analogy with the current climatogeographic boundaries such as the tropics of Cancer or Capricorn. For instance, the boundary between the North and South Australian (as well as that between the South and North Boreal provinces in northern hemisphere) is placed in

the above model at 38° S according to data on the complete disappearance of Pantanelliidae and peak abundance of Parvicingulidae forms, whereas the boundaries at 22° S and 22° N are drawn to isolate the central Tethyan province from the South and North Tethyan zones in accordance with paleomagnetic data, on the one hand, and distribution limits of Parvicingulidae species, on the other. Consequently, this model of radiolarians distribution includes three twisting latitudinal zones, two of which (zones of parvicingulids distribution with their maximum abundance at 38° of latitude) span the interval between 22° and 54° of latitude in both northern and southern hemispheres, which is, as one can see, 32° wide. Kiessling and Scasso (1996), who considered this model from the viewpoint of radiolarians distribution in the Antarctic sections, established deviations exceeding 30°. They also showed that parvicingulids were as abundant in Australian province (50%), as pantanelliids at the sixties south, and concluded that the model of radiolarians distribution within paleolatitudes should be asymmetric, explaining this by difference in thermal regimes of North and South Pacific during the Jurassic.

Our preliminary consideration also showed that the model by Pessagno *et al.* is inconsistent with data on radiolarian assemblages from the north of Russia and should be revised and verified. Especially interesting in this respect are radiolarian assemblages from epicontinental marine deposits of large continents, because paleolatitudes of corresponding sedimentary basins are figured out from reliable paleomagnetic and paleoclimatic data. In particular, the Pechora basin, considered here and located now at 60°–70° N, was displaced for about 20° of latitude to the south during the Tithonian. In accordance with the model by Pessagno *et al.*, this region could be a part of the North Boreal radiolarian province. The recent investigation of belemnites from the region (Riboulleau *et al.*, 1998) also demonstrated that the water temperature in the basin was about 17°C during the Kimmeridgian and Volgian stages, and the basin is assumed to be located northward off 50° N.

Like the Pechora basin, the Paksa Peninsula and middle courses of the Volga River (Vishnevskaya, 1998) are suitable areas for precise age determinations of radiolarian assemblages, because particular sections bear here, as in California, the abundant parvicingulids, but in contrast to the last and other segments of circum-Pacific belt, radiolarians in the afore mentioned areas coexist with ammonites, *Buchia* forms, belemnites, foraminifers, and nannoplankton. Using this situation, Kozlova (1994) have already suggested a scheme of stratigraphic correlation of Late Jurassic radiolarian assemblages with ammonite and foraminiferal zonations.

STUDIED MATERIALS

Radiolarians used in this comparative analysis are from the Kimmeridgian–Volgian sections of the Timan–Pechora oil-and-gas field, Ul'yanovsk area near the Volga River, northern Siberia, and fragmentary Radiolaria-bearing sequences, which are exposed in tectonic terranes of the Koryak Upland in northeastern Russia (Figs. 1–3). We personally collected basic materials in the Ukhta area of the Pechora basin (exposures at the Izhma and Pizhma rivers) and near Ul'yanovsk (Gorodishche section) during the period of 1995–1997, and also in the Koryak Upland during the field seasons of 1989–1990. In addition, we studied radiolarians from rock samples collected by N.I. Filatova, A.I. Dvoryankin, V.N. Grigor'ev, K.A. Krylov, and S.D. Sokolov in various areas of the upland and from collection of Yu.M. Malinovskii, which characterizes sections of the Paksa Peninsula. The analyzed phosphorite samples from the Sysola River basin are from collection at the laboratory of Marine Geology, Moscow State University. Data on radiolarians from 52 drill holes in the Pechora basin are also used in our analysis.

PROCEDURES

Radiolarians were extracted from rocks using the chemical preparation method, namely the siliceous matrix dissolution in hydrofluoric acid. In addition, radiolarians were studied in thin sections of the same rock samples to obtain additional data on taxonomic composition of assemblages and supplementary micropaleontological and lithological information. Radiolarian skeletons were separated from unsolvable residue by selecting them under a microscope with a soft brush. Radiolarian images are shot under the scanning electron microscope.

LATE JURASSIC RADIOLARIAN ASSEMBLAGES FROM THE NORTHEAST OF RUSSIAN PLATE

Khudyaev (1931) and Khabakov (1937) were the first to describe thin sections of rock samples with Late Jurassic radiolarians from northeastern areas of Russian plate. As they noted, the Tithonian–Valanginian radiolarian assemblages of these areas differ from coeval West European faunas by a higher abundance of turriculated nasselarians. These researchers emphasized the following morphological and ecological features of radiolarian skeletons from the Kama–Vyatka region: (1) the larger size ranges of shells as compared to coeval radiolarians from Western Europe; (2) their smoother surface lacking radial apophyses and spines of a complicated structure; and (3) predominance of turriculated forms relative to number of species and total amount of radiolarian specimens.

Later, Kozlova (1971, 1994) demonstrated that radiolarians are dispersed throughout the sequence of Upper Jurassic marine deposits in the northeast of Russian plate. Sections analyzed in this study (Figs. 1, 2) show that this conclusion is correct. After a classical paleontological description of radiolarians from Pechora basin, Kozlova (1994) suggested considering

the assemblage of Timan–Pechora region as typical of the Boreal-Atlantic province. Late Jurassic radiolarians have been discovered in deposits of Moscow syneclise (Bragin and Bragina, 1996) and northern Siberia (Vishnevskaya and Malinovskii, 1995) just recently, because the Upper Jurassic stratigraphy in these regions was traditionally based on ammonites and bivalves *Buchia*, whereas radiolarians were always outside the attention sphere of stratigraphers.

Inasmuch as paleogeography and stratigraphic ranges of radiolarians from northeastern Russia have been recently discussed with a keen interest, we attempted for the first time to compare these and coeval assemblages from northern areas of the country. In general, Eastern Europe is a unique area suitable for elucidation of paleoclimatic affinities of Mesozoic radiolarians, as it spans both the Boreal and Tethyan biogeographic provinces.

Within the northeastern part of the Eastern European platform, Late Jurassic radiolarian assemblages of the Boreal province are known from sedimentary sequences along the Izhma, Pizhma, Unzha, and Sysola rivers, and also from drill holes of the Barents Sea–Pechora region (Fig. 2).

According to composition of macrofaunas (ammonites, buchias, belemnites), the Pechora basin of Kimmeridgian–Volgian time was a part of the Boreal-Atlantic province (Kozlova, 1994). Like in Norway and Spitsbergen, nasselarians from this basin are mostly represented by the genus *Parvicingula*. In contrast to shallow-water deposits of England and North Siberia, where predominant among spongy multichamber radiolarians are spheroid or discoid forms, radiolarian

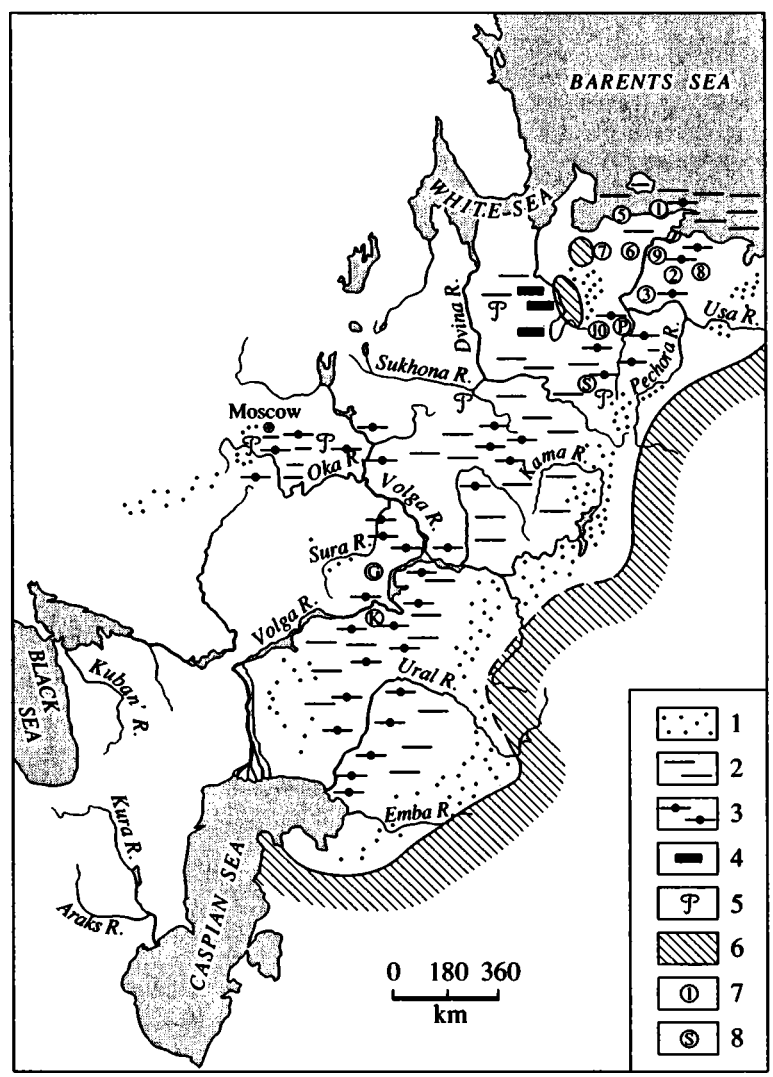

Fig. 1. Paleogeographic scheme of the Volga–Urals region for the Late Jurassic (Volgian) time with analyzed radiolarian-bearing sections of the Pechora basin (encircled numbers): (1) sand; (2) clay; (3) combustible shale; (4) coal; (5) phosphorite; (6) land (?) area; (7) section number; (8) exposures of the Sysola River (S), Gorodishche (G), Kashpir (K), and Pizhma River (P).

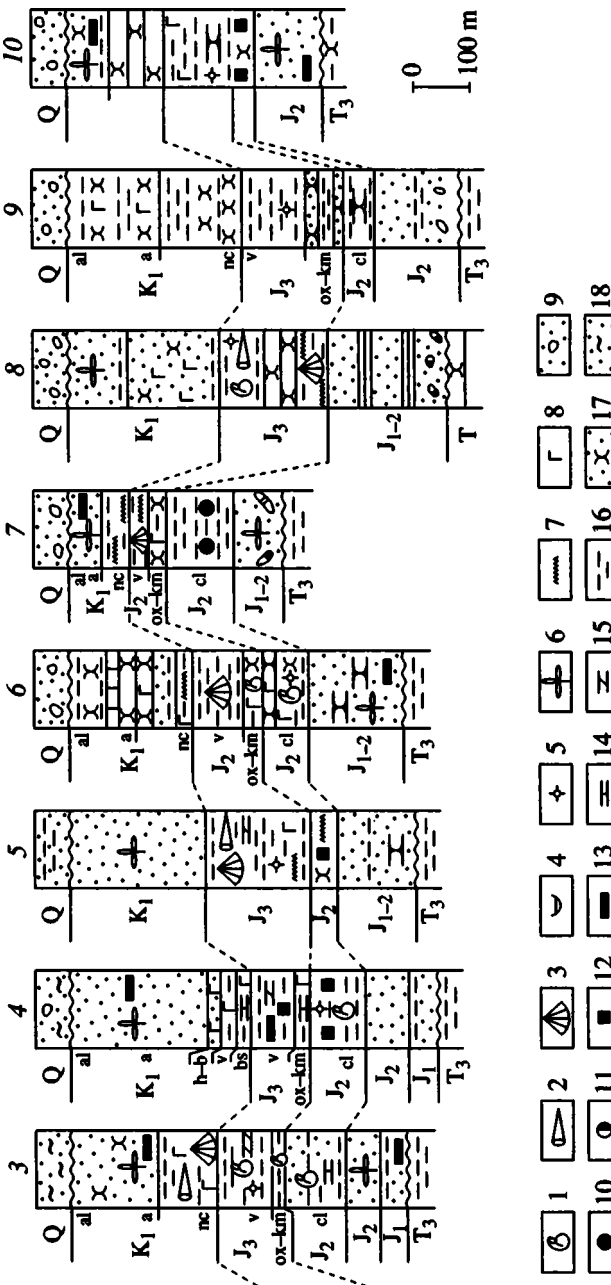

Fig. 2. Upper Jurassic sections of the Pechora basin bearing radiolarians, vertical scale 1 : 10000: (1) ammonites; (2) belemnites; (3, 4) *Buchia* forms; (5) radiolarians; (6) fossil flora; (7) hiatus; (8) glauconite; (9) conglomerate, moraine; (10) siderite nodules; (11) phosphate nodules; (12) pyrite nodules; (13) coal, combustible shale; (14) limestone; (15) marl; (16) clay; (17) sand, sandstone, siltstone; (18) loam. Section numbers correspond to drill holes North Chernorechenskaya (*1*), West Khorveiskaya (2), Khar'yaga-1 (*3*), Khar'yaga-62 (*4*), South Khil'chuiskaya (*5*), Khar'yaga-221 (6), South Khar'yaga-1 (*7*), East Khorveiskaya (8), Verkhne-Shapkina (9), and Yuzhno-Shapkina (*10*).

assemblages from the basin under consideration are extremely rich in turriculated specimens (Vishnevskaya, 1996a, 1996b). This abundance of cyrtoid forms suggests that a stable upwelling zone extended during the Late Jurassic parallel to the Urals foldbelt, along which Boreal radiolarians migrated to the south, as it is recorded in Jurassic sections (Gorodishche) of the Ul'yanovsk region.

Kimmeridgian–Volgian radiolarian assemblages from the Timan–Pechora region, like many assemblages of this age from the Koryak Upland (Vishnevskaya and Filatova, 1996), show preponderance of parvicingulids (Plates I, II). The Kimmeridgian radiolarian fauna from the Barents Sea–Pechora region consists of the following species (Kozlova, 1994; Vishnevskaya, 1998): *Archaeocenosphaera ineaqualis* (Rust), *Praeconosphaera* ex gr. *sphaeroconus* (Rust), *Praeconocaryomma hexagonata* Rust, *"P." dupla* (Kozlova), *Pseudocrucella* aff. *prava* Blome, *Crucella crassa* (Kozlova), *C.* aff. *mexicana* Yang, *Orbiculiforma* cf. *iniqua* Blome, *O.* (?) *retusa* (Kozlova), *Paronaella paenorbis* (Rust), *Pantanellium* (?) *fallax* (Tan), *P. lanceola* (Parona), *P. tierrablankaense* Pessagno et McLeod, *Parvicingula antoshkina* Vish., *P. inornata* Blome, *P.* cf. *blowi* Pessagno, *P. haeckeli* (Pantanelli), *P. burnsensis* Pessagno et Whalen, *P. genrietta* Vish., *P. pizhmica* Kozlova, *P. pusilla* Kozlova, *P. papulata* Kozlova, *P. santabarbaraensis* Pessagno, *P.* (?) *enormis* Yang, *P.* (?) *blackhorsensis* Pessagno et Whalen, *P.* sp. K. Vish., *Excingula* (?) *bifaria* Kozlova, and *Sethocapsa leiostraca* Foreman. Parvicingulids represent over 90% of this assemblage, whose age is determined on the basis of the coexisting ammonite taxon *Amoeboceras kitchini* (Salf.).

Radiolarians from the ammonite *Dorsoplanites panderi* Zone of the Pechora–Urals region are represented mostly by species *Parvicingula papulata* Kozlova, *P. conica* (Khabakov), *P. cristata* Kozlova, *P. rugosa* Kozlova, and *P. simplicima* Kozlova. In the Pechora basin, the majority of species from the genus *Parvicingula* Pessagno have well-developed spines, and an apical horn, and parvicingulids from the Koryak Upland frequently display the same features (Bogdanov and Vishnevskaya, 1991; Plate 16). According to Kozlova (1994), the middle Volgian *Parvicingula papulata* fauna with guide species *Aacaeniotyle uralica* (Rust), *Parvicingula papulata* Kozlova, and *P. simplicima* Kozlova characterizes the lower part of Paromes Formation, and its age is determined on the basis of ammonites *Dorsoplanites* cf. *panderi* (d'Orb.), *Zaraiskites* aff. *scythicus* Vischn., and bivalves *Buchia mosquensis* (Buch). Kozlova considers the Timan–Pechora region as a part of the Boreal-Atlantic province, because the Pechora sea of the Volgian time represented a basin with predominant clayey sedimentation (Fig. 2) and local accumulations of combustible shales (Sedaeva and Vishnevskaya, 1995). During the Kimmeridgian and Tithonian ages, radiolarian communities of the Barents and Pechora seas (Kozlova, 1994) were lacking the thermophilic

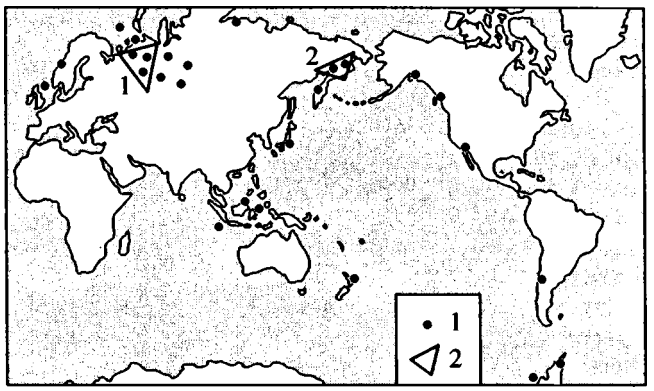

Fig. 3. Distribution scheme of radiolarians from genus *Parvicingula*: (1) localities of parvicingulids; (2) areas in Pechora basin (1) and Koryak Upland (2) with comparable assemblages of Jurassic radiolarians.

genera of the order Nasselaria, such as *Eucyrtidiellum* Baumgartner, *Mirifusus* Pessagno, *Podobursa* Wisniowski, and *Podocapsa* Rust, whose important morphological feature is a large swollen or spheroid segment of a shell. Exotic southern genera *Andromeda* Baumgartner, *Bernoullius* Baum., *Protunuma* Ichikawa and Yao, and *Tethysetta* Dumitrica, as well as some others (*Foremanella* Muzavov, *Eoxitus* Kozur) also have never been encountered in Boreal assemblages from the Pechora region. At the same time, pantanelliids are rather abundant in the latter. In addition, the last group is abundant in Kimmeridgian deposits of the Moscow region, where radiolarian assemblages include the following species (Bragin, 1997): *Pantanellium huazalingoense* Pessagno et McLeod, *P. tierrablankaense* Pessagno et McLeod, *P. moscowiense* Bragin, *Crucella squama* (Kozl.), *Paronaella* sp. aff. *P. kotura* Baum., *Tripocyclia* sp. cf. *T. amajacensis* Pessagno et Yang, *Parvicingula* sp. aff. *P. vera* Pessagno et Whalen, *Praeparvicingula dannae* Bragin, and *Pseudodictyomitrella* (?) *spinosa* Grill and Kozur.

Radiolarian assemblage with *Parvicingula jonesi* Pessagno is distinguished in the Kimmeridgian part of the Dubki section, which extends downward the Gorodishche lectostratotype (middle courses of the Volga River) and is attributed to the ammonite *cymodoce* Zone. In the Gorodishche section, the radiolarian assemblage from the *klimovi* Zone shows the same abundance rate of *Parvicingula* species, dominant amid which is *P. blowi* (Pessagno). In clay beds of the *sokolovi* and *pseudoscythica* zones, radiolarians are scarce, although the redeposited radiolarians are plentiful in phosphate nodules dispersed throughout this interval of the section. The upper *Z. zarajskensis* Subzone of the *Dorsoplanites panderi* Zone, an analogue of the *Watznaueria communis* Zone of nannoplankton zonation, yields the very diverse radiolarian assemblage: *Orbiculiforma* ex gr. *mclaughlini* Pessagno, *Stichocapsa* (?) *devorata* (Rust), *Phormocampe favosa*

Khudyaev, *Parvicingula hexagonata* (Heitzer), *P. cristata* Kozlova, *P. conica* (Khabakov), *P.* aff. *alata* Kozlova, *P. multipora* (Khudyaev), *P.* aff. *haeckeli* (Pantanelli), *P.* aff. *spinosa* (Grill et Kozur), *P.* cf. *Lithocampe terniseriata* Rust, and *Plathycryphalus* (?) *pumilus* Rust (Vishnevskaya, 1998). In other words, representatives of *Parvicingula* genus characteristic of the Boreal province are dominant here like in the Kimmeridgian and early Volgian assemblages from the Gorodishche section and constitute up to 50% of the assemblage. All Late Jurassic assemblages of the Volga River region show close similarity with those from the North Sea (Dyer and Copestake, 1989) and appear to be dwellers of comparable latitudinal zones, where the water temperature was about 18°C (Riboulleau *et al.*, 1998).

An assemblage resembling that from the Pechora basin was distinguished among Rarytkin radiolarian faunas from the Koryak Upland (e.g., species from samples H-212/15a and H-212/6; Vishnevskaya and Filatova, 1996, p. 33). The abundance of pantanelliids in radiolarian assemblages from northern areas of Eastern Europe (Kozlova, 1994; Vishnevskaya, 1996, Bragin, 1997) represents a deviation from the model by Pessagno *et al.* (1987) describing the latitudinal distribution of radiolarians. Another model based on the distribution of Jurassic radiolarians in the Antarctic regions (Kiessling and Scasso, 1996) is also inadequate, since parvicingulids are much more abundant than pantanelliids in the Late Jurassic assemblages of northern Europe.

JURASSIC RADIOLARIANS FROM NORTH SIBERIA

In Siberia, Kozlova (1983) described a radiolarian assemblage from the Upper Jurassic Bazhenovo Formation, which is similar to those from the Pechora basin (Kozlova, 1994). In both regions, the Kimmeridgian–Volgian radiolarian faunas are monotypic, and that from the Bazhenovo Formation is represented by *Acaeniotyle* sp. aff. *A. diaphorogona* (Foreman), *Emiluvia* cf. *chica* For., *Pantanellium lanceola* (Parona), *Staurodictya* cf. *retusa* Kozlova, *Parvicingula multipora* (Khudyaev), *P.* cf. *santabarbaraensis* Pessagno, and *P.* cf. *khabakovi* (Zhamoida). Parvicingulids with well-developed apical horns are dominant in the assemblage, whereas spongy discoid forms and alveolate pantanelliids occur as single specimens and are subordinate. The Volgian assemblage consists of *Crucella* cf. *mucronata* (Rust), *Theocapsa* (?) sp. aff. *T. obesa* Rust, *Parvicingula tetracapsa* (Zham.), *P.* cf. *gracilis* (Khabakov), *P.* sp. aff. *Siphocampe turrita* Rust, *P.* cf. *rostrata* (Khabakov), *P.* cf. *seria* (Rust), and *P. tanella* (Khabakov), among which parvicingulids are dominant again. In Kozlova's opinion (1983), the Bazhenovo fauna exemplifies a typical cold-water assemblage. To support this conclusion, she points out that radiolarian communities from recent bottom sediments of Antarctic regions are of a similar taxonomic structure and include a limited number of widespread species represented, according to Petrushevskaya (1966), mostly by nasselarians.

One more assemblage of radiolarians discovered recently (Vishnevskaya and Malinovskii, 1995) in Oxfordian–Valanginian deposits in the north of Central Siberia (coastal cliffs of the Paksa Peninsula, Laptev Sea) is also almost free of Tethyan elements, being, like the assemblage from Pechora basin, of great scientific interest. The Oxfordian–Valanginian radiolarians from exposures of the Anabar Bay of the Laptev Sea are similar to the Kimmeridgian-Ryazanian assemblage of the North Sea (Dyer and Copestake, 1989). For instance, the Kimmeridgian assemblage from the Urdyuk-Khaya Cape at the Laptev Sea consists of *Orbiculiforma lowreyensis* Pess., *O. mclaughlini* Pess., *Praeconocaryomma hexagonata* (Rust), *Pantanellium* sp., *Parvicingula blowi* Pess, *P. jonesi* Pess., *P. khabakovi* (Zham.), *P. haeckeli* (Pant.), *Praeparvicingula donnae* Bragin, *Archaeodictyomitra apiara* (Rust), and *Zhamoidellum ovum* Dumitrica, dominant among which are *Parvicingula blowi* Pess., *Parvicingula khabakovi* Zhamoida, and *Praeparvicingula donnae* Bragin. On the basis of all these data, we may consider the Pechora and North Siberian assemblages together as characterizing the Boreal radiolarian fauna.

Thus, data on Late Jurassic radiolarians from northern Russia (Pechora, Sysola, Moscow, Volga River, and North Siberian regions) suggest that the distribution zone of pantanelliids should be extended into the North-Boreal province in both available paleobiogeographic models (Pessagno *et al.*, 1987; Kiessling and Scasso, 1996).

SOME RADIOLARIAN ASSEMBLAGES FROM TERRANES OF KORYAK UPLAND

Zhamoida (1972) was first to discover parvicingulids (*Eucyrtidium khabakovi*) in northeastern Russia. Below, we consider radiolarian assemblages of the Koryak Upland (Plates III, IV), which have been macerated from a series of tectonic sheets of the Kuyul ophiolite terrane (Grigor'ev *et al.*, 1995), Rarytkin Ridge, and Anadyr–Velikaya river basins

Plate I. Some species of Late Jurassic radiolarians from the Pechora basin and Koryak Upland: (1–3) *Parvicingula* (?) *blackhorsensis* Pessagno et Whalen, ×210, 185, 185; (4) *P.* (?) ex gr. *khabakovi* Zhamoida, ×150; (5, 10–12) *P.* (?) *elegans* Pessagno et Whalen, ×165, 145, 135, 140; (6–9) *P.* sp. cf. *P.* (?) *elegans* Pessagno et Whalen, ×210, 190, 210, 130. (1, 6, 8) from Pechora River basin, Pizhma River, Sample P; (2, 3, 7–9, 10–12) from Koryak Upland, Malyi Nauchirynai River, Sample 757/6; (4, 5) from Koryak Upland, Pravyi Talyainyn River, Sample H-212-15a.

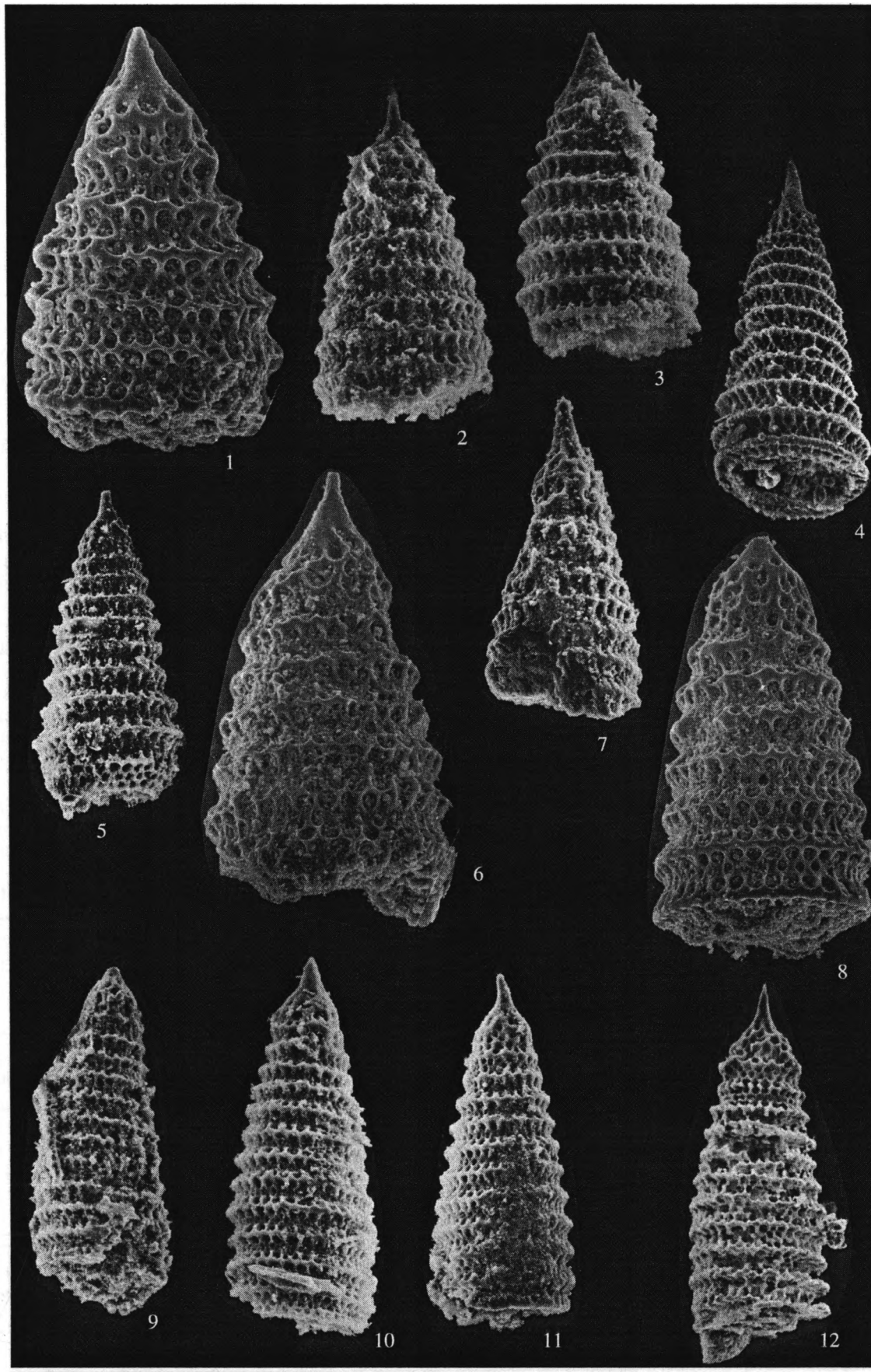
1
2
3
4
5
6
7
8
9
10
11
12

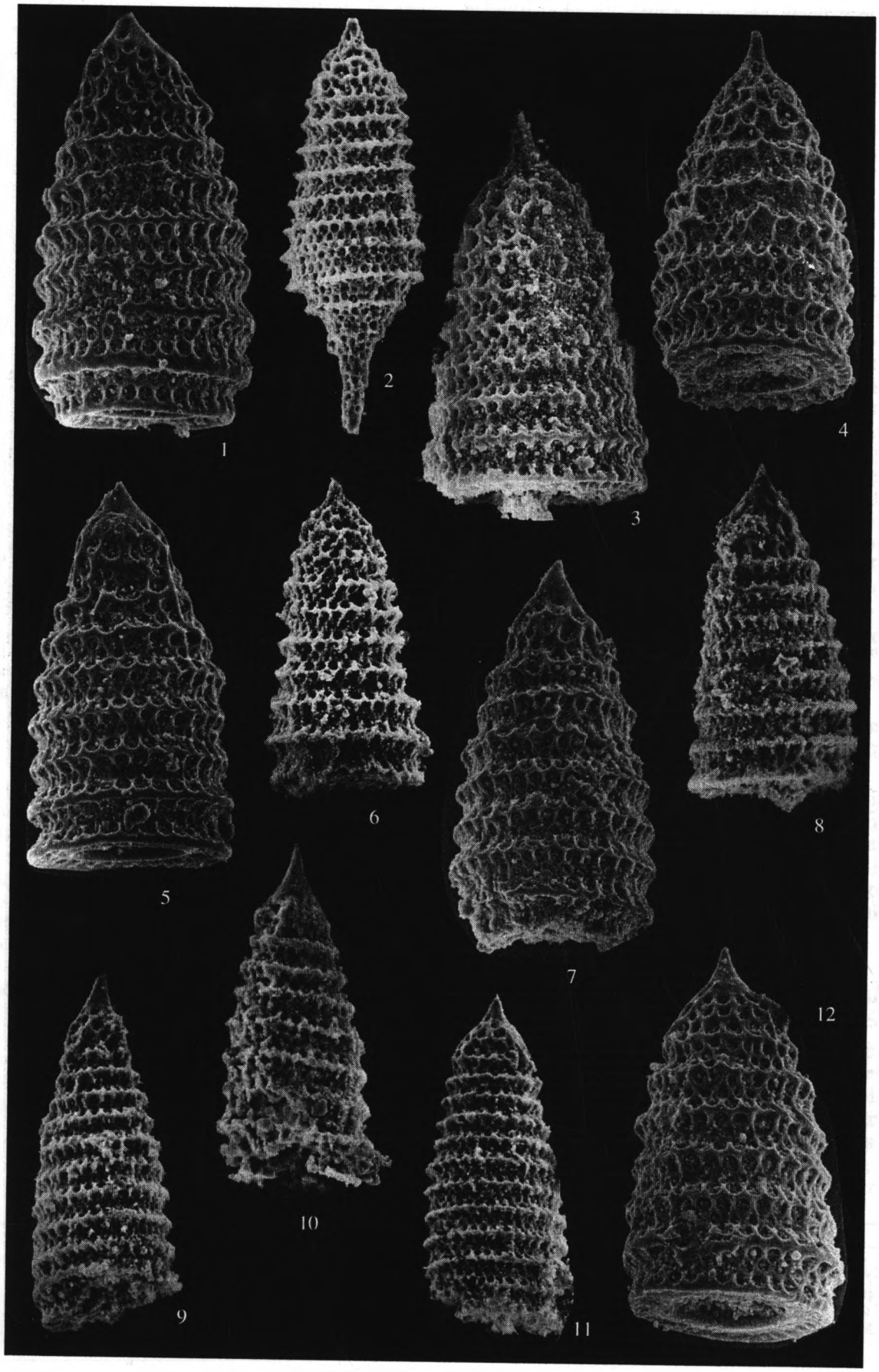
1
2
3
4
5
6
7
8
9
10
11
12

(Vishnevskaya and Filatova, 1996). As the siliceous sedimentary sequences (radiolarite beds) lack other faunas and are intensely fragmented here, the stratigraphic ranges of deposits under consideration have been determined only on the basis of distribution of radiolarians (Vishnevskaya and Filatova, 1996).

The Callovian–Oxfordian assemblage is distinguished in radiolarite and jasper beds intercalated with basaltic flows within a tectonic slice exposed at the Vstrechnyi Creek. For instance, Sample C-2076 from this site yielded the assemblage of *Andromeda* (?) sp., *Archaeodictyomitra apiarium* (Rust), *A. mirabilis* Aita, *Cinguloturris carpatica* Dumitrica, *Dictyomitrella* (?) *kamoensis* Mizutani et Kido, *Eucyrtidiellum unumaense* (Yao), *E.* aff. *E. unumaense dentatum* Baumgartner, *E. nodosum* Wakita, *E.* (?) *ozaiense* Aita, *E. ptyctum* Riedel et Sanfilippo, *E.* sp. A aff. *E. quinatum* Takemura, *Hsuum* sp., *Parahsuum* aff. *P. cruciferum* Takemura, *P.* aff. *P. kanyoense* Sashida, *Parvicingula* ex gr. *blackhorsensis* Pessagno et Whalen, *P.* aff. *P. dhimenaensis* Baumgartner, *P.* aff. *P. vera* Pessagno et Whalen, *Zhamoidellum mikamense* Aita, and *Zh.* sp. Saturnalids are extremely rare in the assemblage, but cyrtoid forms of radiolarians are widespread, and both features presumably characterize the cold-water environments in the habitat basin (Pral'nikova and Vishnevskaya, 1996). Another remarkable genus is *Archaeodictyomitra*, whose representative *A. apiarium* shows morphological features characteristic of this species in the north of Tethyan province (Pral'nikova and Vishnevskaya, 1996). Nasselarians of the genus *Eucyrtidiellum* are represented by six species, many of which display the following morphological features of shells: (1) rather massive and dense walls; (2) hexagonal structure of framework around pores; (3) surface inside hexagons downgrading toward the central pore and tubercles ornamenting the shell surface at the angles of hexagons. The structure of this kind reveals the high packing density of shell elements and is responsible for the shell soundness indicative of ecological and depth characteristic of the habitat basin (Pral'nikova, 1995). The assemblage is rich in parvicingulids, suggesting its origin in the northern part of the Tethyan province. Characteristic Tethyan genera proper, such as *Andromeda* and *Cinguloturris*, are represented by single specimens. According to the concept of unitary assemblages (Baumgartner *et al.*, 1995), the assemblage is of the Callovian–Kimmeridgian age.

An assemblage of Callovian–early Tithonian radiolarians is established in the left-hand side of the Talovka River (Pral'nikova and Vishnevskaya, 1996). Sample M-911/17 from this site yielded the following species: *Acanthocircus dicranacanthos* Squinabol, *A. suboblongus* Yao, *Gorgansium* aff. *G. pulchrum* Kocher, *Pantanellium* cf. *P. riedeli* Pessagno, *P.* sp., *Saitoum dercourti* De Wever, *Triactoma blakei* Pessagno, *Amphipyndax* sp., *Archaeodictyomitra apiarium* (Rust), *A. minoensis* Mizutani, *A. mirabilis* Aita, *A. suzukii* Aita, *Bagotum* aff. *B. zhamoidai* Vishnevskaya, *Canutus* (?) sp., *Eucyrtidiellum ptyctum* (Riedel et Sanfilippo), *E. pyramis* Aita, *E.* sp. B aff. *E. quinatum* Takemura, *Foremanina* (?) aff. *F.* sp. A Baumgartner, *Hsuum* aff. *H. basovi* Vishnevskaya, *H.* aff. *H. belliatulum* Pessagno et Whalen, *H.* aff. *H. inexploratum* Blome, *H. okamurai* Mizutani, *H.* sp., *Mirifusus mediodilatatus* (Rust), *Napora* sp., *Obesacapsula pacifica* Vishnevskaya, *Parvicingula* aff. *P. aculeata* Carter, *P. dhimenaensis* Baumgartner, *P. vera* Pessagno et Whalen, *P.* aff. *P. vera* Pessagno et Whalen, *P.* sp., *Ristola altissima* (Rust), *Stichocapsa japonica* Yao, *S.* sp., *Theocapsa* (?) sp., *Tricolocapsa* sp., *Xitus gifuensis* Mizutani, *X.* aff. *X. gifuensis* Mizutani, *Williriedellum crystallanum* Dumitrica, *W.* aff. *W. crystallanum* Dumitrica, and *Zhamoidellum ovum* Dumitrica (Plate IV). Genera *Triactoma, Archaeodictyomitra, Eucyrtidiellum*, and *Hsuum* are more diverse here than others. The available *Parvicingula* representatives suggest, according to the model by Pessagno *et al.*, that the assemblage originated close to the boundary between the Tethyan and Boreal provinces, since *Parvicingula vera* Pessagno et Whalen is widespread in several localities of the province, e.g., in Kimmeridgian–Tithonian deposits of the Pechora basin (Kozlova, 1994), Kimmeridgian beds of the Moscow syneclise (Bragin, 1997), and Tithonian sediments of the Antarctic Peninsula (Kiessling and Scasso, 1996). The assemblage in question includes, like the previous one, species of genera *Eucyrtidiellum* (three forms) and *Williriedellum*. Species of the last taxon display the same morphological peculiarities (hexagonal packing of structural shell elements) as *Eucyrtidiellum* forms do, and also suggest a specific ecology of paleobasin. Many cyrtoid radiolarians of the assemblage have spongy and hyaline shell structures, which are characteristic of basins adjacent to the Boreal province (Pral'nikova and Vishnevskaya, 1996), but they are found together with a shell fragment of *Mirifusus mediodilatatus* (Rust) widespread in the Tethyan province. Correlating this assemblage with Pechora and Mediterranean faunas on the basis of stratigraphic ranges of *Parvicingula vera, Ristola altissima, Mirifusus mediodilatatus*, and *Zhamoidellum ovum*, we attribute it to the Kimmeridgian–early Tithonian interval.

Unlike this assemblage, radiolarian faunas from the Rarytkin (Sample H-212-15a), Pikas'vayam (Sample C-2799), and Nauchirynai (Sample C-2802) sections of Kimmeridgian–Tithonian radiolarian shales

Plate II. Late Jurassic radiolarian species in common from the Pechora basin and Koryak Upland: (1–3, 6) *Parvicingula* (?) *blowi* Pessagno, ×210, 110, 290, 180; (4, 5) *P. burnsensis* Pessagno et Whalen, ×220, 210; (7–10) *P.* aff. *burnsensis* Pessagno et Whalen, ×210, 170, 150, 210; (11–12) *P.* (?) *enormis* Yang, ×150, 210. (1, 4, 5, 7, 12) from Pechora basin, Pizhma River locality, sample P; others from Koryak Upland localities: (2) Pravyi Konachan River, Sample C-2646-2B; (3) Utesiki River, Sample H-11; (6) Pravyi Talyainyn River, Sample H-212-15a; (8, 9, 11) Malyi Nauchirynai River, Sample 757/6; (10) Malyi Nauchirynai River, Sample 760/1.

Plate III. Jurassic radiolarians from siliceous deposits of tectonic slice exposed at the Veselaya River, Talovka River basin of the Koryak Upland: (1) *Archaeodictyomitra apiarium* (Rust), ×375; (2) *A.* (?) aff. *A. mirabilis* Aita, ×375; (3, 4) *Xitus gifuensis* Mizutani, ×375; (5) *Williriedellum crystallanum* Dumitrica, ×375; (6) *Archaeodictyomitra* aff. *A. suzukii* Aita, ×750; (7) *Hsuum* aff. *H. belliatulum* Pessagno et Whalen; (8) *Eucyrtidiellum pyramis* (Aita), ×375; (9) *E.* sp. B aff. *E. quinatum* Takemura, ×375 (all from Sample M-911/17).

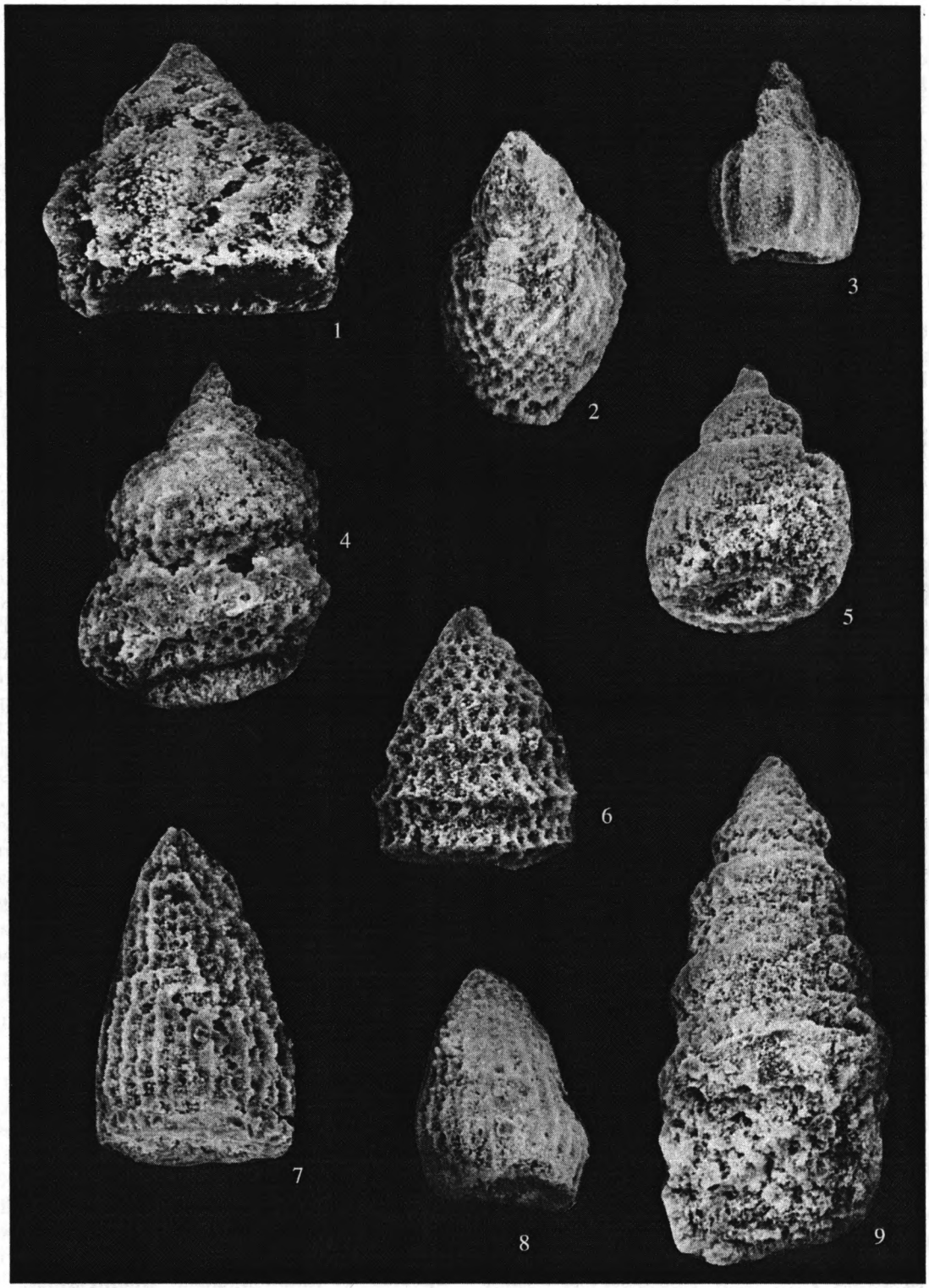

Plate IV. Jurassic radiolarians from siliceous deposits of tectonic slice exposed at the Vstrechnyi Creek, Talovka River basin of the Koryak Upland: (1) *Eucyrtidiellum* (?) *ozaiense* Aita; (2) *E. nodozum* Wakita; (3) *E. ptyctum* (Riedel et Sanfilippo); (4) *E. quinatum* sp. A aff. *E. quinatum* Takemura; (5) *E.* aff. *E. nodozum* Wakita; (6) *Parvicingula* (?) *blackhorsensis* Pessagno et Whalen; (7) *Parahsuum* aff. *P. kanyoense* Sashida; (8) *Archaeodictyomitra* (?) *mirabilis* Aita; (9) *Cinguloturris carpatica* Dumitrica (all from Sample C-2076, ×375).

and jaspers (radiolarites) are extremely rich in parvicingulids (for the sample positions in the sections, see Vishnevskaya and Filatova, 1996). Sample H-212-15a from the first site yielded *Chitonastrum tricuspidatum* (Rust), *Pantanellium* cf. *fischeri* Pess., *Mirifusus fragilis* Baum., *Parvicingula boesii* (Parona), *P.* cf. *dhimenaensis* (Baum.), *P. khabakovi* (Zham.), *P. procera* Pess., *Podobursa helvetica* (Rust), *Dibolachras* aff. *chandrica* Kocher, *Hsuum* (?) *cuestaensis* Pess., and *H. obispaensis* Pess. (Vishnevskaya and Filatova, 1996, p. 36, Plate II). Considering the distribution ranges of genera *Mirifusus* and *Parvicingula* in the Pechora, Bazhenovo, and other regions, we should attribute this assemblage to the Kimmeridgian Age, excluding the Tithonian in contrast to our previous opinion. In the Rarytkin assemblage, parvicingulids represent more than 75% of the total amount of taxa.

In the Pikas'vayam assemblage (Sample C-2799) of *Triactoma echiodes* For., *Ristola altissima* (Rust), *Parvicingula dhimenaensis* Baum., *P. khabakovi* (Zham.), *P.* aff. *vera* Pess. et Whalen, *Hsuum* cf. *maxwelli* Pess., and *H.* cf. *mirabundum* Pess. et Whalen, the abundance of parvicingulids is up to 50%.

Parvicingulids, namely *P.* cf. *elegans* Pess. et Whalen, *P.* ex gr. *khabakovi* (Zham.), and *P.* cf. *vera* Pess. et Whalen, are even more abundant (up to 90%) in the Nauchirynai assemblage (Sample C-2802), where they coexist with single specimens of *Mirifusus* sp. and *Podobursa* cf. *helvetica* (Rust). Species *Parvicingula* ex gr. *khabakovi* (Zhamoida), *P.* cf. *elegans* Pessagno et Whalen, *P. procera* Pessagno, and *P.* cf. *vera* Pessagno et Whalen are thus dominant in all localities, and locally, they represent up to 70% of total amount of radiolarian specimens. Only their coexistence with single species of genera *Andromeda* Baumgartner, *Mirifusus* Pessagno, and *Podobursa* Wishniowski allows us to attribute the assemblages to the North-Tethyan province. Simultaneously, it is not inconceivable that a similar assemblage might exist in the South-Boreal province. The abundance of parvicingulids in particular samples of the Rarytkin (H-212/6), Pikas'vayam (L-10/1), and Nauchirynai (DH-760) sections is 90% and more (Vishnevskaya and Filatova, 1996). None of Tethyan species or genera have been detected in these samples. Most widespread parvicingulid forms are *P. blackhorsensis* Pessagno et Whalen, *P. burnsensis* Pessagno et Whalen, *P. elegans* Pessagno et Whalen, *P.* cf. *inornata* Blome, *P.* (?) *khabakovi* (Zhamoida), and *P. vera* Pessagno et Whalen, which are principal components of Boreal-Atlantic and Arcto-Boreal radiolarian assemblages from northern Russia. As the species morphology in these, Pechora, and North Siberian assemblages is comparable, they all can be considered as characterizing the Boreal zone. The late Callovian–early Tithonian (or Kimmeridgian–Volgian in terms of local scale for the Pechora basin) assemblage from the Malyi Nauchirynai River basin (Sample 757/6 from Filatova's collection) is enigmatic, because dominant forms in this case are species of low latitudes (Vishnevskaya and Filatova, 1996, p. 31, Plate 7), which were widespread in the Tethys during the Late Jurassic (Baumgartner *et al.*, 1995). The abundance of parvicingulids is less than 1%, although they are represented by several species typical of radiolarian assemblages from the Pechora basin (Plate II). According to criteria suggested by Pessagno, this is a warm-water assemblage of the central Tethyan zone. On the one hand, the greater abundance of parvicingulids in lower latitudes of the Pacific province, compared to that in the Tethys, may reflect the close connections of the former with the Arctic basins—in other words, the compositional difference between Mesozoic radiolarian communities in the past Tethyan, Atlantic, and Pacific basins. On the other hand, we may face again the discordance between the real distribution patterns of radiolarians and those suggested in biogeographic models (Pessagno *et al.*, 1987; Kiessling and Scasso, 1996).

Additional data on the Koryak Upland show that the variable abundance of parvicingulids is a characteristic feature: they may represent 50–70 and even 90% of total amount of species in some cases (samples H-212-15 and H-212-15a from the Pravyi Talyainyn River basin, Vishnevskaya and Filatova, 1996) being less abundant (25–50%) in others (samples 2646-2b and H-11 from the Konachan and Utesiki river basins) and locally representing a greater (samples C-2076 and DH-760) or lesser (samples DH-757/6 and M-911/17) admixture to other radiolarians. The same irregular distribution of Parvicingulidae (from 20 to 60%) was observed in North America (Pessagno *et al.*, 1984, 1987; Hull, 1995). At the same time, the distribution patterns of pantanelliids in the Koryak terranes (Vishnevskaya and Filatova, 1996) are similar to those in the north of eastern Europe and differ considerably from biogeographic models based on radiolarian analysis of Californian and Antarctic sections.

A COMPARISON WITH LATE JURASSIC RADIOLARIANS OF THE TETHYS

It is well known that the Kimmeridgian–Tithonian radiolarian assemblages of lower Tethyan latitudes (Baumgartner *et al.*, 1995) are almost completely lacking the *Parvicingula* representatives bearing a horn similar to that of the Pechora or Pacific species. Even Parvicingulidae forms without horn, like Kimmeridgian *Parvicingula* (?) *spinata* (Vinassa) (Baumgartner *et al.*, 1995, Plate 3187, Fig. 1) or *P. haeckelli* (Pantanelli), 1880, Plate 10, Fig. 6, are extremely rare there. Species *P. dhimenaensis* Baumgartner, *P. boesii* (Parona), *P. mashitaensis* Mizutani, *P. cosmoconica* (Foreman), *P. longa* Jud, and *P.* (?) sp. aff. *P. cincta* (Hinde) (Baumgarther *et al.*, 1995) represent a specific group of Tethyan radiolarians lacking the apical horn and tentatively attributed to the genus *Parvicingula*. Only two of the 450 species listed in the guide book on Middle Jurassic–Early Cretaceous radiolarians of the Tethys (Baumgartner *et al.*, 1995) are true representa-

tives of the genus. These are *P.* (?) sp. A from the Bathonian–Callovian beds of the Bahaman basin in Central America (present geographic position at 28° N) and *P.* sp. aff. *P. elegans* Pessagno et Whalen, geographic position of which is not indicated. Some other radiolarians of similar morphology from Mediterranean regions (Rust, 1895, 1898; Heitzer, 1930; Grill and Kozur, 1986) seem to be ambiguously affiliated with this genus as well, and Dumitrica *et al.* (1997) suggested considering them as species of the new genus *Tethysetta* Dumitrica.

CONCLUSION

Radiolarian assemblages from northeastern Russia (Koryak Upland) and other regions of the circum-Pacific belt, which include *Parvicingula* species but are of unknown paleogeographic affinity, can be correlated with the well-studied Kimmeridgian–Tithonian assemblages of the Pechora basin (Kozlova, 1971, 1994) and North Siberia (Kozlova, 1983; Vishnevskaya and De Wever, 1996) much better than with radiolarian faunas of North America (California, Mexico), where they are imprecisely dated and have provincial features unknown in the classical Tethyan assemblages.

The comparative analysis of radiolarians from the Pechora basin, Siberia, and Koryak Upland allowed us to abridge stratigraphic ranges of their assemblages from the Talovka River basin (Sample M-911-17) and Nauchirynai Creek locality to the Kimmeridgian–lower Tithonian, and that of the Rarytkin assemblage (Sample H-212-15a) to the Kimmeridgian.

Restraining the age determination of radiolarian assemblages from the Koryak Upland, the analysis of Late Jurassic radiolarians from the north of European Russia and Siberia extends simultaneously our knowledge of Middle Mesozoic Boreal faunas that is important for deciphering their paleoclimatic affinity, when we study enigmatic terranes in the northwestern Pacific margin.

Preliminary results of the comparative paleontological analysis of radiolarians from the Pechora basin, North Siberia, Tethys, and Koryak Upland show that their cold- and warm-water assemblages really associate with one another in tectonic thrust sheets of the last region (Pral'nikova and Vishnevskaya, 1996). The further investigation of these assemblages seems to be fruitful for better understanding of their paleoclimatic characteristics and distinction criteria.

Distribution patterns of Late Jurassic radiolarians from northern Russia point to the necessity of adequate revision of available models on paleobiogeographic zoning of these organisms. The model should be corrected to fit new data, since otherwise their application may result in erroneous geological interpretations.

ACKNOWLEDGMENTS

The work was supported by the Russian Foundation for Basic Research, project nos. 96-05-64512 and 97-05-65566, and by the International Program "Peri-Tethys," grant no. 96-18. We are grateful to N.I. Filatova, A.I. Dvoryankin, V.N. Grigor'ev, K.A. Krylov, and S.D. Sokolov for the rock samples they donated to our study. We also appreciate critical comments of N.A. Bogdanov, N.Yu. Bragin, V.N. Grigor'ev, G.E. Kozlova, and S.D. Sokolov, which we used to improve the manuscript.

APPENDIX
PALEONTOLOGICAL DESCRIPTION OF SELECTED SPECIES

Family Archaeodictyomitridae Pessagno

Genus *Archaeodictyomitra* Pessagno, 1976

Archaeodictyomitra apiarium (Rust)

Plate III, 1

Lithocampe apiarium Rust: Rust, 1885, 314, Pl. 39 (14), Fig. 8.

Dictyomitra apiarium (Rust): Rust, 1898, p. 58; Nakaseko *et al.*, 1979, Pl. 3, Fig. 4.

Archaeodictyomitra apiara (Rust): Pessagno, 1977b, p. 41, Pl. 6, Figs. 6, 14; De Wever and Thiebault, 1981, p. 585; Nakaseko and Nishimura, 1981, p. 145, Pl. 6, Figs. 2–4; Pl. 15, Figs. 2, 6, not Fig. 7; not Schaaf, 1981, p. 432, Pl. 18, Figs. 2a–2b; Matsuyama *et al.*, 1982, Pl. 1, Fig. 1; Aoki, 1982, Pl. 2, Figs. 11, (?) 12; Matsuoka and Yao, 1985, Pl. 2, Fig. 4; Tanaka *et al.*, 1985, Pl. 1, Figs. 5–6; Conty and Marcucci, 1986, Pl. 1, Fig. 3; Kishida and Hisada, 1986, Fig. 2.8; Matsuoka, 1986a, Pl. 2, Fig. 14; Pl. 3, fig 13; Aita, 1987, p. 64; Kawabata, 1988, Pl. 2, Fig. 9; Wakita, 1988, Pl. 4, Fig. 1; Tumanda, 1988, p. 36, Pl. 2, Fig. 9; Kiessling, 1992, Pl. 1, Figs. 4–5; Steiger, 1992, p. 8, Pl. 25, Figs. 8–9.

Archaeodictyomitra apiarium (Rust): Kocher, 1981, p. 56, Pl. 12, Fig. 13; Schaaf, 1984, p. 92–93, Figs. 1, 3a–3b, 5a–5b; not 2, 4a–4b; Ishida, 1985, Pl. 3, Fig. 4; Suyari and Ishida, 1985, Pl. 2, Figs. 7–10; Aita and Okada, 1986, p. 108, Pl. 1, Fig. 11; Igo *et al.*, 1987, Figs. 2, 14; Pavsic and Gorican, 1987, p. 24, Pl. 2, Fig. 11; Danelian, 1989, p. 142, Pl. 3, Figs. 1–2; Widz, 1991, p. 243, Pl. 1, Fig. 14; Jud, 1994, p. 62, Pl. 3, Figs. 10, 11; Pral'nikova and Vishnevskaya, 1996, p. 241, Fig. 2h, 2l, 2m.

Archaeodictyomitra apiaria (Rust): Wu, Li, 1982, p. 67, Pl. 1, Figs. 15, 16; Ozvoldova and Sykora, 1984, p. 263, Pl. 3, Fig. 6; Baumgartner, 1984, p. 758, Pl. 2, Figs. 5, 6; Ozvoldova, 1990, Pl. 3, Fig. 2; Pl. 5, Fig. 5; not Murchey, 1984, Pl. 1, Fig. 3.

(?) *Archaeodictyomitra directiporata* (Rust): Ozvoldova, 1988, Pl. 4, Fig. 3.

(?) *Archaeodictyomitra* sp. C: Foley *et al.*, 1988, p. 485, Fig. 3, not 10, 11, (?) 12.

(Here and hereafter, synonymy is given after Baumgartner *et al.*, 1995).

Description. The elongated conical shell consists of 8–10 segments and lacks the apical horn. Cephalothorax is of the sphaeroconic shape, while other segments are almost cylindrical. All along the length, the shell is ornamented with 26–30 ribs separating vertical pore rows. Vertical intervals between distinct horizontal pore levels are equal or almost equal to each other. In the distal part, the unequal intervals are sometimes alternating. The horizontal pore rows show variable position within a segment.

Dimensions. Shells are 180–200 μm high and 90–100 μm wide.

Distribution: Upper Jurassic all over the globe and in the Talovka River basin of the Koryak Upland, samples C-2076 and M-911/17.

Archaeodictyomitra (?) *mirabilis* Aita, 1987

Plate IV, 8

Thanarla sp. B, Aita, 1982, Pl. 3, Figs. 1–2b.

Archaeodictyomitra (?) *mirabilis* Aita, 1987, Pl. 1, Figs. 14a–14b; Pl. 9, Figs. 7, 8.

Description. The bell-like subconical shell narrows slightly toward its aperture. Cephalis is rounded, lacking the apical horn. Postabdominal segments are ornamented with 20–24 ribs extending all along the shell and separating pore rows. Intervals between horizontal pore rows increase a little from cephalis toward the apertural end. Small round pores are identical in size. The last segment is somewhat swollen and narrows toward the aperture. Segments grade to each other without constrictions. Elementary cells of shell walls are tetragonal (Pral'nikova, 1995).

Dimensions. Shells are 90 μm high and 60–70 μm wide.

Distribution: Upper Jurassic of Japan and Russia; in the last case, the Talovka River basin of the Koryak Upland, samples C-2076 and M-911/17.

Archaeodictyomitra (?) aff. *A. mirabilis* Aita, 1987

Plate III, 2

As compared to the previous forms, shells are shorter and wider. Their aperture is narrower.

Distribution: Upper Jurassic of Russia, the Talovka River basin of the Koryak Upland, samples C-2076 and M-911/17.

Archaeodictyomitra aff. *A. suzukii* Aita, 1987

Plate III, 6

Archaeodictyomitra sp. A Aita, 1982, Pl. 3, Fig. 14

Archaeodictyomitra sp. Ishida, 1983, Pl. 7, Fig. 9.

Archaeodictyomitra suzukii Aita, 1987, Pl. 2, Figs. 1a–2b; Pl. 9, Fig. 9.

Description. The elongated conical shell is cylindrical in the middle and narrowing toward aperture. The shell is ornamented with 20–22 ribs separating pore rows. Intervals between horizontal pore rows are not equally wide. Elementary cells of shell walls are tetragonal.

Dimensions. Shells are 180 μm high and 75 μm wide.

Distribution: Upper Jurassic of Japan and Russia; in the last case, the Talovka River basin of the Koryak Upland, Sample M-911/17.

Genus *Cinguloturris* Dumitrica: Dumitrica et Mello, 1982

Cinguloturris carpatica Dumitrica

Plate IV, 9

Unnamed multicyrtoid nassellarians: ? Adachi, 1982, Pl. 2, Figs. 9 (?) 10; Yamamoto, 1983, Pl. 1, Fig. 10.

Theoperidae gen. et. sp. indet. 1: Aita, 1982, Pl. 2, Fig. 18.

Theoperid gen. et sp. indet:: Aoki, Tashiro, 1982, Pl. 2, Fig. 9.

Stichomitra sp. A: (?) Yao *et al.*, 1982, Pl. 4, Fig. 20.

Dictyomitra sp. B: 1983, Ishida, Pl. 5, Figs. 3, 4.

Cinguloturris carpatica: Dumitrica, Mello, 1982, p. 23, Pl. 4, Figs. 7–11; Yao, 1984, Pl. 2, Fig. 28; Ishida, 1985a, Pl. 3, Fig. 14; Pl. 4, Figs. 13–14; Matsuoka, Yao, 1985, Pl. 2, Fig. 13; Tanaka *et al.*, 1985, Pl. 1, Fig. 12; Aita, 1985, Figs. 7, 12; Kishida, Hisada, 1986, Pl. 2, Fig. 12; Matsuoka, 1986a, Pl. 2, Fig. 16; Matsuoka, Yao, 1986, Pl. 2, Fig. 14; Aita, 1987, p. 64, Pl. 10, Fig. 12; Ozvoldova, 1988, Pl. 6, Fig. 8; Kawabata, 1988, Pl. 2, Fig. 10; Wakita, 1988, Pl. 4, Fig. (?) 16; Pl. 5, Fig. 8; Kato, Iwata, 1989, Pl. 5, Fig. 5; Pl. 6, Fig. 10; Yasuda, 1989, Pl. 1, Fig. 14; Widz, 1991, p. 244, Pl. 1, Fig. 11; Yao, 1991, Pl. 4, Fig. 11; Matsuoka, 1992, Pl. 3, Fig. 2; Pl. 4, Fig. 1.

Cinguloturris sp. aff. *C. carpatica* Dumitrica: Yao, 1984, Pl. 3, Fig. 19.

Cinguloturris sp. cf. *C. carpatica* Dumitrica: Tanaka *et al.*, 1985, Pl. 1, Fig. 7.

Cinguloturris sp. cf. *C. carpatica* Dumitrica: Kurimoto, 1989, Pl. 1, Fig. 17.

Description. The preserved shell fragment consists of seven segments. Cephalothorax is sphaeroconical and grades into post-thoracic segments, which widen notably up to the third one; afterward, the shell width grows slower. Segments are separated by constrictions, the first of which, between the thorax and subsequent segment is indistinct, but others are better developed. Constrictions are filled with spongy material, whose layer increases the shell diameter up to that in the wide section of a segment.

Dimensions. Shell is 210 μm high and 95 μm wide.

Distribution: Upper Jurassic all over the globe and in Russia; in the last case, the Talovka River basin of the Koryak Upland, Sample C-2076.

Family Eucirtidiellidae Takemura, 1986

Genus *Eucyrtidiellum* Baumgartner, 1984

Eucyrtidiellum nodosum Wakita

Plate IV, 2

Eucyrtidiellum sp. aff. *E. unumaense* (Yao): Matsuoka, 1986, Pl. 2, Fig. 9.

Eucyrtidiellum nodosum Wakita: Wakita, 1988, p. 408, Pl. 4, Fig. 29; Baumgartner, 1995, p. 213, Pl. 3014, Figs. 1–3.

Description. Small spheroid cephalis has an apical horn. Thorax is ornamented with small tubercles. Pore arrangement in abdomen is hexagonal, and pores are surrounded by larger that of the tubercles than they are on thorax. The aperture diameter is almost as wide as thorax.

Dimensions. Shell (cephalis, thorax, and abdomen) is 80–90 μm high; thorax is 20–30 μm high and 35–40 μm wide; abdomen is 40–50 μm high.

Distribution: Upper Jurassic of Japan and Russia; in the last case, the Talovka River basin of the Koryak Upland, Sample C-2076.

Eucyrtidiellum (?) *ozaiense* Aita

Plate IV, 1

Eucyrtidiellum (?) *ozaiense* Aita: Aita, 1987, Pl. 14, Fig. 1.

Description. Shell consists of three segments: sphaeroconical cephalis, conical second segment, and swollen third segment separated from the previous one by a minor constriction. The third segment is ornamented with 12 smooth vertical ribs, the amount of which is lesser than that in *E. pyramis*. Another distinctive feature is absence of ribs on the second segment.

Dimensions. Shell without the apical horn is 45–55 μm high and 60–65 μm wide.

Distribution: Upper Jurassic of Japan and Russia; in the last case, the Talovka River basin of the Koryak Upland, Sample C-2076.

Eucyrtidiellum ptyctum (Riedel et Sanfilippo)

Plate IV, 3

Eucyrtidiellum ptyctum: Riedel and Sanfilippo, 1974, p. 778, Pl. 5, Fig. 7; Pl. 12, Fig. 14; Baumgartner, 1984, p. 764, Pl. 4, Figs. 1–3; Aita, 1987, p. 65, Pl. 4, Figs. 12a–12b; Pl. 10, Fig. 14; Pl. 14, Fig. 3; Baumgartner *et al.*, 1995, Pl. 3017, Figs. 1–8.

Description. Shell has a rounded cephalis and consists of three segments. Pores are missing in the first and third segment and show the hexagonal arrangement in the second one decorated with tubercles around pores. The horizontal row of slightly larger pores separates the second and third segments. The widest third segment is ornamented all around with 14–16 vertical ridges.

Dimensions. Shell without the apical horn is 35–45 μm high and 25–30 μm wide thus being twice lesser than the holotype and specimens from the Tethys and California (Baumgartner *et al.*, 1995).

Distribution: Bajocian–lower Tithonian of the Tethys, Japan, and Russia; in the last case, the Talovka River basin of the Koryak Upland, samples C-2076 and M-911/17.

Eucyrtidiellum pyramis (Aita)

Plate III, 8

Eucyrtidium (?) *pyramus* (Aita): Aita et Okada, 1986, p. 109, Pl. 6, Figs. 8–13; Pl. 7, Figs. 1a–2b.

Eucyrtidiellum pyramis (Aita): Aita, 1987, p. 65, Pl. 14, Fig. 2; Baumgartner, 1995, p. 216, Pl. 3019, Figs. 1, 2(H).

Description. Three-segment shell has the mucronated conical cephalis swollen downward and grading without a constriction into the conical thorax. Shell walls in the second and third segments are ornamented with 14 vertical smooth-wavy ribs. A horizontal pore row is distinct within a minor constriction between the second and third segments. The third segment is almost as high as a half of the shell and widest as compared to others; being conical in the upper portion, it is cylindrical below.

Dimensions. Shell is 55–65 μm high and 35–40 μm wide.

Distribution: Tithonian of Japan and Russia; in the last case, the Talovka River basin of the Koryak Upland, Sample M-911/17.

Eucyrtidiellum sp. A aff. *E. quinatum* Takemura

Plate IV, 4

Eucyrtidiellum quinatum Takemura: Takemura, 1986, Pl. 12, Figs. 16–18.

Description. Shell consists of five segments widening sequentially. Constriction between the first and second segment is indistinct, but further downward, this morphological element is more developed. Between the third and fourth segments, it is clearly seen because the latter is considerably wider than the former. The fourth and fifth segments are almost equally wide, and constriction between them is decorated with large pores surrounded by wall depressions. On the cephalis, porosity is hardly seen, being distinct in other parts of the shell. Pores and tubercles in between show the hexagonal arrangement and are joint neatly. The aperture diameter is almost as wide as that of the constriction between the fourth and fifth segments.

An abrupt widening of the shell beginning from the fourth segment differs it from *E. quinatum* Takemura. In addition, its fifth segment is slightly wider than the fourth one, whereas the last segment of *E. quinatum* is narrower than the previous element. The hexagonal arrangement of pores and tubercles is more regular in

the shell under discussion, which is also lesser in size than the holotype *E. quinatum* Takemura.

Dimensions. Shell is 130–140 μm high and 90–100 μm wide (4–5th segments).

Distribution: Callovian–Oxfordian of Japan and Russia; in the last case, the Talovka River basin of the Koryak Upland, Sample C-2076.

Eucyrtidiellum sp. B aff. *E. quinatum* Takemura

Plate III, 9

Eucyrtidiellum quinatum Takemura: Takemura, 1986, Pl. 12, Figs. 16–18.

Description. Shell consists of five segments widening cone-like toward the last hemispheric segment, which closes around the aperture. Constrictions are notable on both sides of the fourth segment, and the lower one between 4th and 5th segments is marked by a row of large pores located inside concavities. Three initial segments have indistinct boundaries on the shell surface. Porosity obscure on the smooth surface of cephalis is more distinct on other segments. Hexagonal ridges around pores are flattened. In comparison with *E. quinatum* Takemura, the distinctive features are as follows: shell shows an abrupt widening beginning from the fourth segment, which is narrower, however, than the fifth one in contrast to reversed proportions of these segments of *E. quinatum*; the hexagonal arrangement of pores is more regular than in photograph published by Takemura; the shell surface is smoother, because pores are less frequent and smaller in diameter. In comparison with *E.* sp. A aff. *E. quinatum* Takemura, we noted the following distinctions: three initial segments have no constriction in between; widening of the fourth segment is more abrupt; shell surface is smoother; round pores are situated in the center of hexagonal platelets framed by low-relief ridges; intervals between pores are 2–3 times greater than their diameters; the aperture is lesser in diameter.

Dimensions. Shell is 120–130 μm high and 85–90 μm wide at the level of the 4–5th segments.

Distribution: Middle–Upper Jurassic of Japan and Russia; in the last case, the Talovka River basin of the Koryak Upland, Sample M-911/17.

Family Hsuidae Pessagno, 1977

Genus *Hsuum* Pessagno, 1977

Hsuum aff. *H. belliatulum* Pessagno et Whalen

Plate III, 7

Hsuum belliatulum Pessagno et Whalen: Pessagno and Whalen, 1982, p. 131, Pl. 7, Figs. 7, 8, 12, 18, 22; Pl. 13, Fig. 3.

Description. Shell is conical to subcylindrical in shape, with the cephalis, thorax, and abdomen forming a hemisphere crowned with a short horn. Vertical cuneate ribs are more numerous in the distal, than in the proximal part of the shell. Additional ribs appear close to the middle of the shell length. Between the ribs, there are visible pairs of vertical pore rows. Pores are large (diameter up to 1/2–2/3 of the rib width) and arranged chequerwise; some of them approach a hexagon in shape. In the postabdominal part, the amount of ribs grows from 14 to 16–18.

In comparison with *H. belliatulum* Pessagno et Whalen, the form has more massive ribs embossed at the shell surface, but its vertical pore rows are less regular.

Dimensions. Specimen lacking a shell part is 120–140 μm high and 110–115 μm wide.

Distribution: Middle–Upper Jurassic of California and Russia; in the last case, Kimmeridgian–lower Tithonian, the Talovka River basin of the Koryak Upland, Sample M-911/17.

Genus *Parahsuum* Yao, 1982

Parahsuum aff. *P. kanyoense* Sashida

Plate IV, 7

Parahsuum kanyoense Sashida: Sashida, 1988, Pl. 1, Figs. 14, 15, 20–24; Pl. 2, Fig. 4.

Description. Shell is conical, widening below cephalis quickly, but slower below the second or third segment, where it is approaching the cylindrical shape. Cephalis is dense, crowned with not a prominent horn. The tetragonal framework of the shell consists of vertical and horizontal pore rows separated by vertical ridges. On the lateral wall, there are 12–14 ridges. In particular specimens, ridges are dichotomous, and their amount somewhat increases from cephalis toward the last segment

Dimensions. Shell is 110–140 μm high and 85–110 μm wide (size ranges of four specimens). Shell size is 1.5–2 times less than that in original description.

Distribution: Middle Jurassic of Japan and Russia; in the last case, Callovian–Oxfordian, the Talovka River basin of the Koryak Upland, Sample C-2086.

Family Parvicingulidae Pessagno

Genus *Parvicingula* Pessagno, 1977

Parvicingula (?) *blackhorsensis* Pessagno et Whalen, 1982

Plate I, 1–3; Plate IV, 6

Parvicingula blackhorsensis Pessagno et Whalen: Pessagno and Whalen, 1982, p. 137, Pl. 10, Figs. 10–12; Pl. 13, Fig. 14.

Parvicingula blackhorsensis (?) Pessagno et Whalen: Blome, 1984, p. 357, Pl. 9, Figs. 6, 11, 15, 22; Pl. 15, Figs. 3, 8.

Description. Shell is wide-conical. Cephalis, thorax, and abdomen are perforated by small pores. Postabdominal chambers show three pore rows each. These hexagonal pores of a much larger size are arranged chequerwise. Beginning from the abdomen, chambers grow quickly in width and slower in height. Chambers

are separated from each other by tubercular embossed rings.

Dimensions. Shell without broken horn is 110 μm high and 90 μm wide.

Distribution: Middle–Upper Jurassic of California and Russia; in the last case, lower Kimmeridgian, *Amoeboceras kitchini* Zone, Ukhta region, Pechora River, Sample P; Koryak Upland, Rarytkin Ridge, samples H-11, H–212, 4626; Malyi Nauchirynai River, Sample 757/6; Talovka River basin, Sample C-2076.

Parvicingula cf. *blowi* Pessagno
Plate II, 1–3, 6

Parvicingula blowi Pessagno: Pessagno, 1977, p. 85, Pl. 8, Figs.11–14.

Parvicingula blowi Pessagno: Pessagno *et al.*, 1984, p. 26, Pl. 2, Figs. 14–15, 1989.

Parvicingula blowi Pessagno: Dyer and Copestake, p. 227, Pl. 2, Figs. 3–4, 1995.

Parvicingula blowi Pessagno, Hull, p. 21, pl. 3, Figs. 6, 18, 22.

Distribution: Middle–Upper Jurassic of California; Upper Jurassic (lower Kimmeridgian) of Russia: *Amoeboceras kitchini* Zone, Ukhta region, Pechora River, Sample P; Koryak Upland, Rarytkin Ridge, Sample H-212-15a, Utesiki River, Sample N–11.

Parvicingula burnsensis Pessagno et Whalen
Plate II, 4–5

Parvicingula burnsensis Pessagno et Whalen: Pessagno and Whalen, 1982, p. 136, Pl. 9, Figs. 5–7, 14–15, 19–20; Pl. 13, Fig. 2.

Parvicingula cf. *burnsensis* Pessagno et Whalen: Vishnevskaya, 1992, p. 27, Pl. 1, Fig. 15.

Parvicingula burnsensis Pessagno et Whalen: Kozlova, 1994, Pl. 3, Figs. 5–6.

Parvicingula burnsensis Pessagno et Whalen, Vishnevskaya, 1994, p. 217, Fig. 14:19.

Distribution: Middle–Upper Jurassic of California; Upper Jurassic (lower Kimmeridgian) of Russia, *Amoeboceras kitchini* Zone, Ukhta region, Pizhma River, Pechora River basin, Sample P.

Parvicingula aff. *burnsensis* Pessagno et Whalen
Plate II, 7–10

Distribution: Upper Jurassic (lower Kimmeridgian) of Russia, *Amoeboceras kitchini*, Ukhta region, Pechora River, Pechora River basin, Sample P; Koryak Upland, Nauchirynai Creek, samples 757/6, DH-760.

Parvicingula (?) elegans Pessagno et Whalen
Plate I, 5 and 10–12

Parvicingula elegans Pessagno et Whalen: Pessagno and Whalen, 1982, p. 138, Pl. 10, Figs. 7, 16, 20; Pl. 13, Figs. 9, not 1994.

Parvicingula elegans Pessagno et Whalen: Kozlova, Pl. 4, Figs. 3–4.

Parvicingula sp. aff. *P.* aff. *P. elegans* Pessagno et Whalen: Baumgartner *et al.*, 1995, p. 408, Pl. 3188, Figs. 1–2.

Distribution: Middle–Upper Jurassic of California and Russia; in the last case: lower Kimmeridgian, *Amoeboceras kitchini*, Ukhta region, Pechora River, Sample P; Koryak Upland, Nauchirynai Creek, Sample H-757-6 and Rarytkin Ridge, Sample H-212-15a.

Parvicingula (?) *enormis* Yang
Plate II, 11–12

Parvicingula (?) *enormis* Yang: Yang, 1993, p. 118, Pl. 19, Figs. 6, 13, 18; Pl. 20, Figs. 5, 6, 15, 22.

Distribution: Middle–Upper Jurassic of California; Upper Jurassic (lower Kimmeridgian) of Russia: *Amoeboceras kitchini* Zone, Ukhta region, Pechora River, Sample P; Koryak Upland, Nauchirynai Creek, Sample 757-6.

Parvicingula ex gr. *khabakovi* (Zhamoida)
Plate I, 4

Eucyrtidium khabakovi Zhamoida: Dundo and Zhamoida, 1963, p. 82, Pl. 2, Figs. 9–10; Pl. 4, Fig. 6.

Eucyrtidium khabakovi Zhamoida: Zhamoida, 1972, p.120b, Pl. 12, Figs. 7–8; Pl. 13, Fig. 5.

Parvicingula khabakovi Zhamoida: Vishnevskaya and Kazintseva, 1990, Pl. 4, Fig. 5.

Parvicingula ex gr. *khabakovi* Zhamoida: Vishnevskaya and Filatova, 1996, Pl. 2, Fig. 12.

Distribution: Upper Jurassic (lower Kimmeridgian) of Russia: *Amoeboceras kitchini*, Ukhta region, Pechora River, Sample P; Koryak Upland, Rarytkin Ridge, Sample H-212-15a.

Family Xitidae Pessagno
Genus *Xitus* Pessagno, 1977
Xitus gifuensis Mizutani
Plate III, 3–4

Xitus gifuensis Mizutani: Mizutani, 1981, p.180, Pl. 59, Figs. 1, 2a–2b, 3–4; Adachi, 1982, Pl. 3, Figs. 1–2; Wakita, 1988, Pl. 5, Fig. (?) 9; Pl. 6, Fig. 20; Baumgartner *et al.*, 1995, p. 640, Pl. 3294, Figs. 1–3.

Description. The cone-like shell is ornamented with large smooth tubercles, which are arranged chequerwise. Intervals between pores are slightly greater than pore diameters. Pores tend to surround tubercles, although this type of their distribution is inconsistent. Cephalis is perforated by small chaotic pores.

Dimensions. The incomplete shell specimen is 100–120 μm high and 70–80 μm wide.

Distribution: upper Kimmeridgian–lower Valanginian of Japan; Kimmeridgian–lower Tithonian of Russia, Koryak Upland, Talovka River basin, Sample M-911/17.

Family Williriedellidae Dumitrica

Genus *Williriedellum* Dumitrica, 1970

Williriedellum cf. *W. crystallanum* Dumitrica

Plate III, 5

Williriedellum crystallanum Dumitrica: Dumitrica, 1970, p. 69, Pl. 10, Figs. 60a–c, 62–63; Widz, 1991, p. 257, Pl. 4, Figs. 21–22.

Williriedellum cf. *crystallanum* Dumitrica: Adachi, 1982, Pl. 4, Figs. 8 (?), 9; Wakita, 1988, Pl. 5, Fig. 25; Kiessling, 1992, Pl. 1, Fig. 14.

Description. Shell is rounded, almost oval. Dense shell walls consist of hexa- to pentagonal facets, which are slightly concave. Facets are perforated by small cylindrical pores (three to ten in each), which are arranged into oblique rows. The apical horn is missing. Aperture is rather large.

Dimensions. Shell is 155–170 μm high and 130–140 μm wide.

Distribution: Upper Jurassic all over the globe; Kimmeridgian–lower Tithonian of Russia, Koryak Upland, Talovka River basin, Sample M-911/17

Reviewers I.A. Basov and N.Yu. Bragin

REFERENCES

Aita, J., Middle Jurassic to Lower Cretaceous Radiolarian Biostratigraphy of Shikoku with Reference to Selected Sections in Lombardy Basin and Sicily, *Sci. Rep., Tohoku Univ.*, 1987, vol. 58, no. 1, pp. 1–91.

Baumgartner, P.O. and INTERRAD, Jurassic–Cretaceous Working Group, Middle Jurassic to Lower Cretaceous Radiolaria of Tethys, *Mem. Geol., Lausanne*, 1995, no. 23, pp. 1–1172.

Blome, C.D., Middle Jurassic (Callovian) Radiolarians from Carbonate Concretions, Alaska and Oregon, *Micropaleontol.*, 1984, vol. 30, no. 4, pp. 343– 389.

Bogdanov, N.A. and Vishnevskaya, V.S., Significance of Radiolarians for Tectonostratigraphy of Northeastern Russia, in *Paleontologo-stratigraficheskie issledovaniya fanerozoya Dal'nego Vostoka (po resul'tatam radiolyarievogo analiza dlya kartirovaniya)* (Paleontological-Stratigraphic Studies on the Phanerozoic in the Far East: Results of Radiolarian Analysis for Cartography), Vladivostok: Akad. Nauk SSSR, 1991, pp. 20–30.

Bragin, N.Y., Radiolaria from the Phosphorites Basal Horizons of the Volgian Stage in the Moscow Region, *Rev. Micropaleontol.*, 1997, vol. 4, no. 4, pp. 285–296.

Bragin, N.Yu. and Bragina, L.G., Radiolarians from Upper Jurassic–Cretaceous Deposits of the Moscow Region, in *X seminar po radiolyariyam XLII sessii VPO Rossii* (X Seminar on Radiolarians, XLII Session of Russian Paleontological Society), Moscow, 1996, p. 12.

Dumitrica, P., Immenhauser, A., and Dumitrica-Jud, R., Mesozoic Radiolarian Biostratigraphy from Masirah Ophiolite, Sultanate of Oman, Part 1: Middle Triassic, Uppermost Jurassic and Lower Cretaceous Spumellarians and Multisegmented Nassellarians, *Bull. Nat. Mus. Natural Sci.*, 1997, no. 9, pp. 1–107.

Dundo, O.P. and Zhamoida, A.I., Stratigraphy of Mesozoic Deposits in the Velikaya River Basin and Characteristic Assemblage of Valanginian Radiolarians, in *Geologiya Koryakskogo nagor'ya* (Geology of the Koryak Upland), Moscow: Gosgortekhizdat, 1963, pp. 65–90.

Dyer, R. and Copestake, P., A Review of Latest Jurassic to Earliest Cretaceous Radiolaria and Their Biostratigraphic Potential to Petroleum Exploration in the North Sea, in *Northwest European Micropaleontology and Palynology*, London, 1989, pp. 214–235.

Grigor'ev, V.N., Sokolov, S.D., Krylov, K.A., *et al.*, Geodynamic Typofication of Triassic–Jurassic Complexes of Volcanic and Siliceous Rocks of the Kuyul Terrane (Koryak Upland), *Geotektonika*, 1995, no. 3, pp. 59–69.

Grill, J. and Kozur, H., The First Evidence of the *Unuma echinatus* Radiolarian Zone in the Rudabanya Mts. (Northern Hungary), *Geol. Palaont. Mitt. Innsbruck.*, 1986, vol. 13, no. 11, pp. 239–275.

Heitzer, I., Die Radiolarienfauna der mitteljurassischen Kieselmergel im Sonnwendgebirge, *Jahrb. geol. L.A. Wien*, 1930, no. 80, pp. 381–406.

Hull, M.D., Morphologic Diversity and Paleogeographic Significance of the Family Parvicingulidae (Radiolaria), *Micropaleontol.*, 1995, vol. 41, no. 1, pp. 1–48.

Khabakov, A.V., Radiolarian Fauna from Upper Jurassic and Lower Cretaceous Phosphorites of the Vyatka and Kama River Basins, *Ezheg. Vses. Paleontol. O-va*, 1937, vol. 11, pp. 90–120.

Khanchuk, A.I., Grigor'ev, V.N., Golozubov, V.V., *et al.*, *Kuyul'skii ofiolitovyi terrein* (The Kuyul Ophiolite Terrane), Vladivostok: Akad. Nauk SSSR, 1990.

Khudyaev, J., On the Radiolaria in Phosphates in the Region of the Syssola River, *Trans. Geol. Prospect. Service of U.S.S.R.*, 1931, no. 46, pp. 1–48.

Kiessling, W. and Scasso, R., Ecological Perspectives of Late Jurassic Radiolarian Faunas from the Antarctic Peninsula, *Geo Research Forum, Switzerland*, 1996, vols. 1–2, pp. 317–326.

Kozlova, G.E., Radiolarians Discovered in Lower Kimmeridgian Deposits of the Timan–Urals Region, *Dokl. Akad. Nauk SSSR*, 1971, vol. 201, no. 5, pp. 1175–1177.

Kozlova, G.E., Distribution of Radiolarians in the Bazhenovo Formation of West Siberia, in *Paleogeografiya i biostratigrafiya yury i mela Sibiri* (Jurassic–Cretaceous Paleogeography and Biostratigraphy of Siberia), Moscow: Nauka, 1983, pp. 47–55.

Kozlova, G.E., Mesozoic Radiolarian Assemblage of the Timan–Pechora Oil Field, *Proc. Sankt-Petersburg International Conference*, St. Petersburg, 1994, pp. 60–75.

Pantanelli, D., I diaspri della Toscana e i loro fossili, *Atti della reale Academia nazionale del Lincei, Mem. della Classe di Scienze fisiche, matematiche e naturali*, 1880, vol. 8, pp. 35–66.

Pessagno, E.A., Jr., Lower Cretaceous Radiolarian Biostratigraphy of Great Valley Sequences and Franciscan Complex, California Coast Ranges, *Contrib. Cushman Found. Foraminiferal Res.*, 1977a, no. 15, pp. 1–87.

Pessagno, E.A., Jr., Upper Jurassic Radiolaria and Radiolarian Biostratigraphy of the California Coast Ranges, *Micropaleontol.*, 1977b, vol. 23, no. 1, pp. 117–134.

Pessagno, E.A., Jr., Blome, C.D., and Longoria, J.F., A Revised Radiolarian Zonation for the Upper Jurassic of

Western North America, *Bull. Am. Paleont.*, 1984, vol. 320, pp. 1–51.

Pessagno, E.A., Jr., Longoria, J.F., McLeod, N., and Six, W.M., Studies of North American Jurassic Radiolaria, Part 1: Upper Jurassic (Kimmeridgian–Upper Tithonian) Pantanelliidae from the Taman Formation, East–Central Mexico: Tectonostratigraphic, Cronostratigraphic and Phylogenetic Implications, *Contrib. Cushman Found. Foraminiferal Res.*, 1987, no. 23, pp. 1–55.

Pessagno, E.A., Jr. and Whalen, P.A., Lower and Middle Jurassic Radiolaria (Multicyrtid Nassellariina) from California, East–Central Oregon and the Queen Islands, B.C., *Micropaleontol.*, 1982, vol. 28, no. 2, pp. 11–169.

Petrushevskaya, M.G., Radiolarians of Plankton and Bottom Sediments, in *Geokhimiya kremnezema* (Geochemistry of Silica), Moscow: Nauka, 1966, pp. 219–245.

Pral'nikova, I.E., Hexagonal and Tetragonal Frameworks in the Structural Evolution of Radiolarian Skeletons, in *Tez. Mikropaleontol. O-va, Tomsk. Gos. Univ.*, (Abstracts of Micropaleontol. Soc., Tomsk State Univ.), Tomsk, 1995, pp. 86–87.

Pral'nikova, I.E. and Vishnevskaya, V.S., Middle–Late Jurassic Radiolarian Assemblages from Oceanic Rock Complexes of the Kuyul Terrane (Koryak Upland, Northeastern Russia) and Their Paleogeographic Affinity, *Dokl. Ross. Akad. Nauk*, 1996, vol. 351, no. 2, pp. 240–245.

Riboulleau, A., Baudin, F., Daux, V., *et al.*, Evolution de la paleotemperature des eaux de la plate–forme russe au cours du Jurassique superieur, *Sciences de la terre et des planetes, Acad. Sci. Paris*, 1998, no. 326, pp. 239–246.

Rust, D., Beitrage zur Kenntniss der fossilen Radiolarien aus Gesteinen des Jura und der Kreide, *Palaeontographica*, 1885, vol. 31 (ser. 3), pp. 269–321.

Rust, D., Neue Beitrage zur Kenntniss der fossilen Radiolarien aus Gesteinen des Jura und der Kreide, *Palaeontographica*, 1898, vol. 45, pp. 1–67.

Sashida, K., Lower Jurassic Multisegmented Nassellaria from the Itsukaichi Area, Western Part of Tokyo Prefecture, Central Japan, *Sci. Rep. Inst. Geosci., Univ. Tsukuba*, 1988, vol. 9, nos. 1–4, pp. 1–27.

Sedaeva, G.M. and Vishnevskaya, V.S., Jurassic Paleoenvironments of the North–Eastern European Platform, *Zonenshain Conference on Plate Tectonics, GEOMAR*, Kiel, 1995, p. 205.

Sokolov, S.D., *Akkretsionnaya tektonika Koryakskо-Chukotskogo segmenta Tikhookeanskogo poyasa* (Accretionary Tectonics of the Koryak–Chukchi Segment of Circum-Pacific Belt), Moscow: Nauka, 1992.

Takemura, A., Classification of Jurassic Nassellarians (Radiolaria), *Palaeontographica*, 1986, vol. 195A, pp. 5–86.

Vishnevskaya, V.S., Significance of Mesozoic Radiolarians for Tectonostratigraphy in Pacific Rim Terranes of the Former USSR, *Palaeogeogr., Palaeoclimatol., Palaeoecol.*, 1992, no. 96, pp. 23–39.

Vishnevskaya, V.S., *Parvicingula* as Indicator of Jurassic to Early Cretaceous Paleogeographical and Sedimentological Paleoenvironments within North Peri-Tethys, in *Moscow Peri-Tethys Workshop*, Moscow, 1996a, pp. 30–31.

Vishnevskaya, V.S., Radiolarians of Peri-Tethys and Their Stratigraphic Significance, *Dokl. Ross. Akad. Nauk*, 1996b, vol. 346, no. 5, pp. 638–641.

Vishnevskaya, V., The Domanikoid Facies of the Russian Platform and Basin Paleogeography, *Mem. Mus. Nat. Hist.*, 1998, no. 177, pp. 38–62.

Vishnevskaya, V.S. and De Wever, P., About Possibility to Correlate North Peri–Tethyan Radiolarian Events with Other Zonations, in *Moscow Peri-Tethys Workshop*, Moscow, 1996, pp. 31–32.

Vishnevskaya, V.S. and Filatova, N.I., Mesozoic Terranes of the Northwest Pacific Continental Margin (Russia): Radiolarian Ages and Sedimentary Environments, *Island Arc*, 1994, vol. 3, pp. 199–220.

Vishnevskaya, V.S. and Filatova, N.I., Mesozoic Radiolarian Biostratigraphy of Northeastern Russia, *Tikhookean. Geol.*, 1996, vol. 15, no. 1, pp. 16–44.

Vishnevskaya, V.S. and Kazintsova, L.I., Cretaceous Radiolarians of the USSR, in *Radiolyarii v biostratigrafii* (Radiolarians in Biostratigraphy), Sverdlovsk: Akad. Nauk SSSR, 1990, pp. 44–59.

Vishnevskaya, V.S. and Malinovskii, Yu.N., Radiolarians from the Reference Section of Oxfordian–Valanginian Deposits of the Paksa Peninsula, Anabar Bay, North Siberia, in *Tez. Micropaleontol. O-va, Tomsk. Gos. Univ.*, (Abstracts of Micropaleontol. Soc., Tomsk State Univ.), Tomsk, 1995, p. 66.

Wakita, A., Early Cretaceous Melange in the Hida–Kanayama Area, Central Japan, *Bull. Geol. Surv. Jpn.*, 1988, vol. 39, no. 6, pp. 367–421.

Yang, Q., Taxonomic Studies of Upper Jurassic (Tithonian) Radiolaria from the Taman Formation, East–Central Mexico, *Palaeoworld, Nanjing Inst. Geol. Paleontol., Acad. Sinica*, 1993, vol. 3, pp. 1–165.

Zhamoida, A.I., *Biostratigrafiya mezozoiskikh kremnistykh tolshch Vostoka SSSR* (Mesozoic Biostratigraphy of Siliceous Deposits in the Eastern USSR), Leningrad: Nedra, 1972.

Stratigraphy and Geological Correlation, Vol. 7, No. 5, 1999, pp. 492–500. Translated from Stratigrafiya. Geologicheskaya Korrelyatsiya, Vol. 7, No. 5, 1999, pp. 84–92.
Original Russian Text Copyright © 1999 by Bragina, Ben'yamovskii, Zastrozhnov.
English Translation Copyright © 1999 by MAIK "Nauka/Interperiodica" (Russia).

The Upper Cretaceous Radiolarians, Foraminifers, and Stratigraphy of the Southeastern Russian Plate, the Right-Bank Volga Region near Volgograd

L. G. Bragina*, V. N. Ben'yamovskii*, and A. S. Zastrozhnov**

* *Geological Institute (GIN), Russian Academy of Sciences, Pyzhevskii per. 7, Moscow, 109017 Russia*
** *Volgograd Hydrogeological Expedition, ul. Nezhdanovoi 8, Volgograd, 400135 Russia*

Received January 27, 1997; in final form, May 15, 1998

Abstract—Paleontological study of the Upper Cretaceous sediments from wells 502 and 28 in the Volgograd region revealed distinct radiolarian and foraminiferal assemblages. Two stratigraphic levels, Coniacian-Santonian and upper Campanian, are recognized on the basis of radiolarians. Foraminiferal and radiolarian zones of the same section are first correlated to each other in the Volgograd region, and coeval assemblages from the Moscow syneclise and Volgograd region are compared.

Key words: *Upper Cretaceous, stratigraphy, radiolarians, foraminifers, European paleobiogeographical area, Volga region*

The Upper Cretaceous sediments of the studied region are represented by three lithostratigraphic units. The lower one is arenaceous, the middle is carbonate, and the upper unit that constitutes the major part of the section is composed of siliceous clayey and silty arenaceous rocks. The middle, Turonian-Coniacian unit, yields foraminifers. Radiolarians were encountered at several levels of the upper unit. These two microfossil groups are of great importance for the age determination of the studied sediments.

The latest research (Bragina, 1987, 1994; Vishnevskaya and Kazintsova, 1990) showed that the Late Cretaceous radiolarians require a more thorough investigation. Up to now, the Cretaceous radiolarian zonation in the Russian plate is not developed. Therefore, when estimating age of fossil assemblages, paleontologists use zonations suggested for subtropical and tropical areas notably remote from the study region. To develop a similar Cretaceous zonation for the Russian plate, it is necessary to reveal the radiolarian assemblages, whose stratigraphic position in the section is defined on the basis of associated traditional fossil groups. This paper is an attempt to approximate the solution to the problem. The sections of boreholes drilled near Volgograd, namely, Well 502 (the Zarya Village) and Well 28 (the Peskovatka Village) were basic objects for the investigation.

We suggest to divide the Upper Cretaceous sediments into the following units: (1) the Peskovatka sequence of the Albian–Cenomanian sands and limestones; (2) the Dubovka sequence (Turonian-Coniacian and lower Santonian limestones and marls) named for the Dubovka Village adjacent to Well 28 that penetrated the complete section of the sequence; (3) the Nariman sequence (Santonian and lower Campanian clays and argillites) named after the Nariman Village; (4) the Zarya sequence (upper Campanian clays and siltstones) named after the Zarya Village adjacent to Well 502; and (5) the Bereslavka sequence (upper Campanian and Maastrichtian silts and sands) named after the Bereslavka Village, which is situated 10 km north of Well 502.

Let us consider these lithostratigraphic units penetrated by Well 28 near the Peskovatka Village. The studied Upper Cretaceous section (see the figure) is described upward from the base.

The Peskovatka Sequence

Bed 1 (depth range from 494 to 465 m): greenish gray quartz sands, fine-grained, at the top, green and bearing glauconite; the thickness is 25 m.

The Dubovka Sequence

Bed 2 (depth range from 465 to 457 m): grayish white loose chalk with the basal layer of sandy chalk grading into calcareous sandstone; at a depth of 461 m the foraminifer assemblage of the *Hedbergella holzli* Zone was found. The assemblage includes the following characteristic planktonic foraminifers: *Hedbergella paradubia* Sigal, *H. bornholmensis* Douglas, *H.* aff. *caspia* (Vassilenko), and *Rugoglobigerina ordinaria* Subbotina. The thickess is 8 m.

The sample from the depth of 458 m yielded foraminifer species missing below: *Arenobulimina presli*

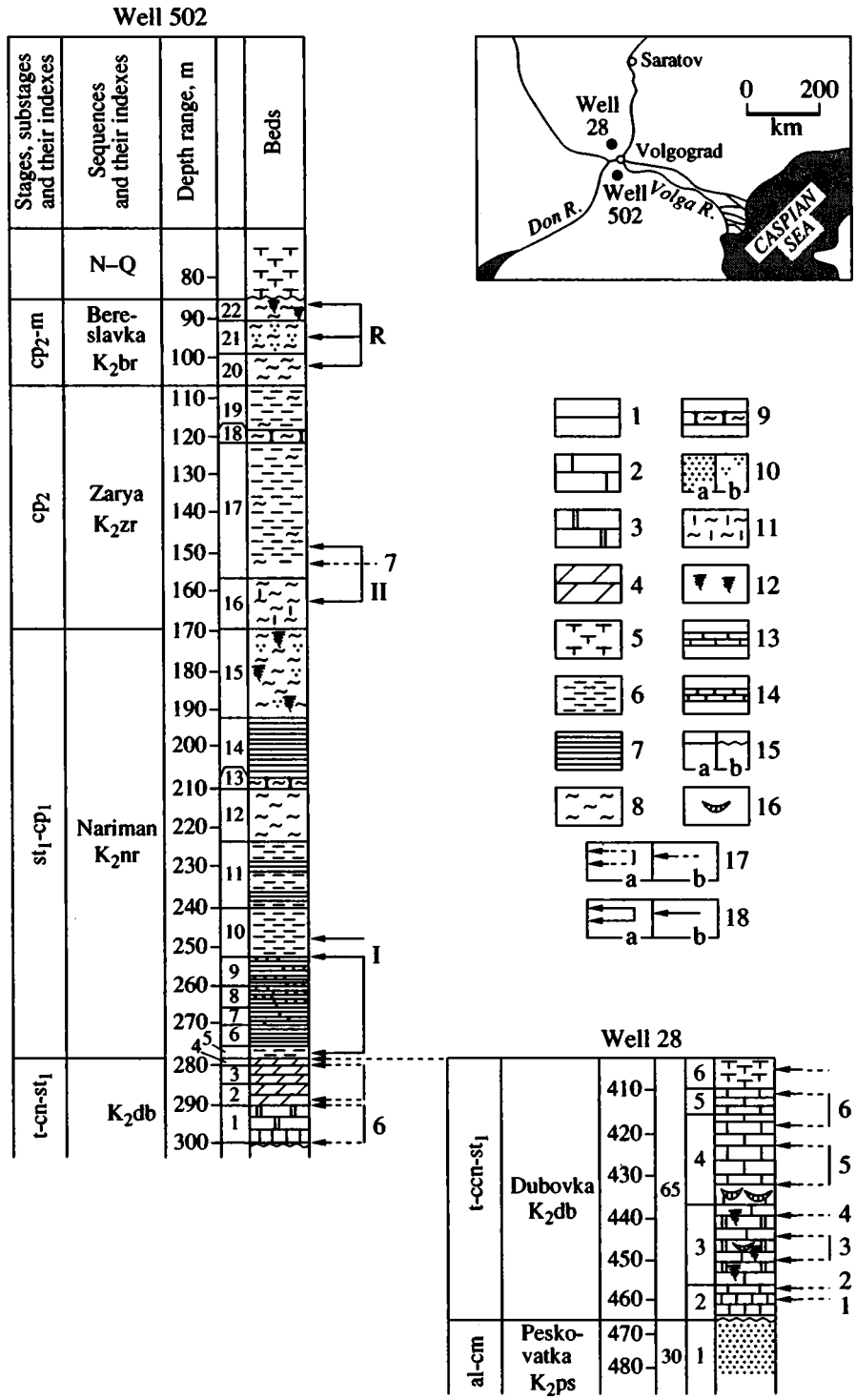

Sections of wells 502 and 28 with their localities indicated in the inset map: (1) chalklike limestone; (2) limestone; (3) calcareous chalk; (4) siliceous marl; (5) carbonate clay; (6) silty clay; (7) argillite; (8) clayey silt; (9) glauconitic siltstone; (10) sand (a) and glauconitic sand (b); (11) calcareous silt; (12) bioturbation; (13) slightly calcareous argillite; (14) silty argillite; (15) conformable (a) and unconformable (b) boundaries; (16) inoceram fragments; (17) foraminifer findings (a) and beds (b); (18) radiolarian findings (a) and beds (b).

(Reuss), *A. orbignyi* (Reuss), and *Gavelinella moniliformis* (Reuss), which make it possible to correlate the host sediments with the *Gavelinella moniliformis* Zone. The thickness is 8 m.

Bed 3 (depth range from 457 to 435 m): light-gray chalklike limestones displaying strong bioturbation and bearing inoceram fragments and crinoid columals. In the interval from 450 to 445 m, sediments contain the foraminifer assemblage of the *Ataxophragmium nautiloides* Zone with characteristic species *Marssonella* sp., *M. oxycona* (Reuss), *M. araksensis* Azizbekova, *Ataxophragmium nautiloides* Vassilenko, and *Gavelinella kelleri* (Mjatliuk). The first occurrence of *Gavelinella praeinfrasantonica* (Mjatliuk) was recorded at a depth of 440 m. The thickness is 22 m.

Bed 4 (depth range from 435 to 412 m): light-gray to greenish limestones, dense, massive, with thin (0.4–0.1 m) interlayers of clayey darker limestones. The strongly bioturbated and inoceram fragment-crammed limestone layer occurs at a depth of 433.5 m. At the depth of 433 and 424 m, the foraminifer assemblage of the *Stensioeina granulata granulata* Zone is found. It includes the following species: *Ataxophragmium compactum* Brotzen, *Stensioeina granulata granulata* (Olbertz), *Gyroidina turgida* (Hagenow), *Osangularia whitei* (Brotzen), and *Gavelinella infrasantonica* (Balakhmatova).

At a depth of 418 m, there are detected foraminifer species not encountered below: *Arenobulimina senonica* (Voloshina), *Orbignyna variabilis* (d'Orbigny), *Globorotalites michelinianus* (d'Orbigny), and *Stensioeina exsculpta exsculpta* (Reuss). The latter is the index species of the corresponding foraminifer zone, to which we attribute this assemblage. The thickness is 21 m.

Bed 5 (depth range from 412 to 407 m): light greenish gray clayey limestones, displaying bioturbation, hard, with dense interlayers. The very impoverished foraminifer assemblage of the *Stensioeina exsculpta exsculpta* Zone was found at a depth of 411 m. The thickness is 5 m.

Bed 6 (depth range from 407 to 400 m): gray carbonate clay grading upward into dark-gray carbonate-free clay; the transition to the overlying noncarbonate sediments of the Nariman sequence is gradual. Scarce foraminifers of the *Stensioeina exsculpta exsculpta* Zone occur at a depth of 405 m. The thickness is 7 m.

Data on Well 502 elucidate the lithology of younger deposits. The following units are recognized here from the base upward (figure).

The Dubovka Sequence

Bed 1 (depth range from 300 to 290 m): white-gray chalklike limestones, hard, thick platy, intercalated with hard calcareous chalk; sediments contain the foraminifer assemblage of the *Stensioeina exsculpta exsculpta* Zone, including the index species, *Globorotalites michelinianus* (d'Orbigny), *Stensioeina granulata granulata* (Olbertz), *Gavelinella umbilicatula* (Mjatliuk), and *G. infrasantonica* (Balakhmatova). The thickness is 10 m.

Bed 2 (depth range from 290 to 285 m): light-gray marls, partly siliceous, dense and platy; *Ataxophragmium nautiloides* Vassilenko and *Stensioeina granulata perfecta* Koch show their first occurrence at the depth of 289 and 286 m, respectively. The thickness is 5 m.

Bed 3 (depth range from 285 to 280 m): light siliceous marls with interlayers of silica-free varieties; the transition to overlying deposits is gradual. The thickness is 5 m.

Bed 4 (depth range from 280 to 278 m): gray siliceous clayey marl; the foraminifer assemblage of the *Stensioeina exsculpta exsculpta* Zone with predominant *Stensioeina granulata granulata*, scarce *Eponides concinnus plana* Vassilenko, *Cibicidoides praeeriksdalensis* Vassilenko, and *Bolivinita eleyi* Cushman still occurs in the bed. The thickness is 2 m.

The Nariman Sequence

Bed 5 (depth range from 278 to 275 m): light-gray siliceous clay, slightly carbonate; at a depth of 277.5 m, the radiolarian assemblage of *Euchitonia santonica–Pseudoaulophacus floresensis* Zone was encountered. It includes *Acaeniotyle* aff. *diaphorogona* Foreman, *Archaeospongoprunum cortinaensis* Pessagno, *Cromyodruppa concentrica* Lipman, *Crucella cachensis* Pessagno, *Euchitonia santonica* Lipman, *Histiastrum aster* Lipman, *H. latum* Lipman, *Orbiculiforma vacaensis* Pessagno, *O. quadrata* Pessagno, *Patellula euessceei* Empson-Morin, *P. planoconvexa* (Pessagno), *Pentinastrum subbotinae* Lipman, *Praeconocaryomma californiaensis* Pessagno, *Pseudoaulophacus floresensis* Pessagno, *Pseudoaulophacus praefloresensis* Pessagno, *Rhopalastrum tumidum* Lipman, *Septinastrum dogeli* Gorbovetz, *Stylosphaera pusilla* Campbell et Clark, *Amphipyndax stocki* (Campbell et Clark), *Dictyomitra densicostata* Pessagno, *D. multicostata* Zittel, and *Xitus asymbatos* (Foreman). The thickness is 3 m.

Bed 6 (depth range from 275 to 270 m): dark-gray to black siliceous argillites with shelly jointing. The thickness is 5 m.

Bed 7 (depth range from 270 to 265 m): dark-gray to black argillites with brown spots, slightly calcareous. The thickness is 10 m.

Bed 8 (depth range from 265 to 260 m): dark-gray to black silty, carbonate argillites. The thickness is 5 m.

Bed 9 (depth range from 260 to 252 m): dark-gray and black argillites, somewhat silty, slightly micaceous, carbonate-free to slightly calcareous. The thickness is 8 m.

Bed 10 (depth range from 252 to 240 m): dark-gray and black somewhat silty clay, micaceous, with shelly jointing; at the depth of 248 m, the considerably impoverished radiolarian assemblage was found. It is represented by *Cromyodruppa concentrica* Lipman, *Histiastrum aster* Lipman, *H. latum* Lipman, *Rhopalastrum*

tumidum Lipman, and *Dictyomitra densicostata* Pessagno. The thickness is 8 m.

Bed 11 (depth range from 240 to 233 m): dark-gray to black, dense clay, partially argillite-like. The thickness is 3 m.

Bed 12 (depth range from 223 to 210 m): dark-gray to black clayey micaceous siltstone. The thickness is 13 m.

Bed 13 (depth range from 210 to 207 m): gray, strongly micaceous silt, glauconitic, clayey, displaying a week bioturbation; fragments of small pelecypods were found at the top of the bed. The thickness is 3 m.

Bed 14 (depth range from 207 to 192 m): black and dark-gray silty micaceous argillite. The thickness is 15 m.

Bed 15 (depth range from 192 to 169 m): dark-gray to greenish silts, showing strong bioturbation, micaceous, with brown spots and glauconite nests. The thickness is 23 m.

The Zarya Sequence

Bed 16 (depth range from 169 to 156 m): dark-gray and black silts, siliceous, partly calcareous; the *Patellula planoconvexa–Amphibrachium mucronatum–Amphipyndax tylotus* radiolarian assemblage was encountered at the depth of 163 m. It consits of the following species: *Amphibrachium mucronatum* Lipman, *A. sibiricum* Gorbovetz, *Cromyodruppa concentrica* Lipman, *Histiastrum aster* Lipman, *H. latum* Lipman, *Patellula euessceei* Empson-Morin, *Patellula planoconvexa* (Pessagno), *Pentinastrum subbotinae* Lipman, *Porodiscus* aff. *cretaceous* Campbell et Clark, *Septinastrum dogeli* Gorbovetz, *Spongodiscus volgensis* Lipman, *Spongoprunum crassum* Lipman, *Amphipyndax tylotus* Foreman, *Dictyiomitra densicostata* Pessagno, *D. multicostata* Zittel, *Archaeodictyomitra* ex gr. *squinaboli* Pessagno, *Stichomitra cechena* Foreman, and *S. campi* (Campbell et Clark). The thickness is 13 m.

Bed 17 (depth range from 156 to 120 m): dark-gray, black, and greenish brown clays, dense, micaceous, silty in places, carbonate-free, massive or platy; the following agglutinated foraminifers were found at the depth of 153.5 m: *Rhabdammina* sp., *Bathysiphon* sp., *Rhizammina* sp., *Saccammina* sp., *Haplophragmoides* sp., *Ammobaculites* sp., and *Spiroplectammina* sp. Calcareous foraminifers *Dentalina* sp., *Nodosaria* sp., *Stylostomella?* sp., and young specimens of *Brotzenella monterelensis* (Marie), *Cibicidoides aktulagayensis* Vassilenko, and *C. voltzianus* (d'Orbigny) were identified there as well. The *Patellula planoconvexa–Amphibrachium mucronatum–Amphipyndax tylotus* radiolarian assemblage occurs up to the depth of 148 m. The thickness is 36 m.

Bed 18 (depth range from 120 to 118 m): gray and dark-gray to black siltstones, clayey (strongly clayey at the base), micaceous, carbonate-free, bearing dispersed coalified detritus. The thickness is 2 m.

Bed 19 (depth range from 118 to 106 m): dark-gray to greenish brown clay, micaceous, somewhat silty, carbonate-free. The thickness is 12 m.

The Bereslavka Sequence

Bed 20 (depth range from 106 to 99 m): dark-gray to black siltstone, with greenish brown spots, slightly micaceous, carbonate-free, clayey in places and displaying a week bioturbation. The thickness is 5 m.

Bed 21 (depth range from 99 to 90 m): dark-gray to black, slightly brownish silt, sandy, locally showing admixture of fine-grained quartz-glauconite sand; a layer with nests of glauconitic sand occurs at the base of the bed. The thickness is 9 m.

Bed 22 (depth range from 90 to 85 m): dark-gray, strongly micaceous silt, with local signs of bioturbation; the rock is carbonate-free. The thickness is 5 m.

The beds 20–22 (depth interval 104–85 m) yield an impoverished, poorly preserved radiolarian assemblage. It includes representatives of *Amphibrachium, Pentinastrum,* and *Septinastrum* genera associated with scarce nassellarians *Stichomitra campi* (Campbell et Clark) and *Theocampe animula* Gorbovetz.

The discussed sediments are overlaid by the 85-m-thick sequence of Neogene-Quaternary deposits.

BIOSTRATIGRAPHY

Foraminifers

Foraminifers are abundant in the sediments of the Dubovka sequence and occur in deposits of the Zarya sequence as well. The following assemblages were distinguished in the section from the base upward.

(1) The *Hedbergella holzli* assemblage (Dubovka sequence, Well 28, Bed 2, depth of 461 m) is characterized by predominance of planktonic *Hedbergella* forms, including *H. holzli* (Hagn et Zeil), *H. bornholmensis* Douglas, and *H. paradubia* Sigal, which associate with *Rugoglobigerina ordinaria* Subbotina. The assemblage is referred to the Early Turonian *Hedbergella holzli* Zone (Naidin *et al.*, 1984a, 1984b). Large accumulations of planktonic *Hedbergella* shells were recorded at the Cenomanian-Turonian boundary in the sections of Western Europe, Mediterranean, and Atlantic Ocean (Robaszynski, 1984; Robaszynski *et al.*, 1982).

(2) The *Gavelinella moniliformis* assemblage (Dubovka sequence, Well 28, Bed 2, depth of 458 m) was distinguished because of presence of the index species and *Arenobulimina presli* (Reuss) and *A. orbignyi* Brotzen characteristic of the Upper Turonian. A similar assemblage is characteristic of the *Gavelinella moniliformis* Zone of the lower upper Turonian in the Mangyshlak and Caspian region (Naidin *et al.*, 1984a, 1984b), whereas in the western Russian platform, this zone corresponds to the uppermost Turonian (Akimets *et al.*, 1991).

(3) The *Ataxophragmium nautiloides* assemblage (Dubovka sequence, Well 28, Bed 3, depth of 450–445 m) was distinguished because of presence of the index species and other forms typical of the *Ataxophragmium nautiloides* Zone. Its characteristic species are *Arenobulimina presli* (Reuss), *Marssonella* sp., *M. oxycona* (Reuss), *M. araksensis* Azizbekova, *Gyroidina nitida* (Reuss), *Eponides karsteni–concinna* Brotzen, and *Gavelinella kelleri* (Mjatliuk). In the eastern part of the European paleobiogeographical area (EPA), this zone corresponds to the Upper Turonian (Naidin *et al.*, 1984a, 1984b).

(4) The *Gavelinella praeinfrasantonica* assemblage (Dubovka sequence, Well 28, Bed 3, depth of 440 m) is recognized because of appearance of the index species, although forms of the previous assemblage still occur in sediments. The deposits of the zone are attributed to the early Coniacian in the east of the EPA (Naidin *et al.*, 1984a, 1984b).

(5) The *Stensioeina granulata granulata* assemblage (Dubovka sequence, Well 28, Bed 4, depths of 433 and 424 m) is characterized by the first occurrence of a series of forms, namely of the index species, *Ataxophragmium compactum* Brotzen, *Gyroidina turgida* (Hagenow), *Globorotaloides michelinianus* (Orbigny), *Osangularia whitei* (Brotzen), and *Gavelinella infrasantonica* (Balakhmatova). Moreover, *Gavelinella moniliformis* (Reuss), *Gyroidina nitida* (Reuss), and *Marssonella* representatives have their last occurrence at this level. The assemblage is referred to the synonymous zone, which is distinguished in the lower upper Coniacian of the Mangyshlak and eastern Caspian region (Naidin *et al.*, 1984a, 1984b). In Western Germany, the zone ranges throughout the Lower Coniacian (Koch, 1977). The first occurrence level of *Stensioeina granulata granulata* (Olbertz) and *Osangularia whitei* (Brotzen) is recorded in the mid-Coniacian deposits of the eastern EPA (Mangyshlak, Caspian and Volga regions, and Belarus), Western Germany, and France (Koch, 1977; Robaszynski and Amedro, 1980).

(6) The *Stensioeina exsculpta exsculpta–Stensioeina granulata perfecta* assemblage (Dubovka sequence, Well 28, Bed 4, depth of 418 m; Bed 5, depth of 411 m; Dubovka sequence, Well 502, Bed 1, depths of 300–290 m) is recognized as being the first occurrence of its index species. Its eponymous zone is recorded in the upper Coniacian and lower Santonian of western Kazakhstan and Western Germany (Naidin *et al.*, 1984a, 1984b; Koch, 1977). In the Dnieper–Donets depression and Belarus, the *Stensioeina exsculpta exsculpta* Zone corresponds to the lower part of the *Gavelinella infrasantonica* Zone and to the top of the *Gavelinella costulata* Zone, which range throughout the uppermost Coniacian and lowermost Santonian deposits (Grigelis *et al.*, 1980; Akimets *et al.*, 1991).

(7) The *Haplophragmoides–Spiroplectammina* beds (Zarya sequence, Well 502, Bed 17, depth of 153.5 m) were distinguished in the lower part of the Zarya sequence. They are characterized by a peculiar assemblage composed of agglutinated forms and scarce calcareous nodosariids and anomalinids, including *Brotzenella monterelensis* (Marie) and *Cibicidoides votzianus* (d'Orbigny), which are important in stratigraphic aspect and mark the lower part of the upper Campanian within the whole EPA (Naidin *et al.*, 1984b).

Radiolarians

Three radiolarian assemblages are distinguished.

(1) The *Euchitonia santonica–Pseudoaulophacus floresensis* assemblage (Nariman sequence, Well 502, Beds 5–9, depths of 277.5–250 m) is represented by *Acaeniotyle* aff. *diaphorogona* Foreman, *Archaeospongoprunum cortinaensis* Pessagno, *Cromyodruppa concentrica* Lipman, *Crucella cachensis* Pessagno, *Euchitonia santonica* Lipman, *Histiastrum aster* Lipman, *H. latum* Lipman, *Orbiculiforma vacaensis* Pessagno, *O. quadrata* Pessagno, *Patellula euessceei* Empson-Morin, *P. planoconvexa* (Pessagno), *Pentinastrum subbotinae* Lipman, *Praeconocaryomma californiaensis* Pessagno, *Pseudoaulophacus floresensis* Pessagno, *P. praefloresensis* Pessagno, *Rhopalastrum tumidum* Lipman, *Septinastrum dogeli* Gorbovetz, *Stylosphaera pusilla* Campbell et Clark, *Amphipyndax stocki* (Campbell et Clark), *Dictyomitra densicostata* Pessagno, *D. multicostata* Zittel, and *Xitus asymbatos* (Foreman) (Plate I–II).

Since sediments 12.5 m downward in the Dubovka section (Bed 1) contain the foraminifer assemblage of the *Stensioeina exsculpta exsculpta* Zone (the uppermost Coniacian–lowermost Santonian), the overlying *Euchitonia santonica–Pseudoaulophacus floresensis* radiolarian assemblage cannot be older than this level.

According to listed species, the assemblage under discussion is rather diverse and dominated by discoidal morphotypes. For instance, the representatives of *Histiastrum, Rhopalastrum*, and *Orbiculiforma* genera are most abundant. The assemblage includes species of a wide geographic ranges, such as, *Amphipyndax stocki, Dictyomitra densicostata, D. multicostata*, and *Xitus asymbatos*, which associate with forms that appeared in the Coniacian like *Orbiculiforma vacaensis*. However, some species cited by Lipman (1952) as characteristic of the Santonian in the Russian plate (*Euchitonia santonica, Histiastrum aster*, and *H. latum*), dominate in the assemblage. It is also notable that the assemblage in question has only one third of its species common with the Santonian radiolarians of the Ul'yanovsk Volga region (Bragina, 1987); these are *Histiastrum aster, Rhopalastrum tumidum, Septinastrum dogeli*, and *Dictyomitra densicostata*. The similarity is considerably higher at the generic level because both assemblages are characterized by different species of the same genera. It is of particular interest that *Spongoprunum articulatum*, characteristic and predominant in both Santonian

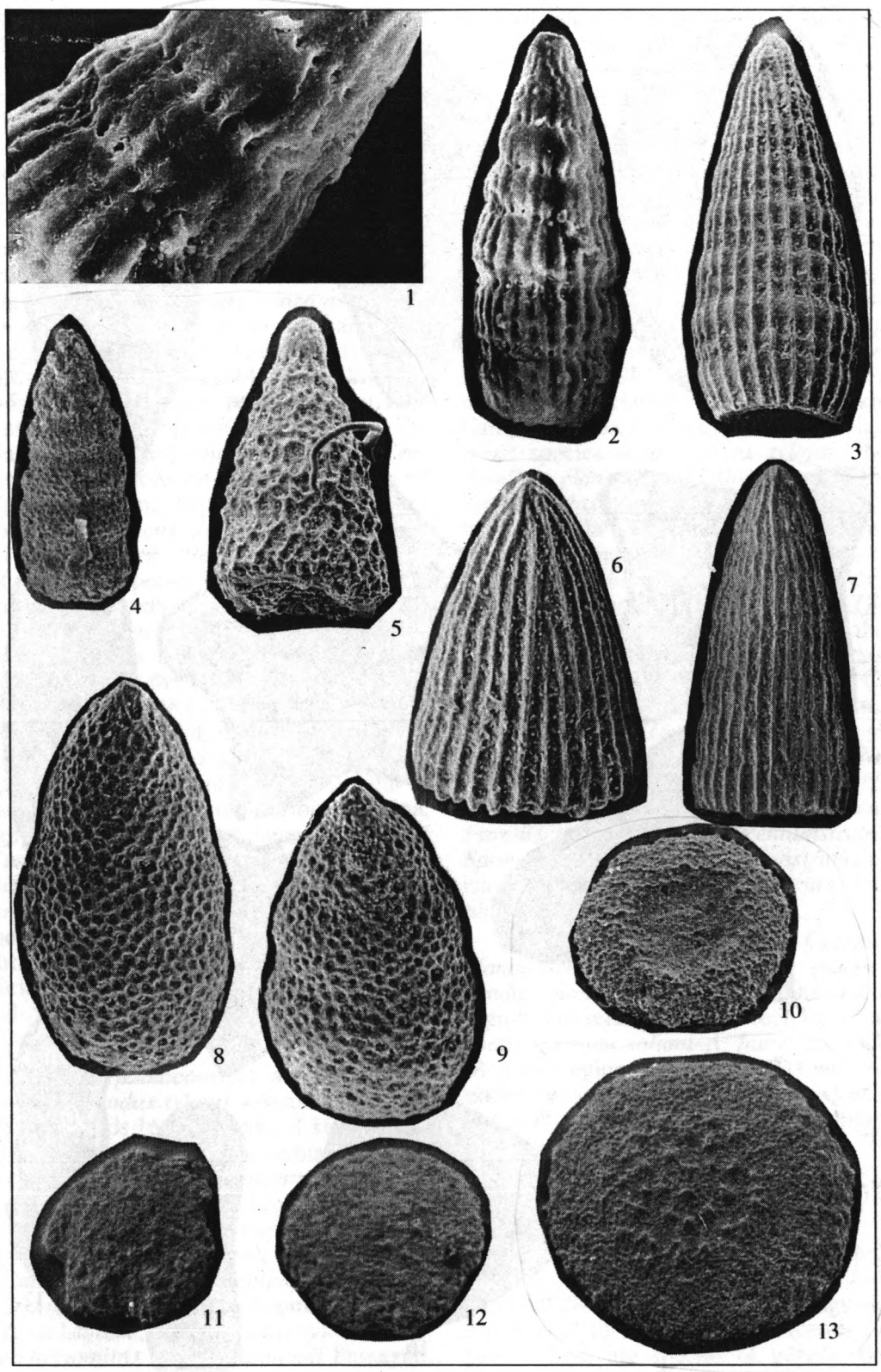

Plates I, II. Late Cretaceous radiolarians from the Volgograd Volga region.

Plate I. (1) *Dictyomitra densicostata* Pessagno, shell fragment, ×400; (2) *D. densicostata* Pessagno, ×200; (3) *D. multicostata* Zittel, ×200; (4) *Stichomitra cechena* Foreman, ×100; (5) *Amphipyndax tylotus* Foreman, ×200; (6, 7) *Dictyomitra* ex gr. *squinaboli* Pessagno: (6) ×300, (7) ×200; (8, 9) *Stichomitra campi* (Campbell et Clark), ×300; (10) *Orbiculiforma vacaensis* Pessagno, ×100; (11) *Patellula verteroensis* (Pessagno), ×100; (12, 13) *P. euessceei* Empson-Morin: (12) ×100, (13) ×200.

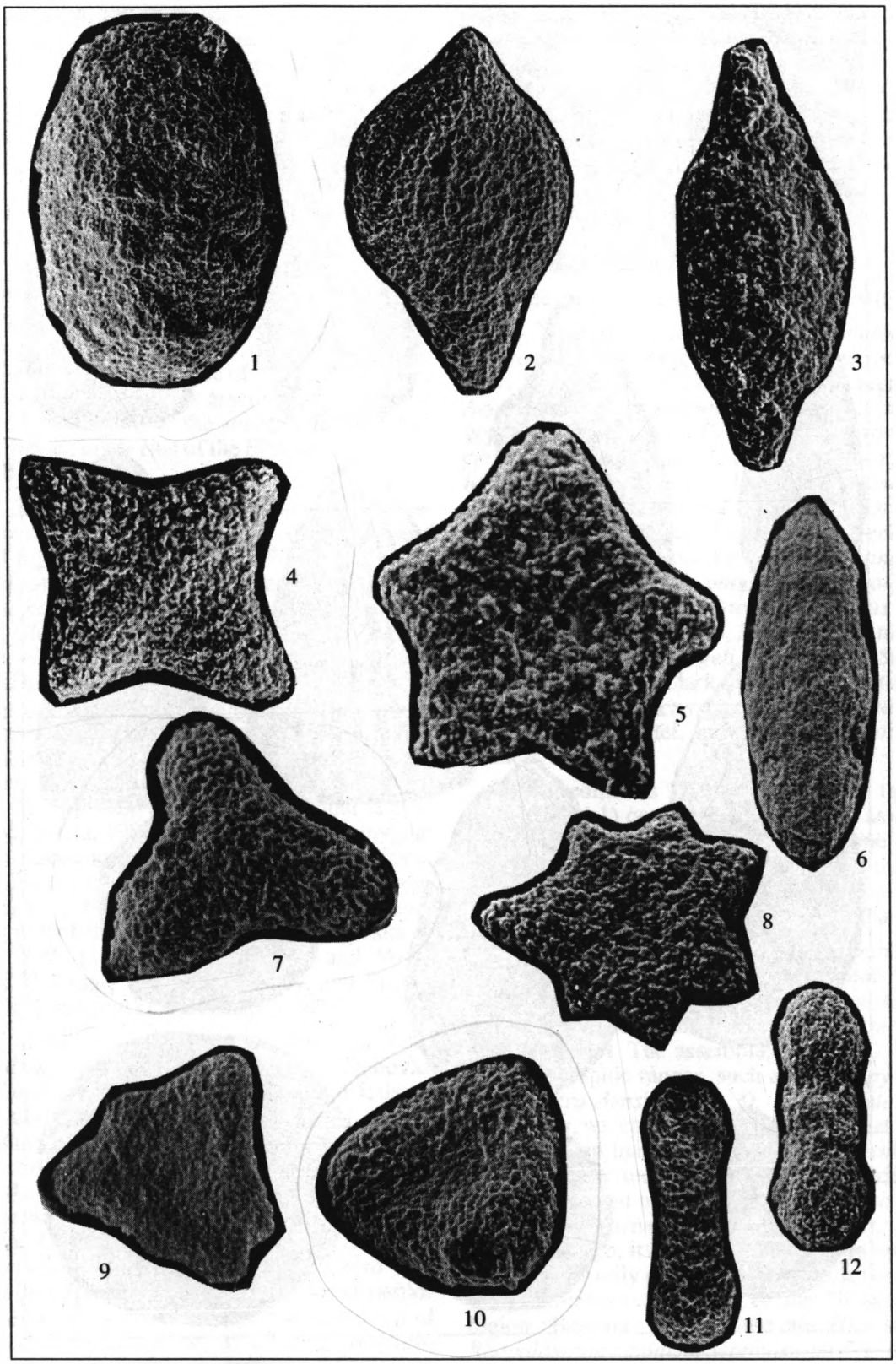

Plate II. (1) *Cromyodruppa concentrica* Lipman, ×200; (2) *Spongodiscus* sp., ×200; (3) *Spongoprunum crasum* Lipman, ×200; (4) *Histiastrum aster* Lipman, ×200; (5, 9) *Pentinastrum subbotinae* Lipman, ×200; (6) *Amphibrachium sibiricum* Gorbovetz, ×100; (7) *Rhopalastrum tumidum* Lipman, ×200; (8) *Septinastrum dogeli* Gorbovetz, ×100; (10) *Euchitonia santonica* Lipman, ×200; (11, 12) *Amphibrachium mucronatum* Lipman, ×100.

and Campanian deposits of the Ul'yanovsk region (Bragina, 1987), was not found in the studied assemblage. The difference may be a result of the lower stratigraphic position of the studied assemblage. Many its species (nearly a half) are also typical of the Santonian assemblage of the Penza region (Lipman, 1952). However, the Coniacian–Santonian assemblages from the Usa River region of the northern Russian plate (Amon, 1994), have only three species in common with the discussed assemblage, namely, *Cromyodruppa concentrica, Orbiculiforma quadrata*, and *O. vacaensis*. Amon distinguished the *Dictyomitra triara aspinosa–Pseudoaulophacus* sp. assemblage in the Santonian of the Volga region (Amon and De Wever, 1994). As he did not list all species of the assemblage, any comparison is impossible in this case. It is also relatively difficult to establish the relationships between the Coniacian–Santonian *Orbiculiforma quadrata–Crucella irwini* assemblage from the Khot'kovo Group of the Moscow region (Bragina, 1994) and the *Euchitonia santonica–Pseudoaulophacus floresensis* assemblage distinguished in this work. We can only state that almost all of the latter species occur in the Moscow region, however, the studied assemblage (Bragina, 1994) is much more impoverished. Moreover, the Moscow regional assemblages lack the dominant species unlike the discussed one. In the Moscow syneclise, Vishnevskaya and Kazintsova (1990) distinguished the Coniacian *Archaeospongoprunum bipartitum–A. triplum* and Santonian *Euchitonia santonica* assemblages. Eighty percent of species in these assemblages are present in all assemblages from the Moscow region (Bragina, 1994), and approximately a half of them is typical of the studied assemblages from the Volgograd region. It is interesting that a half of the *Euchitonia santonica–Pseudoaulophacus floresensis* assemblage is represented by species known and described from the Californian subtropical province (Foreman, 1968; Campbell and Clark, 1944; Pessagno, 1976). The studied assemblage also includes several unknown species that require the further description.

(2) The *Patellula planoconvexa–Amphibrachium mucronatum–Amphipyndax tylotus* assemblage (Zarya sequence, Well 502, beds 16–17, depths of 163–148 m) contains *Amphibrachium mucronatum* Lipman, *A. sibiricum* Gorbovetz, *Cromyodruppa concentrica* Lipman, *Histiastrum aster* Lipman, *H. latum* Lipman, *Patellula euessceei* Empson-Morin, *Pentinastrum subbotinae* Lipman, *P. planoconvexa* (Pessagno), *Porodiscus* aff. *cretaceous* Campbell et Clark, *Septinastrum dogeli* Gorbovetz, *Spongodiscus volgensis* Lipman, *Spongoprunum crassum* Lipman, *Amphipyndax tylotus* Foreman, *Archaeodictyomitra* ex gr. *squinaboli* Pessagno, *Dictyomitra densicostata* Pessagno, *D. multicostata* Zittel, *Stichomitra campi* (Campbell et Clark), *S. cechena* Foreman, *Theocampe animula* Gorbovetz, and includes almost all the species of the underlying *Euchitonia santonica–Pseudoaulophacus floresensis* assemblage. The assemblage is also distinct because of a high predominance of spongy forms. However, other species, namely the numerous representatives of *Amphibrachium* and *Spongoprunum* genera are abundant here. Another peculiarity of the assemblage is that some nassellarians, like *Stichomitra campi* and *Theocampe animula* described from the Campanian of West Siberia (Kozlova and Gorbovetz, 1966), are almost as abundant as the spongy forms. We should note in addition the presence of *Amphipyndax tylotus* unknown previously in the Russian plate. Its first finding is extremely important, as it is the zonal species in the late Campanian-Maastrichtian tropical assemblages (Sanfilippo and Riedel, 1985). The occurrence of *Amphibrachium* and *Spongoprunum* forms also indicates the Campanian age (Lipman, 1952) of the assemblage. Therefore, the majority of species of the assemblage is known from the Campanian. According to the stratigraphic range of the zonal species *Amphipyndax tylotus*, the age of the *Patellula planoconvexa–Amphibrachium mucronatum–Amphipyndax tylotus* assemblage should correspond the late Campanian. This conclusion is confirmed by the distribution of foraminifers of the *Brotzenella monterelensis* (Marie)–*Cibicidoides votzianus* (d'Orbigny) assemblage encountered at the same level. The comparison with the Campanian assemblage of the Ul'yanovsk region revealed only one third of species in common; these are *Amphibrachium mucronatum, Cromyodruppa concentrica, Histiastrum aster, H. latum, Dictyomitra densicostata*, and *D. multicostata*. The similarity with assemblages of the same age from West Siberia is higher. In this case, species in common (two thirds) are *Cromyodruppa concentrica, Histiastrum aster, H. latum, Porodiscus cretaceous, Pentinastrum subbotinae, Spongodiscus volgensis, Septinastrum dogeli, Amphibrachium mucronatum, A. sibiricum*, and *Theocampe animula*.

The analogues of the upper Campanian *Patellula planoconvexa–Amphibrachium mucronatum–Amphipyndax tylotus* assemblage are unknown in the Moscow region. The relationship between the younger *Archaeospongoprunum salumi–A. hueyi* assemblage from the Moscow region (Bragina, 1994) and the assemblage under consideration is relatively clear. The latter is obviously younger, as it contains *Amphipyndax tylotus* and coexisting numerous prunoids. Therefore, the *Archaeospongoprunum salumi–A. hueyi* assemblage from the Moscow region is not younger than the middle Campanian.

(3) The third assemblage is recorded in the depth interval of 104–85 m. It is characterized by predominance of discoid forms with a spongy skeleton, which are typical to the Upper Cretaceous in the Russian plate. These are species of genera *Amphibrachium, Pentinastrum*, and *Septinastrum*. Among nassellarians, only scarce *Stichomitra* and *Theocampe* forms were encountered (Plates I, II). Unfortunately, the poor preservation of microfossils and low taxonomic diversity suggest only rather wide Campanian–Maastrichtian range of the assemblage.

CONCLUSION

Main conclusions of this study are as follows.

(1) The radiolarian *Euchitonia santonica–Pseudoaulophacus floresensis* assemblage occurs in the Nariman sequence above the foraminiferal assemblage of the *Stensioeina exsculpta exsculpta* Zone. Thus, the radiolarian assemblage is of the late Coniacian–Santonian age.

(2) The radiolarian *Patellula planoconvexa–Amphibrachium mucronatum–Amphipyndax tylotus* assemblage found in the Zarya sequence at the occurrence level of foraminifers *Brotzenella monterelensis* and *Cibicidoides votzianus*, which are characteristic of the lower upper Campanian within the whole European paleobiogeographical area.

(3) In composition, the studied radiolarian and foraminiferal assemblages are similar to the Boreal (West Siberian) microfossil faunas. This suggests a past connection between the West Siberian and East European basins.

Reviewers I.A. Basov and V.S. Vishnevskaya

REFERENCES

Akimets, V.S., Ben'yamovskii, V.N., and Kopaevich, L.F., The Western Part of the European USSR and Western Kazakhstan, Upper Series, in *Prakticheskoe rukovodstvo po mikrofaune SSSR. Foraminifery mezozoya* (Guide to the USSR Microfauna: Mesozoic Foraminifers), Leningrad: Nedra, 1991, vol. 5, pp. 192–210.

Amon, E.O., A Review of Upper Cretaceous Biostratigraphy of the Polar Urals, in *Novye dannye po stratigrafii verkhnego paleozoya–nizhnego kainozoya Urala* (New Data on the Upper Paleozoic–Lower Cenozoic Stratigraphy of the Urals), Yekaterinburg: Ural. Otd. Ross. Akad. Nauk, 1994, pp. 109–138.

Amon, E.O. and De Wever, P., Upper Cretaceous Biostratigraphy of the Borders of the Ural Belt: Western Siberian and Eastern Volga–Ural Basins, in *Peri-Tethyan Platforms*, Paris, 1994, pp. 229–262.

Ben'yamovskii, V.N., Kopaevich, L.F., Akimets, V.S., *et al.*, Upper Cretaceous Foraminifer Stratigraphy of the Volga Region near Ul'yanovsk, *Izv. Akad. Nauk SSSR, Ser. Geol.*, 1988, no. 5, pp. 65–74.

Bragina, L.G., Abstracts of Papers, *VI konferentsiya molodykh uchenykh GIN AN SSSR* (VI Conf., Young Scientists of Geol. Inst. Akad. Nauk SSSR), Moscow: Nauka, 1987, pp. 1–7.

Bragina, L.G., Upper Cretaceous Radiolarians and Stratigraphy of the Khot'kovo Group of the Moscow Region, *Byull. Mosk. O-va. Ispyt. Prir., Otd. Geol.*, 1994, vol. 69, no. 2, pp. 91–100.

Campbell, A.S. and Clark, B.L., Radiolaria from Upper Cretaceous of Middle California, *Spec. Pap. Geol. Soc. Am.*, 1944, vol. 57, pp. 1–61.

Foreman, H., Upper Maastrichtian Radiolaria of California, *Paleontol. Spec. Pap.*, 1968, no. 3, pp. 1–82.

Grigelis, A.A., Akimets, V.S., and Lipnik, E.S., Phylogeneses of Benthic Foraminifers as a Basis of of the Upper Cretaceous Zonation (The East European Platform as an Example), *Vopr. Mikropaleontol.*, 1980, no. 23, pp. 145–159.

Koch, W., Stratigraphie der Oberkreide in Nordwestdeutschland (Pompeckjeche Scholle), part 2: Biostratigraphie der Oberkreide und Taxonomie von Foraminiferen, *Geol. Jahrb.*, 1977, no. 38, pp. 11–123.

Kozlova, G.E. and Gorbovets, A.N., Radiolarians from the Upper Cretaceous–Upper Eocene of the West Siberian Lowland, *Tr. Vses. Nauch.-Issled. Geol.-Razved. Inst.*, 1966, no. 248, pp. 1–158.

Lipman, R.Kh., Materials for Comprehensive Study of Late Cretaceous Radiolarians from the Russian Platform, in *Paleontologiya i stratigrafiya* (Paleontology and Stratigraphy), Moscow: Gos. Izd. Geol. Lit., 1952, pp. 24–45.

Naidin, D.P., Ben'yamovskii, V.N., and Kopaevich, L.F., *Metody izucheniya transgressii i regressii (na primere pozdnemelovykh basseinov Zapadnogo Kazakhstana)* (Investigation Methods of Trangressions and Regressions the Upper Cretaceous Basin of Western Kazakhstan as an Example), Moscow: Mosk. Univ., 1984a.

Naidin, D.P., Ben'yamovskii, V.N., and Kopaevich, L.F., The Upper Cretaceous Biostratigraphic Zonation of the European Paleobiogeographic Area, *Vestn. Mosk. Univ., Ser. 4, Geol.*, 1984b, no. 5, pp. 3–15.

Pessagno, E.A., Jr., Radiolarian Zonation and Stratigraphy of Upper Cretaceous Portion of the Great Valley Sequence, *Micropaleontol.*, 1976, no. 2, pp. 1–96.

Robaszynski, F., The Albian, Cenomanian and Turonian Stages in Their Type Regions, *Bull. Geol. Soc. Denmark*, 1984, vol. 33, pp. 191–198.

Robaszynski, F., Alcayde, G., Amedzo, F., *et al.*, Le Touronian de la Region-Type: Sinemurois et Touraine stratigraphie, biozonations, sedimentologie, *Bull. Centres Rech. Explor. Prod. EL-Aquitaine*, 1982, vol. 6, no. 1, pp. 119–225.

Robaszynski, F. and Amedro, F., Synthese biostratigraphique de L'Aptien au Santonien du Boulonnais a parties de sept groupes paleontologiques: foraminiferes, nannoplankton, dinoflagelless et macrofaunes, *Rev. Micropaleontol.*, 1980, vol. 22, no. 4, pp. 195–225.

Sanfilippo, A. and Riedel, W.R., Cretaceous Radiolaria, in *Plankton Stratigraphy*, Cambridge: Cambridge Univ., 1985, pp. 631–712.

Vishnevskaya, V.S. and Kazintsova, L.I., Cretaceous Radiolarians of the USSR, in *Radiolyarii v biostratigrafii* (Radiolarians in Biostratigraphy), Sverdlovsk: Ural. Otd. Akad. Nauk SSSR, 1990, pp. 44–58.

Stratigraphy and Geological Correlation, Vol. 7, No. 5, 1999, pp. 501–507. Translated from Stratigrafiya. Geologicheskaya Korrelyatsiya, Vol. 7, No. 5, 1999, pp. 93–99.
Original Russian Text Copyright © 1999 by Degtyarev, Dubinina, Orlova.
English Translation Copyright © 1999 by MAIK "Nauka/Interperiodica" (Russia).

Stratigraphy and Structural Peculiarities of the Lower Paleozoic Carbonate–Siliceous–Tuffaceous Complex of the Chingiz Range (Eastern Kazakhstan)

K. E. Degtyarev, S. V. Dubinina, and A. P. Orlova

Geological Institute, Russian Academy of Sciences, Pyzhevskii per. 7, Moscow, 109017 Russia

Received February 26, 1997; in final form, May 26, 1997

Abstract—Sections of the Middle Cambrian–Middle Ordovician carbonate–siliceous–tuffaceous complexes of eastern Kazakhstan, which are characterized by different groups of fossils (conodonts, graptolites, brachiopods, trilobites), are described for the first time. The heterofacies sections are subdivided into two types. They are first established to occupy an intermediate position in the structural–facies zonation of Chingiz Range, between volcanosedimentary and siliceous–basaltic sequences. It is inferred that the carbonate–siliceous–tuffaceous deposits presumably accumulated in a marginal part of a back-arc basin in the vicinity of a volcanic island arc.

Key words: *Middle, Upper Cambrian; Lower, Middle Ordovician; conodonts, graptolites, trilobites, brachiopods, carbonate–siliceous–tuffaceous complexes, island arc, back-arc basin*

It was established during past decades that the Lower Paleozoic complexes of eastern Kazakhstan are of the fold-and-nappe structure (*Tektonika Kazakhstana...*, 1982; Samygin, 1984, and others); therefore natural successions of several stratigraphic units are rarely retained in the modern structure. The uninterrupted sequences of carbonate, siliceous and terrigenous rocks comprising organic remains of different age are often interpreted to be blocks and erratic masses in olistostromes (Kopyatkevich, 1981; Samygin, 1981, 1990; Samygin and Kheraskova, 1994). Only detailed biostratigraphic studies and large-scale geological mapping of such sequences allow olistostromes to be discriminated from intensely dislocated, heterofacies and relatively continuous sections.

We conducted such studies in the central part of the Chingiz Range. Since the mid-1960s, the Mayan trilobites were found here on the right bank of Kol'denen River (Fig. 1) in limestones at the base of a thick carbonate–siliceous–tuffaceous section resting with an unconformity on older intermediate to basic volcanic rocks and granitoids (*Geologiya...*, 1962; *Geologiya SSSR*, 1972). The whole sequence was attributed on the basis of these findings to the Middle Cambrian. Trilobites of the Late Cambrian appearance and the Arenigian–Llanvirnian graptolites, which were found later in terrigenous rocks of the same section, made it possible to consider the Middle Cambrian limestones as blocks in the Arenigian–Llanvirnian olistostrome (Kopyatkevich, 1981). It was established later (Samygin, 1981) that the olistostrome is overridden by a major allochthonous complex composed of the Upper Cambrian–lower Llanvirnian volcanosedimentary sequences and encloses blocks of the Middle and Upper Cambrian limestones and of the Arenigian–Llanvirnian graptolitic shales. On the basis of these data, the olistostrome was dated back to the late Llanvirnian (Samygin, 1990; Samygin and Kheraskova, 1994).

In the Kol'denen River basin, we performed geological mapping and collected different groups of organic remains at several stratigraphic levels. This allowed us to establish that the olistostromal strata are lacking in the region, where the carbonate–siliceous–tuffaceous complex is of the Middle-Cambrian–Middle-Ordovician age. Sections of these heterofacies deposits can be divided into two types occupying the intermediate position in the structural–facies zoning of the Chingiz Range, namely between volcanosedimentary and siliceous–basaltic sequences.

Conodonts were identified by S.V. Dubinina, graptolites by A.P. Orlova, brachiopods by G.T. Ushatinskaya, trilobites by M.K. Apollonov.

DESCRIPTION OF THE CARBONATE–SILICEOUS–TUFFACEOUS COMPLEX

The Middle-Cambrian–Middle-Ordovician carbonate–siliceous–tuffaceous sequences are exposed on the right bank of Kol'denen River in the vicinity of Kopa Creek. The sequences overlie with an unconformity the Amga Formation of volcanic and granitoid rocks and underlie an allochthon of the complicated structure, which is composed of the Upper Cambrian–lower Arenigian differentiated volcanic series of the Tort-

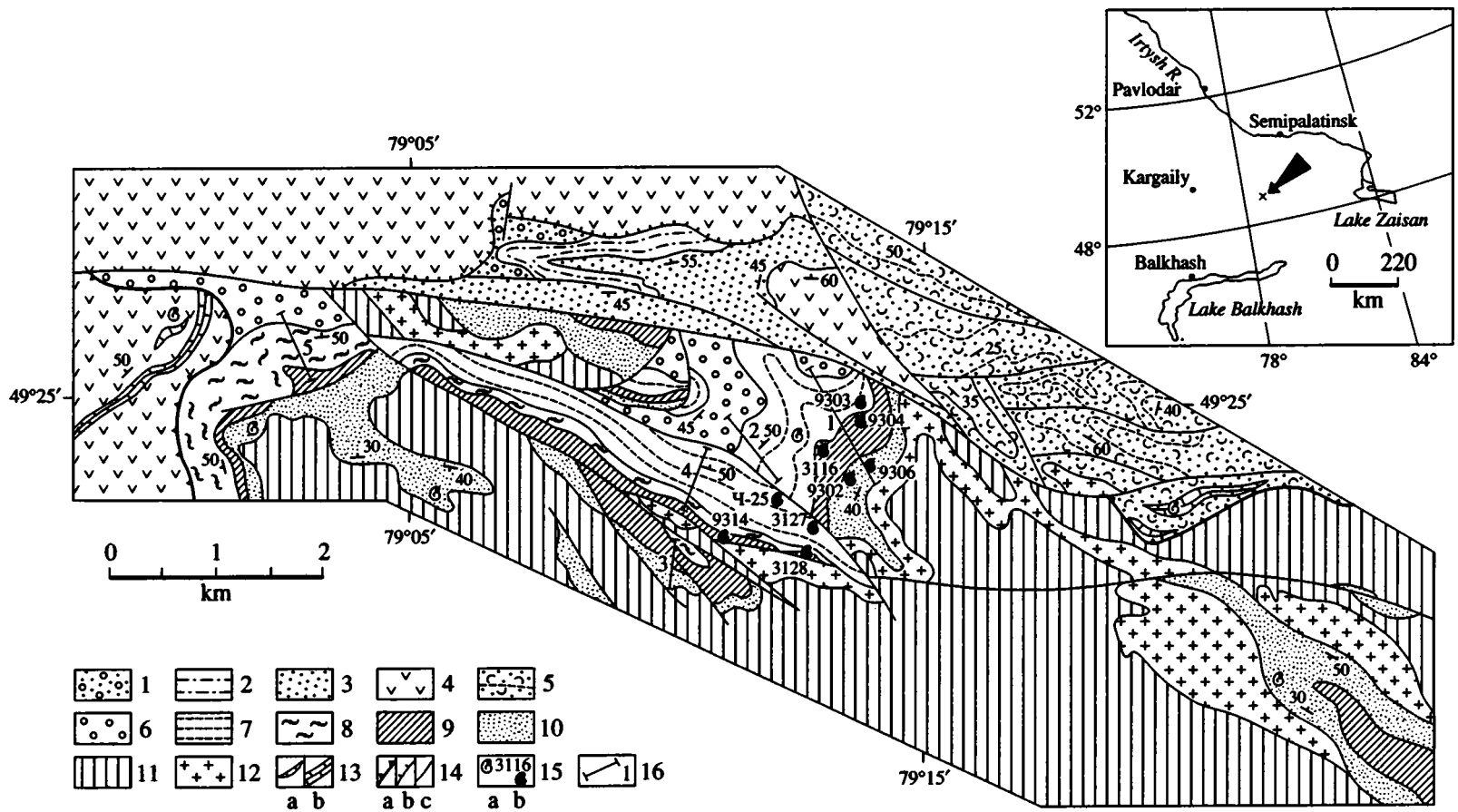

Fig. 1. Geological sketch map of middle courses of the Kol'denen River, central part of the Chingiz Range (modified after I.F. Nikitin, M.A. Orenburgskii, S.G. Samygin, and R.A. Kopyatkevich).

(1–5) Central Chingiz nappe: (1–3) Naiman Formation of cobble conglomerate (1), black siliceous siltstone (2), and of sandstone member and limestone horizons and lenses (3); (4) Saryshok Formation of andesites and basaltic andesites, intercalated with limestone lenses; (5) Upper Cambrian–Lower Ordovician volcanogenic–tuffaceous–terrigenous sequence; (6–10) carbonate–siliceous–tuffaceous complex divided into: (6) member of coarse-grained sandstones and conglomerates with limestone blocks, (7) member of siltstones, tuffites, and tephroites, (8) member of siliceous siltstones and clayey jaspers, (9) siliceous member, and (10) member of calcareous siltstones and sandstones with limestone lenses; (11) lowermost mid-Cambrian volcanogenic strata; (12) Middle Cambrian granitoids; (13) limestone lenses (a) and horizons (b); (14) tectonic boundaries of thrust nappes (a) and separate thrust slices (b), other faults (c); (15) sampling points for organic remains (SP) as reported by previous researchers (a) and studied in this work (b); (16) sections described in the text and their numbers.

kuduk Group (ϵ_3–O_{1tr}) and Saryshok Formation (O_{1ar}) (*Geologiya SSSR*, 1972; Nikitin, 1972) and of the upper Arenigian–lower Llanvirnian siliceous–terrigenous deposits of the Naiman Formation (O_{1ar3}–O_{1ln}) (Nikitin, 1972; Orlova, 1993) (Fig. 1). We have studied several carbonate–siliceous–tuffaceous sections spanning the interval from basal beds of the Mayan Stage of the Middle Cambrian to the uppermost Arenigian or probably the lowermost Llanvirnian included.

The first section is studied on the right bank of the Kopa Creek in the eastern part of the area (Fig. 1). Here, the carbonate–siliceous–tuffaceous deposits overlie with an unconformity the Amga granites (Fig. 2, Section 1). The section consists of the following units (from the base upward):

(1) Quartz–feldspathic sandstones and gravelstones overlain by green calcareous siltstones with thin lenses and horizons of gray limestones bearing poorly preserved trilobites (30 m thick).

(2) Calcareous, thin-layered, green, and violet siltstones with abundant carbonate–siliceous concretions of various size that yield undeterminable fragments of trilobites and articulate brachiopods (20 m thick).

(3) Gray to pink, layered, organogenic–detrital limestones with calcarenite horizons, the rocks enclose interlayers of carbonate breccia and bright green tuffosilicites. The Mayan (Middle Cambrian) brachiopods (SP 9306) *Stipnotreta inaequalis* Ushat., *Homotreta* cf. *captiosa* (Koneva), *Kotylotreta undata* Koneva, *Erbotreta* sp., *Acrothele* sp., *Oepikites* sp., and *Micromitra* sp. were macerated from limestones. From limestones of the unit, N.K. Ivshin identified earlier (*Geologiya SSSR*, 1972) the Mayan trilobites *Menevia venulosa* (Salt.), *Peronopsis fallax* Linnars., *Hypagnostus*

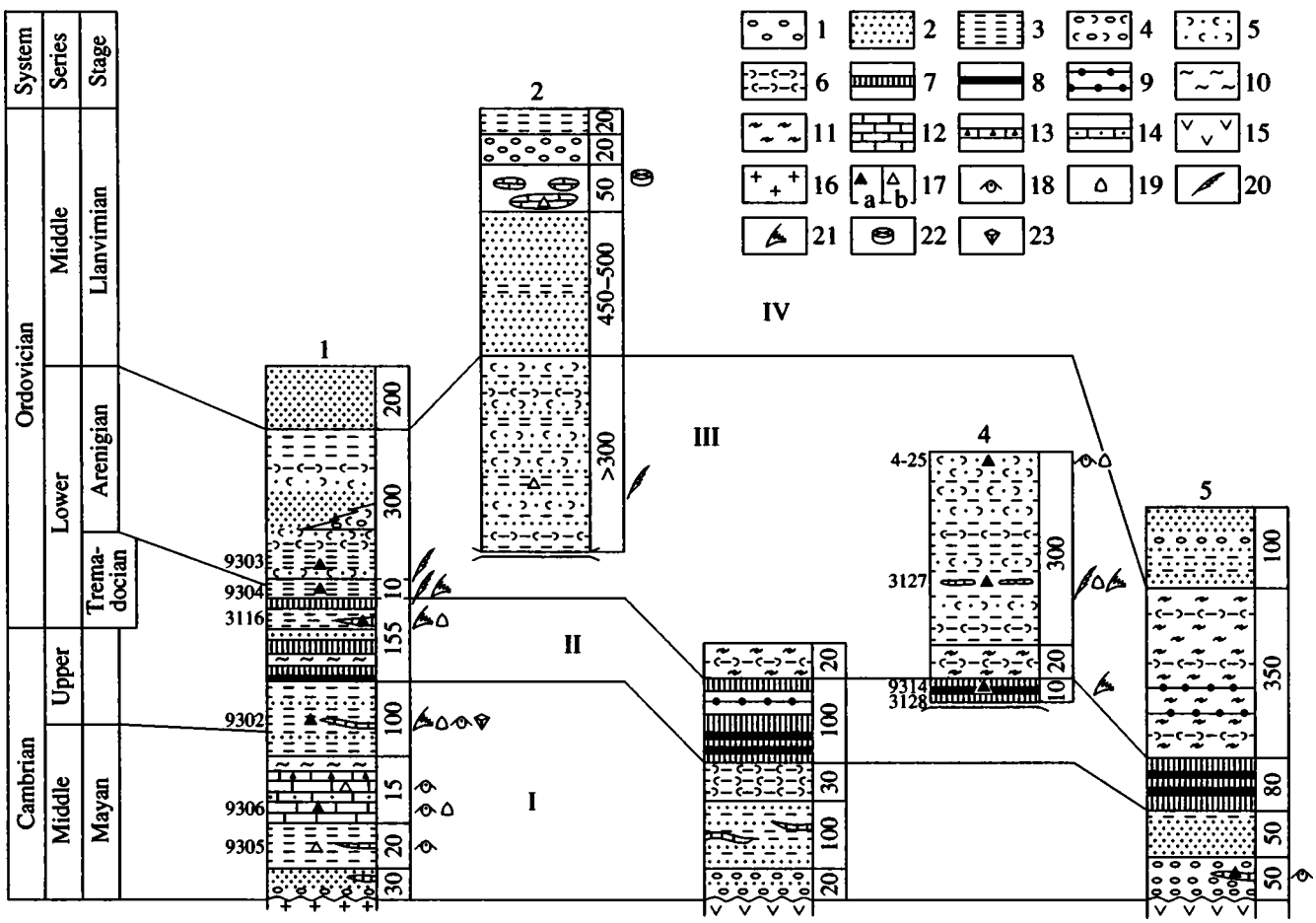

Fig. 2. Correlated sections of the carbonate–siliceous–tuffaceous complex:

(1) conglomerate; (2) sandstone; (3) siltstone; (4) tuffaceous conglomerate; (5) tuffstones and tephroids; (6) tuffaceous siltstone, (7) cherts; (8) phthanite; (9) red jasper; (10) siliceous siltstone; (11) cherry-red and green clayey jaspers; (12) limestone; (13) carbonate breccia; (14) calcarenite; (15) basaltic andesite; (16) granite; (17) sampling points for organic remains (SP) studied in this work (a) and reported by previous researchers (b); (18) trilobites, (19) brachiopods, (20) graptolites, (21) conodonts, (22) crinoids, (23) *Conularia*.

Sections: (I) terrigenous–carbonate member; (II) siliceous member; (III) tuffaceous-terrigenous member; (IV) terrigenous member.

Brogg., *Basocephalus* ex gr. *nominalis* Ivsh., *Olenoides* Meek, and *Kootenia* Walc. (15 m thick).

(4) Green and gray sandstones and siltstones with thin horizons and lenses of gray limestones and rare interlayers of coarse-grained calcareous sandstones; conodonts (SP 9302) macerated from the limestone interlayer in the upper part of the member are *Phakelodus tenius* (Muller), *"Phakelodus" cavatus* Dubinina, *"Barnesodus" planus* Dubinina, *Proconodontus magezhuangensis* An, and *Viirodus* sp. of the Late Cambrian *Proconodontus* Zone. Siltstones yielded undeterminable fragments of trilobites which, according to Apollonov's conclusion, are of the Cambrian appearance; the same rocks bear inarticulate brachiopods and gastropods and show impressions of poorly preserved *Conularia* (100 m thick).

(5) Siliceous siltstones and black to green-gray silty sandstones with numerous horizons of black banded phthanites and rare lenses of gray crystalline limestones. After dissolving, the limestones of the upper part of the member (SP 3116) yielded the Late Cambrian conodonts *Phakelodus tenius* (Miller), *"Proconodontus"* sp. and inarticulate brachiopods (155 m thick).

(6) Black foliated siltstones and fine-grained sandstones with abundant undeterminable fragments (SP 9304) of inarcticulate brachiopods, Arenigian graptolites *Tetragraptus* cf. *quadribrachiatus* (Hall), and conodonts *Acodus* sp. and *Scandodus* sp. of the late Tremadocian–early Arenigian appearance (10 m thick).

(7) Medium-grained tuffaceous siltstones and sandstones with frequent interlayers of green siliceous tuffites and tephroids; the rocks are intercalated with lenses of coarse volcaniclastic and tuffaceous conglomerates. Siltstones often enclose carbonate concretions. The Arenigian graptolites *Tetragraptus quadribrachiatus* (Hall), *Expansograptus* sp., and *Phyllograptus* sp. (SP 9303) are macerated together with conodonts of poor preservation from green siltstones 20 m above the member base (over 300 m thick).

(8) Coarse-grained, predominantly quartz sandstones with rare siltstone interlayers (more than 200 m thick).

The total thickness of the section described is 830 m.

The upper part of the section is exposed on the left bank of Kopa Creek, in the central part of the area (Fig. 2, Section 2). The following succession of units is distinguished there in the syncline limb (from the base upward).

(1) Alternating green siltstones and medium-grained tuffaceous sandstones with numerous horizons of siliceous tuffites and tephroids (an analogue of Unit 7 in the previous section); known from the unit (Kopyatkevich, 1981) are the Arenigian–Llanvirnian graptolites *Tetragraptus quadribrachiatus* (Hall) (300 m thick).

(2) Coarse-grained, quartzitic sandstones with interlayers of siltstones and aleurotuffites, the analogue of Unit 8 in the previous section (500 m thick).

(3) Sandstones, similar to those of Unit 2 with embedded, presumable slump bodies and smaller blocks of gray crystalline limestones, which yield rare fragments of undeterminable crinoids (50 m thick).

(4) Conglomerates with small- and medium-sized pebbles of limestones and black siliceous siltstones (20 m thick).

(5) Black siliceous siltstones (20 m thick).

The total thickness of the section is 840 m.

The second of the studied sections is located southwest of the previous one on the left bank of Kopa Creek, in the central part of the area (Fig. 2, Sections 3, 4). The carbonate–siliceous–tuffaceous rocks overlie here the Amgan volcanic rocks with unconformity. The rock sequence is of the imbricated structure; it was reconstructed on the basis of two separate intervals. The first one corresponds to the lower part of the section:

(1) Volcaniclastic medium-pebbled conglomerates with fragments of basic and intermediate volcanic rocks (20 m thick).

(2) Green to tobacco-colored polymictic calcareous sandstones with lens-like interlayers of bedded arenaceous limestones (100 m thick).

(3) Green to violet tuffites and silty tuffstones (30 m thick).

(4) Gray bedded cherts with numerous interlayers of black banded phthanites and horizons of red bedded jaspers (100 m thick).

(5) Thin-bedded cherry-red to green and gray tuffites and siltstones (20 m thick).

The section terminates in the core of the syncline; its total thickness is 170 m.

The second fragment of the section is exposed further north, being a partial continuation of the part described above (Fig. 2, Section 4). Exposed there north of the tectonic contact with the Amginian volcanic rocks are the following units (from the base upward):

(1) Gray bedded cherts with phthanite interlayers (an analogue of Bed 4 in the previous section), in which there were found conodonts (SPs 9314 and 3128) *Viirodus impressus* Dubinina, *Eoconodontus* (*E.*) cf. *alisonae* Landing, *Eoconodontus* (*E.*) *notchpeakensis* (Miller), *Phakelodus tenuis* (Muller), *Proaconodontus latus* (Van Wamel), *Proaconodontus latus entis* Dubinina, *Proaconodontus jilinensis* (Chen et Gong), *Proaconodontus sagittalis* Dubinina, *Prooneotodus rotundatus* (Druce et Jones), and *Prooneotodus gallatini* (Muller). These conodonts are characteristic of the uppermost Cambrian *alisonae* Zone (10 m thick).

(2) Cherry-red to green thin-bedded tuffites and siltstones (20 m thick).

(3) Siltstones, siliceous tuffites, tephroites, and tuffstones thin-bedded as a rule; carbonate concretions are often encountered in siltstones. Abundant inarticulate brachiopods are found throughout the whole interval. The late Arenigian graptolites *Loganograptus logani* (Hall), *Tetragraptus quadribrachiatus* (Hall), and *Expansograptus* cf. *extensus* (Hall) were collected from the middle part of the unit (SP 3127), and carbonate concretions at the same sampling point yielded the middle Arenigian conodonts *Prioniodus* (*P.*) *deltatus longibasis* McTavish, prioniodiform el. *Prioniodus* (*P.*) *deltatus* (Lindstr.), prioniodiform el. et prioniodinaform el. *Paroistodus paralellus* (Pander), and drepanodiform el. et oistodiform el., *Tropodus sweeti* (Serpagli). The upper part of the bed (SP Ch-25) yielded the Arenigian–Llanvirnian trilobites *Niobides* (?) sp., *Cybelurus* sp. (over 300 m thick).

The total thickness of the section is more than 330 m.

Uppermost rocks of the section are missing from this profile, but they appear to be similar in composition to those from the section of the first type.

The third section is studied in the western part of the area, on the left bank of Tomarshi Creek (Fig. 1), where the carbonate–siliceous–tuffaceous sequence overlies the Amginian basalts and basaltic andesites in the core of a small anticline. Resting above them are the following units (Fig. 2, Section 5):

(1) Cobble and boulder conglomerates with calcareous cement; the rocks are composed of fragments of volcanic rocks. Small lenses of organogenic limestones with the Mayan trilobites are found among the conglomerates (*Geologiya SSSR*, 1972). The unit is 50 m thick.

(2) Green calcareous sandstones and siltstones (50 m thick).

(3) Gray bedded cherts alternating with black banded phthanites (80 m thick).

(4) Cherry-red to green siliceous siltstones rhythmically alternating with thin interlayers of tuffites and red jasper in the upper parts of the rhythms (350 m thick).

(5) Calcareous green sandstones, gravelstones, and small-pebbled conglomerates (100 m thick).

The total thickness is 630 m.

The last section bears rare fossils, but in composition and structure, it is obviously correlative with the previous sections.

GENERAL CHARACTERISTICS OF THE SECTIONS

The sections described are of two types, each consisting of four members distinct in composition of coeval rocks.

Sections of the first type (Fig. 2, Sections 1–4; Fig. 3, Section 3a) are typical of the eastern and central parts of the area.

Member 1 ($\epsilon_{2m}-\epsilon_3$) of the terrigenous–carbonate composition is distinguished in the lower part of the sections. The member is composed of calcareous limestones, sandstones, and siltstones. Carbonate–siliceous concretions occur as extended horizons in these rocks. A persistent layer of bedded organogenic–detrital limestones, calcarenites, and carbonate breccia is distinguished in the middle part of the member. The member rocks (especially in its lower and middle parts) yield abundant fragments of larger trilobites, as well as articulate and inarticulate brachiopods. This abundance of benthonic fauna suggests that sediments accumulated at a small depth interval of a gentle slope.

This inference is confirmed by good preservation of thin phosphatic tests of inarticulate brachiopods, which experienced an insignificant transportation. The carbonate content distinctly decreases in rocks of the upper part of the member (Upper Cambrian) that indicates some deepening, although insignificant, of the sedimentation basin. Fragments of five faunal groups are found there: conodonts, brachiopods, trilobites, gastropods, and *Conularia*.

Member 2 (ϵ_3–O_{1tr}) is mainly composed of siliceous rocks, among which gray cherts and phthanites dominate, whereas jaspers are more rare. In addition to siliceous rocks, there are horizons of fine-grained sandstones and siltstones, and also the limestone lenses. This part of the section is poor in benthonic faunal groups, as only conodonts are encountered there, whereas inarticulate brachiopods macerated from carbonate interlayers are very rare. The member lithology and fossils suggest an abrupt increase in the sedimentation depth of mid-Late Cambrian.

Member 3 (O_{1ar}) is of a tuffaceous–terrigenous composition and consists of siliceous tuffites, tephroids, and siltstones intercalated with various tuffaceous and volcaniclastic sandstones, and with lenses of tuffaceous conglomerates. Gradation and slumping structures are typical of these rocks. A great amount of inarticulate brachiopods, which are found buried in their lifetime position throughout the whole section, is a characteristic feature of the member. Conodonts from carbonate concretions of the member and imprints of graptolites are buried in their lifetime position as well. The member composition may indicate that sedimentation was synchronous to the calc-alkaline volcanism. The fossil preservation attests to calm sedimentation conditions at a remarkable distance from volcanic foci. The permanent presence of carbonate material suggests that the basin depth did not exceed the carbonate compensation depth (CCD).

Member 4 ($O_{2ln?}$) is composed of quartz and quartz-feldspathic sandstones and siltstones. Limestone blocks with poorly preserved fragments of crinoids occur in the upper parts of the member. According to the rock composition, the volcanic activity ceased at the time of the member accumulation, and the depth of sedimentation was small.

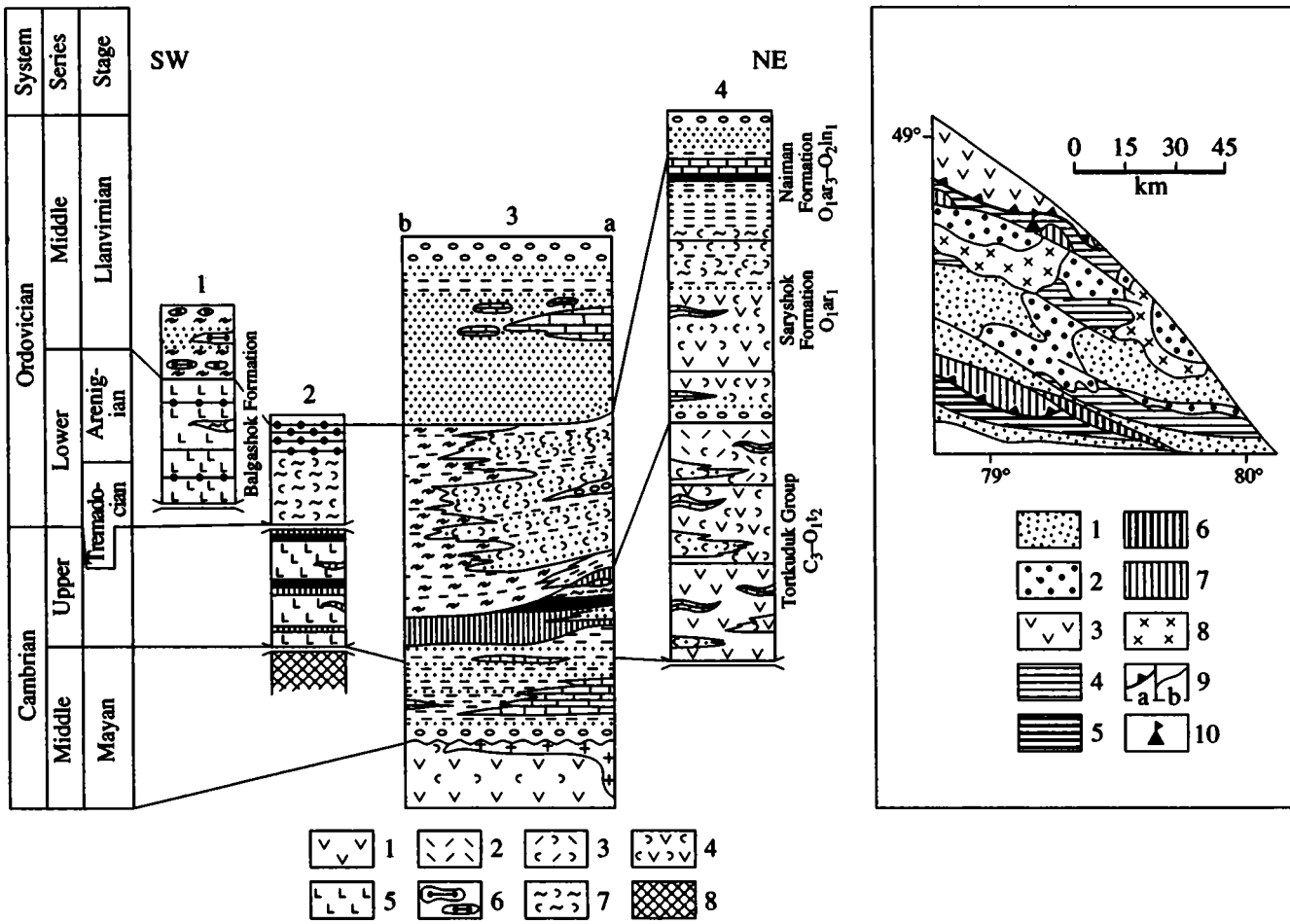

Fig. 3. Correlation between the Middle Cambrian–Llanvirnian sections of central and southwestern parts of the Chingiz Range: (1) andesite; (2) rhyolite; (3) rhyolitic tuffs; (4) andesitic tuffs; (5) basalts; (6) blocks and bed fragments of red jasper; (7) siliceous tuffite; (8) gabbro–ultramafic part of the ophiolite section (other symbols as in Fig. 2).

The inset map shows the location of main structural–facies zones in the southwestern part of the Chingiz Range: (1) Silurian terrigenous sequences; (2) Upper Ordovician complexes; (3) Upper Cambrian–Lower Ordovician volcanogenic and volcanosedimentary rocks of the Central Chingiz nappe (Section 4); (4) Middle Cambrian–Llanvirnian carbonate–siliceous–tuffaceous complex (sections 3a, 3b); (5–6) siliceous–basaltic sequences and ophiolites divided into (5) Lower Ordovician (Section 1) and (6) Upper Cambrian parts (Section 2); (7) Lower–Middle Cambrian complexes; (8) Upper Silurian granodiorites; (9) thrust (a) and other (b) faults; (10) location of the studied area.

The first-type section of the carbonate–siliceous–tuffaceous sequence is 1350–1400 m thick.

The second-type sections are typical of the western part of the area (Fig. 2, Section 5; Fig. 3, Section 3b). Siliceous and siliceous–tuffaceous rocks dominate here, whereas carbonates are missing. The absence of coarse pyroclastic material evidence for a larger distance to volcanic foci. The section is poorly characterized by organic remains; its thickness is about 600–700 m. All these features may indicate a larger depth of the sedimentation basin as compared to that of the first-type section, although the scarcity of organic remains does not allow us to confirm this inference by biofacies analysis.

POSITION OF CARBONATE–SILICEOUS–TUFFACEOUS COMPLEX IN THE STRUCTURAL–FACIES ZONING OF THE CHINGIZ RANGE

In the main part, the rock sequence studied (members 2–4) is synchronous to the volcanosedimentary sequence distinguished long ago in the central part of Chingiz Range, i.e., to the Tortkuduk Group (ϵ_3–O_{1tr}) and Saryshok (O_{1ar}) and Naiman (O_{1ar3}–O_{2ln}) formations, whose distribution zone is located east of the area studied in this work (Fig. 3, Section 4). Dominant in the lower part of the latter (ϵ_3–O_{1ar}) are calc–alkaline differentiated volcanic series, and pyroclastic to volcanoclastic rocks, which are intercalated with thick lenses

and horizons of algal limestone bearing diverse trilobite assemblages (*Geologiya...*, 1962; *Geologiya SSSR*, 1972; Nikitin, 1972). The upper part of this sequence (O_{1ar3}–O_{2ln}) is composed of siliceous–tuffaceous–terrigenous rocks characterized by graptolite and conodont assemblages (Nikitin, 1972; Orlova, 1993) and formed under conditions of gradual cessation of volcanic activity. This volcanosedimentary complex can be correlated with sequences of recent island-arc systems (Samygin, 1990; Samygin and Kheraskova, 1994).

Age analogues of the carbonate–siliceous–tuffaceous complex are known southwest of the studied area as well, i.e. in southwestern piedmonts of the Chingiz Range (Fig. 3, Sections 1, 2). The Upper Cambrian and Lower Ordovician siliceous–basaltic and siliceous sequences, which are spatially related to ophiolites, are widespread there (Nikitin *et al.*, 1992; Koren' *et al.*, 1993; Tolmacheva, 1996). The admixture of tuffaceous and terrigenous material is entirely absent in the last sequences, and only conodonts and radiolarians are encountered as organic remains. Therefore, the siliceous–basaltic and siliceous rock complexes appear to be formed in a back-arc basin with an oceanic crust at a large distance from the volcanic island arcs.

Hence, in the structural–facies zoning of the Chingiz Range, the carbonate–siliceous–tuffaceous complex occupies on the one hand, a position between the zone of volcanosedimentary deposits, where volcanic rocks are differentiated, and the siliceous–basaltic sequences, on the other. This suggests that the studied complex formed in the marginal part of the back-arc basin in the vicinity of the volcanic island arc.

ACKNOWLEDGMENTS

The work was supported by the Russian Foundation for Basic Research, project no. 94-05-16934.

Reveiwers T.N. Koren' and A.Yu. Rozanov

REFERENCES

Geologiya Chingizskoi geoantiklinornoi zony (Tsentral'nyi Kazakhstan) (Geology of the Chingiz Geoanticlinal Zone: Central Kazakhstan), Alma-Ata: Nauka, 1962.

Geologiya SSSR. T. XX. Kniga 1 (Geology of the USSR, Vol. 20, Book 1), Moscow: Nedra, 1972.

Kopyatkevich, R.A., The Early Ordovician Olistostrome of the Chingiz Ridge, *Izv. Akad. Nauk KazSSR, Ser. Geol.*, 1981, no. 1, pp. 41–43.

Koren', T.N., Lytochkin, V.N., Popov, L.E., and Tolmacheva, T.Yu., *Biostratigraficheskii analiz pelagicheskikh strukturno-veshchestvennykh kompleksov paleozoya dlya tselei GSP-50 i 200. Metodicheskie rekomendatsii Roskomnedra* (Biostratigraphic Analysis of the Paleozoic Pelagic Structural–Lithological Complexes for the Geological Mapping 50 and 200: Methodical Recommendations), St. Petersburg: Vseross. Geol. Inst., 1993.

Nikitin, I.F., *Ordovik Kazakhstana, Stratigrafiya* (The Ordovician of Kazakhstan, Stratigraphy), Alma-Ata: Nauka, 1972, vol. 1.

Nikitin, I.F., Zhilkaidarov, A.M., and Frid, N.M., The Ordovician Siliceous–Basaltic Complex of the Southwestern Chingiz Region, *Izv. Akad. Nauk KazSSR, Ser. Geol.*, 1992, no. 4, pp. 57–70.

Orlova, A.R., New Data on Graptolites and Conodonts from the Naima Formation (Lower Ordovician) of the Chingiz Ridge, Central Kazakhstan, *Byull. Mosk. O-va Ispyt. Prir., Otd. Geol.*, 1993, vol. 69, no. 1, pp. 43–47.

Samygin, S.G., The Caledonian Overthrust Sheets of the Chingiz Ridge, Eastern Kazakhstan, *Dokl. Akad. Nauk SSSR*, 1981, vol. 275, no. 3, pp. 709–713.

Samygin, S.G., Central and Eastern Kazakhstan, in *Tektonicheskaya rassloennost' i regional'nye geologicheskie issledovaniya* (The Tectonic Layering and Regional Geological Investigations), Moscow: Nauka, 1990, pp. 180–189.

Samygin, S.G. and Kheraskova, T.N., Formations and Sedimentational Environments within the Early Paleozoic Active Margin (Chingiz Ridge, Central Kazakhstan), *Litol. Polezn. Iskop.*, 1994, no. 3, pp. 86–102.

Tektonika Kazakhstana. Ob"yasnitel'naya zapiska k Tektonicheskoi karte Vostochnogo Kazakhstana, masshtab 1 : 2 500000 (Tectonics of Kazakhstan: Explanatory Notes to the Tecotnic Map of Eastern Kazakhstan, Scale 1 : 2 500 000), Moscow: Nauka, 1982.

Tolmacheva, T.Yu., The Late Cambrian–Early Ordovician Pelagic Conodonts of Central Kazakhstan, *Cand. Sci. (Geol.–Min.) Dissertation*, St. Peterburg., Vseross. Geol. Inst., 1996.

Stratigraphy and Geological Correlation, Vol. 7, No. 5, 1999, pp. 508–518. Translated from Stratigrafiya. Geologicheskaya Korrelyatsiya, Vol. 7, No. 5, 1999, pp. 100–110.
Original Russian Text Copyright © 1999 by Volokhin, Mikhailik, Burii.
English Translation Copyright © 1999 by MAHK "Наука/Interperiodica" (Russia).

Triassic Siliceous Formation in the Khor River Basin (Central Sikhote Alin)

Yu. G. Volokhin, E. V. Mikhailik, and G. I. Burii

Far East Institute of Geology, Far East Division, Russian Academy of Sciences, pr. 100-letiya Vladivostoka 159, Vladivostok, 690022 Russia

Received February 12, 1997; in final form, August 4, 1997

Abstract—In the Khor River middle courses, the Triassic siliceous formation about 430 m thick represents the transgressive–regressive megacyclothem composed of carbonate–siliceous deposits bearing conodonts of the middle Anisian to late Norian (Rhaetian ?) period of time. The decreased thickness of upper Ladinian (24 m) and Carnian (27 m) beds is associated with cryptic intraformational hiatuses that is established within the siliceous sequence exposed along the Lyamfana Creek in close proximity to the Khankai massif. The hiatuses are correlated with events of erosion that affected terrigenous shelf deposits of the South Primor'e, Arsen'ev, and Alchan zones. The bed sequence within the carbonate–siliceous megacyclothem corresponds to cycles of the global eustatic changes of sea level during the Triassic. The thick carbonate deposits of the Sikhote Alin basin accumulated at the time of maximum sea-level stand (Carnian–middle Norian), when there was the sea transgression over the Khankai land. Silica accumulation rates during the Anisian (2.8–3.0 g/cm^2/1000 years) and Ladinian (2.7–3.1 g/cm^2/1000 years) were similar to current parameters characterizing the biogenic silica precipitation in the Far East marginal seas, some inner sea basins (e.g., the Sea of Azov), and coastal upwelling zones (Peru–Chile region). They were one order of magnitude higher than rates of pelagic silica accumulation in the northern and equatorial Pacific. The much slower silica accumulation during the Carnian (0.33 g/cm^2/1000 years) and Norian (0.62–0.63 g/cm^2/1000 years) was compensated by carbonate sedimentation that seems to be a response to migration of habitat areas of siliceous and calcareous plankton during the transgressive epochs interrelated with the eustatic sea-level changes.

Key words: *Sikhote Alin, Triassic, cherts, carbonates, conodonts, sea-level changes, sedimentation rate*

INTRODUCTION

Understanding of geological history of folded regions directly depends on reconstructions of pre-accretionary structures of sedimentary sequences revealing the natural cycles of sedimentogenesis. The available medium- to large-scale geological maps of the Sikhote Alin were produced when this principle was being violated, and the highly deformed sequences were studied inadequately in the litho-biostratigraphic aspect. They actually represent maps of "tectono-stratigraphic" complexes and are almost useless for analysis of original sedimentary basins and pre-accretionary geological history of the region. Boundaries between these complexes usually do not coincide with natural boundaries of geological formations and represent either limits of submarine landslide bodies, or tectonic contacts that originated later. Plankton-bearing siliceous deposits include persistent facies rich in microfauna and representing the ideal reference levels for structural analysis of accretionary prisms of the region.

In the Sikhote Alin, radiolarian siliciliths are known amid Upper Paleozoic, Jurassic, and Cretaceous deposits being most widespread in Triassic sequences. The Triassic siliceous formation of regional significance consists of cherty and cherty–carbonate facies (Volokhin, 1985; Volokhin *et al.*, 1987). The carbonate–siliceous sequences are typical of the Central Sikhote Alin and Amur–Ussuri (Nadan'khada–Khabarovsk) zones located at a certain distance from old continental massifs (Khankai, Kentei, and Bureya). Closer to the latter, there are widespread the cherty Triassic sequences.

In the northern and central Sikhote Alin, the Triassic carbonate–siliceous deposits are exposed in the upper and middle reaches of the Anyui River, close to the Dzhaur River head, and in middle courses of the Gur River. They are attributed to the Dzhaur Formation that was originally considered as the Late Triassic–Late Jurassic in age (*Resheniya tret'ego...*, 1982), and now is thought to be of the Early Triassic–Late Jurassic age (*Resheniya chetvertogo...*, 1994). In the central Sikhote Alin, outcrops of carbonate–siliceous Triassic beds were studied at the left (Kabuli River basin and middle courses of the Katen River) and right-hand (downstream from the Kolomi River mouth) sides of the Khor River. In accordance with the available scheme of tectonic zoning, these beds are included into the Dzhaur Formation within the area located to the east of the Central Sikhote Alin fault (Fig. 1), whereas to the west of this structural line, they are assumed to be a part of the Krasnaya

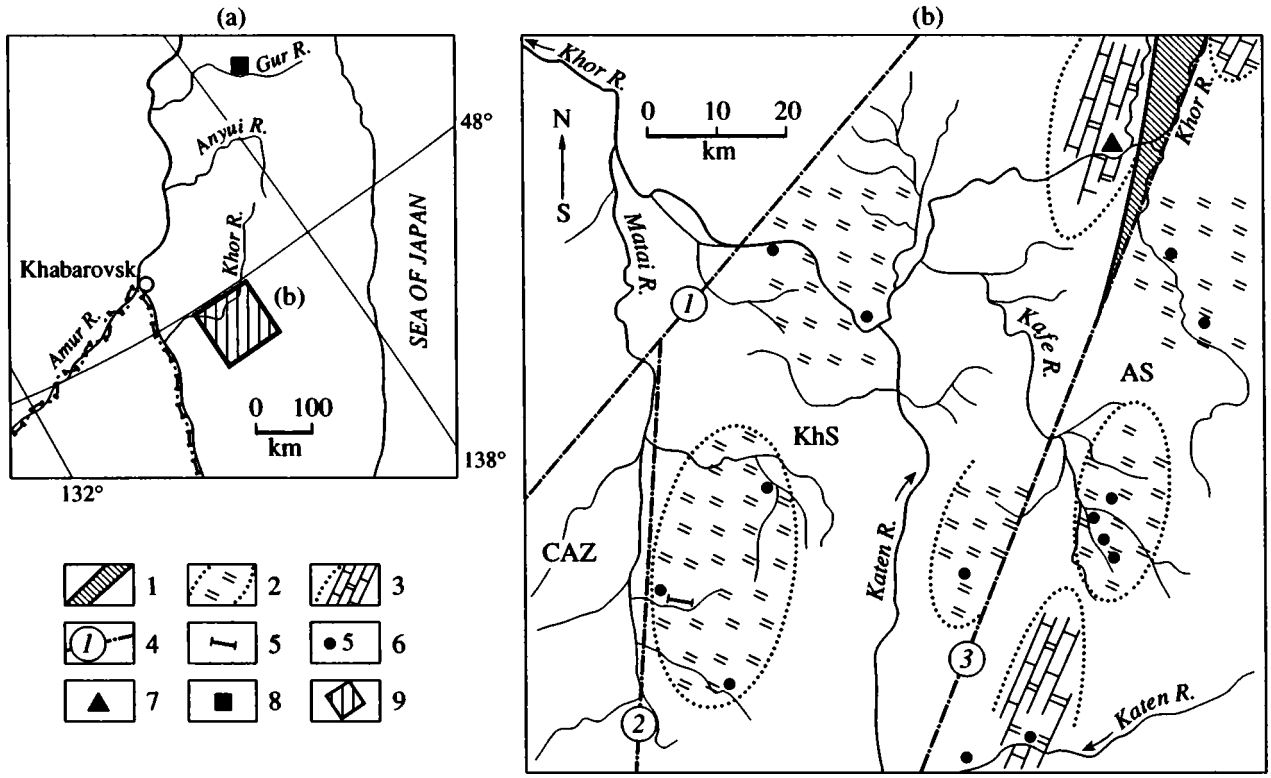

Fig. 1. Geographic position of the study area (a) and facies scheme (b) compiled by using data of Shevelev (1988), Klets (1995) and Burii *et al.* (1990) for the Triassic siliceous formation in the Khor River basin: (1) Khor metamorphic complex; (2) siliceous and (3) carbonate–siliceous facies of the formation; (4) Alchan (*1*), Arsen'ev (2) and Central Sikhote Alin (*3*) faults; (5) Lyamfana Creek section (after Burii *et al.*, 1990); (6) exposures of siliceous and carbonate–siliceous Triassic rocks after Klets (1995); (7) section described in this work; (8) Gur River section; (9) study area in geographic scheme; (CAZ) Central Alchan structural-lithologic zone with Khor (KhS) and Anyui (AS) subzones.

Rechka Formation of the Late Triassic–Late Jurassic age (Shevelev, 1988). Our facies scheme of Triassic deposits in the Khor River basin (Fig. 1) shows however that both "structural-facies" or "structural-lithologic" zones represent a result of invalid tectonic zoning, because the facies boundaries do not coincide with principal tectonic elements such as the deep-rooted faults.

SECTION AT THE RIGHT-HAND SIDE OF THE KHOR RIVER

The Triassic carbonate–siliceous facies are exposed better than elsewhere in the Khor River cliffs located 2 km downstream from the mouth of the Kolomi River, the right-hand tributary of the former. Cherty and limy beds belong here to the southeastern limb of a large syncline (synform ?), within which the distance between flanks (along the base of Triassic cherts) is about 2.5 km. The syncline core is composed of Lower–Middle Jurassic (?) terrigenous deposits. In the northwestern and southeastern limbs, the Triassic cherts overlie the silty-shale sequence impregnated by sills (80–200 m thick) of phyric basalts and diabases. V.I. Anoikin and his colleagues, who mapped this area, tentatively attributed the latter to the Upper Triassic.

In exposures located below the Kolomi River mouth, chert and limestone beds experienced displacement along faults striking northeastward and were affected by fault-related folding; the faulted blocks are narrow (50–70 m) and separation amplitude is insignificant (Fig. 2). Studying the lithology of this section, which had been previously considered formerly as being barren of fossils, we macerated conodonts from 57 rock samples and identified them as ranging in age from the middle Anisian to the late Norian–Rhaetian, inclusive. We distinguished 25 sedimentary members grouped into 7 units 355–381 m thick in total and representing an integral carbonate–siliceous megacyclothem (Fig. 3), which consists of subdivisions characterized below (from the base upward).

Unit (1) of Siliceous Shales and Silty Shales (More that 13 m Thick)

Member 1: siliceous shales, gray to greenish gray, exhibiting lenticular lamination, medium- to thin-bedded; thickness of elementary cycles (Tec) = 2–6 cm; subordinate interbeds of clayey chert and black silty

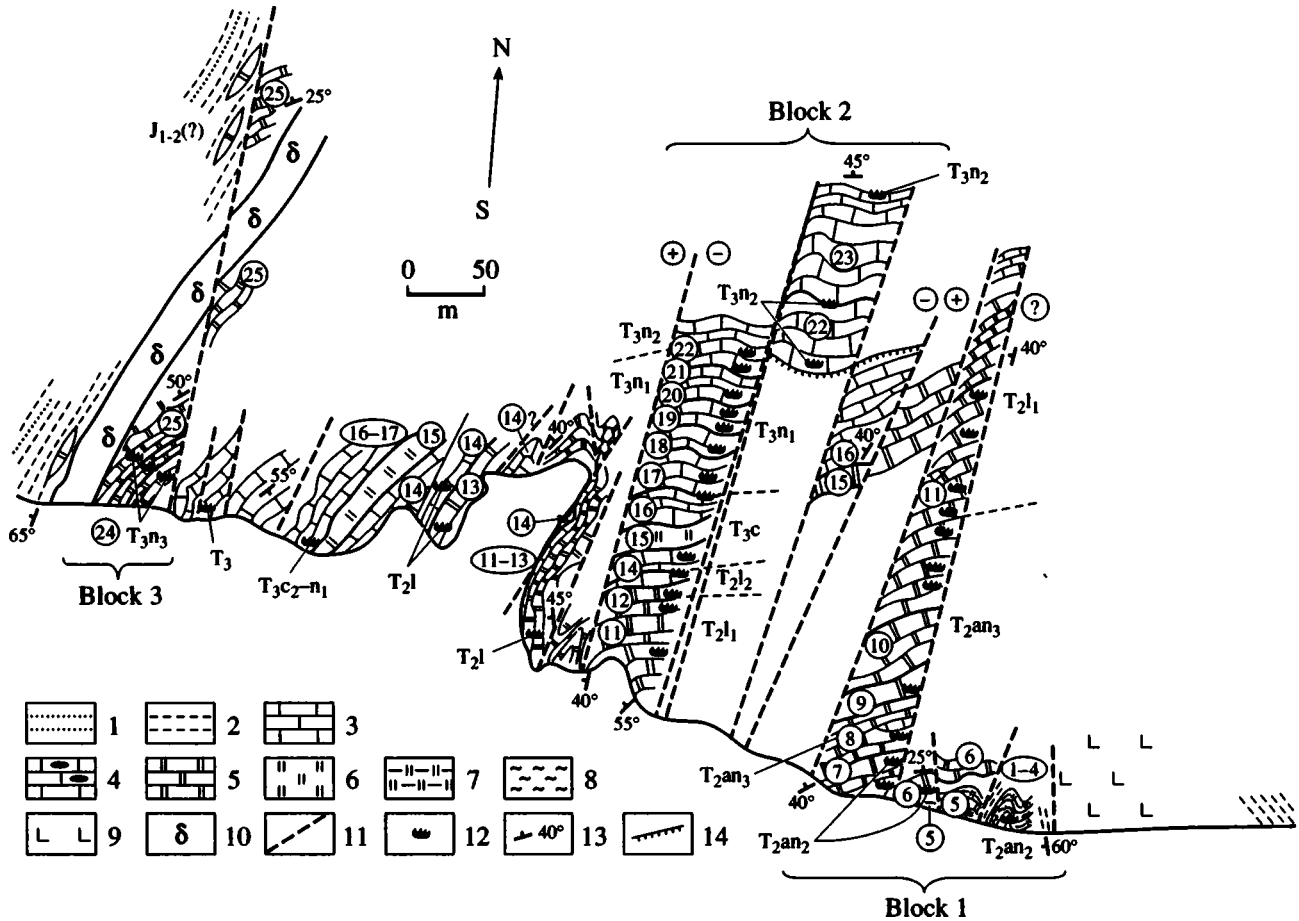

Fig. 2. Geological plan of exposures of Triassic siliceous formation at the right-hand side of the Khor River 2 km downstream from the Kolomi River mouth: (1) sandstone; (2) siltstone or shale; (3) limestone; (4) limestone with cherty nodules and lenses; (5, 6) chert beds; (7) clayey chert; (8) siliceous shale; (9) diabase and phyric basalt; (10) K-lamproite; (11) faults; (12) conodont fauna; (13) strike and dip angle; (14) steep cliffs (encircled numbers denote the recognized members).

shale (10–15%); conodonts *Paragondolella bulgarica* Budurov et Stephanov and *Neogondolella constricta* (Mosher et Clark) occur in the lower part of the member (3 m thick).

Member 2: siliceous shales, gray, thin-bedded (Tec = 1–3 cm); subordinate (1 : 5 to 1 : 10) interbeds of black shale, one of which (0.3 m thick) is fine-bedded and situated in the upper part of the member (1.4 m thick).

Member 3: clayey chert, gray, showing subhorizontal lamination, thin-bedded (Tec = 1–6 cm, 3–4 cm in average); intercalated black shale interbeds (2 m thick).

Member 4: black shale with rare lenses of clayey chert and cherty shales (more the 6 m thick).

Further upward, the interval of 10–12 m is unexposed, marked by debris of black cherty shale, and interpreted as corresponding to the fault zone.

Unit (II) of Clayey Cherts (25–30 m)

Member 5: clayey cherts, gray to charcoal gray, thick-bedded (Tec = 10–25 cm, usually 15–25 cm), with subhorizontal lamination; rocks are intercalated with interbeds of black silty shale (1–40 cm) and occasional clayey phthanite; lower beds yielded *Neogondolella* sp. indet. and *Paragondolella* sp. indet.; *Neogondolella* sp. indet. together with rod-like conodonts are characteristic of the middle portion, and *Paragondolella* cf. *bulgarica* Budorov et Stepanov occur in the upper one (25–30 m thick).

The overlying 1-m-thick interval is unexposed and corresponds to the contact between units (II) and (III).

Unit (III) of Platty Cherts (145–165 m)

Member 6: cherts, gray, thick-bedded (Tec = 12–30 cm, usually from 15 to 25 cm), displaying subhorizontal lamination, intercalated with rare beds (up to 1 m thick) of medium-platty chert (Tec = 3–6 cm) bearing *Paragondolella bulgarica* at the base (6 m thick).

Member 7: cherts, gray to bluish green, displaying subhorizontal to lens-like bedding and thick-bedded general structure (Tec = 8–12 cm); lentils and interbeds

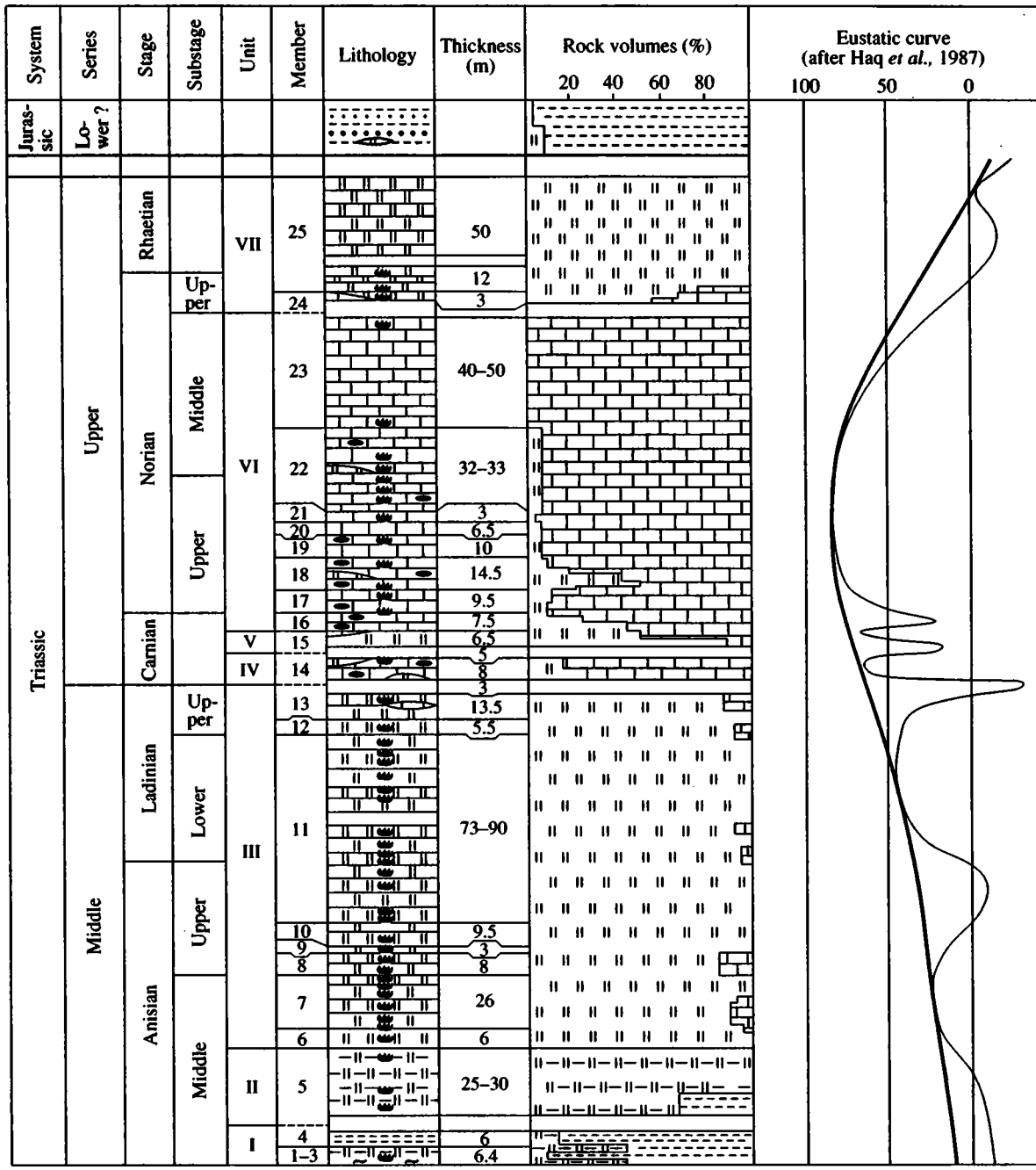

Fig. 3. Stratigraphy and lithology of the Khor River section (symbols as in Fig. 2).

of cherty dolomite constitute 5–10% of the member; conodont remains from basal and middle beds belong to the Middle Triassic genera *Neogondolella, Paragondolella*, and *Gladigondolella*, though they are undeterminable at the species level; *Neogondolella* cf. *constricta* (Mosher et Clark) and *Neospathodus* cf. *kockeli* (Tatge) are identified in samples collected 4 m below the member top (26 m thick).

Member 8: cherts, gray to greenish blue, thick-bedded (Tec = 2–16 cm and 8–10 cm in average), interca-lated with subordinate (1 : 6 to 1 : 7) interbeds (0.5–7 cm) of light gray and pale dolomites and limy-dolomitic cherts; *Neogondolella constricta* (Mosher et Clark) and *Neogondolella* sp. indet. characterize basal and middle beds, respectively (8 m thick).

Member 9: cherts, light gray to greenish white, all pale at the weathered surface; rocks are thin-bedded (Tec = 0.5–1.5 cm), bearing *Paragondolella hanbulogi* Sudar et Budurov near the member top (3 m thick).

Member 10: cherts gray to brownish at the weathered surface, displaying lens-like bedding and thick-bedded structure (Tec = 20–25 cm); rocks are intercalated with rare interbeds of thin-bedded chert (Tec = 3–10 cm) bearing *Neogondolella* sp. indet. (9.5 m thick).

Member 11: cherts, light gray (almost white), locally bluish green, pinkish to brown at the weathered surface, thick- to coarse-bedded in structure (Tec = 10–40 cm); minor dolomite lentils and rare intercalations of thin-bedded cherts (Tec = 1–3 cm) yielded *Neogondolella* sp. indet. at the level of 5.8 m above the base, *Paragondolella* cf. *hanbulogi* 2 m above this level, remains of M- or S-elements of *Ellisonia* forms 6 m higher than the last mark, and then successively *Neogondolella mombergensis* (Tatge) (+2.5 m upward), *N.* cf. *mombergensis* and *Sephardiella* sp. indet. (+3.7 m upward), and *Paragondolella* sp. indet. (+3.3 m upward); overlying cherty dolomite beds bear *N.* cf. *mombergensis* and *Paragondolella* aff. *excelsa* Mosher (+5.4 m upward), and higher (+6.5 m) *N.* cf. *mombergensis* coexists with *Sephardiella* sp. indet. juv. In this block, the uncompleted thickness of the member is 40 m.

The upper continuation of the sequence is detected in a narrow tectonic block located 115–125 m to the west, near the slope foot (Fig. 2). This part of the member consists of gray to bluish gray, subparallel-bedded cherts (Tec = 10–50 cm), which are intercalated with interbeds and lentils (up to 2 cm thick) of calcareous dolomite (upper 25 m). Samples from the base of the exposure yielded *Sephardiella mungoensis* (Diebel) and *Neogondolella mombergensis*. Three meters higher we recovered *Sephardiella* sp. indet. In the upper portion, we detected an assemblage of *Paragondolella* cf. *excelsa, Neogondolella* cf. *mombergensis, N.* sp. juv. aff. *excentrica* Budurov et Stephanov, and *Sephardiella* sp. indet. juv. (10 m below the top); rocks above this level bear *Neogondolella* sp. (6.7 m below the top). The upper portion is 33–52 m thick, and the total thickness of Member 11 is 73–90 m.

Member 12: cherts, gray to light gray, thin- to thick-bedded (Tec = 2–10 cm), displaying subhorizontal or lens-like lamination; rocks are intercalated with lentils and interbeds (1–3 cm) of limestone, dolomite, and calcareous chert; uppermost beds bear *Gladigondolella tethydis* (Huck.) juv. and *Paragondolella* cf. *tadpole* (Hayashi) (5.5 m thick).

Member 13: cherts, charcoal gray, brownish to tawny when weathered, medium- to thick-bedded (Tec = 8–15 cm in lower beds and 6–10 cm in upper portion); rocks are intercalated with lenses and interbeds (1–3 cm) of black chert in the middle interval and with subordinate (1 : 5 to 1 : 10) carbonate interbeds (1–2 cm) in the upper one; uppermost beds bear *Paragondolella* cf. *excelsa* and *Neogondolella* sp. indet. (13.5 m thick).

The interval atop (3 m thick) is concealed under the talus apron, and beds above it are attributed to the next unit.

Unit (IV) of Carbonate Rocks (8–16 m)

Member 14: limestone, siliceous limestone, and dolomite beds, black to charcoal gray, medium- to thick-bedded, intercalated with subordinate (15–20%) lenses and interbeds (1–3 cm) of gray chert; *Neogondolella* cf. *praeangusta* Kozur, Mirauta et Mock and *Paragondolella* cf. *foliata* Budurov are discovered at the level of 1 m below the top. The apparent thickness of the unit is estimated to be 16 m (unexposed lower and upper intervals included).

Unit (V) of Bedded Cherts (More than 6.5 m)

Member 15: cherts, taupe colored, pale and brecciated at the base, enclosing black lentils and undeterminable conodont remains; close to the top (interval 1.5 m thick), rocks enclose frequent (30–40%) carbonate lenses (0.5–3 cm) (more than 6.5 m thick).

Unit (VI) of Carbonate Rocks

Member 16: limestone beds, gray to charcoal gray, intercalated with lenses and nodules of taupe chert (20–30% in average, and up to 40–50% close to the base); conodont remains are undeterminable (7.5 m thick).

Member 17: limestone beds, dark gray, massive or vaguely bedded, enclosing cherty nodules, lenses (up to 8 cm thick and about 10% in volume), and remains of conodonts *Epigondolella abneptis* (Huck.), *Metapolygnathus vialovi* (Buryi), and *M.* cf. *primitia* Mosher (9.5 m thick).

Member 18: limestone beds, charcoal gray and gray, medium- to thick-bedded, intercalated with nodules and lenses (1–8 cm) of gray chert (15–20% in average and up to 50% close to the base); species *Metapolygnathus* cf. *vialovi* Buryi occur near the base and in the middle beds (14.5 m thick).

Member 19: limestone beds, gray to charcoal gray, rhythmically thick-bedded (Tec = 10–35 cm), with interbeds (0.5–1 m) of fine- to medium-bedded nodular cherts; rocks enclose conodonts *Metapolygnathus* cf. *linguiformis* Mosher and *M.* sp. juv. aff. *vialovi* (10 m thick).

Member 20: limestone beds, charcoal gray, thick-bedded and sporadically massive (Tec = 20–100 cm), enclosing rare chert interbeds with fine or more coarse lamination (Tec = 2–6 cm); conodonts *Metapolygnathus* sp. are recovered from basal beds, and *Metapolygnathus* aff. *permicus* (Hayashi) together with *M. vialovi* occur 0.8 m below the top (6.5 m).

Member 21: limestone beds, gray to charcoal gray; alternating bed packets consist of thin-bedded (Tec = 1–3 cm) and thick- to coarse-bedded (Tec = 15–20 cm) rock varieties (3 m thick).

Member 22: limestone beds, charcoal or gray in color, thick- to coarse-bedded (Tec = 5–20 cm), enclosing cherty lenses and nodules (2–3%); in general, the member is more massive than rocks below and above it;

conodont assemblages occurring at different levels are one of *Epigondolella* cf. *abneptis* and *Metapolygnathus vialovi* (basal bed), another of *Metapolygnathus* cf. *nodosus* (Hayashi) and *M.* cf. *vialovi* (5 m above the base), assemblage of *Epigondolella abneptis, Metapolygnathus primitia* Mosher and *Ancyrogondolella triangularis* Budurov (+3 m upward), assemblage of *Metapolygnathus vialovi, M. spatulatus* (Hayashi), *Paragondolella steibergensis* Mosher, *Epigondolella multidentata* Mosher, *E. abneptis* and *Ancyrogondolella triangularis* (+2.5 m upward), and assemblage of *Metapolygnathus* sp. indet. and *Epigondolella abneptis* (+3 m upward). Topmost beds of the member are exposed in another block, 38 m to the east from the fault line (Fig. 2), where they bear *Epigondolella abneptis* and *E. multidentata.* The estimated total thickness of the member is 32–33 m.

Member 23: limestone beds, gray to charcoal gray, fine- to thick-bedded (Tec = 1–25 cm, most often 10–15 cm); *Metapolygnathus* cf. *spatulatus* and *Neogondolella* sp. are from basal level, and *Epigondolella* aff. *bidentata* Mosher coexists with *Metapolygnathus spatulatus* near the apparent top of the member (40–50 m thick).

Overlying beds are studied in the western side of the locality (Fig. 2), within a small tectonic Block 3, where they are bounded by the Upper Triassic limestone sequence (Block 3) and K-lamproite dike separating them from overlying terrigenous shales.

Unit (VII) of Bedded Cherts (More than 15 m)

Member 24: cherty beds, light gray to greenish, fine- to medium-bedded, showing lenticular lamination and intercalated with lenses (2–10 cm) of limestone and calcareous chert (15–25% in average and up to 50% in the middle interval); basal beds yielded *Epigondolella* aff. *mostleri* (Kozur et Mostler) (3 m thick).

Member 25: cherts, gray to light gray and greenish, medium-bedded (Tec = 2.5–15 cm and 3–4 cm in average), with lenticular lamination in basal interval and subhorizontal-laminated in the middle; near the dike, cherts are brecciated and impregnated by quartz veins (upper 6-m-thick interval); conodonts *Parvigondolella* sp. indet., *Misikella* cf. *posthernsteini* Kozur et Mock, and *Epigondolella* cf. *slovakensis* Kozur are recovered from basal beds (apparent thickness is 12 m).

Bedded cherts of Member 25 are also exposed in another block located 400 m northward (Fig. 2), where a normal fault separates them from black shales of the overlying terrigenous sequence. The complete thickness of Unit (VII) is about 65 m.

The sequence of cherts and limestones, exposed between the second and third blocks is similar in lithology with members 13–17 (Fig. 2). These rocks yielded *Neogondolella* sp., *Sephardiella* sp., *Metapolygnathus vialovi*, and *Epigondolella* sp.

AGE SUBSTANTIATION FOR UNITS AND MEMBERS

We attribute members 1–7 to the middle Anisian, because they bear the conodont assemblage of *Paragondolella bulgarica, Neospathodus* cf. *kockeli,* and *Neogondolella constricta.* The first species is characteristic of the uppermost lower (Bitinian) and middle Anisian (Pelsonian) in Bulgaria and Italy (Budurov, 1980; Pisa *et al.*, 1980). *Neogondolella constricta* is widespread in the middle Anisian–lower Ladinian beds of Nevada, Bulgaria, and Italy (Mosher and Clark, 1965), whereas *Neospathodus kockeli* is an index species of the middle Anisian deposits in Germany, Bulgaria, and some other regions (Tatge, 1956).

Members 8–10, together with lower beds of Member 11, are considered to be the late Anisian in age, because they bear *Paragondolella hanbulogi* characteristic of this substage (Sudar and Budurov, 1979), while, on the contrary, *Paragondolella bulgarica* and *Neospathodus kockeli* are missing from this level. The upper Anisian boundary is placed at the disappearance level of *P. hanbulogi*, above which we established the presence of *Neogondolella mombergensis* and *Sephardiella* forms suggesting the Ladinian age of host deposits (Tatge, 1956; March *et al.*, 1990).

The lower Ladinian beds are marked by the oexistence of *Neogondolella mombergensis* and *Paragondolella* aff. *excelsa.* In addition to *N. mombergensis*, samples from middle beds of Member 11 yielded first specimens of *Sephardiella mungoensis* typical of the uppermost lower and upper Ladinian. Accordingly, they mark the boundary beds between these substages.

The upper Ladinian includes members 12 and 13 bearing the characteristic assemblage of *Gladigondolella tethydis, Paragondolella* cf. *tadpole*, and *P.* cf. *excelsa* (Kovacs and Kozur, 1980).

The overlying Member 14, where we detected *Neogondolella* cf. *praeangusta* and *Paragondolella* cf. *foliata*, is definitely of the early Carnian age, since the first form is known from coeval deposits in Romania (Kovacs and Kozur, 1980), and the second one is typical of the Ladinian–Carnian boundary beds in Yugoslavia, Bulgaria, and Sikhote Alin region (Budurov, 1975; Burii, 1989). In Japan, the *P. foliata* Zone spans the Ladinian–Carnian boundary interval above the *Sephardiella (Carinella) mungoensis* Zone of the Ladinian and below the *Neogondolella polygnathiformis* Zone of the Carnian (Igo and Koike, 1983).

Members 15 and 16, where conodont remains are undeterminable, are attributed with due precautions to the upper Carnian Substage.

Member 17 that yielded the late Carnian–early Norian species *Metapolygnathus* cf. *primitia* and *M. vialovi* in association with the late Norian *Epigondolella abneptis* (Buryi, 1996) is considered as a subdivision of the lower Norian.

The early Norian conodont assemblage is also characteristic of members 18–21 and of lower beds of Member 22. In the assemblage from the upper part of Member 22, *Epigondolella abneptis* characteristic of the early Norian coexists with first specimens of *E. multidentata* typical of the middle Norian (Mosher, 1970). Accordingly, the lower–middle Norian boundary is placed inside Member 22 at the first occurrence level of *E. multidentata*.

Member 23 is considered to be of the middle Norian age, because *Metapolygnathus spatulatus* typical of this substage is recovered from its basal and uppermost beds. In the last case, this species coexists with the late Norian (after Kovacs and Kozur, 1980) *Epigondolella bidentata*, and the top beds of the member may be as young as the last substage.

The late Norian conodonts are characteristic of members 24 and 25, and one of them (*Misikella posthernsteini*) is widespread even in Rhaetian deposits. *Epigondolella* aff. *slovakensis* from the last rock sample studied in this work is the index species of topmost Norian beds in Slovakia (Kovacs and Kozur, 1980), and other beds of Member 25 could be of the same age. According to Kozur (1989), the first occurrence level of *Misikella posthernsteini* corresponds to the Norian–Rhaetian boundary. As the upper part of Member 25, where cherts experienced metamorphic transformations, includes only undeterminable conodont remains, it could be corresponding already to the Rhaetian Stage.

The Triassic siliceous formation of the Khor River section is almost complete. Remaining problems concern only the uppermost beds of Member 25 (Rhaetian–basal Jurassic ?) and the interval (several to few dozens of meters) between members 23 and 24 (topmost middle–basal upper Norian). The total thickness of middle Anisian–upper Norian deposits in the studied section is 355–381 m. The complete thickness of siliceous deposits in the Khor River basin could be as high as 430 m or slightly over.

PRINCIPAL STRUCTURAL FEATURES AND BOUNDARIES OF SILICEOUS FORMATION IN THE KHOR RIVER BASIN

From the field studies, we estimated volumetric proportions between main rock types in individual members and particular horizons (see Fig. 3). The cyclic structure of the formation is distinct despite the fact that the section is faulted and some its intervals are unexposed. The studied deposits of the Khor River basin represent the carbonate–siliceous megacyclothem. As abundance of terrigenous material progressively grows toward the base of megacyclothem (basal Anisian), the proportion of siliceous material decreases. At the top of megacyclothem, the upper Norian–Rhaetian bedded cherts are conformably overlain by the Jurassic terrigenous deposits. Carbonate rocks of the Carnian–middle Norian interval are predominant in the middle of megacyclothem. Subordinate lentils and interbeds of carbonate rocks are also characteristic of the middle–upper Anisian, Ladinian, and upper Norian, whereas the increased abundance, or even predominance of siliceous rocks is typical of certain members within the upper Carnian and lower Norian intervals corresponding to inner mesocyclothems of the formation.

The problem of upper age limit of the formation in the Khor River basin still remains inadequately solved, though our and some other data (Burii *et al.*, 1990; Shevelev, 1988; Klets, 1995) suggest that the megacyclothem is limited at the top by the Triassic–Jurassic boundary or by basal Jurassic strata. Terrigenous deposits above cherts of Member 25 yield only radiolarians, which are poorly preserved. Their basal beds are composed of black silty shales intercalated with subordinate interbeds (1–2 cm) and lenses of gray, locally clayey cherts, and this suggests a gradual transition from Member 25 to terrigenous deposits. Above this level, black silty shales enclose interbeds of volcaniclastic graywacke displaying turbidite structures. In lithology, the terrigenous deposits are similar to sediments of the Khungari Formation of the Gur River basin. To the west of the section studied (near the village of Khody, the right-hand side of the Matai River), siltstone beds (up to 400 m thick) overlying the Triassic cherts yielded the Early–Middle Jurassic radiolarians (Shevelev, 1988). In the section at the Lyamfana Creek, the Upper Triassic cherts directly grade upward into silty shales with Early Jurassic radiolarians (Burii *et al.*, 1990). Consequently, we provisionally consider the terrigenous deposits above Member 25 as corresponding in age to the Early–Middle Jurassic.

The lower boundary of the formation in question is also problematic. The contact between this formation and "underlying" volcanogenic terrigenous complex is actually disturbed by the hypabyssal basaltic intrusion (sill ?). This intrusion seems to be young (Middle–Late Jurassic ?), because it is similar in petrographic features to other Jurassic subalkaline basaltoids known in the region and was responsible for transformation of the middle Anisian rocks of members 1–6 into hornfels. Unfortunately, the age of volcanogenic terrigenous rocks proper is unknown.

In other areas of the Khor River basin (middle courses of the Katen River and exposures of the Matai River), the Triassic siliceous formation is thought to overlie the Late Permian volcanogenic-terrigenous deposits (Shevelev, 1988). The oldest Triassic forms *Neospathodus triangularis* and *N. homeri* (uppermost beds of the Olenekian) were detected by Klets (1995) in siliceous tuffoargillites overlying a thick sequence of volcanogenic rocks (Upper Permian ?) in outcrops located 90 km southward of the studied site. Taking this into consideration, we believe that the lower limit of siliceous formation is approaching the Induan–Olenekian boundary in age.

COMPARISON BETWEEN SECTIONS OF THE KHOR AND GUR RIVER BASINS

Burii was first to discover in 1983 the Middle (Ladinian) and Late Triassic conodonts from the stratotype of the Dzhaur Formation (Kakdyamu Cliffs of the Gur River), which has been formerly considered as being barren of organic remains (Volokhin, 1985). Afterward it was established that the stratotype includes four units of bedded cherts separated by units of carbonate beds at the base of the Carnian (7–8.5 m), within the upper Carnian (78 m), and in the lower–middle Norian (102–113 m). All these units are interrelated in lithological respect and represent a megacyclothem that is 385–425 m thick. The Gur River section includes all Triassic stages and substages from the upper Anisian (*Neogondolella constricta* Beds) to the middle–upper Norian (*Epigondolella postera* Beds). Bedded cherts crowning this sequence yielded specimens of the Upper Triassic *Epigondolella* forms at the basal level only. Higher they contain undeterminable conodonts and are tentatively dated back to the middle–late Norian (Volokhin *et al.*, 1987). The top member of clayey cherts (6 m) underlies black silty shales of the Jurassic Khungari Formation.

The original description of the Dzhaur Formation stratotype (Gur River locality) should be corrected with respect to the Carnian–Norian boundary that was placed at the base of the carbonate unit VI (Volokhin *et al.*, 1987) and must be displaced now 52–57 m downward, in the middle of the carbonate unit IV (the base of Member 18), where the first occurrence level of *Epigondolella abneptis* is recorded. Another correction concerns the age of black shales situated below unit I of bedded cherts and separated from the latter by a fault. The stratigraphic position of the shales was considered as corresponding to the Anisian Stage that is incorrect. Later field observations in the Anyui River basin (Volokhin *et al.*, 1996) demonstrated that Anisian beds are composed of chert and jasper and represent constituents of the Triassic siliceous formation.

The considered sections of Khor and Gur river basins are attributed to the Krasnaya Rechka and Dzhaur formations, respectively. In their structure, thickness (about 400 m), lithology, and age, the sections are similar. Both exhibit sedimentary cycles, where lower and upper sequences of bedded cherts are separated by carbonate deposits confined to the intermediate Carnian–middle Norian interval. In the Gur River section, the total thickness of carbonate rocks is greater (about 200 m), and their sequence includes two lower Norian horizons of submarine landslides. Many Anisian beds are unexposed here, but the top of the formation grades (across the member of clayey cherts) into the overlying Jurassic formation of terrigenous rocks. Basal beds of the formation under consideration and zone of transition to underlying terrigenous (or volcanogenic terrigenous) deposits are better represented in the Khor River section. The maximum thickness of the Triassic formation is in the Gur River basin, where it could be up 500 m, if the Anisian bedded cherts and jaspers are its constituents.

As compared to sections consisting of siliceous facies only, where the Middle–Upper Triassic deposits are from dozens of meters (Burii *et al.*, 1990; Volokhin *et al.*, 1990) to 200–250 m thick (section of the Dubovaya Sopka, Klets, 1995), the studied section of carbonate–siliceous deposits is much thicker.

RATES OF SEDIMENTATION AND SILICA ACCUMULATION

The detailed subdivision of the section that is established in accordance with distribution patterns of conodont fauna of a high resolution potential allows the accumulation rates of Triassic deposits to be calculated using the recent calibration of the geological time scale (Ross *et al.*, 1994). We used the following thickness parameters of sedimentary units and time ranges of Triassic ages: 122 m and 7 m.y. for the Anisian; 84 m and 6 m.y. for the Ladinian; 27 m and 8 m.y. for the Carnian; 131–141.5 m and 8 m.y. for the Norian. Calculating sedimentation rates of free silica (SiO_2), we took into consideration the content of siliceous rocks in the units and members (Fig. 3), the average rock density of 2.6 g/cm^3, and free silica content assumed to be equal to that in Ladinian beds of the Gur River section (85%), which is greater than the average value for siliceous deposits of Sikhote Alin (77.4%), but better characterizes rocks of the carbonate–siliceous formation. For clayey cherts and siliceous shales of members 1–5, the free silica content was taken equal to 54% that is characteristic of this rock types in average within the Sikhote Alin region (Volokhin, 1985).

The calculated sedimentation rates (mm/k.y.) are as follows: 17.4 for the Anisian; 12.8–14.0 for the Ladinian; 3.4 for the Carnian; and 16.4–17.7 for the Norian. The silica accumulation rates (free SiO_2 g/cm^2/k.y.) are 2.8–3.0 for the Anisian, 2.7–3.1 for the Ladinian, 0.33 for the Carnian, and 0.62–0.63 for the Norian. Thus, both parameters were at the maximum during the Anisian and Ladinian ages. The decreased silica accumulation during the Norian time was compensated by the more intense carbonate sedimentation. The Carnian minimum of silica accumulation and sedimentation rate seems to be caused however by some other factors, which will be considered below (they could be active as well during the late Ladinian time). The Ladinian silica accumulation rate was higher in general within the Khor River area than in the Gur River section, where it was 1.8–2.0 g/cm^2/k.y. (Volokhin *et al.*, 1987).

Prior to this work, we calculated sedimentation and silica accumulation rates for the Dal'negorsk, Gur and Ussuri river areas (Volokhin *et al.*, 1987, 1990) using the geological time scale by Harland *et al.* (1985), which is closer to the scale by Ross *et al.* (1994) than to another scale suggested by Harland and his colleagues

(Harland *et al.*, 1989). Thus, our data on silica accumulation rates during the Triassic ages, which are calculated here and have been published earlier, are comparable within the error range of two indicated scales.

Within distribution areas of carbonate–siliceous facies, the silica accumulation was more intense (5–10 times faster) than in sedimentation areas of siliceous facies only, presumably because of erosion of radiolarian muds and silica transport into the deep-water settings (Volokhin *et al.*, 1990). In general, the estimated rates of biogenic silica accumulation in Triassic basins were greater than these parameters characterizing the same process in the northern and equatorial belts of pelagic sedimentation in oceans. They were close to rate magnitudes typical of hemipelagic oceanic zones, marginal and intracontinental seas (Bering Sea, Sea of Okhotsk, and Sea of Azov), and Peru–Chilean upwelling zone, but considerably lower than in the Californian and Southwest African upwelling zones (De Master, 1981; Volokhin, 1985, Table 38).

STRUCTURE OF THE SECTION AND GLOBAL EUSTATIC CYCLES

The described Khor River section is a rare example of well-exposed and almost complete Triassic sequence of carbonate–siliceous facies of the Sikhote Alin region. It was accumulated in a deep zone of the Sikhote Alin sea, and variable proportions of rocks within the section show the distinct correlation with global sea-level changes thus reflecting dependence of sedimentation on eustatic factors and related transgressive–regressive cycles (Fig. 3).

In the known curve of sea-level fluctuations (Haq *et al.*, 1987), one of the high-stand maximums spans the Carnian–Norian interval, when exactly the carbonate rocks become predominant in the Khor River section, whereas minimums mark the Rhaetian–Jurassic and Permian–Induan boundaries, near to which siliceous beds are in contact with terrigenous or volcanogenic–terrigenous deposits. The short-term periods (mesocyclothems) of sea-level drops at the end of the Anisian and especially remarkable at the terminal Ladinian time and in the middle and latest Carnian correspond to most siliceous members of the section and have resulted in reduced thickness of upper Ladinian and Carnian beds. Cryptic intraformational hiatuses are established by Burii and Filippov (1991) in the Lyamfana Creek section, 95 km to the southwest of the Khor River locality, where the bed sequence is composed of siliceous facies only. These hiatuses characteristic of the upper Ladinian, Carnian and Norian mark levels of siliceous mud erosion and may be a result of the same events. However, the highly siliceous Member 18 in the lower Norian interval of the Khor River section does not correspond to any global cycle. It could reflect influence of some regional factors, e.g., of transgressive–regressive cycles related to local tectonic movements or to some other events.

An impact of global eustatic sea-level fluctuations on composition and cyclic structure of the Triassic siliceous deposits in the Sikhote Alin was most decisive at least for the carbonate–siliceous facies. Within basins of the Khor, Gur, and Anyui rivers, the formation can be classed with a megacyclothem, whose central part is composed of carbonate rocks grading up and downward first into bedded cherts, then into siliceous clay beds, and finally into terrigenous (or terrigenous–volcanogenic) deposits. At the time of high sea level stand, when the sea advanced into adjacent land, the carbonate sedimentation replaced the siliceous one in central areas of the Sikhote Alin basin.

The Triassic siliceous formation is of the "planktonogenic" type. Radiolarian skeletons represent the main fraction of sedimentary material in siliceous beds (Volokhin, 1985). Pelitomorphic limestones have been considered earlier as chemogenic in origin because of absence of macrofauna (Dagys *et al.*, 1984; Klets, 1995), but they may equally be of the planktonic-detrital microalgal or microalgal–foraminiferal type (Volokhin *et al.*, 1987). We believed formerly (Volokhin *et al.*, 1987) that the transition from siliceous to carbonate sedimentation in the Sikhote Alin basin was caused by changes in the carbonate compensation depth. However, the established correlation between carbonate units of the Khor River section and epochs of high sea-level stands (transgressions) suggests that transitions of this kind depended not on the above factor, but on migration of habitat areas of calcareous and siliceous plankton. Actually, the epochs of sea level rise lead to decrease of the carbonate compensation depth because of a lower temperature gradient and depressed circulation of oceanic water masses, whereas the result of sea level drops is inverse (Haq *et al.*, 1987). In addition, the described parageneses and compositions of rocks, as well as high silica accumulation rates, are characteristic of marginal sea basins, where the carbonate compensation depth is shallower than in oceanic areas of pelagic sedimentation.

In sections of terrigenous shallow-shelf deposits of the Arsen'ev and Alchan zones, mesocycles of sea level drop and regression correspond to epoch of erosion of the Lower Triassic and Anisian deposits preserved within a small area only. The Ladinian beds are almost missing here, but the Upper Triassic beds are widespread (Burago *et al.*, 1969). The same period of erosion of terrigenous shelf sediments is also recorded in the South Primor'e zone, where "by the beginning of the Carnian Age, the continental type of sedimentation became widely predominant and continued until the new early Norian regression of the Boreal sea" (Burii and Zharnikova, 1980, p. 45).

CONCLUSION

The section exposed at the right-hand side of the Khor River (downstream from the Kolomi River mouth) exemplifies the carbonate–siliceous facies of

the Triassic siliceous formation of the Sikhote Alin. Units of bedded cherts and carbonate rocks are interrelated here via gradual lithological transitions and constitute the Anisian–Rhaetian (?) megacyclothem about 430 m thick. The megacyclothem structure reflects the global eustatic sea-level fluctuations of the Triassic period. Carbonate units of the section accumulated in the past basin during the maximum sea level stand in the Carnian–middle Norian time, whereas bedded cherts were deposited, when the sea level lowered. The sea level was at the minimum in the early–middle Anisian and Early Jurassic (?) times of accumulation of terrigenous and siliceous-clay deposits. The short-term periods (mesocycles) of sea level drop were responsible for the thickness decrease characterizing the upper Ladinian and Carnian beds. Near the continental margin (exposures of the Lyamfana Creek) and within terrigenous shelf deposits of the Khankai microcontinent, the same events are recorded in the form of intraformational erosion hiatuses within siliceous facies of the Triassic formation.

In Anisian and Ladinian ages, rates of sedimentation and silica accumulation were comparable with these parameters currently established in the Sea of Okhotsk, Bering Sea, Peru-Chilean upwelling zone, and in some marginal or intracontinental seas, but they were greater than in open pelagic zones of the Pacific Ocean. In the Carnian and Norian, the silica accumulation rate decreased, and this type of sedimentation was replaced by accumulation of carbonate sediments. This event appears to be caused by the sea level rise and transgression responsible for the displacement of habitat areas of siliceous and calcareous plankton closer to the shoreline.

The established influence of global eustatic sea-level fluctuations on composition and structure of planktonogenic sediments opens a new methodic perspective for the detailed correlation of shallow- and deep-water deposits. This is also important for the retrospective analysis of events in adjacent land areas, where their records are worse preserved in general.

The Early Triassic was a time of initial accumulation of siliceous formation in the Sikhote Alin, presumably above the terrigenous (siliceous–clayey or clayey-silty) deposits, where fauna abundance is low. Some researchers suggest in contrast that bedded cherts persistently accumulated in the Sikhote Alin basin from the Permian to Middle Jurassic (Rudenko and Panasenko, 1990) or from the Early Carboniferous to Late Triassic inclusive (Shevelev and Kuz'min, 1990). We consider it unreasonable to unite in a single formation all Upper Permian and Middle–Upper Triassic bedded cherts even if they are similar in lithology. According to our observations, the proportion of terrigenous material is growing toward the base of the Triassic formation almost everywhere in the region: in the Olenekian beds of the Dal'negorsk region; in the middle Anisian beds near the villages of Uborka and Samarka at the right-hand side of the Ussuri River (Volokhin *et al.*, 1990); in the Anisian beds of the Anyui River basin, and other areas of the Sikhote Alin folded zone.

It seems to be equally unreasonable to attribute Triassic and Middle–Upper Jurassic siliceous beds to a single stratigraphic subdivision as it is done, for instance, in the case of the Dzhaur and some other formations (*Resheniya tret'ego...*, 1982; *Resheniya chetvertogo...*, 1994). Such a decision appears to be workable for solving stratigraphic problems by means of biostratigraphic methods only, when lithostratigraphy and original succession of sedimentary units within highly deformed sequences are inadequately studied and lithologic variations and transitions (interrelations) between members and units are underestimated. In our opinion, the aforementioned sequences belong to different formations corresponding to different sedimentation cycles and are individual in their structure and composition.

ACKNOWLEDGMENTS

We are grateful to Yu.D. Zakharov for critical analysis of our manuscript and valuable comments. The work was supported by the Russian Foundation for Basic Research, project no. 95-05-14129a.

Reviewers I.A. Basov and N.Yu. Bragin

REFERENCES

Budurov, K.J., *Paragondolella foliata* sp. n. (Conodonta) von der Trias des Ost-Balkans, *Rev. Bulgar. Geol. Soc.*, 1975, vol. 36, no. 1, pp. 79–81.

Budurov, K.J., Conodont Stratigraphy of the Balkanide Triassic, *Riv. Ital. Paleontol.*, 1980, vol. 85, nos. 3–4, pp. 767–780.

Burago, A.I., Burii, I.V., and Bersenev, I.I., The Triassic System, in *Geologiya SSSR, Primorskii krai* (Geology of the USSR, Primorskii Krai), Moscow: Nedra, 1969, pp. 197–228.

Burii, G.I., *Konodonty i stratigrafiya triasa Sikhote-Alinya* (Triassic Conodonts and Stratigraphy of the Sikhote Alin), Vladivostok: Dal'nevost. Otd. Akad. Nauk SSSR, 1989.

Burii, G.I. and Filippov, A.N., Cryptic Hiatuses in the Triassic Siliceous Formation of the Sikhote Alin, *Izv. Akad. Nauk SSSR, Ser. Geol.*, 1991, no. 7, pp. 136–139.

Burii, I.V. and Zharnikova, N.K., The Ladinian Flora-Bearing Beds of the Middle Triassic in the Southern Primor'e, *Byull. Mosk. O-va Ispyt. Prir., Otd. Geol.*, 1980, vol. 55, no. 3, pp. 45–53.

Burii, G.I., Filippov, A.N., and Rudenko, V.S., Stratigraphy and Depositional Environments of the Triassic Siliceous Formation on the Right Bank of the Matai River (the Khor-Anyui Subzone of the Central Sikhote-Alin), in *Litogenez i rudoobrazovanie v drevnikh i sovremennykh morskikh basseinakh Dal'nego Vostoka* (Lithogenesis and Ore Formation in Ancient and Recent Sea Basins of the Far East), Vladivostok: Dal'nevost Otd. Akad. Nauk SSSR, 1990, pp. 5–16.

Buryi, G.I., Evolution of Late Triassic Conodont Platform Elements, *Acta Micropaleontol. Sin.*, 1996, vol. 13, no. 2, pp. 135–142.

Dagis, A.A., Anoikin, V.I., and Klets, T.V., First Finds of Conodonts in the Upper Triassic Siliceous Deposits, in *Stratigrafiya, fauna i flora triasa Sibiri* (The Triassic Stratigraphy, Fauna, and Flora of Siberia), Moscow: Nauka, 1984, pp. 22–26.

De Master, D.J., The Supply and Accumulation of Silica in the Marine Environment, *Geochim. Cosmochim. Acta*, 1981, vol. 45, no. 10, pp. 1715–1732.

Haq, B.U., Hardenbol, J., and Vail, P.R., Chronology of Fluctuating Sea Levels since the Triassic, *Science*, 1987, vol. 235, pp. 1156–1167.

Harland, W.B., Armstrong, R.L., Cox, A.V., Craig, L.E., Smith, A.G., and Smith, D.G., *A Geologic Time Scale 1989*, Cambridge: Cambridge: Univ., 1989.

Harland, W.B., Cox, A.B., Llewellyn, N.G., *et al.*, *A Geological Time Scale*, Cambridge: Cambridge Univ., 1982. Translated under the title *Shkala geologicheskogo vremeni*, Moscow: Mir, 1985.

Igo, H. and Koike, T., Conodont Biostratigraphy of Chert in the Japanese Islands, in *Siliceous Deposits in the Pacific Region*, Iijima, A., Hein, J.R., and Siever, R., Eds., Amsterdam: Elsevier, 1983, pp. 65–78.

Klets, T.V., *Biostratigrafiya i konodonty triasa srednego Sikhote-Alinya* (The Triassic Biostratigraphy and Conodonts of the Middle Sikhote-Alin), Novosibirsk: Novosib. Gos. Univ., 1995.

Kovacs, S. and Kozur, H., Stratigraphische Reichweite der wichtigsten Conodonten (ohne Zahnreihenconodonten) der Mittel- und Obertrias, *Geol. Palaontol. Mitt. Innsbruck*, 1980, vol. 102, pp. 47–78.

Kozur, H., Significance of Events in Conodont Evolution for the Permian and Triassic Stratigraphy, *Curier Forsch. Inst. Senckenberg* (Frankfurt), 1989, no. 117, pp. 385–408.

March, M., Budurov, K., and Hirsch, F., *Sephardiella* nov. gen. (Conodonta), Emendation of *Carinella* (Budurov, 1973) from the Ladinian (Middle Triassic) Type Area in Catalonia (N.E. Spain), Sephardic Province, *Courier Forsch. Inst. Senckenberg*, 1990, no. 118, pp. 197–201.

Mosher, L.C., New Conodont Species as Triassic Guide Fossils, *J. Paleontol.*, 1970, vol. 44, no. 4, pp. 737–742.

Moscher, L.C. and Clark, D.L., Middle Triassic Conodonts from the Prida Formation of Northwestern Nevada, *J. Paleontol.*, 1965, vol. 39, no. 4, pp. 551–565.

Pisa, G., Perri, C., and Veneri, P., Upper Anisian Conodonts from Dont and M. Bivera Formations, Southern Alps (Italy), *Riv. Ital. Paleontol.*, 1980, vol. 85, nos. 3–4, pp. 807–828.

Resheniya chetvertogo mezhduvedomstvennogo regional'nogo stratigraficheskogo soveshchaniya po dokembriyu i fanerozoyu yuga Dal'nego Vostoka i Vostochnogo Zabaikal'ya. Khabarovsk, 1990 (Resolutions of 4th Interdepartmental Regional Conf. on Precambrian and Phanerozoic Stratigraphy of the Southern Far East and Eastern Baikal Region), Khabarovsk: KhGGP, 1994.

Resheniya tret'ego mezhduvedomstvennogo regional'nogo stratigraficheskogo soveshchaniya po dokembriyu i fanerozoyu Dal'nego Vostoka SSSR, Vladivostok, 1978 (Resolutions of 3d Interdepartmental Regional Conf. on Precambrian and Phanerozoic Stratigraphy of the Far East, Vladivostok, 1978), Magadan, GKP SVPGO, 1982.

Ross, C.A., Baud, A., and Menning, M., A Time Scale for Project Pangea, in *Pangea: Global Environments and Resources*, Embry, A.F., Beachamp, B., and Glass, D.J., Eds., Calgary: C.S.P.G., 1994, pp. 81–83.

Rudenko, V.S. and Panasenko, E.S., Permian Albaillellaria (Radiolarians) from the Panty Formation of the Primor'e, in *Novye dannye po biostratigrafii paleozoya i mezozoya yuga Dal'nego Vostoka* (New Data on Paleozoic and Mesozoic Biostratigraphy of the Southern Far East), Vladivostok: Dal'nevost. Otd. Akad. Nauk SSSR, 1990, pp. 117–124.

Shevelev, E.K., Khor–Anyui i Khabarovsk–Vandan Structural–Formational Zones, in *Mikstity Sikhote-Alinskoi skladchatoi sistemy* (Mixtites of the Sikhote Alin Folded System), Vladivostok: Dal'nevost Otd. Akad. Nauk SSSR, 1988, pp. 33–62.

Shevelev, E.K. and Kuz'min, S.P., New Stratigraphic Data on the Badzhal Zone, in *Novye dannye po biostratigrafii paleozoya i mezozoya yuga Dal'nego Vostoka* (New Data on Paleozoic and Mesozoic Biostratigraphy of the Southern Far East), Vladivostok: Dal'nevost. Otd. Akad. Nauk SSSR, 1990, pp. 72–80.

Sudar, M.N. and Budurov, K.J., New Conodonts from the Triassic in Yugoslavia and Bulgaria, *Geol. Balc.*, 1979, vol. 9, no. 3, pp. 47–52.

Tatge, U., Conodenten aus dem germanischen Muschelkalk, *Palaontol. Zeitschr*, 1956, vol. 30, pp. 108–147.

Volokhin, Yu.G., *Kremnevye porody Sikhote-Alinya i problema proiskhozhdeniya geosinklinal'nykh kremnevykh tolshch* (Cherts of the Sikhote Alin and Origin of Geosynclinal Cherty Sequences), Vladivostok: Dal'nevost. Nauch. Tsentr Akad. Nauk SSSR, 1985.

Volokhin, Yu.G., Burii, G.I., Filippov, A.N., and Mikhailik, E.V., The Carbonate–Siliceous Facies in the Geosynclinal Triassic Deposits of the Sikhote Alin, in *Geosinklinal'nye osadochno-vulkanogennye formatsii sovetskogo Dal'nego Vostoka* (Geosynclinal Sedimentary–Volcanogenic Formations of the Soviet Far East), Vladivostok: Dal'nevost. Otd. Akad. Nauk SSSR, 1987, pp. 70–91.

Volokhin, Yu.G., Burii, G.I., Rudenko, V.S., and Filippov, A.N., Triassic Siliceous Formation of the Southern Sikhote Alin, *Izv. Akad. Nauk SSSR, Ser. Geol.*, 1990, no. 4, pp. 45–57.

Volokhin, Yu.G., Mikhailik, E.V., Burii, G.I., and Rudenko, V.S., The Pre-Accretion Structure of the Triassic Siliceous Formation of the Sikhote Alin, in *Zakonomernosti stroeniya i evolyutsii geosfer* (Structure and Evolutionary Trends of Geospheres), Khabarovsk: Tikhookean. Inst. Geol., Dal'nevost. Otd. Ross. Akad. Nauk, 1996, pp. 60–63.

Stratigraphy and Geological Correlation, Vol. 7, No. 5, 1999, pp. 519–520. Translated from Stratigrafiya. Geologicheskaya Korrelyatsiya, Vol. 7, No. 5, 1999, pp. 111–112.
Original Russian Text Copyright © 1999 by Chernysheva.
English Translation Copyright © 1999 by МАИК "Наука/Interperiodica" (Russia).

A Tribute to the 90th Birthday of Boris Borisovich Chernyshev (1909–1941)

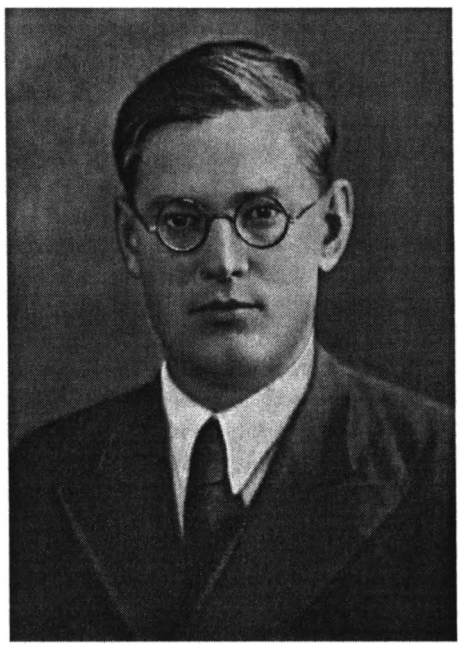

Boris Borisovich Chernyshev, an outstanding paleontologist, dedicated his research mainly to the Middle Paleozoic tabulate corals and brachiopods of the Arctic, Siberia, and Mongolia. Though his life was cut short in the Great Patriotic War, he left a brilliant legacy in science as one of the pioneers in his field of research. By disposition, he was a typical naturalist. He was born on December 19, 1909, in the town of Yeisk (Krasnodar Territory) to the family of Boris Isidorovich Chernyshev, the well-known geologist, paleontologist, and future member of the Ukrainian Academy of Sciences. Until 1918, Chernyshev lived in Yeisk with his grandfather, a teacher at the local school and a descendent from a family of Kuban Cossacks; he finished school in Dnepropetrovsk. When still a schoolboy, he worked in geological field parties, first with his father and later with D.I. Sokolov. In 1929, he entered the Pedological–Geological Department of the Physico-Mathematical Faculty at the Leningrad University. In 1930, after reorganizations in geological service and education, he and his colleagues were transferred to the Leningrad Mining Institute (LMI), which he graduated in 1934.

As a student, Chernyshev was extremely interested in geological and biological sciences, read special books, popular–science literature and scientific papers. He was active in the students' scientific society, attended the lectures of V.I. Vernadskii, R.F. Gekker, K.M. Deryugin, and listened to discourses of A.P. Karpinskii and A.V. Lunacharskii. Chernyshev was an amiable man, a true friend, and a nature lover. In spring and summer, he spent a lot of time in the country with, his younger brother Oleg, a future biologist. In winter, his favorite pastime was that of an enthusiastic radio ham operator. By the end of his student years, he took to photography and became a professional photographer of people and landscapes; later, he photographed the fauna he studied. In his monograph on Silurian brachiopods of Mongolia and Tuva, the paleontological tables were edited from his photos.

When still a student at the LMI, Chernyshev had his summer practicum in the Caucasus and Urals. By this time, he was well qualified for field research after his work with the expeditions when still a schoolboy. This experience was augmented by inborn orderliness and self-discipline. He made up detailed lists of equipment and personal belongings long before field work and carefully packed them in a good time with his fishing-tackle and hunting outfit. He filled thick copybooks with notes ranging from useful general information to mathematical formulas and cooking recipes. B.P. Markovskii, his former instructor in field work, remarked ironically, but approvingly, that Chernyshev made plans of his return a fortnight before starting on field work. His diploma paper on the materials of field research in the Urals was dedicated to the stratigraphy and fauna of the Domanik horizon in one of the regions of Bashkiria (Bashkortostan) and received highest honors.

On graduation from the LGI, Chernyshev was taken on the staff of the Commission on Mongolia (which was then in Leningrad) at the Geological Institute of the Academy of Sciences of the USSR as a scientific worker, and his first task was to study the Silurian faunas of Mongolia and Tuva. During his first two years with this Commission, he wrote two monographs on brachiopods and tabulate corals, which were published in 1937 and received high appraisal from specialists, among them D.V. Nalivkin, who remarked on the high level of research and the reliability of determinations and conclusions. In May 1936, Chernyshev moved from the Commission on Mongolia to the All-Union Arctic Institute (VAI), where he continued his paleontological researches, and in 1938 he became the Head of the Paleontological Chamber. That year, he becarne a member of the All-Union Paleontological Society and worked in the Polar Urals during field seasons of 1937

and 1938. The materials that he collected on the Paleozoic Pai-Khoi deposits are demonstrated in a glass case at the Museum of the Central Institute of Geological Exploration for Base and Precious Metals (TsNIGRI). By mid 1938, Chernyshev had six published works, and three papers were prepared for publication; according to Nalivkin, by their significance they exceeded the demands required of a Candidate Dissertation.

Chernyshev had the ability to be enthusiastic about anything he had to do. He was equally interested and persevering in the study of both brachiopods and tabulate corals, but actually the latter became the main object of his research. At the same time, he finished a monograph study on graptolites, tetracorals and calcareous algae of the Lower Paleozoic. With the same enthusiasm, he worked in summer with the geological survey parties and showed considerable organizational acumen. Moreover, he had the gift of establishing friendly contacts with people, a family trait also characteristic of his father and brother. Chernyshev's life and work were extremely organized; he scrupulously carried out any commitments that he undertook. Owing to the strict regulation of his day and maximal use of his time, he soon became familiar with the very essence of the problems under study and could make an appreciable contribution to their solution. His scientific works, since the first paper published soon after his graduation from the LGI, Chernyshev, wrote straightway and ready for publication after previous deep deliberation of every statement. Even his field reports on geological studies were substantial and could be printed without further corrections. Nonetheless, Chernyshev found pleasure in recreations: he was an enthusiastic radio and photography amateur; he was fond of cinema and greatly enjoyed art exhibitions and the theater.

In April 1941, Chernyshev was appointed Senior Geologist on the expedition of the "Glavsevmorput" (the Main North Seaway Administration) to the Arctic regions, but the beginning of the Great Patriotic War of 1941–1945 frustrated his plans. In the first days of the war, Chernyshev enlisted in the civil volunteer corps and at the same time received summons from the District Military Registration and Enlistment Commissariat, which directed him to the advanced courses of the Red Army Commanding Corps in the vicinity of Leningrad. In August 1941, Chernyshev was sent on a mission to Leningrad and could spend a few hours with his family and see his recently-born daughter and his beloved five-year old son, who died in 1943 during evacuation to the rear of the country. After finishing the courses in the rank of junior lieutenant, Boris Borisovich went to the front. Every two or three days, he wrote letters home full of anxiety about the family, and optimism and hope for the forthcoming happy and peaceful life. The last letter was sent on November 12, 1941, from the railway station Mga region in the Leningrad District, where at that time the army was engaged in a furious military combat. In 1967, the All-Union Arctic Institute put up a memorial stele with the names of its collaborators, who perished at the battle-front; the name of Boris Borisovich Chernyshev is among them.

In the short period of his scientific activity (1934–1941) Chernyshev wrote several articles and monographs, twelve of which were published; the manuscripts of his two monographs were lost during evacuation of the Arctic Institute from Leningrad, which was then under siege. A list of works by Chernyshev on corals is given in the book *The History of Study of Paleozoic Corals and Stromatoporoids* published in 1973, where it is noted that he was one of the first researchers of tabulate and other corals recovered from different areas in the Arctic region, Mongolia, Tuva, the Main Devonian Field, and the Kuznetsk basin. Moreover, Chernyshev prepared a description of Silurian graptolites of the Arctic and Silurian brachiopods of Mongolia and Tuva, thus outlining for the first time the specific features of the Tuva–Mongolian paleobasin, which is often called *Tuvellian* after the *Tuvaella* genus of brachiopods distinguished by him. All Chernyshev's works received high praise from specialists, among whom were D.V. Nalivkin, I.I. Gorskii, B.P. Markovskii, and M.E. Yanishevskii, whereas the monograph on Silurian brachiopods of Mongolia and Tuva, according to E.V. Vladimirskaya, still serves as a reference book for specialists working in this field. In 1951, a posthumous edition of Chernyshev's monograph on tabulate corals from the Kuznetsk basin became extremely popular. In addition, he laid the foundation for study on dwelling mode of tabulate corals and was first to remark on symbiosis of favositids and tubular worms. This phenomenon drew the attention of many geologists, as is testified by the numerous publications on this topic in the past 30 years. The contribution of Chernyshev's valuable study on Paleozoic faunas is evident from nine coral species named after him.

In the obituary written by Nalivkin and Sokolov (published in the *All-Union Paleontological Society Annual*, vol. 13, 1949), the authors expressed their high opinion of Chernyshev's merits in the development of the Paleozoic paleontology, biostratigraphy and paleogeography of Northern Eurasia and remarked on his role as a pioneer in the study on many Silurian and Devonian faunas. Chernyshev was an outstanding specialist and indomitable traveler–naturalist. He made a valuable contribution to paleontological science, which was greatly appreciated by his contemporaries and followers. No doubt, he could have done much more. Academician Nalivkin singled him out among his disciples and used to say that he had the makings of an outstanding scientist.

N. E. Chernysheva

Subscribe to the journals from the Russian Academy of Sciences

Translated and Published by МАИК "Наука/Interperiodica"
Distributed Worldwide by INTERPERIODICA

Copy this form to mail or fax your order today

	TITLE	Volume	ISSN	ISSUES	RATE IN US DOLLARS US/CAN	INTERNATIONAL	YOUR ORDER
❑	Agricultural Chemistry	3	1560-0890	4	$558	$643	$ _____
❑	Biophysics	44	0006-3509	6	$2400	$2496	$ _____
❑	Computational Mathematics and Mathematical Physics	39	0965-5425	12	$2137	$2600	$ _____
❑	Doklady Earth Sciences	364-369A	1028-334X	9	$2691	$3095	$ _____
❑	Doklady Mathematics	59-60	1064-5624	6	$1289	$1481	$ _____
❑	Entomological Review	79	0013-8738	9	$1996	$2296	$ _____
❑	Environmental Geoscience	2	Pending	4	$564	$640	$ _____
❑	Eurasian Soil Science	32	1064-2293	12	$1897	$2181	$ _____
❑	Geochemistry International	37	0016-7029	12	$2138	$2459	$ _____
❑	Geology of Ore Deposits	41	1075-7015	6	$906	$1041	$ _____
❑	Geomagnetism and Aeronomy	36	0016-7932	6	$555	$638	$ _____
❑	Geomagnetism and Aeronomy	37	0016-7932	6	$555	$638	$ _____
❑	Geomagnetism and Aeronomy	38	0016-7932	6	$623	$715	$ _____
❑	Geotectonics	33	0016-8521	6	$528	$574	$ _____
❑	Herald of the Russian Academy of Sciences	69	1019-3316	6	$1223	$1554	$ _____
❑	Izvestiya, Atmospheric and Oceanic Physics	35	0001-4338	6	$735	$790	$ _____
❑	Izvestiya, Physics of the Solid Earth	35	1069-3513	12	$775	$853	$ _____
❑	Journal of Communications Technology and Electronics	44	1064-2269	12	$2472	$2843	$ _____
❑	Journal of Computer and Systems Sciences International	38	1064-2307	6	$1947	$2240	$ _____
❑	Journal of Ichthyology	39	0032-9452	9	$1715	$1972	$ _____
❑	Laser Physics	9	1054-660X	6	$1029	$1242	$ _____
❑	Oceanology	39	0001-4370	6	$654	$705	$ _____
❑	Paleontological Journal	33	0031-0301	6	$1281	$1474	$ _____
❑	Pattern Recognition & Image Analysis	9	1054-6618	4	$647	$743	$ _____
❑	Petroleum Chemistry	39	0965-5441	6	$2627	$2733	$ _____
❑	Petrology	7	0869-5911	6	$906	$1041	$ _____
❑	The Physics of Metals and Metallography	87-88	0031-918X	12	$2198	$2530	$ _____
❑	Polymer Science. Series A	41	0965-545X	12	$2435	$2805	$ _____
❑	Polymer Science. Series B	41	1560-0904	6	$928	$1068	$ _____
	Both Series A & B. $200 discount				$3163	$3673	$ _____
❑	Proceedings of the Steklov Institute of Mathematics	224-227	0081-5438	4	$946	$1090	$ _____
❑	Russian Journal of Inorganic Chemistry	44	0036-0236	12	$2521	$2899	$ _____
❑	Russian Journal of Mathematical Physics	6	1061-9208	4	$528	$600	$ _____
❑	Russian Journal of Physical Chemistry	73	0036-0244	12	$2521	$2899	$ _____
❑	Russian Journal of Zoology	3	1560-0912	4	$544	$623	$ _____
❑	Stratigraphy and Geological Correlation	7	0869-5938	6	$906	$1041	$ _____
❑	Studies on Russian Economic Development	10	1075-7007	6	$655	$754	$ _____
❑	Thermal Engineering	46	0040-6015	12	$1417	$1630	$ _____
❑	Thermophysics and Aeromechanics (only distribution)	6	0869-8643	4	$603	$724	$ _____
						TOTAL	_____

❶ Name _____
Institution _____
Address _____
_____ State _____
City _____ Country _____
Zip/Postal Code _____
Telephone (_____)

Delivery is not made until payment is received

To order by phone call **1 800 633-4931**
or (205) 995-1567 outside the US and Canada

❷ ❑ My payment for $_____ is enclosed.
OR
❑ Bill me. My library's purchase order number is _____

❸ Send this order and payment to:
INTERPERIODICA
P.O. Box 1831
Birmingham, AL 35201-1831
Or fax this order form to (205) 995-1588

Order now for immediate delivery. All journals will be published in 1999!

МАИК "НАУКА/INTERPERIODICA" PUBLISHING

is pleased to present to the international scientific community simultaneous Russian- and English-language publication of the journals of the Russian Academy of Sciences

International Academic Publishing Company "NAUKA/INTERPERIODICA" (МАИК "НАУКА/INTERPERIODICA"), in cooperation with the Russian Academy of Sciences, publishes the results of research in all fields of modern science performed by leading scientists and scientific institutions from Russia, the CIS, and other countries. Simultaneous English translation of the journals is provided by INTERPERIODICA Publishing, the translation division of МАИК "НАУКА/INTERPERIODICA". Today, scientists around the world have direct access to the most significant Russian research at the time it is first published in Moscow – at the time it is most relevant to the worldwide scientific community. In addition to more timely publication, readers benefit from more precise translations of each journal, provided by a carefully chosen team of scientific translators with direct access to the authors and editors. English versions of the journals published by МАИК "НАУКА/INTERPERIODICA" are distributed worldwide by INTERPERIODICA, Kluwer Academic/Plenum Publishers, and the American Institute of Physics.

МАИК "НАУКА/INTERPERIODICA" 1999 volumes include the following titles:

- *Agricultural Chemistry*
- *Biophysics*
- *Computational Mathematics and Mathematical Physics*
- *Doklady Earth Sciences*
- *Doklady Mathematics*
- *Entomological Review*
- *Environmental Geoscience*
- *Eurasian Soil Science*
- *Geochemistry International*
- *Geology of Ore Deposits*
- *Geomagnetism and Aeronomy*
- *Geotectonics*
- *Herald of the Russian Academy of Sciences*
- *Izvestiya, Atmospheric and Oceanic Physics*
- *Izvestiya, Physics of the Solid Earth*
- *Journal of Communications Technology and Electronics*
- *Journal of Computer and Systems Sciences International*
- *Journal of Ichthyology*
- *Journal of Journals*
- *Laser Physics*
- *Oceanology*
- *Paleontological Journal*
- *Pattern Recognition and Image Analysis*
- *Petroleum Chemistry*
- *Petrology*
- *Polymer Science, Series A*
- *Polymer Science, Series B*
- *Proceedings of the Steklov Institute of Mathematics*
- *Russian Journal of Inorganic Chemistry*
- *Russian Journal of Mathematical Physics*
- *Russian Journal of Physical Chemistry*
- *Russian Journal of Zoology*
- *Stratigraphy and Geological Correlation*
- *Studies on Russian Economic Development*
- *The Physics of Metals and Metallography*
- *Thermal Engineering*
- *Thermophysics and Aeromechanics**

* *Thermophysics and Aeromechanics* is only distributed by МАИК "НАУКА/INTERPERIODICA" Publishing

Please direct all inquiries about the above journals to: **INTERPERIODICA**, P.O. Box 1831, Birmingham, AL 35201-1831.
For faster service call toll-free (800) 633-4931 or (205) 995-1567 (outside US and Canada). Fax: (205) 995-1588, E-mail: interperiodica@ebsco.com

- *Applied Biochemistry and Microbiology*
- *Biochemistry (Moscow)*
- *Biology Bulletin*
- *Colloid Journal*
- *Cosmic Research*
- *Doklady Biochemistry*
- *Doklady Biological Sciences*
- *Doklady Biophysics*
- *Doklady Botanical Sciences*
- *Doklady Chemical Technology*
- *Doklady Chemistry*
- *Doklady Physical Chemistry*
- *Glass Physics and Chemistry*
- *High Energy Chemistry*
- *High Temperature*
- *Human Physiology*
- *Inorganic Materials*
- *Instruments and Experimental Techniques*
- *Journal of Analytical Chemistry*
- *Journal of Evolutionary Biochemistry and Physiology*
- *Kinetics and Catalysis*
- *Lithology and Mineral Resources*
- *Microbiology*
- *Molecular Biology*
- *Programming and Computer Software*
- *Protection of Metals*
- *Radiochemistry*
- *Russian Journal of Applied Chemistry*
- *Russian Journal of Bioorganic Chemistry*
- *Russian Journal of Coordination Chemistry*
- *Russian Journal of Developmental Biology*
- *Russian Journal of Ecology*
- *Russian Journal of Electrochemistry*
- *Russian Journal of General Chemistry*
- *Russian Journal of Genetics*
- *Russian Journal of Marine Biology*
- *Russian Journal of Organic Chemistry*
- *Russian Journal of Plant Physiology*
- *Russian Microelectronics*
- *Solar System Research*
- *Theoretical Foundations of Chemical Engineering*
- *Water Resources*

Please direct all inquiries about the above journals to: **Kluwer Academic/Plenum Publishers**, 233 Spring Street, New York, NY 10013. Phone: (212) 620-8467. Fax: (212) 807-1047, E-mail: journals@plenum.com

- *Acoustical Physics*
- *Astronomy Letters*
- *Astronomy Reports*
- *Crystallography Reports*
- *Doklady Physics*
- *Optics and Spectroscopy**
- *Physics of Atomic Nuclei*
- *Plasma Physics Reports*

Please direct all inquiries about the above journals to: **American Institute of Physics**, Circulation and Fulfillment Services, 500 Sunnyside Boulevard, Woodbury, NY 11797-2999 USA. Tel. (516) 576-2270, (800) 344-6902. Fax: (516) 349-9704, E-mail: sub@aip.org

**Optics and Spectroscopy*: Optical Society of America, 2010 Massachusetts Ave., NW, Washington, DC 20036-1023, Attn.: Publications Department. Tel. (202) 223-8130, (800) 582-0416. Fax: (202) 223-1096.

International Academic Publishing Company "NAUKA/INTERPERIODICA" (МАИК "НАУКА/INTERPERIODICA")
Profsoyuznaya ul., 90, Moscow, 117864, Russia, Phone: 7 (095) 3361600; Fax: 7 (095) 336 0666,
E-mail:compmg@maik.rssi.ru, http://www.maik.rssi.ru